Synthesis of compound libraries for the study of glucose uptake and splicing inhibition

Dissertation
For the achievement of the academic degree of the
Doctor in Natural Sciences
(Dr. rer. nat.)

Submitted to

Faculty of Chemistry and Chemical Biology

Technical University Dortmund

by

Javier de Ceballos Cerrajería

From Santander, Spain

Dortmund 2017

The following work was performed from September 2012 until February 2017 under the supervision of Prof. Dr. Herbert Waldmann at the Max Planck Institute for Molecular Physiology in Dortmund.

1st Examiner: Prof. Dr. Herbert Waldmann

2nd Examiner: Prof. Dr. Daniel Summerer

Some of the work described in this doctoral thesis can be found in the scientific publication:

Identification of a small molecule inhibitor that stalls splicing at an early step of spliceosome activation

Anzhalika Sidarovich, Cindy L. Will, Maria M. Anokhina, Javier Ceballos, Sonja Sievers, Dmitry E. Agafonov, Timur Samatov, Penghui Bao, Berthold Kastner, Henning Urlaub, Herbert Waldmann, Reinhard Lührmann, *eLIFE,* just accepted.

Dedicated to Helena and my family

for their continuous support.

1. Abstract/Zusammenfassung

Despite having the same "purpose", the uncontrollable cellular growth to the detriment of the organism, cancer presents itself in humans in great variety of forms. This variety makes developing effective treatments a highly challenging task. Nevertheless, cancer has a handful of hallmarks that are present almost ubiquitously in all types of tumours. Among them is the upregulated glucose uptake, known as the Warburg effect. However, there has yet to be a drug or treatment that makes use of this aberrant cancer metabolism. This is due to the lack of potent glucose uptake inhibitors. The identification of small molecules that efficiently target the glucose uptake is hence of high value. Through an in-house established glucose uptake assay, new scaffolds were identified as glucose uptake inhibitors, such as the Glupins. This novel identified scaffold presented a natural product-like structure and a high potency. In the present work, a synthetic route towards the Glupin core was established. The structure-activity relationships of the Glupin class was extensively studied by the synthesis of a library of analogues. The analogue, (+)-Glupin-1, was discovered as one of the most potent glucose uptake and was therefore selected for further biological studies.
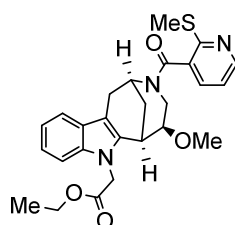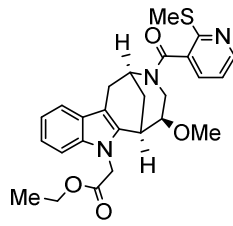

(+)-Glupin-1

The splicing process, the process by which premature messenger RNA is transformed into a mature form ready to be translated, is performed by a highly complex machinery, the spliceosome. The splicing process occurs in a series of steps, each of them catalysed by a different spliceosome complex constituted by many proteins and ribozymes. Decades of research on the spliceosome complex have provided an understanding of the process but much remains to be discovered. The in-house identification of a novel splicing inhibitor, **cp028**, enabled the isolation of a previously unknown spliceosome stage. In this work, the **cp028** compound was studied with the synthesis of a library of analogues around its core. The library of analogues was assayed as splicing inhibitors yielding a SAR analysis of this novel class.

Furthermore, efforts towards the identification of the **cp028** target were made. **Cp028** joins a short list of powerful splicing inhibitor that have allowed for a deeper study of the splicing process and opens the door for the identification of novel key protein players of this highly complex process.
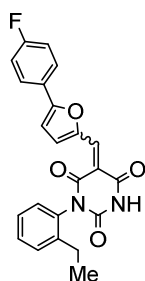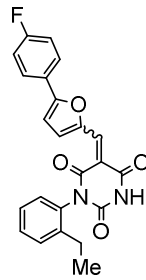

cp028

Krebs ist das unkontrollierte Wachstum von Zellen zum Nachteil des Gesamtorganismus. Auf zellulärem Niveau sind die Eigenschaften von Krebszellen jedoch sehr unterschiedlich, was eine effektive Behandlung von Tumorerkrankungen erschwert. Es gibt jedoch einige Merkmale, die von fast allen malignen Tumorzellen geteilt werden, unter anderem ein veränderter zellulärer Metabolismus. Dieser äußert sich häufig in erhöhter Aufnahme von Glukose und einer erhöhten Glykolyserate, auch Warburgeffekt genannt. Bisher fehlen jedoch effektive Wirkstoffe, die dieses Charakteristikum von Krebszellen nutzen, um selektiv Krebszellen zu adressieren. Die Identifikation von wirksamen Hemmern der Glukoseaufnahmen ist deshalb von großem Interesse. Durch einen intern etablierten zellulären Glukoseaufnahmetest im Hochdruchsatzverfahren konnten verschiedene kleine Moleküle mit gemeinsamen Grundstrukturen, die die Glukoseaufnahme von kultivierten Krebszellen effizient inhibieren identifiziert werden. Eine dieser Substanzklassen, die Glupine, basiert auf einem naturstoffähnlichen Grundgerüst, dessen Synthese im Rahmen dieser Arbeit etabliert wurde und auf dessen Grundlage eine Substanzbibliothek hergestellt wurde um eine Struktur-Wirksamkeitsbeziehung zu erstellen. Die Substanz (+)-**Glupin-1** wurde als wirksamstes Mitglied dieser Molekülklasse identifiziert und für weitere biologische Studien genutzt.

(+)-Glupin-1

Das Spleißen von prä-mRNA wird von einer fein regulierten molekularen Maschinerie aus Enzymen und Ribozymen gesteuert, dem Spleißosom. Obwohl seit vielen Jahrzehnten untersucht, sind viele Details des komplexen Assemblierungsprozess des Spleißosoms bis heute nicht komplett verstanden. Mit Hilfe eines neu identifizierten Inhibitors des Spleißens, **cp028**, konnte ein bisher unbekannter Spleißosom-Komplex entdeckt werden. Auf Grundlage dieses Inhibitors wurde im Rahmen dieser Arbeit eine Substanzbibliothek hergestellt und auf ihre Aktivität in Bezug auf die Inhibierung des Spleißens getestet. **Cp028** erweitert die bisher kurze Liste von Inhibitoren des Spleißings und eröffnet die Möglichkeit neue Schlüsselproteine dieses hoch komplexen Prozesses zu identifizieren.

cp028

Table of Contents

Splicing Inhibition

Glucose Uptake Inhibition

2. Introduction

2.1. Glucose Uptake

The monosaccharide *D*-glucose is the principal source of energy in humans as it fuels the tricarboxylic acid cycle (TCA). Furthermore, it is a main source for anabolic pathways that feed from the TCA cycle and is involved in glycosylation processes. Hence, glucose is a key player in metabolism and cell homeostasis. It is the hydrolysis productof more complex sugars such as starch, sucrose or lactose, obtained from the diet. Although potentially synthesised by the liver, the levels of glucose in blood and tissues are mainly modulated by the synthesis and hydrolysis of the polysaccharide glycogen, which is used as a glucose reserve.The uptake of glucose and other hexoses into cells can be promoted by two different types of transporters: the sodium-glucose transporters (SGLTs) and the facilitative glucose transporters (GLUTs).[1-2] The SGLTs are a family of symporters that use the Na^+-K^+ gradient to actively transport glucose into the cells. Given this mode of transport, these symporters are situated where glucose needs to be absorbed or recovered against the glucose gradient at the membrane, such as the intestines or the renal tubules.The main two transporters of this family are SGLT 1 and 2.The first has a high affinity but low capacity of glucose transport and is present at the small intestine membrane and at the proximal tubules(kidneys). The SGLT2, on the other hand, hasa low affinity but a high capacity and ispresentmostly at the proximal tubules (kidneys). The second family of transporters responsible for glucose uptake is the GLUT family.

2.1.1.The GLUT transporter family

The family of GLUTs is a group of transporters that promote glucose diffusion across the membrane in a bidirectional manner according to the concentration gradient. This family is responsible for glucose uptake in the vast majority of tissues and presents a wide variety of affinities, substrate specificities and different cellular localisations.[2] This array of characteristics ensures a tight control of glucose uptake into the different tissues according to cellular requirements and to glucose availability. The GLUT family comprises 14 members which are classified into three subfamilies according to sequence similarities (Figure 1). The most studied subfamily is the well-characterizedclass 1, that comprises the GLUT1 to 4 plus the recently identified GLUT14.[3] The main difference within this subgroup is the distribution across tissues: GLUT1, ubiquitously expressed, is responsible for the basal supply of glucose to all tissues but

exhibits higher expression on erythrocytes and the brain, whereit representsthe main transporter at the blood brain barrier.[4-5] GLUT1 has a K_m of 3-7 mM for glucose uptake.Since the average glucose concentration in blood is around 5mM, GLUT1 has the ability to transport glucose at a high rate.[6]The second member, GLUT2, displays a comparatively low affinity for glucose (K_m of 15-20 mM) and other sugars but has a high transport capacity.[6] It is mostly expressed on the liver, pancreas and kidney, and its main function is believed to be glucose-sensing.[7-8] GLUT3 presents the highest affinity for glucose (K_m of ca. 2 mM) and is highly expressed in the neurons at the brain, where glucose is in high demand and of high priority.[2] GLUT14 is almost identical to GLUT3 but is specifically expressed in the testis.[3] The last GLUT transporter of the class 1 is GLUT 4, whose main characteristic is its insulin-dependent regulation. GLUT4 is stored in vesicles and is recruited to the membranes upon insulin stimulation.It is mostly expressed in adipocytes, and heart and muscle tissue.[9]
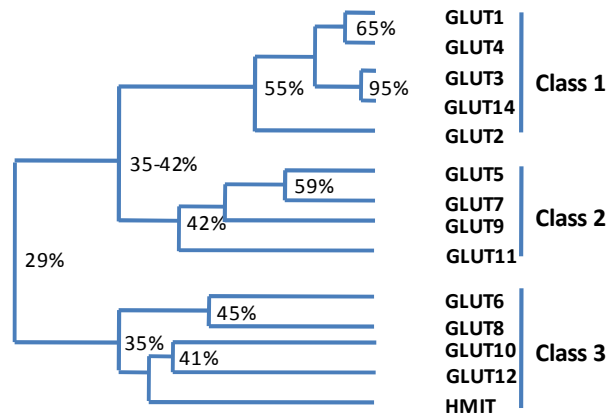
Figure 1. Dendrogram of all members of the GLUT transporter family. The numbers represent the percentages of sequence identity. Adapted from Scheepers *et al*.[2]

2.1.2.GLUT structure and glucose uptake mechanism

The GLUT transporters share a common core structure of two symmetrical six transmembrane α-helix domains, where both termini face the intracellular side (Figure 2a). The transmembrane domains form a cavity that allows glucose to diffuse by the rocker-switch alternative-access mechanism, in which the substrate-binding site is available from both sides of the membrane*via* conformational changes (Figure 2b).[10] The recent solution of the crystal structures of several GLUT transporters has enabled a deeper understanding of the mechanism and functions of the different members.[11-13] The GLUT1 structure was reported in 2014 by Deng and co-workers in an inward-open conformation bound to nonyl-glucopyranoside.[11] This structure complements,

and was resolved with the aid of, the previously reported bacterial homologue of glut1-4, crystallized in an outward-facing conformation bound to glucose.[14]
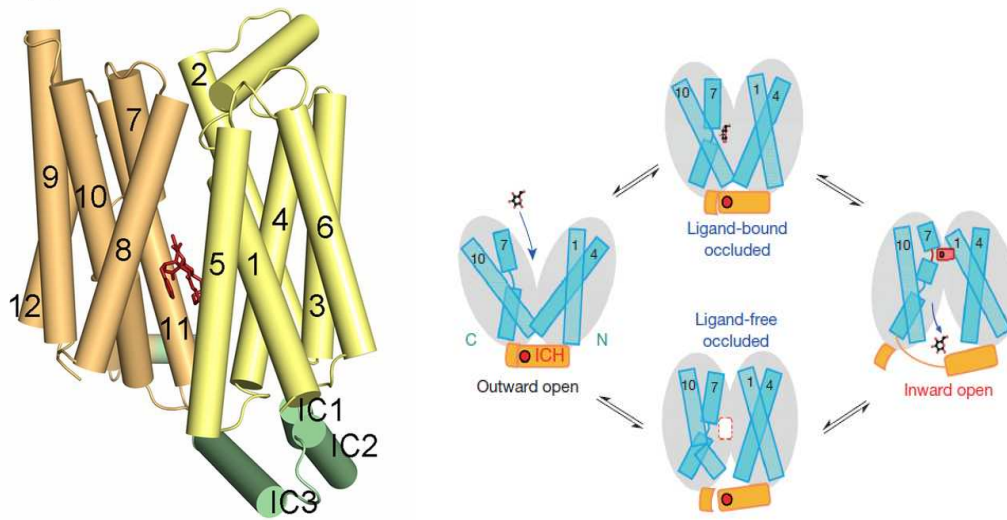
Figure 2. a) Illustration of the human GLUT1 transporter crystal structure (PDB: 4PYP).[11] Adapted from Kapoor *et al.*[15] The drawing shows the *N*-terminal (yellow) and the *C*-terminal (orange) domains and the intracellular (IC) domains (green). Cytochalasin B is represented by the red-stick structure at its binding site. The α-helix domains are represented as rods.**b)** Rocker-switch predicted alternative access transport for the GLUT1transporter. Adapted from Deng*et al.*[11]

2.1.3.Regulation of glucose uptake

Glucose uptake can be considered controlled, at its simplest stage, by the presence or lack of glucose in the extracellular media. This is particularly true for unicellular organisms in which up-regulation or down-regulation of the glucose metabolism is mostly driven by an extracellular nutrient-sensing mechanism. Nevertheless, in higher organisms such as humans, the extracellular media has no shortage of nutrient supply. Consequently, the glucose metabolism needs to be regulated by external signalling factors (e.g. growth factors) to prevent, for example, aberrant cell proliferation. The GLUT transporters are regulated by a series of transcriptional pathways and direct protein or compound interactions. When a greater glucose metabolism is needed, for example in proliferating cells, signalling factorspromote the up-regulation of the glucose uptake capacity. This occurs by modulating the GLUT transporters ability, as for the growth factor IL-3 (interleukin-3),[16] or by over-expressing the GLUT transporters at the membrane, as for the hormone insulin.[17] The main mechanism of glucose uptake regulation is insulin secretion by the pancreas, which transiently recruits GLUT4 to cell membranes of

insulin-responsive tissues. The PI3K/Akt/mTOR pathway is another important regulator of glucose metabolism by, among other mechanisms, increasing the presence of GLUT1 at the cell surface (Figure 3).[18-19] Furthermore, the PI3K/Akt/mTOR pathway also regulates the activation of HIF-1(hypoxia inducible factor-1 alpha),which promotes the over-expression of the GLUT transporters.[20] HIF-1 activation can also be triggered by alterations in ROS levels or in hypoxic conditions (Figure 3). The transcription factor MYC has also been shown to control the expression of the GLUT1 transporter as well as other glycolytic enzymes (Figure 3).[21]
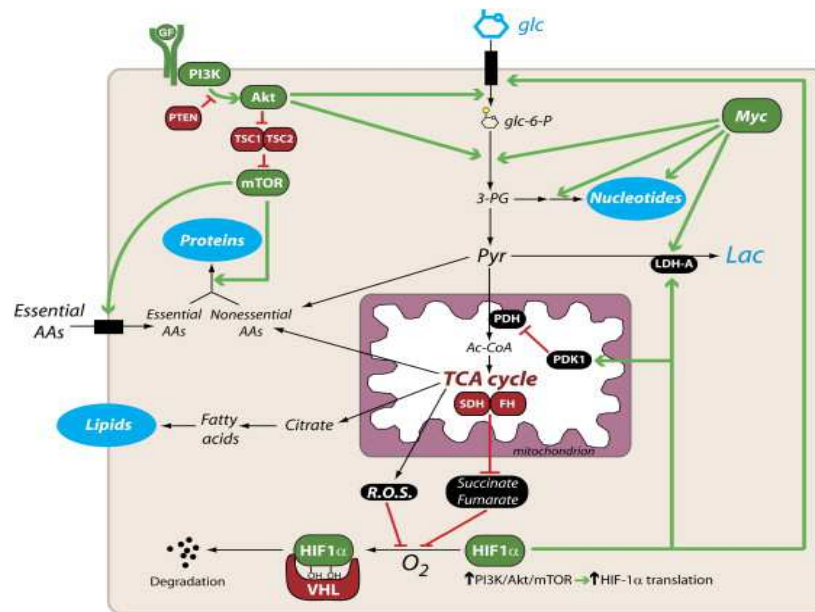
Figure 3. Transcriptional activation of GLUT1 expression regulated by the PI3K/Akt/mTOR signaling pathway, the transcription factors HIF-1 and Myc. Adapted from DeBerardinis *et al.*[19]

Another mechanism for the regulation of glucose uptake is the direct interaction with natural compounds such as methylxanthines and ATP, or proteins such as Stomatin. Methylxanthines bind to the external face of the transporter in a non-competitive mode of inhibition promoting a conformational change that down-regulates glucose uptake.[22] Glucose uptake is also regulated by glycolysis and the oxidative phosphorylation product ATP. Hence, at high ATP/ADP ratios, the triphosphate analogue binds to GLUT1 promoting conformational changes that decrease the transport activity.[23-24] The transmembrane protein Stomatin has also been shown to interact and modulate the function of GLUT1.[25]

Some post-translational modifications can also influence GLUT activity. For example, phosphorylation of GLUT1 by protein kinase C (PKC) is reported to increase its cell surface localisation and hence glucose uptake.[26] This phosphorylation is promoted by growth factors

such as VEGF or by aberrant mutations. *N*-glycosylation of the glucose transporter-1 is required for maintaining a high affinity for glucose and, as a consequence, a high glucose uptake.[27]

2.1.4. Glucose uptake as apart of glucose metabolism

The GLUT transporters represent the first proteins involved in the glycolytic route to convert glucose to pyruvate, which generatestwo molecules of ATP in the process. The glycolytic route is an anaerobic energy-producing process which is highly conserved from the early unicellular organisms, where it represents the main energy source, to high organisms that make further catabolic use of pyruvate to increase the free energy release of the overall process. The glycolytic enzymes include key glucose metabolism regulators like hexokinase (HK),[28] or phosphofructokinase (PFK).[29-30] The GLUT transporters have no affinity for glucose-6-phosphate and since the transport of glucose goes according to the concentration gradient, HK directly regulates the glucose uptake rate. Furthermore, TCA intermediates such ascitrate or ATP are known inhibitors of PFK, and hence of the glycolytic route (Figure 4).

Aerobic organisms, in terms of energy production, metabolize glucose down to carbon dioxide and water. The energy production of this process is18 times higher than anaerobic fermentation (the glycolytic route). The resulting pyruvate from glycolysis is transferred to the mitochondria where it is transformed into acetyl-CoA. Acetyl-CoA then feeds the TCA cycle generating the H^+ and reduced cofactors (NADH and $FADH_2$) necessary for oxidative phosphorylation(OXPHOS) (Figure 4). This pathway is highly conserved in complex organisms because of its high efficiency in ATP production. The mitochondrial metabolic activity is connected to the GLUT transporters through a series of complex signalling pathways, thus enabling "feedback" from energy production at the organelle to regulate glucose uptake. For example, elevation of ROS, generated in the mitochondria, plays an important part in activation of the HIF-1 transcription factor and hence promotes GLUT1 expression (see section 2.1.3.).[20, 31] Increased glucose uptake results in the generation of higher quantities of NAD(P)H (mainly through the pentose phosphate pathway), that can revert the elevated ROS levels.[32] The reverse process has also been reported. When GLUT1 is inhibited or mutated, the ROS levels increase.[33]
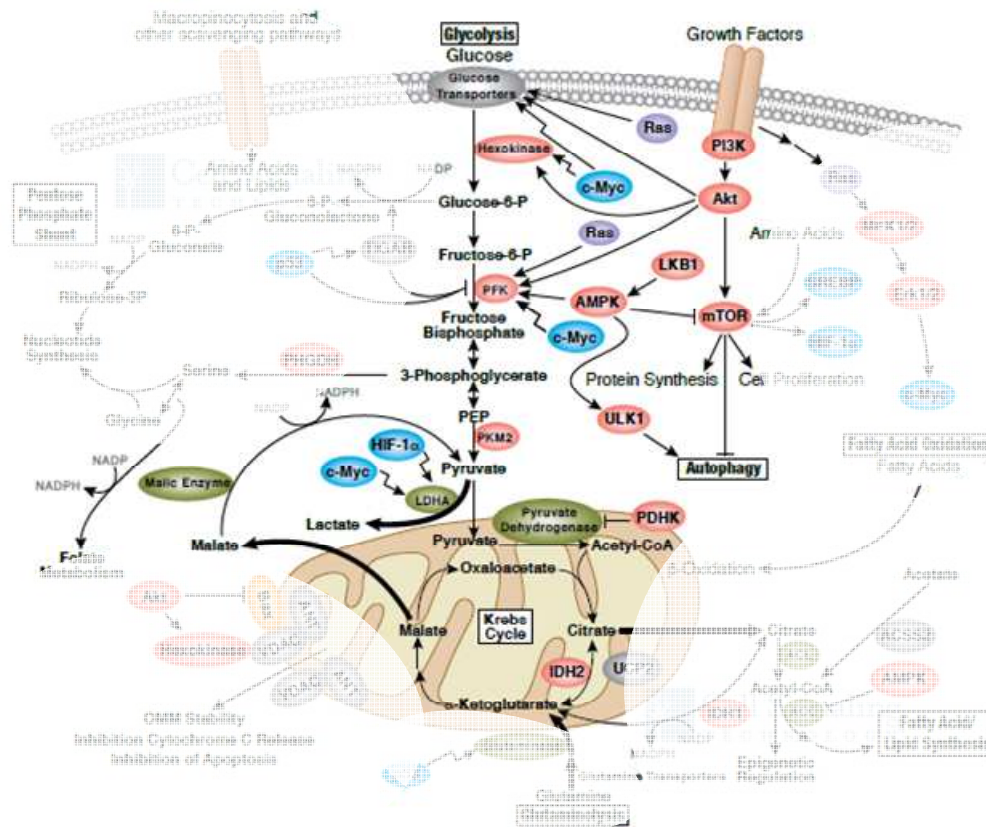
Figure 4. Signalling network around the glucose metabolic pathways. The glycolytic route occurs in the cytosol and is regulated by many transcriptional pathways and the allosteric inhibition of the glycolytic enzymes. Pyruvate can then enter the mitochondria to feed the TCA cycle. Illustration reproduced courtesy of Cell Signaling Technology, Inc. (www.cellsignal.com).

In conclusion, the uptake of glucose, the main energy source and a major feed source to the anabolic routes, is highly regulated by the enzymes and signalling pathways involved in the glucose metabolic routes, glycolysis and the TCA cycle. Hence, variations in glucose uptake have an extended effect throughout cell metabolism.

2.2. Glucose Uptake in Cancer: the Warburg Effect

In 1923, Otto Heinrich Warburg (1883-1970, Nobel laureate in medicine in 1931) observed that, in the presence of sugar, cancerous tissues displayed a much higher (over 70-fold) lactic acid production than healthy tissues (Figure 5).[34-35] Furthermore, he observed that the Pasteur effect (*i.e.* decrease or complete stop of the fermentation process in the presence of oxygen) did not

seem to apply to cancerous tissues. In normoxia (normal oxygen concentrations in the media), the tumours continued to produce high quantities of lactic acid.[36] Warburg hypothesised that the presence of lactic acid fermentation indicated an impaired respiration in the tumours and that this impaired respiration was the cause of carcinogenesis. The presence of such aerobic glycolysis in cancer cells was later named the Warburg effect.

Nr.	Art des Gewebes	*Ohne* Zucker		*Mit* Zucker (2,5 g : 1000 ccm)		Pro Milligramm und Stunde aus Zucker gebildete Milchsäure
		Gewicht des Schnittes mg.	Nach 60 Min. beobachtete Druckänderung mm	Gewicht des Schnittes mg	Nach 60 Min. beobachtete Druckänderung mm	mg
1	Tumor	4,0	− 44	4,5	+ 174	0,069
2	,,	2,6	− 20	2,3	+ 121	0,078
3	,,	2,4	− 16	2,3	+ 124	0,078
4	,,	4,1	− 38	3,9	+ 196	0,075
5	,,	3,3	− 31	3,6	+ 162	0,081
6	Leber	3,2	− 13	4,0	− 12	weniger als 0,001
7	,,	2,6	− 8	3,3	− 7	,,
8	,,	4,6	− 21	4,4	− 19	,,
9	,,	4,8	− 19	3,7	− 17	,,
10	Niere	2,0	− 61	2,0	− 62	,,
11	Herz	2,1	+ 3	1,9	− 3	,,

Figure 5. Changesin pressure caused by the carbon dioxide generated from the acidification of extracellular media in the presence of a bicarbonate solution. Picture taken from Warburg and Minami (1923).[34] Columns (from left to right): Type of tissue. Tumour, liver, kidney and heart. Weight of the tissue slice, without sugar. Change in pressure after 60 minutes, without sugar. Weight of the tissue slice, with sugar. Change in pressure after 60 minutes, with sugar. Lactic acid generated per mg and h.

This hypothesis was soon to be refuted when studies revealed a functioning respiration mechanism across many types of cancers.[37] Nevertheless, his observations have not been disputed and remain a hallmark in cancer metabolism. Contrary to healthy cells, excluding highly proliferative cells such as embryos, cancer cells engage, almost ubiquitously, in aerobic glycolysis, regardless of the extent to which respiration is performed. A high fermentation rate means a higher glucose demand which is met through the over-expression of the GLUT transporters, particularly the GLUT1 and GLUT3 members.[38-39] The rationale behind this behaviour in cancer is still under debate, but it has become clear that the Warburg effect

provides an evolutionary advantage to the cancer cells compared to the surrounding tissues.[40-42] In the past decade, the scientific community has accepted the hypothesis that cancerous cells engage in aerobic glycolysis to boost the anabolic routes with glycolytic intermediates.[40, 43] This allows for fast cell division and tumour proliferation. This hypothesis is partly supported by the observed aerobic glycolytic phenotype in fast proliferating healthy cells such as lymphocytes.[44] Nevertheless, aerobic glycolysis could appear as a hypoxia defense mechanism but also confers a phenotypic advantage to the tumour,which would further promote aerobic glycolysis regardless of the oxygen levels. For example, the acidification of the extracellular media has been hypothesised to confer a proliferation advantage to the tumour, which has adapted to it, in contrast to the healthy surrounding tissues to whichit becomes toxic, thus facilitating the tumour invasiveness.[42] Overall, there is still not clear understanding of the original causes of aerobic glycolysis.

The mechanisms by which the aerobic glycolysis phenotype is achieved are not fully clear. Many signalling pathways have been discovered to promote the necessary metabolic changes to acquire the aerobic glycolytic phenotype, but the molecular mechanism that triggers those pathways has yet to be fully understood. Since glycolysis is highly up-regulated, the pathways and transcription factors that regulate key glycolytic enzymes (see section 2.1.4.), such as glucose transporters or hexokinase, have been extensively studied.[20, 45-46]
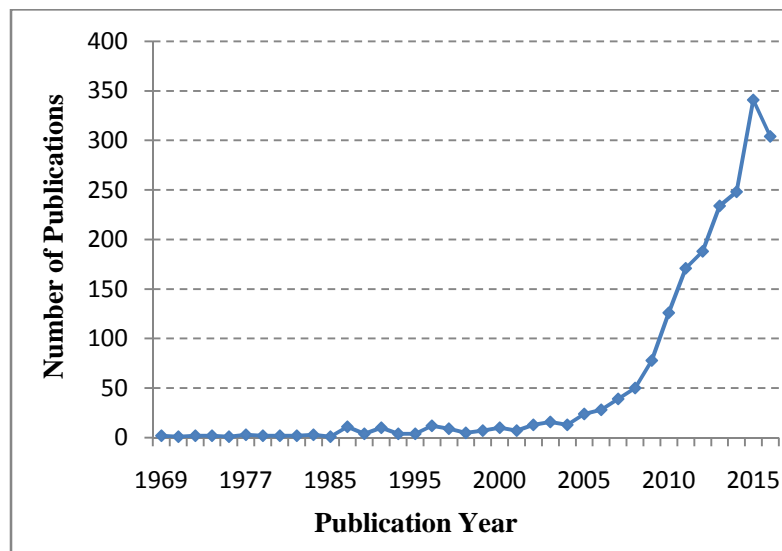

Figure 6. Number of publications per year since 1969. Source: Web of Science, under the theme search of "Warburg Effect".

In the last decade, the interest of the scientific community in the Warburg effect has increased exponentially (Figure 6). Being one of the hallmarks of cancer, the Warburg effect has lately been viewed as a potential window in the fight against cancer.[47] Based on the high dependence of most cancers on glucose, deprivation of it would sensitize tumours towards cancer therapies. This idea has sparked, at both the academic and industrial levels, the search for inhibitors of the glycolytic route, including glucose uptake.

2.3. Targeting Glucose Metabolism in Cancer

For many decades, the selectivity towards cancer cells in medicaltreatments has mainly been based on their higher proliferative character. Chemotherapeutic agents that target characteristic cell proliferation processes, such as cell division, have a stronger toxic effect on the cells with higher proliferation rates. Famous examples are Cisplatin, a chemotherapeutic drug that targets DNA replication, or the cytoskeletal natural product Taxol, which interferes with mitotic spindle assembly. Nevertheless, the recent characterization of alterations in tumour metabolism, such as the highly up-regulated glycolysis (see section 2.2.), have opened a new window for a more selective targeting of cancer.[48] Consequently, a variety of drugs targeting tumour metabolism are currently under study, including in clinical trials.[49]

A very common metabolic alteration found in cancer is aerobic glycolysis. The increased glycolytic flux indicates a strong dependence on glucose metabolism, which if inhibited or dysregulated should impair cancer cell growth or viability. Consequently, several compounds have been developed targeting known upstream oncogene modulators of the glycolytic route, such asHIF, PI3K, AKT or mTOR.[49] Furthermore, much research has also been dedicated to developing inhibitors of the enzymes involved in glucose metabolism (Figure 7).[50-51]
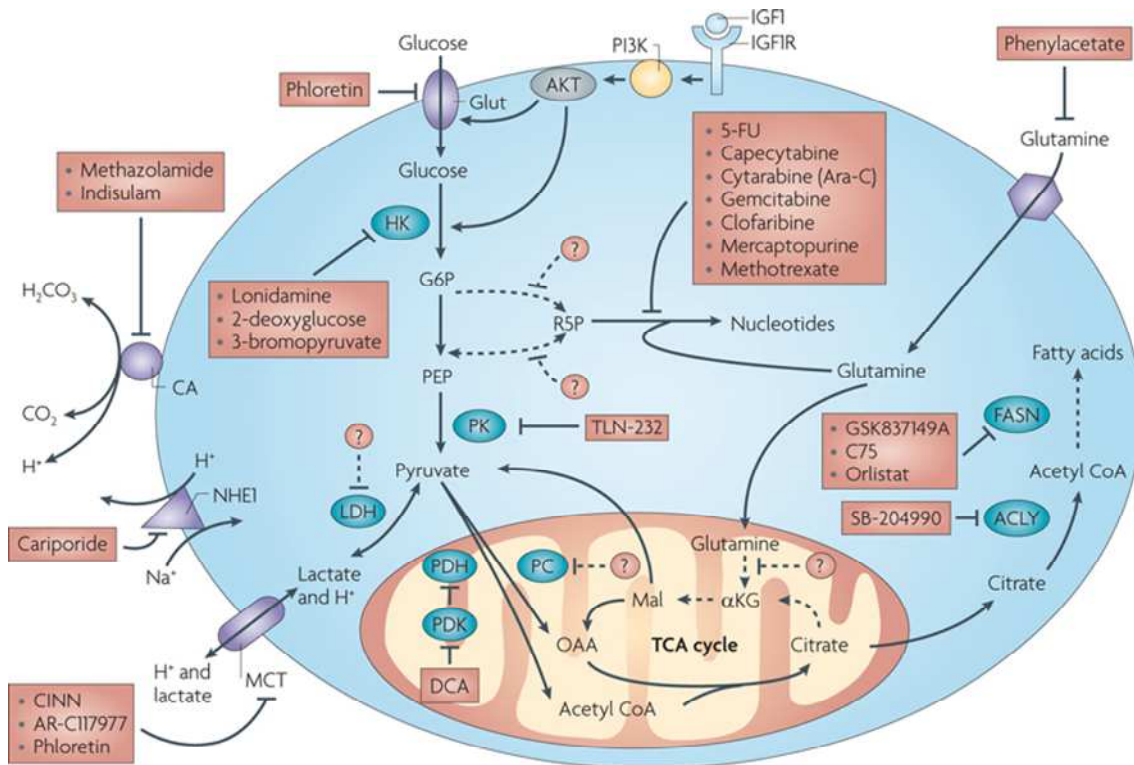
Nature Reviews | Cancer

Figure 7. Metabolic pathways and enzymes with inhibitors that have entered clinical trials. Figure from Tennant *et al*.[49]

Examples below targeting enzymes involved in glucose metabolism will be discussed. A selection was made for representative examples of compounds that have entered clinical trials, further validating modulation of the Warburg effect as a promising anti-cancer therapy. The GLUT inhibitors, which bear more importance for the work of this doctoral thesis, will be discussed in more detail (see section 2.4.).

2.3.1.Targeting hexokinase

The glycolytic enzyme hexokinase, particularly the isoform 2 (HK2), has been found up-regulated in many cancers and has thus received much attention as a potential cancer target, The glucose analogue 2-deoxyglucose (2-DG), which cannot be metabolised in glycolysis, acts as a competitive inhibitor of hexokinase, obstructing glycolytic flux (Figure 7). 2-DG has been subjected to several clinical trials against different solid tumours, alone or in combination with other chemotherapeutic drugs. 2-DG alone, however, has displayed very discouraging results in early clinical trials due partly to the fact that the maximal tolerated dose of 2-DG is approximately one order of magnitude below the average glucose concentrations in the blood.[52]

Nevertheless, 2-DG remains in clinical trials in combination with other drugs.[53-54] Other hexokinase inhibitors that made it into clinical trialsare, 3-bromopyruvate (3-BrPA) and lonidamine. 3-BrPA, displayed good results against liver cancer when administered locally in animals but has yet to conclude successfully a clinical trial.[55]

2.3.2. Targeting pyruvate kinase

The final step of glycolysis, which is catalysed by pyruvate kinase (PK), consists on transferring the phosphate group from phosphoenolpyruvate to ADP, generating ATP and pyruvate (Figure 7). PK is considered a very promising target because in proliferative tissues, including tumours, an alternative spliced form (PKM2) is expressed rather than the normal tissue splice variant, PKM1.[56] This selectivity window was addressed by Vander Heiden *et al.* by developing PKM2 inhibitors.[57] It has also lead to compounds in clinical trials such as the cyclopeptide TLN-232. This PKM2 inhibitor showed promising results in phase II of clinical trials against metastatic melanoma and renal cell carcinoma. Nevertheless, the PK is currently not considered as a useful target in cancer.

2.3.3. Targeting lactate dehydrogenase

Another important glycolytic enzyme targeted is lactate dehydrogenase (LDH) (Figure 7). LDH is the enzyme responsible for the conversion of pyruvate into lactate and has been found over-expressed in many cancers. The natural product gossypol was shown to inhibit LDH and, consequently, the synthesis of pyruvate. After lead optimization studies, the gossypol analogue AT-101 was developed and submitted to clinical trials. Nevertheless, positive results are scarce and cannot be directly linked to the inhibition of LDH.[53]

2.3.4. Targeting pyruvate dehydrogenase

Down-regulationof the aerobic glycolytic flux has also been achieved by "diverting" the glycolytic intermediate pyruvate to the mitochondrial respiration process rather than allowing it to be converted into lactate (as in aerobic glycolysis). Pyruvate dehydrogenase(PDH, the enzyme responsible for converting pyruvate into acetyl-CoA) can be activated by inhibiting a known PDH positive regulator, pyruvate dehydrogenase kinase (PDHK) (Figure 7). The result is a down-regulated aerobic glycolytic flux that can impair tumour growth. The small molecule dichloroacetate (DCA), was found to inhibit PDHK, thereby activating PDH and promotingtumour size reductions in mice. DCA was hence subjectedto several clinical trials against differenttumours, but no clear clinical benefits have yet been discovered.[53]

2.4. Targeting the Facilitative Glucose Transporters

As for the above-mentioned glycolytic enzymes, small molecule inhibition of the GLUT transporters hasalso been reported to impair cancer growth and viability. For example, the glucose inhibitor compound 30 (Table 1) displayed a cytotoxic effect against prostate adenocarcinoma cells while not affecting healthy cells.[58] Compound 30 was, however, devalidated. Another GLUT inhibitor, WZB117 (Table 1) was shown to impair cell proliferation of A549 lung cancer cells more efficiently than that of NL20 healthy lung cells.[59] The natural product Phloretin was reported to induce apoptotic cell death of B16 melanoma cells by inhibition of glucose transport.[60] The biological effects of these glucose uptake inhibitors in cancer cells further validate the idea of selectively targeting cancer by depriving it from glucose. However, due to the striking lack of selective and potent GLUT inhibitors, a glucose transport inhibitor has yet to enter a clinical trial.[61] Furthermore,the GLUT inhibitor Cytochalasin B, despite being a toxic compound andpreventing actin polymerization, continues to be used as the standard tool compound.[62]

The first low nanomolar GLUT inhibitor, the natural product Glucopiericidin A (GPA), was discovered in 2009 by Kitagawa and co-workers(Table 1). GPA was found to inhibit protrusion growth in combination with the known metabolic respiration inhibitor piericidin A (PA).[63] The authors could identify the GLUT transporters as the targets of GPA through a chemical genomic screening of small molecules with identified targets that would emulate GPA´s activity in combination with PA. Interestingly, GPA contains in its structure a glucose molecule (Figure 8), which may suggest a "glucose-directed" GLUT interaction. GPA was identified from a microbial broth and was not chemically synthesised.

The identification of novel glucose uptake inhibitors was enabled by the development of a pairwise chemical genetic screen by Ulanovskaya and co-workers.[64] In this screen, the authors suppressed the oxidative phosphorylation process and measured the ATP decrease upon compound treatment. If oxidative phosphorylation is inhibited, ATP production comes solely from the glycolytic path, hence a decrease in ATP concentration would identify a glycolytic inhibitor, hence potentially a GLUT inhibitor. The authors, however, could only report compounds of low micromolar activity like pyrrolidinone 12 (Table 1). Nevertheless, based on this assay, Bayer Pharmaceuticals established a high throughput screening(HTS)assay and developed the first series of highly potent glucose uptake inhibitors. Compounds Bay-GLUT1,

BAY-876, GLUT-i1 and GLUT-i2 (Table 1, Figure 8) were reported in 2016 while this doctoral thesis doctoral thesis work was performed.

Table 1. Potency, mode of action and GLUT selectivity of some reported glucose uptake inhibitors.

Compound	Reported in	IC$_{50}$ (µM)	Assay	Cell line	Mode of action[b]	GLUT 1-4 selectivity	Ref
BAY-GLUT1[a]	2016	0.311	^{3}H-2DG[c]	DLD-1 (CHO-K1 HeLaMaTu)	Competitive	1	65
		0.025	ATP detection[d]				
WZB117[a]	2012	~0.5	^{3}H-2DG	A549	-	-	66, 59
Phloretin	1964	1-50	^{3}H-2DG	SW620	-	-	67, 68
Cytochalasin B	1972	~0.5	^{3}H-2DG	Various	Non competitive	Non selective	15, 62
Cmpd. 30[a]	2012	2.0	^{3}H-2DG	LNCaP	Non competitive	Non selective	58
Pyrrolidinone 12[a]	2011	2.0	^{3}H-2DG	A549, CHO and ghosts	Non competitive	-	64
	2011	10.0	ATP detection[c]				
Indinavir	2002	50-100	^{3}H-2DG	GLUT4 oocytes	Non competitive	4	69
Glucopiericidin A	2010	0.005	^{3}H-2DG	A431, 3T3-L1 adipocytes	-	unselective to 1 and 4	70
GLUT-i1	2016	0.267	ATP detection[c]	DLD1	-	1 and 4	15
GLUT-i2	2016	0.140	ATP detection[c]	DLD1	-	1 and 4	
BAY-876[a]	2016	0.002	ATP detection[c]	DLD1	Competitive	1	71
PUG-1	2016	0.450	^{3}H-2DG	CHO (GLUT1 transfected)	-	-	72

IOmed-341[a]	2014	< 1.0	[3]H-2DG	HEK-293	-	unselective	73

[a] Compound is a representative example of a reported library. [b] Compared to the natural substrate glucose. [c] [3]H-2DG: [^{3}H]-2-deoxy-*D*-glucose. [d] In the presence of a mitochondrial respiration inhibitor.
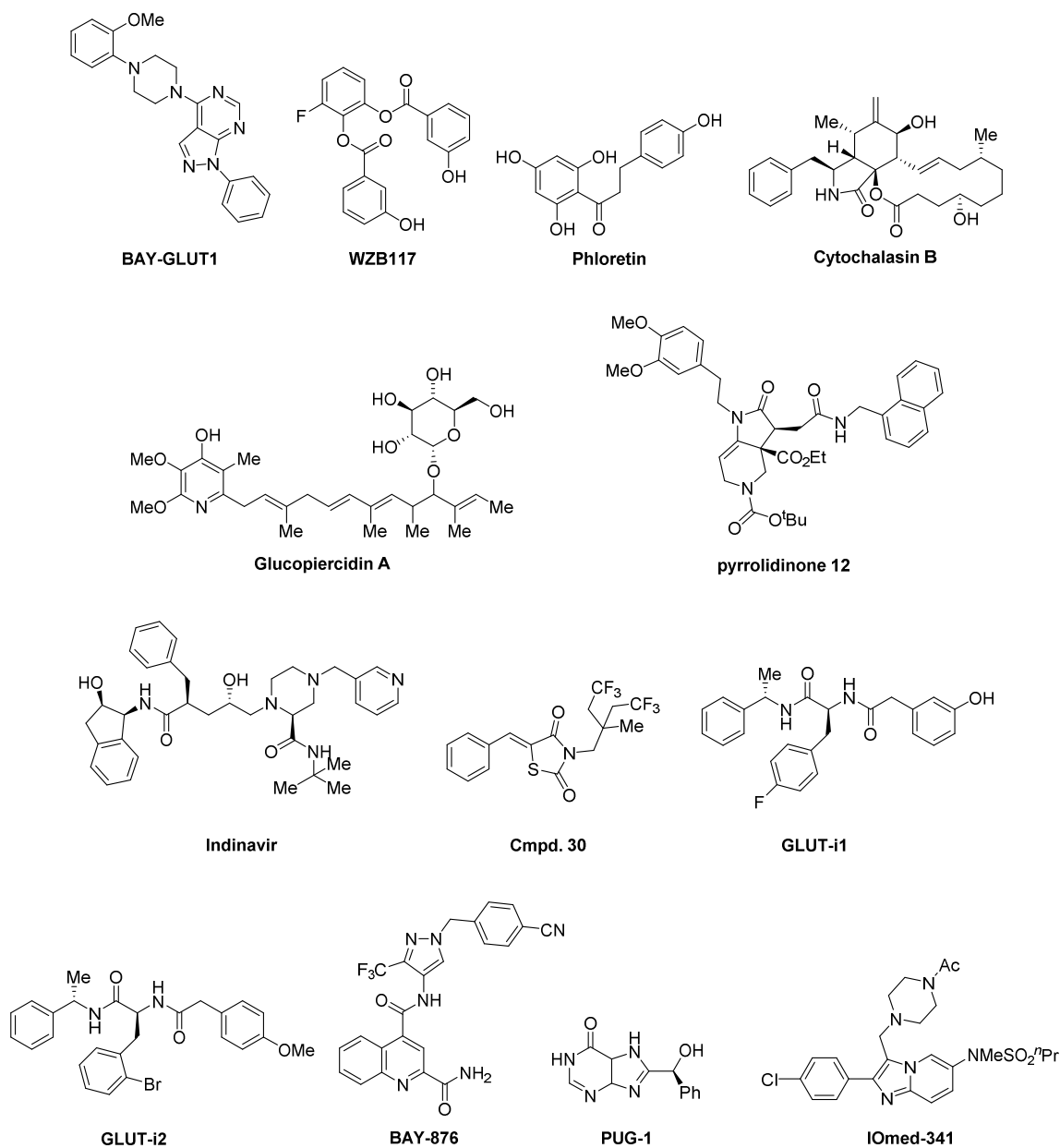

Figure 8. Chemical structures of the glucose uptake inhibitors of Table 1.

Bay-GLUT1 was reported as the first potent GLUT1 selective inhibitor. The following reported GLUT inhibitor, BAY-876 displayed a much higher potency coupled with a very high selectivity towards GLUT1. The identification of these inhibitors has, however, not led to any clinical trials. This may suggest that inhibiting GLUT1 alone may not be sufficient to kill or

sensitize cancer cells, and other receptor family members over-expressed in cancers such as GLUT3 may have to be targeted as well.[38-39, 74] It is possible that cancer cells overexpress GLUT3 or another transporter as a survival mechanism if GLUT1 is targeted. If so, a high selectivity towards any transporter migth be a disadvantage in cancer treatment.

In conclusion, it is my belief that the current trend of targeting the altered mechanism of cancer, particularly the GLUT transporters, has to be accompanied by the development of novel glucose uptake inhibitors and that further effort in this direction is necessary and will eventually lead to a powerful and selective cancer-targeting drug.

3. Aims of the Project

Despite the extensive variety of unique characteristic mutations of each type of cancer, tumors present a series of general trends or hallmarks. The Warburg effect is an example of a cancer hallmark. As such, the scientific community has accepted the potential of targeting the dysregulated metabolism of cancer, in general, and the Warburg effect in particular. The scarcity of potent and selective compounds that target the glucose transport mechanism is, therefore, the inspiration behind this project.

The general aim of this project is the identification of potent glucose uptake inhibitors. Identification of such compounds would meet a growing demand of GLUT inhibitors in the drug development area and provide the scientific community with more reliable tool compounds to inhibit the glucose uptake.

The general aim of this project was envisioned to be met by first; to identify a chemical core structure with glucose uptake-inhibiting properties. Second, to establish a suitable synthetic route for the compound class. Third, to synthesise a library of analogues of this class that can provide a structure-activity-relationship analysis. Once met, these objectives will allow for a biological characterization of a selected glucose uptake inhibitor.

This chemical biology project isa cooperative effort with the dissertation project of Melanie Schwalfenberg, in which the biological part is addressed.

4. Results and Discussion:

4.1. Screening Assay and Compound Class Identification

Based on the lack of compounds targeting the glucose facilitative transporters (GLUTs), there is a strong need for identification of compounds with novel scaffolds that can efficiently inhibit glucose uptake. There are several reported assays to study glucose uptake; so far, the use of radio-labelled [^{3}H]-glucose has been the gold standard. However, due to the use of a radioactive compound, this method is not suitable for a medium/high-throughput assay. Our group has developed an assay monitor glucose uptake in cells, by adaptating the reported procedure by Yamamoto *et al.*[75-76] This method uses a non-hydrolysable analogue of glucose, 2-deoxy-D-glucose (2DG), which is also taken up by glucose transporters (Figure 9). 2DG is taken up by the GLUT transporters into the cell where it is directly phosphorylated by hexokinases to yield 2-deoxy-D-glucose-6-phosphate (2DG6P). Unlike its glucose analogue, 2DG6P cannot be further metabolised because it lacks the 2-hydroxyl group and consequently accumulates in cells. At this point the cells are lysed and the lysate is depleted from NADH. Subsequent NAD$^+$ and glucose-6-dehydrogenase addition prompts the oxidation of 2DG6P to 6-phospho-2-deoxyglucoronic acid (2DGA6P). During this reaction, the nicotinamide cofactor NAD$^+$is reduced to NADH which can be used to reduce the non-fluorescent resazurin to the fluorescent resorufin, a process catalysed by the enzyme diaphorase. By measuring resorufin fluorescence, the amount of glucose taken up can be quantified. The reported assay by Yamamoto *et al.* was adapted to the COMAS screening facilities. The cell line of choice, HCT116, had given the best signal to noise ratios. The glucose uptake assay was then run on a library of over 150,000 compounds with an initial hit rate of 0.44%.
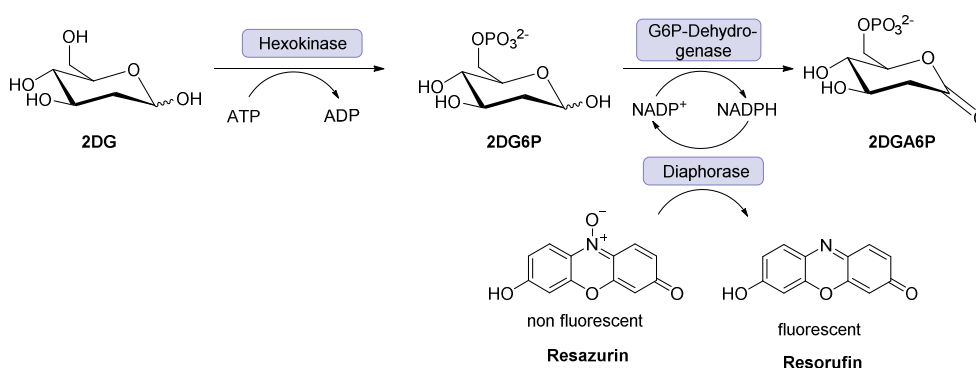

Figure 9. Assay scheme for the detection of glucose uptake. Assay established by Melanie Schwalfenberg and the COMAS screening facility in Dortmund.

All compounds that induced at least a 70% inhibition of glucose uptake, were further tested by different orthogonal assays: against diaphorase inhibition or interaction with the fluorescent readout. Furthermore, their ability to inhibit hexokinase and their cytotoxicity were assayed. After the validation assays, the active compounds were subjected to IC_{50} determination. A total of 121 compounds were found to inhibit glucose uptake in a dose-dependent manner with IC_{50} values ≤ 10 μM.

The active hits were clustered into different families according to their core scaffolds. Based on the relatively manageable number of hits, the clustering was performed by simple observation. For this purpose, the substituents of the different heterocycles were removed to obtain the core scaffolds but the presence of different heteroatoms in the core structure was allowed to vary within members of the same class when the similarities were readily observed. In this fashion, most of the active hits could be grouped into 9 families (Figure 10). Recently, members of the compound classes represented by analogues **2**, **3** and **4** were reported in the literature as glucose uptake inhibitors by Bayer Pharma and collaborators.[15, 65, 71] These reports further validate our assay and the identified hits as starting points for the synthesis of libraries around them.
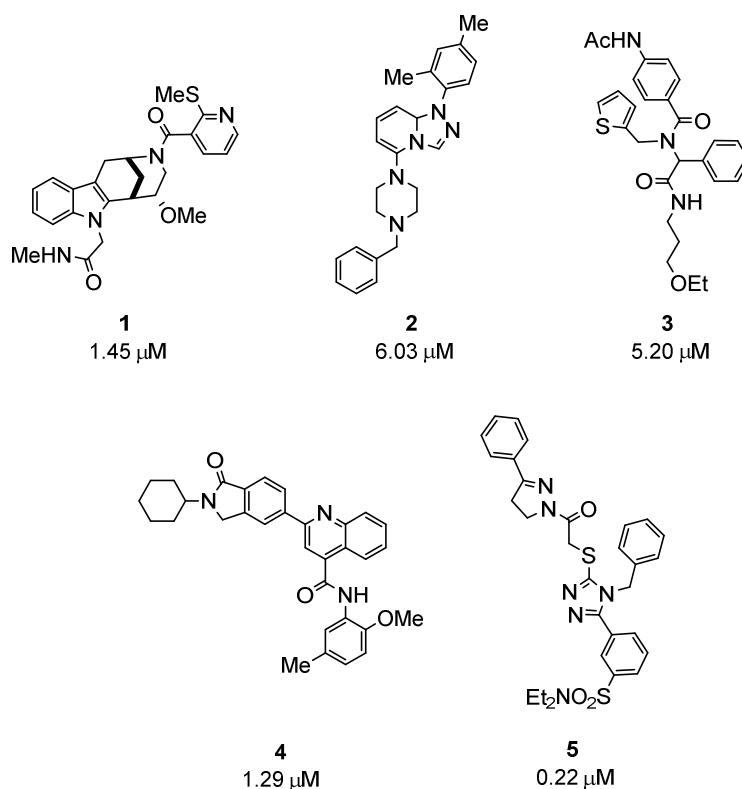

Figure 10. Representative analogues of some of the identified classes.

Compound **5** (Figure 10) had no common core scaffold with any other active hit from our assay. Other singletons (ungrouped active hits) were found in the assay but a clear common core scaffold with compound **5** could not be identified (Figure 11a). A similarity search in our complete library showed several compounds, such as **10** and **11** (Figure 11b), with the same core scaffold as compound **5** albeit with no activity as glucose uptake inhibitors. Nevertheless, compound **5** presented a very high potency with an IC_{50} around 200 nM. At the time, this compound represented, to the best of our knowledge, the most potent glucose-uptake-inhibiting synthetic compound. Consequently, despite not having identified any other active member of this class, I decided to further study the structure of triazole **5** as a potential glucose-uptake-inhibiting class of compounds.
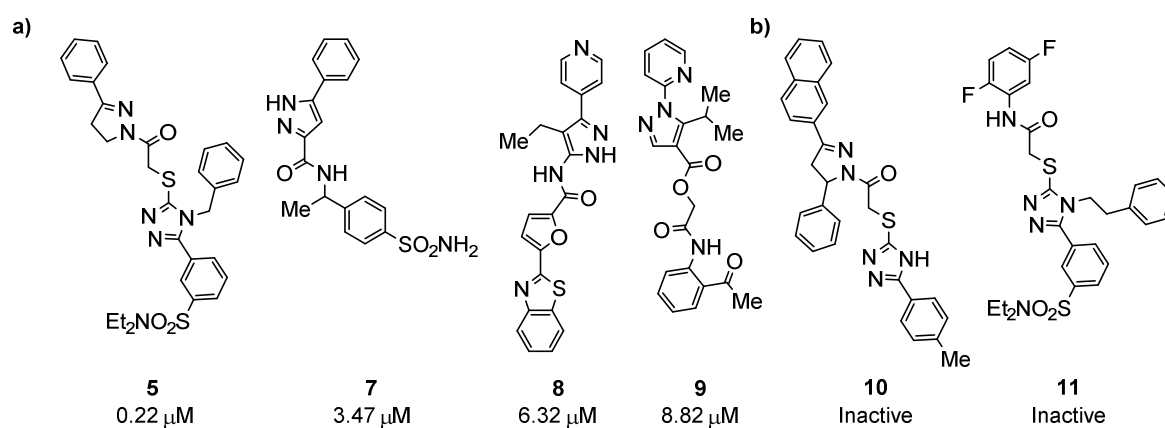

Figure 11.a) Other active singletons. **b)** Inactive analogues from the same compound class represented by compound 5.

The core-scaffold of the family represented by compound **1** (Figure 10), from here on referred to as the Glupin family, was identified in two other active compounds (Figure 12a). This common scaffold consists of a fused tryptamine-morphan hybrid moiety (Figure 12b). Besides the compounds **1**, **12** and **13**, I could identify additional analogues in the library that shared the same scaffold and presented a wide range of potencies (IC_{50}s > 10 μM) (see Experimental Part).

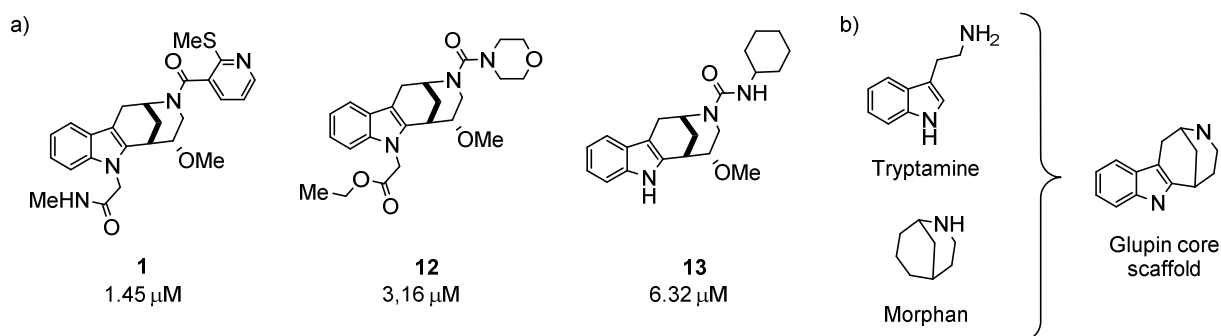**Figure 12. a)** Active hits of the Glupin family identified in the assay and their IC$_{50}$ values as glucose uptake inhibitors. **b)** Tryptamine-morphan Glupin core scaffold.

Both the tryptamine and the morphan scaffolds can be found across natural products, especially in alkaloids derived from tryptophan or the opioid morphine from which morphan takes its name. Although a similar core scaffold can be found in the Strychnos family of alkaloids, *e.g.* Strychnine and Brucine (Figure 13a), the Glupin core is not present in nature. Furthermore, since its first appearance in the literature as a potential opioid, this novel scaffold has remained virtually chemically unexplored (Figure 13b).[77-80] Its strong potency, natural product-like structure and the synthetic challenge of exploring this scaffold, led me to select the Glupin compound class for further study.
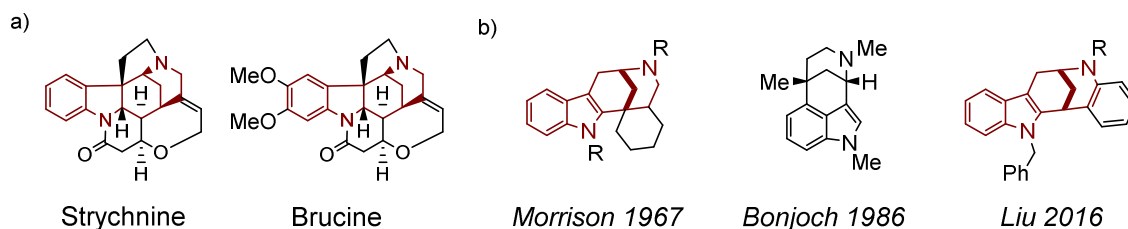

Figure 13. a) Tryptamine-morphan examples in nature. **b)** Examples of synthetic compounds with a tryptamine-morphan scaffold.[77, 81-82]
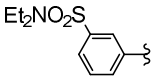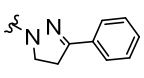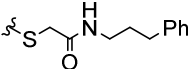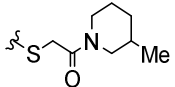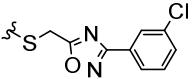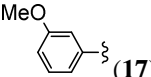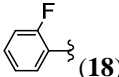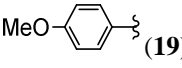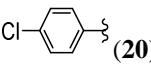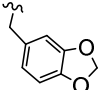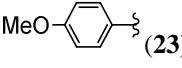
4.2. Validation of the Selected Compound Classes

4.2.1. Compound class of triazole 5

In order to validate the class represented by triazole **5** (Figure 10) as a glucose uptake inhibiting scaffold, a selection of 21 close analogues was purchased from Enamine (Table 2). All the purchased analogues showed significantly lower activities in single point measurements than compound **5**. The potencies were within the 60 to 70% range of residual glucose uptake compared to the parent compound (set as 0%). Furthermore, when the dose-response effect was

measured, all compounds except for the parent compound showed an $IC_{50} > 30$ µM. These results were not very promising, since regardless of the substitutions around the core, the analogues displayed a constant inactivity and only triazole **5** showed a big potency leap. Given that no active analogues were obtained to delineate an initial SAR, this class of compounds was not further explored as glucose uptake inhibitors.

Table 2. Selected examples of the commercial library of analogues of compound 5.

Entry	R¹(cpd)	R²	R³	Activity (%)[a]	IC_{50}(µM)[b]
1[c]	Et₂NO₂S	benzyl	pyrazoline-Ph	0	0.22 ± 0.06
2	cpd. **5**[d] (**14**)	cpd.**5**	S-CH₂-C(O)-NH-CH₂CH₂-Ph	16 ± 3	> 30 µM
3	cpd.**5**(**15**)	cpd.**5**	S-CH₂-C(O)-N-piperidine-Me	28 ± 7	> 30 µM
4	cpd.**5**(**16**)	cpd.**5**	S-CH₂-oxadiazole-(3-Cl-Ph)	29 ± 8	> 30 µM
45	MeO (**17**)	furan	cpd.**5**	35 ± 7	> 30 µM
6	F (**18**)	cpd.**5**	cpd.**5**	35 ± 6	> 30 µM
7	MeO (**19**)	CH₂-Ph	cpd.**5**	36 ± 20	> 30 µM
8	Cl (**20**)	furan	cpd.**5**	38 ± 8	> 30 µM
9	Ph-(**21**)	furan	cpd.**5**	45 ± 19	> 30 µM
10	Ph-(**22**)	benzodioxole	cpd.**5**	47 ± 5	> 30 µM
11	MeO (**23**)	-Cy	cpd.**5**	50 ± 11	> 30 µM

| 12 | (24) | cpd.**5** | cpd.**5** | 53 ± 10 | > 30 µM |
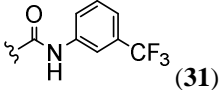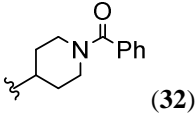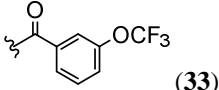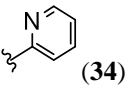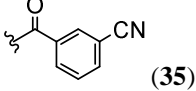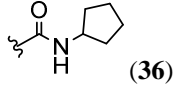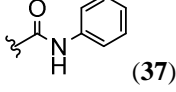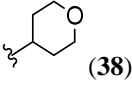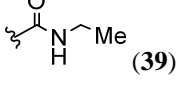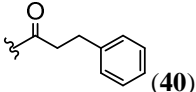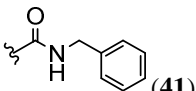
Assay performed in HCT cells, n=3; **[a]** Glucose uptake % residual activities compared to compound **5** assigned arbitrarily as 0% of glucose uptake with a compound concentration of 30 µM;**[b]** Activities given as IC_{50}(µM) ± SD (n ≥ 3). Compounds with IC_{50}> 30 µM were considered inactive; **[c]** Entry 1 corresponds to compound **5**; **[d]** cpd.**5** = same structure as compound **5**.

4.2.2. Glupins

In order to validate the Glupin class, a set of 19 close analogues was purchased from Edelris (Table 3). These analogues were selected based on variations of compounds **1**, **12**, and **13**, while maintaining the tryptamine-morphan core scaffold. It should be noted that all of the commercial compounds (including the ones in our in-house library) were racemic mixtures. The introduction of an ethyl ester at the indole (R^3, Table 3) led to a 25-fold potency increase (entry 2, (**+/-**)-**Glupin-1**). The same potency leap, arising from the introduction of the ester moiety on position R^3, was observed when either a 2-pyrazine or a morpholinecarboxy group was present on the morphan nitrogen (R^1) (entries 6,7 and 3, 9 resp.). In combination with the pyrazine group, the free amide at the R^3 position did not yield any activity, suggesting that the free amide was detrimental for activity (entry 8). On the other hand, on position R^1, heteroaromatics such as furan or thiophene led to active compounds, but both showed only low micromolar potencies (entries 4 and 5). Some ureas on R^1 delivered inactive compounds (entries 9, 10 and 18). In contrast to compound **13** (Figure 4a), the rest of the compounds with no *N*-substitution at the indole (R^3=H) were inactive (entries 11 to 16, 19 and 20). Comparing **13** (Figure 12) with **36** (entry 15), revealed that introduction of a bigger group on R^2, such as 2-pyridine, was deleterious to the activity. In the rest of the compounds where the indole was not *N*-substituted, the lack of activity could then be attributed to an unsuitable R^1 substitution (entries 11 to 13), to an introduction of the bulkier 2-pyridine group on R^2 (entries 14 to 16, 19 and 20) or by a combination of both.

Table 3. Commercial library of analogues of the Glupin compound class.

Entry	R^1(cpd)	R^2	R^3	IC$_{50}$ (μM)[a]
1	(1)	-Me	-CH$_2$CONHMe	1.45 ± 0.6
2	((+/-)-Glupin-1)	-Me	-CH$_2$CO$_2$Et	0.051 ± 0.025
3	(12)	-Me	-CH$_2$CO$_2$Et	3.16 ± 0.6
4	(25)	-Me	-CH$_2$CO$_2$Et	3.4 ± 0.3
5	(26)	-Me	-CH$_2$CONHMe	16 ± 1
6	(27)	-Me	-CH$_2$CONHMe	Inactive
7	(28)	-Me	-CH$_2$CO$_2$Et	2.0 ± 0.4
8	(29)	-Me	-CH$_2$CONH$_2$	Inactive
9	(30)	-Me	-CH$_2$CONHMe	Inactive

10	(31)	-Me	-CH$_2$CONHMe	Inactive
11	(32)	-Me	-H	Inactive
12	(33)	-Me	-H	Inactive
13	(34)	-Me	-H	Inactive
14	(35)		-H	Inactive
15	(36)		-H	Inactive
16	(37)		-H	Inactive
17	(38)	-Me	-CH$_2$CONHMe	Inactive
18	(39)	-Me	-CH$_2$CONHMe	Inactive
19	(40)		-H	Inactive
20	(41)		-H	Inactive

[a]Activities given as IC$_{50}$(μM) $\pm$ SD (n $\geq$ 3). HCT 116 cell line. Compounds with IC$_{50}$> 30μM were considered inactive.

The variety of activities found in this set of analogues and especially the discovery of (+/-)-**Glupin-1** (entry 2) as a highly potent novel glucose uptake inhibitor, encouraged me to further pursue the Glupin class.

4.3. Synthesis of Glupins

To access the Glupin scaffold, I aimed to establish a synthesis towards **(+/-)-Glupin-1** and analogues. I envisioned a synthetic route with ketomorphan **B** as key intermediate compound (Figure 14a), which upon Fischer indole synthesis[83] and subsequent indole alkylation would afford the target compound. The synthesis of such ketomorphans was already describedby the Bonjoch group (Figure 14b)[84] and is based on an acid-catalysed diastereoselective intramolecular aldol reaction. In this step, both the aldehyde and the ketone are protected as acetals and are *in situ* deprotected with the same acidic conditions that promote the aldol reaction. Following the reported conditions, the analogue of **C**, pyridine **42**, was prepared. Unfortunately, **42** proved unstable to the acidic conditions necessary for the next step.
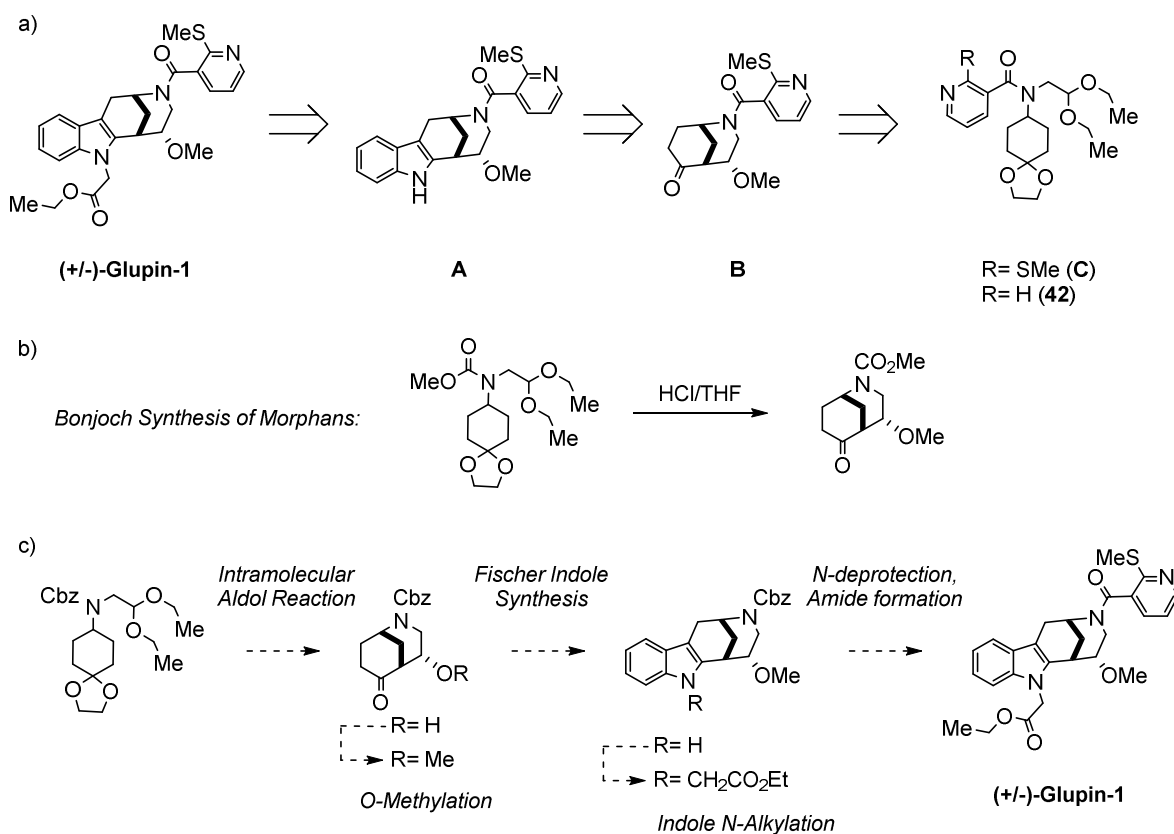
Figure 14. a) Retrosynthetic proposal for the Glupin class. **b)**Bonjoch synthesis of morphans. **c)** Synthetic route for **(+/-)-Glupin-1**.

At this point, it was resolved to introduce a Cbz protecting group on the morphan nitrogen, which would not only solve the stability problems but would also allow for a more efficient study of the R^1 position. The synthetic route was hence established with the use of a protecting group (Figure 14c). The main challenges met for establishing this synthetic route are described in the next sections.

4.3.1. One-pot synthesis of the tryptamine-morphan core scaffold

Following the reported procedures for the synthesis of morphans, ketomorphan **44** was synthesised (Figure15). **44** was then refluxed in acetic acid with phenl hydrazine to yield indole **45** in a Fischer indole synthesis. The Fischer indole synthesis consists on a hydrazone formation between a ketone and a phenyl hydrazine, a subsequent rearrangement and amine attack to an imine to form a pyrrolidine ring. A final step of ammonia elimination affords the indole ring fused to the ketone framework (Scheme 1).
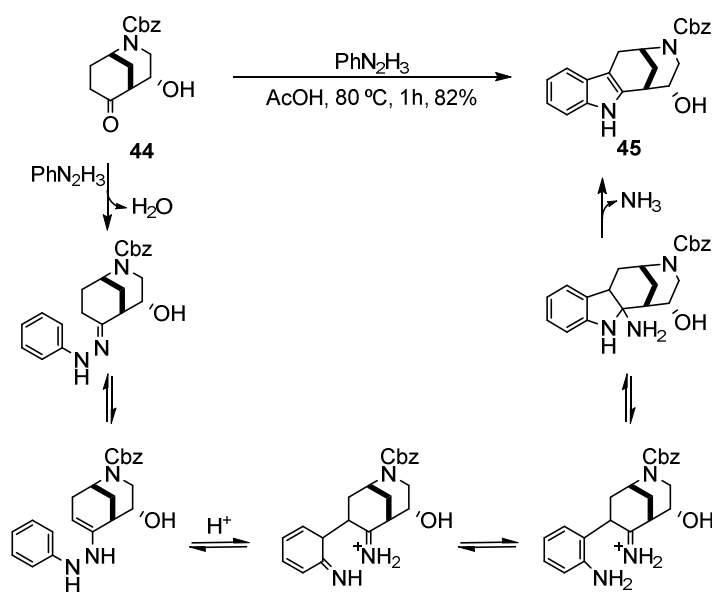
Scheme 1. Mechanism of the Fischer indole synthesis.

This robust reaction has been reported with a wide variety of acidic conditions; substoichiometric and stoichiometric, based on Lewis and Brønsted acids and in a wide variety of solvents. It was therefore envisioned that the acidic conditions, promoting the intramolecular aldol reaction to yield **44**, could also promote the formation of the indole ring if the hydrazine was added to the reaction. Accordingly, phenyl hydrazine was added to the reaction when the starting material was no longer detected (ca. 3 hours). After 30 minutes, full conversion was reached and indole **45** could be isolated in a high yield (Scheme 2).
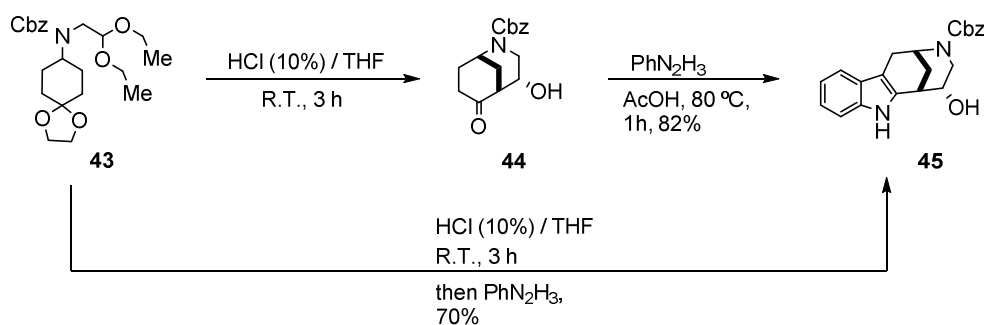
Scheme 2. One-pot synthesis of the Glupin core scaffold.

With compound **45** in hand, I attempted to methylate the alcohol group selectively over the indole. For this purpose, an inorganic base was used in combination with methyl iodide. The reaction needed heating to proceed and even then good conversions were not achieved (Table 4, entries 1 to 3). Increasing the number of equivalents of methyl iodide had little effect on the yield (entry 3). Notably, when the proton spectra of the starting material (**43**) and the product (**45**) (in DMSO-d^6) were compared, a disappearance of a signal at 10.63 ppm was found, which suggested that the indole rather than the alcohol had been methylated. Based on this result, the same conditions were applied but with ethyl 2-bromoacetate as the electrophile. Despite the poor conversion, the desired indole-alkylated product (**47**) was obtained using these conditions. Nevertheless, product and starting material co-eluted and could only be isolated as a mixture (entry 4). When switching to a stronger base (NaH), full conversions were achieved, however, a mixture of mono-alkylated and di-alkylated products was isolated (entry 5). These two compounds showed very similar R_f and could not be purified without the use of preparative HPLC. The temperature was then lowered to 0 ℃, so as to promote selectivity towards mono-alkylation, however the yield dropped to 34% and the product was again isolated as a mixture (entry 6). Even when only half of the electrophile equivalents was used and the reaction was conducted at 0 ℃, di-alkylation was observed (entry 7). Very short reaction times were achieved by heating to 90 ℃, but again no selectivity towards the mono-alkylated product was found (entry 8).

Table 4. *N*-, *O*-Alkylation attempts on compound **45**.
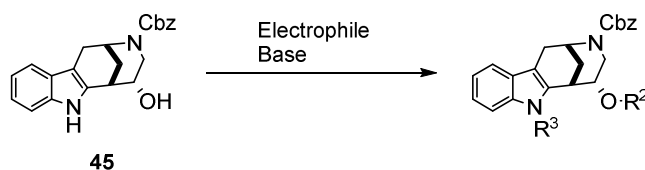
Entry	Electrophile (eq)	Base (eq)	Solvent	T (ºC)	Product	Yield(%)
1	MeI (1.2)	K$_2$CO$_3$(3)	DMF	r.t.	-	-
2	MeI (1.2)	K$_2$CO$_3$(3)	DMF	r.t. to 90	R^3=Me, R^2=H, (**46**)	29
3	MeI (3)	K$_2$CO$_3$(3)	DMF	r.t. to 90	R^3=Me, R^2=H, (**46**)	35
4	BrCH$_2$CO$_2$Et (3)	K$_2$CO$_3$(3)	DMF	90	R^3=CH$_2$CO$_2$Et, R^2=H, (**47**)	34[a]
5	BrCH$_2$CO$_2$Et (1)	NaH(2.5)	DMF	R.T	R^3=CH$_2$CO$_2$Et, R^2=H, (**47**)	53[b]
6	BrCH$_2$CO$_2$Et (1)	NaH(2.5)	DMF	0	R^3=CH$_2$CO$_2$Et, R^2=H, (**47**)	34[b]
7	BrCH$_2$CO$_2$Et (0.5)	NaH(2.5)	DMF	0	-	-[c]
8	BrCH$_2$CO$_2$Et (1)	NaH(5)	DMF	90	-	-[d]

[a] Isolated as a mixture with **45**; **[b]** Isolated as a mixture with the di-alkylated product R^3=CH$_2$CO$_2$Et, R^2= CH$_2$CO$_2$Et; **[c]** Mixture of mono-, di-alkylated product and **45**; **[d]** Reaction time: 10 min.

Since achieving selectivity between the NH and OH nucleophiles of indolomorphan **45** proved too inefficient for the synthesis of (+/-)-Glupin-1, I shifted my focus to a stepwise process in which the hydroxyl group would be methylated before constructing the indole ring.

4.3.2. *O*-Methylation of alcohol 44

In a stepwise fashion, alcohol **44** was to be methylated before proceeding with the indole synthesis. The possibility of selectively alkylating the hydroxy group of compound **44,** despite the presence of an enolisable ketone, was envisioned. The use of a relatively weak inorganic base should promote the *O*-alkylation rather than the *C*-alkylation. Accordingly, typical conditions for ether synthesis such as potassium carbonate and methyl iodide were used. To my surprise, the use of one equivalent of methyl iodide in the presence of potassium carbonate in excess did, however, not yield any conversion (Table 5, entry 1). Addition of the phase transfer catalyst tetrabutylammonium iodide (TBAI) did not enhance the reaction (entry 2). Use of a stronger base as caesium carbonate also failed to achieve any conversion (entry 3). When the temperature was raised to 56 ºC, addition of MeI did not promote any reactivity (entries 4 and 5). Increasing the temperature to 80 °C in MeCN failed as well to convert any starting material after 2 days (entry 6). High temperatures in DMF in the presence of caesium carbonate did promote reactivity, but the conversion was very low after 2 days and mixtures of mono- and di-alkylated products were detected by HPLC-MS (entry 7). When using diisopropylamine (DIPEA) or pyridine as bases, similar results were obtained (entries 9 and 10).

Table 5. *O*-Methylation attempts (I).
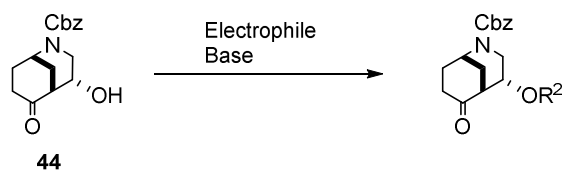
Entry	Electrophile (eq)	Base (eq)	Solvent	T (ºC)	Conversion (%)[a]
1	MeI (1)	K_2CO_3(3)	acetone	r.t.	0
2	MeI (1)	K_2CO_3(3)	acetone	r.t.	0[b]
3	MeI (1)	Cs_2CO_3(3)	acetone	r.t.	0[b]
4	MeI (1)	K_2CO_3(3)	acetone	56	0[b]
5	MeI (3)	K_2CO_3(3)	acetone	56	0[b]
6	MeI (1)	K_2CO_3(3)	MeCN	82	0[b] [c]
7	MeI (1)	Cs_2CO_3(3)	DMF	r.t. to 80	< 20[b,c]
8	MeI (3)	K_2CO_3(3)	MeCN	82	<20[b,c]
9	MeI (3)	DIPEA(1.2)	MeCN	r.t. to 80	<20[c]
10	MeI (3)	-	pyridine	r.t. to 80	<20[c]

[a] After 2 days; [b] Addition of 0.1 eq of TBAI; [c] Mono- and di-alkylated products among others, and starting material.

At this point, I decided to force the generation of the alkoxide by the use of a stronger base, like NaH. The use of the hydride base with alcohol **44** in the presence of MeI in DMF yielded no conversion, regardless of the amount of electrophile used (Table 6, entries 1 and 2). On the other hand, when the electrophile was changed to a more reactive one, as allyl bromide, the reaction was promoted albeit with low conversions (entries 3 and 4). A similar reactivity was observed for chloromethoxymethane; in the presence of a phase transfer catalyst the reaction took place but less than 20% conversion was achieved. Since more reactive electrophiles were able to promote the reaction to a certain extent, the powerful methylating agent, dimethyl sulphate, was explored (entries 6 to 11). However, **44** was methylated only under harsh conditions. Either high excess of dimethyl sulphate (entry 8) or high temperatures (entry 9) were needed to achieve reasonable conversions. Nevertheless, a mixture a products was detected. Meerwein Salt (Me_3OBF_4), a more powerful methylating agent, was tested, but showed no success in converting any starting material (entry 12). Finally, I tried to install a silyl protecting group with literature-reported conditions but no conversion was observed either (entry 13).

Table 6. *O*-Methylation attempts (II).
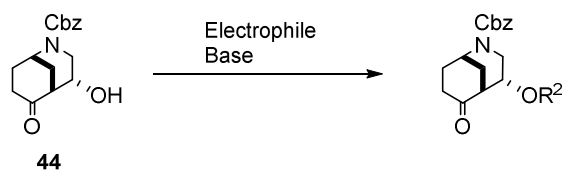
Entry	Electrophile (eq)	Base (eq)	Solvent	T (ºC)	Conversion (%)[a]
1	MeI (1)	NaH (1)	DMF	r.t.	0
2	MeI (3)	NaH (1)	DMF	r.t.	0
3	Allylbromide (1)	NaH (1)	DMF	r.t.	<10[b]
4	Allylbromide (3)	NaH (1)	DMF	r.t.	<20
5	MeOCH$_2$Cl (2)	DIPEA (4)	CH$_2$Cl$_2$	r.t. to 40	20
6	Me$_2$SO$_4$ (1)	K$_2$CO$_3$(3)	DMF	r.t.	0
7	Me$_2$SO$_4$ (3)	K$_2$CO$_3$(3)	DMF	r.t.	0
8	Me$_2$SO$_4$ (10)	K$_2$CO$_3$(3)	DMF	r.t.	<40[c]
9	Me$_2$SO$_4$ (1)	K$_2$CO$_3$(3)	DMF	100	<40[c]
10	Me$_2$SO$_4$ (1)	NaH (1.2)	DMF	r.t. to 90	<20
11	Me$_2$SO$_4$ (1)	-	Pyridine	r.t. to 90	<20
12	Me$_3$OBF$_4$ (1+2)	2,6-lutidine	CH$_2$Cl$_2$[d]	r.t.	0
13	TBDMSCl (1.5)	Imidazole (1.5)	DMF	r.t. to 90	0

All reactions were performed with 0.2 equivalents of TBAI; **[a]** After 2 days; **[b]** Product was detected by HPLC; **[c]** Complicated mixture; **[d]** Molecular sieves were used.

A literature search of similar transformations revealed that no examples of alkylations in similar compounds had been reported. I envisioned that, since this scaffold is the product of an intramolecular aldol reaction, an equilibrium between the aldol and retro-aldol reactions could be taking place in solution, and the presence of a base could be promoting the latter. I decided to install functional groups on **44** whose reaction was promoted by acidic conditions. Gratifyingly, *O*-benzylation of **44** was achieved in moderate yield with benzyl 2,2,2-trichloroacetimidate and catalysed by triflic acid (compound **48**, Table 7, entry 1). Furthermore, tetrahydropyran (THP) protection catalysed by acidic pyridinium *p*-toluenesulfonate (PPTS) afforded **49** in an excellent yield (Table 7, entry 2). Attempts to methylate with TMSCHN$_2$ in acidic conditions led, however, to very complicated mixtures (entry 3). Nonetheless, since acidic conditions were discovered to be more suitable to functionalise this position, I decided to test the Lewis acid silver oxide for methylation. The use of 1.5 equivalents of both the electrophile and Ag$_2$O resulted in 20% yield of isolated product in the case of methyl iodide (entry 4), but did not promote any conversion in the case of allyl bromide (entry 5). This observation was not surprising, since silver (I) activates the iodine atom towards a nucleophilic attack more

efficiently than bromine. The use of excess of methyl iodide alone did not have a strong effect on the yield (entry 6), but the addition of the catalyst in excess afforded **50** in a 64% yield. Addition of the silver oxide in portions over 12 h did not seem to have any effect on the reaction outcome.

Table 7. *O*-Methylation attempts (III).
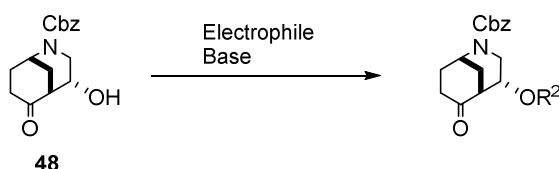
Entry	Electrophile (eq)	Catalyst (eq)	Solvent	T (ºC)	R^2(cpd)	Yield (%)
1	Benzyl 2,2,2-trichloroacetimidate (2)	F$_3$CSO$_3$H (0.07)	CH$_2$Cl$_2$/Hex.	0º to r.t.	-Bn (**48**)	58
2	DHP (1.5)	PPTS (0.1)	CH$_2$Cl$_2$	r.t.	2-THP (**49**)	96
3	TMSCHN$_2$(1)	BF$_3$OEt$_2$ (0.1)	CH$_2$Cl$_2$	0	-Me	_[a]
4	MeI (1.5)	Ag$_2$O (1.5)	CH$_2$Cl$_2$	r.t.	-Me(**50**)	20[b]
5	Allylbromide (1.5)	Ag$_2$O (1.5)	CH$_2$Cl$_2$	r.t.	-Me	0[b]
6	MeI (5)	Ag$_2$O (1.5)	CH$_2$Cl$_2$	r.t.	-Me	24[b]
7	MeI (5)	Ag$_2$O (5)	CH$_2$Cl$_2$	r.t.	-Me	64[b,c]
8	MeI (5) [d]	Ag$_2$O (5)	CH$_2$Cl$_2$	r.t.	-Me	65[d]

[a] Very complicated mixture; [b] Reaction time: 72h; [c] 25% of the starting material was recovered; [d] Addition in portions over 12 h.

In summary, alkylation of ketomorphan **44** proved inefficient under standard base-promoted conditions but was efficient in the presence of an excess of silver oxide and methyl iodide. This reaction was considered adequate to continue the synthesis **(+/-)-Glupin-1**.

4.3.3. Indole *N*-alkylation

Despite the difficulties in alkylating alcohol **44**, it was readily acetylated with acetyl chloride in CH$_2$Cl$_2$/pyridine to yield *O*-acetyl compound **51** (Scheme 3). While the methylation of **44** was still being investigated, compound **51** was used to further explore the Glupin synthesis.
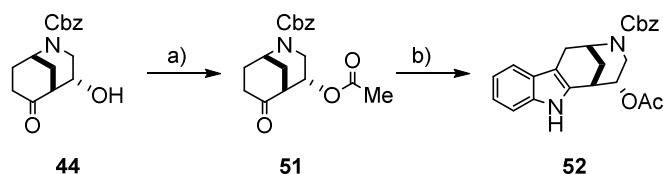
Scheme 3. Part of the synthesis of the *O*-acetyl analogue of **(+/-)-Glupin-1**. **a)** AcCl, CH$_2$Cl$_2$/Pyr., 3 h, -10º, 69%; **b)** PhN$_2$H$_3$, AcOH, reflux, 1.5 h, 76%.

Compound **51** was readily converted into **52** when subjected to Fischer indole synthesis conditions. The acid and solvent, chosen to promote this reaction was acetic acid. Even at 120 ºC, both the acetyl group and the Cbz protecting groups were stable and the reaction was completed in 1.5 h in a high yield (Scheme 3). Before achieving efficient conditions for the *N*-alkylation of the indole, a small screen was performed (Table 8).

Table 8. Indole *N*-alkylation of the *O*-acetyl intermediate **52**.
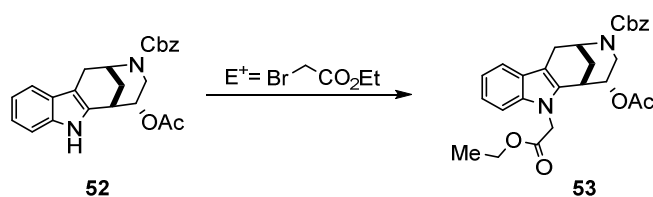
Entry	Base (eq)	Eq. of E$^+$	Solvent	T (ºC)	Conversion(%)
1	K$_2$CO$_3$(1.1)	1.05	DMF	r.t.	< 30
2	K$_2$CO$_3$(3.0)	1.05	DMF	r.t.	<50
3	K$_2$CO$_3$(3.0)	3	DMF	r.t.	< 70
4	K$_2$CO$_3$(3.0)	3.0	DMF	80	<80[a]
5	K$_2$CO$_3$(3.0)	10	DMF	r.t.	< 50[a]
6	K$_2$CO$_3$(3.0)	3	CH$_2$Cl$_2$	r.t.	< 50[b]
7	K$_2$CO$_3$(3.0)	3	CH$_2$Cl$_2$/H$_2$O	r.t.	_[b]
8	K$_2$CO$_3$(3.0)	3	CH$_2$Cl$_2$	r.t.	< 50[c]
9	Cs$_2$CO$_3$(3.0)	3	DMF	r.t.	100
10	Cs$_2$CO$_3$(1.2)	1.2	DMF	r.t.	< 70

[a] The product could only be isolated with starting material and an impurity; [b] Reaction performed with 0.3 equivalents of TBAI; [c] Reaction performed with 0.3 eq of NaI.

Based on the attempts of *N*-alkylation on compound **45** described above (see section 4.3.1.), it seemed that the use of potassium carbonate as a base was suitable for this position. A slight excess of both base and electrophile (ethyl 2-bromoacetate) yielded only a 30% conversion before the reaction stalled (entry 1, Table 8). Whereas increasing the equivalents of the base

improved the conversion to 50% (entry 2), an excess of base and electrophile improved the conversion up to 70% (entry 3). However, as described above, the indole-alkylated product did not differ much in polarity from the starting material and was thus not separable. Full conversion of this reaction was hence needed before proceeding with the synthesis of Glupin-1. When the reaction was heated or a large excess of the electrophile was used, a fast appearance of an impurity was observed (entries 4 and 5). The use of a phase transfer catalyst in dichloromethane yielded ca. 50% conversion (entry 6) and the addition of sodium iodide, that would promote the iodo/bromo exchange and hence further activate the electrophile, had no effect on the yield (entry 8). A H_2O/CH_2Cl_2 biphasic mixture with the PTC led to no conversion (entry 7). In order to promote full conversion a stronger base was tested, and to my delight, when excess of caesium carbonate was used the reaction led to full conversion in under 3 hours and the product could be isolated in very high yield (entry 9). In spite of the caesium carbonate´s higher basicity, an excess of it and of the electrophile had to be employed to achieve full conversion (compare entries 9 and 10). The optimised conditions (entry 9) were applied successfully in the synthesis of **(+/-)-Glupin-1**.

4.3.4. Synthesis (+/-)-Glupin-1

Once the *O*-methylated ketomorphan **50** was successfully synthesised (see section 4.3.2.), the indole ring was easily constructed by Fischer indole synthesis.[83] The conditions optimised for the indole *N*-alkylation of compound **45** were applied to indole **57** to yield compound **58** (Scheme 4). The Cbz protecting group was removed by hydrogenation (1 atm) catalysed by palladium over charcoal, to afford intermediate **59** in 86% yield.
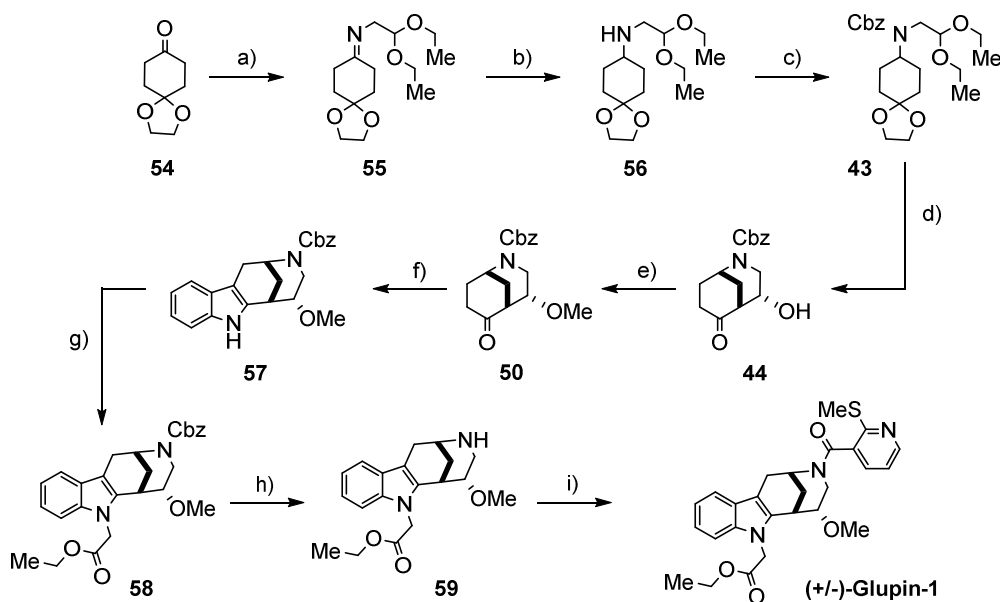
Scheme 4. Synthetic route for **(+/-)-Glupin-1**.**a)** $H_2NCH(CH_2OEt)_2$, CH_2Cl_2, M.S., 4 h, r.t., 99%; **b)** $NaBH_4$, MeOH, r.t., 12 h, 99%; **c)** CbzCl, K_2CO_3, MeCN, 12 h, r.t., 75%; **d)** HCl (10%)/THF, 3 h, r.t., 88%; **e)** MeI, Ag_2O, CH_2Cl_2, 72 h, r.t., 64%; **f)** PhN_2H_3, AcOH, reflux, 1.5 h, 74%; **g)** $BrCH_2CO_2Et$, Cs_2CO_3, DMF, 6 h, r.t., 88%; **h)** H_2, Pd/C, EtOH, 5 h, r.t., 86%; **i)** 2-(methylthio)nicotinic chloride, NEt_3, CH_2Cl_2, 12 h, r.t., 53%.

Removal of the Cbz group also eliminated the mixture of rotamers observed by NMR as an amide bond was no longer present. The *anti*-configuration of the morphan ring, which had been assumed so by literature precedents was then confirmed by a NOESY experiment (Figure 15). The NOE-interaction between the hydrogen atoms on the morphan bridge (H_A) with the hydrogen atom attached to the same carbon as the methoxy group (H_D) indicates that the bridge and the methoxy groups were in an *anti*-configuration. Furthermore, when the morphan ring was constructed by the intramolecular aldol reaction, an additional inseparable product (approximately 10%) was identified. This side-product of the same mass was the *syn* isomer of compound **44** (the methylene bridge and the hydroxy group point in the same direction), and could only be separated after the Fischer indole synthesis. As mentioned above, the major isomer was characterized as the *anti*-configuration (at the compound **57** stage) indicating that the diastereoselectivity of the acid-catalysed intramolecular aldol reaction was 9:1 *anti* to *syn*.
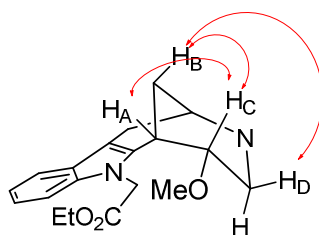
Figure 15. Confirmation of the anti configuration of the substituted morphan ring. Some of the NOE interactions are shown in red .

Finally, introduction of the thiomethylnicotinoyl group on position R^1 of **59** was readily achieved with the corresponding nicotinoyl chloride to yield **(+/-)-Glupin-1** in 53% yield.

The final synthesis established for **(+/-)-Glupin-1** started from the inexpensive 1,4-cyclohexanedione monoethyleneacetal (**54**) and was achieved in 9 steps with an overall yield of 12% and with the use of one protecting group (Scheme 4). The activity of the synthesised **(+/-)-Glupin-1** as a glucose uptake inhibitor matched the activity found for the commercial batch (Table 9), validating this route for further study of the Glupin class of glucose uptake inhibitors.

Table 9. Validation of the synthetic route to **(+/-)-Glupin-1**.

Batch	IC$_{50}$ (µM)
Commercial	0.051 ± 0.025
Synthesised	0.055 ± 0.017

HCT 116 cell. (n ≥ 3).

4.4. Determination of a Structure-Activity Relationship for the Glupin class

The ynthetic route established for **(+/-)-Glupin-1**, enabled the preparation of a small library of Glupin analogues. Testing the activities of such a library allowed me to gain insight into the SAR analysis of this class of compounds. Variations of the synthetic route were required to

study the different positions of the Glupin scaffold, but the main synthetic strategy remained constant. The objectives of creating a SAR analysis are well-known; to gain insight into the essential parts of the parent compound for activity; to find potential attachment points to couple the parent compound with other groups (solid phase, fluorescent dyes etc); and to discover new members of the class that may present higher activities than the parent compound. Furthermore, in a typical medicinal chemistry drug project the establishment of a library of analogues opens the door for comparison of other properties among the library compounds that can later on be considered important, such as permeability, solubility or plasma stability. In this project, a collaboration with the Lead Discovery Center (LDC, Dortmund) was established to investigate some of those properties. The aim of this collaboration was to establish if the Glupin class could be developed into an anticancer drug candidate. Nevertheless, my principal aim in this thesis was to explore the above mentioned objectives of a Glupin SAR analysis.

4.4.1. Validation of the tryptamine-morphan core scaffold of the glupin compound class

In order to validate the core scaffold identified for the Glupin family, two key compounds were synthesised. In the first one, the indole ring of the tryptamine moiety was eliminated (**60**, Figure 16). In the second, the morphan bicycle was replaced by a simple cyclohexyl core (**66**). Both analogues showed no activity against the glucose uptake, validating the fused core of the tryptamine and morphan fragments.
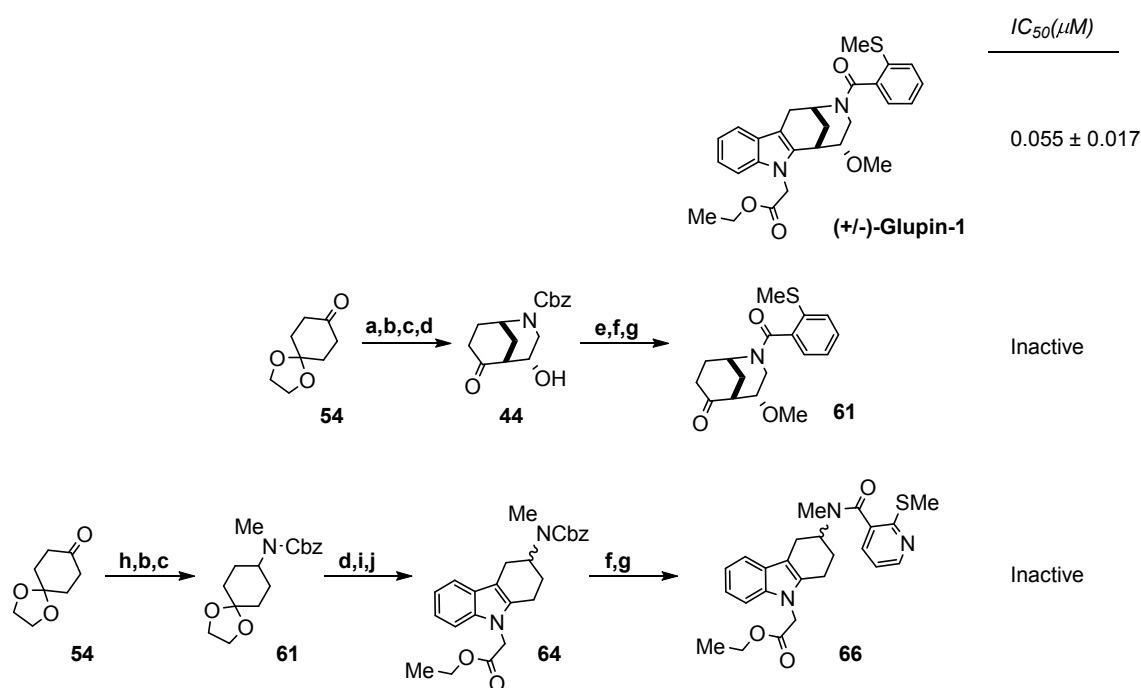

Figure 16. Synthetic scheme to validate the Glupin Scaffold. a) $H_2NCH(CH2OEt)_2$, CH_2Cl_2,

M.S., 4 h, R.T; b) NaBH$_4$, MeOH, r.t., 12 h; c) CbzCl, K$_2$CO$_3$, MeCN, 12 h, R.T; d) HCl (10%)/THF, 3 h, R.T; e) MeI, Ag$_2$O, CH$_2$Cl$_2$, 72 h, R.T; f) H$_2$, Pd/C, EtOH, 5 h, R.T; g) 2-(methylthio)nicotinic chloride, NEt$_3$, CH$_2$Cl$_2$, 12 h, R.T; h) MeNH$_2$, CH$_2$Cl$_2$, M.S., 3 h, R.T; i) PhN$_2$H$_3$, AcOH, reflux, 1.5 h; j) BrCH$_2$CO$_2$Et, Cs$_2$CO$_3$, DMF, 6 h, r.t.

With the Glupin core validated, I then moved to create a library of Glupin analogues. Four positions of the Glupin scaffold were selected for modification based on the chemical structure (Figure 17). Three of them had already been somewhat explored with the commercial library but required significant further analysis. As position R^1 is introduced in the last step of the synthesis, it was the most accessible for SAR analysis and was therefore explored first.
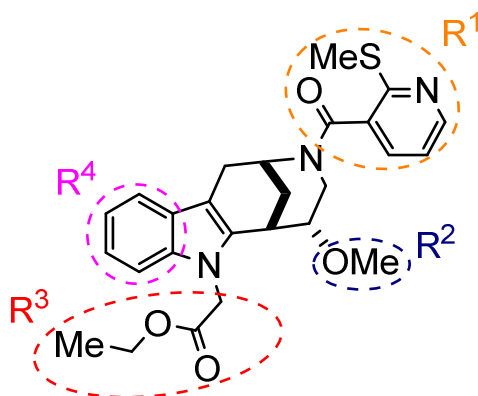
Figure 17. Glupin structure positions explored by SAR.

4.4.2. SAR analysis for position R^1

To explore different substitutions of position R^1 a series of aroyl chlorides was introduced to intermediate **59** in the last step of the synthetic route (Table 10). Except the 2-thiomethyl nicotinoyl chloride that was commercially available, the rest of the R^1 groups were purchased as carboxylic acids and subsequently transformed into the respective aroyl chlorides with thionyl chloride (SOCl$_2$). This approach was successful for most of the analogues (see the Experimental Part for each case) and in the cases were the chloride could not be synthesised, TBTU (*O*-(benzotriazol-1-yl)-N,N,N′,N′-tetramethyluroniumtetrafluoroborate) was employed to activate the carboxylic acid *in situ*. Based on the data from the commercial analogues (see Table 3), I decided to focus more on the 2-substituted nicotinic ring instead of exploring a wide range of heterocycles and other alkyl groups as R^1.

Table 10. SAR analysis of the Glupin position R[1].
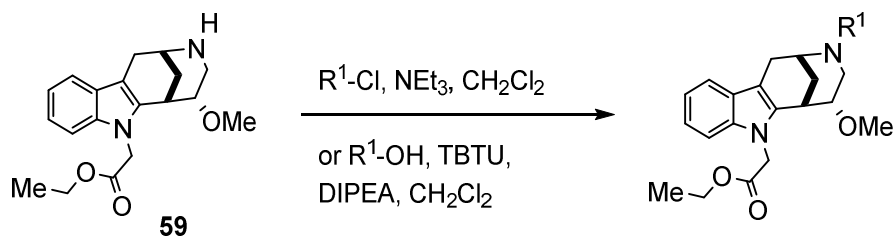
Entry	R[1]	Activity[a]	Entry	R[1]	Activity	Entry	R[1]	Activity
1[b]	(SM, O)	0.055± 0.017	8	(OEt) (73)	0.22 ± 0.07	15	(80)	13 ± 3
2	(Cl) (67)	0.093 ± 0.041	9	(F) (74)	0.54 ± 0.16	16	(81)	14 ± 5
3	(CF₃) (68)	0.12 ± 0.03	10	(75)	1.4 ± 0.2	17	(82)	3.0 ± 0.4
4	(SPh) (69)	0.14 ± 0.07	11	(SO₂Me) (76) (GK)	1.7 ± 0.7	18	(SMe, Me) (83)	0.20 ± 0.01
5	(SⁿF) (70)	0.19 ± 0.12	12	(77)	>30	19	(SMe, Br) (84)	9.35 ± 0.03
6	(Br) (71)	0.18 ± 0.06	13	(78)	24 ± 3	20	(SMe, F₃C) (85)	6.7 ± 1.6
7	(OM) (72)	0.23 ± 0.05	14	(79)	2.3 ± 0.8	21	(SMe, CF₃) (86)	14 ± 4

GK: Synthesised by Dr. Karageorgis.**[a]** Activities given as $IC_{50}(\mu M) \pm SD$ ($n \geq 3$). HCT 116 cell line; **[b]** Entry 1 corresponds to **(+/-)-Glupin-1**.

First the position 2 of the parent R[1] thiomethyl nicotinic group was explored. All of the groups introduced were commercially available as the corresponding nicotinic acids. Most of the 2-substituted nicotinoyl residues maintained high potencies albeit with loss of activity compared

to (+/-)-Glupin-1 (entries 1 to 11). Morpholino and methylsulfonyl residues (entries 10 and 11, respectively) showed strongly decreased activity around the low micromolar range but only the very bulky *tert*-butyl amide led to a complete loss (entry 12). Exchange of thiomethyl for a thiophenyl group on position 2 of the nicotinic ring led to a 3-fold decrease in activity (entry 4). Notably, an addition of two carbons on the sulfur, resulted in a 4-fold drop in activity (entry 5). Chloride and bromide analogues, showed high potencies although a 2- to 4-fold decrease in activity was observed (entries 2 and 6). However, fluorine, potentially as a result of its smaller size, had a bigger drop in activity at this position (entry 9). Exchange of the thiomethyl for the analogous methoxy and ethoxy groups led to a potency drop of at least 2-fold (entries 7 and 8). Based on the 2 position of the thiomethyl group at the pyridine ring and the carbonyl moiety in α, I envisioned that a nucleophilic substitution on the 2 position could be taking place *in vivo*. However, the decreased activity in the fluoro and methylsulfonyl analogues (entries 9 and 11) suggested that this was not the case. When I removed the substitution at the pyridine 2 position (entry 14) the activity resulted in a low single digit micromolar activity. Nevertheless, this compound could be compared with picolinic and isonicotinic analogues (entries 13 and 15, respectively) to hint at the most active pyridine disposition of R^1. The nicotinic pattern remained the most potent. Notably, the pyrimidine-5-carbonyl analogue (**81**), displayed a 7-fold loss of activity compared to the nicotinic analogue (entry 16).

The inconclusive activity pattern at this position in relation with the size may be due to the rotation around the carbonyl-aryl bond. When isolated, these compounds are an atropoisomeric mixture around the carbonyl-aryl bond. The two atropoisomers could not be separated by chromatography and were therefore measured as a mixture. The atropoisomers were easily detected in the ^{1}H and ^{13}C NMR spectra. Besides the expected signal splitting from the rotameric mixture around the amide bond, further splitting was observed in the analogues where the 2-position of the nicotinic acid was occupied. Nevertheless, this mixture was inseparable and the activity of all analogues was measured as a mixture.
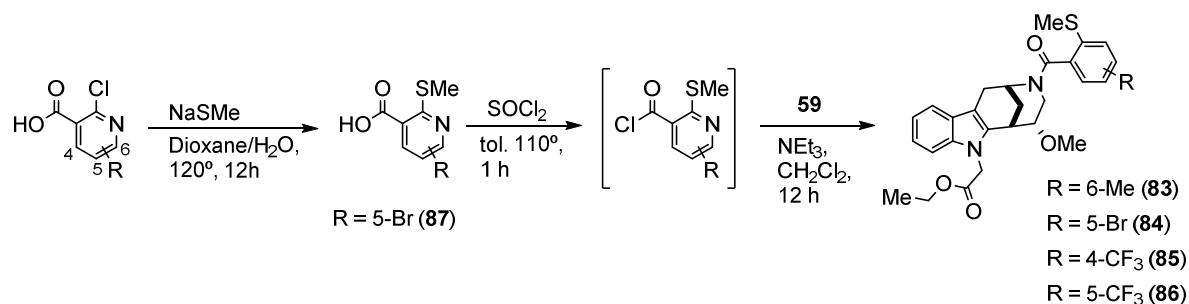
Scheme 5. Synthetic scheme for positions 4,5 and 6 of the nicotinic acid on R^1.

To finalize the SAR study for R^1, positions 4, 5 and 6 of the nicotinic acid group were explored. The commercially available 2-chloronicotinic acids were reacted with sodium methanethiolate at 120 °C in a mixture of dioxane and water (Scheme 5).[85] The reaction was carried out in sealed tubes. The resulting 2-methylthionicotinic acids were transformed into the nicotinoyl chlorides *in situ* and reacted with intermediate **59** to afford the analogues with substitutions on position 4, 5 and 6.The 5-bromo nicotinic intermediate was isolated for characterization, but the compounds can be reacted *in situ* as crudes.Due to the lack of available 2-chloro nicotinic acids only 4 analogues (methyl, trifluoromethyl and bromo substituted) were synthesised. Position 6 tolerated the methyl substitution with only a small decrease in activity (Table 10, entry 18), but trifluoromethyl substitution on positions 4 and 5 strongly reduced the potency (entries 19 to 20) and the same was observed for the bromo analogue on position 5.

In summary, all analogues explored for this position showed less potency than the parent compound, **(+/-)-Glupin-1**. The thiomethyl group was found essential for the high activity. Inactive compounds were found only when very bulky groups were introduced in position 2 of the nicotinic acid ring, or with small groups on positions 4 and 5.

4.4.3.SAR analysis for position R^2

With position R^1 studied, I turned my focus towards the methoxy group at the morphan ring (R^2 position). To study this position the variations had to be made at the ketomorphan stage of the general synthesis (compound **44**, Scheme 4). As described before (see 3.3.3.) this position was readily acetylated to give **51** (Scheme 3). This compound was carried through the Glupin synthesis to obtain the Glupin analogue **89** (Scheme 4). No modifications from the general Glupin synthesis procedures were needed. **89** was subjected to hydrolysis conditions (LiOH in H_2O/THF) to cleave both ester groups present. The crude product was re-esterified with sulphuric acid in ethanol to afford the free alcohol **90**.

Since **44** had shown low reactivity towards typical alkylation conditions, I envisioned that Tsuji-Trost chemistry may offer a reactive enough electrophile and no basic media would be needed. In this fashion, alcohol **44** was allylated following the reported conditions for allylation of α-hydroxy carbonyls compounds by Schmidt *et al.*(Scheme 6).[86] The allylated product **91** was also carried through the Glupin synthesis to obtain compound **93**. Hydrogenation conditions for removing the Cbz afforded the expected *O*-propyl product that was converted into the Glupin analogue **95**. When **93** was, however, treated with HBr in acetic acid, only the Cbz group was reduced and allylated Glupin analogue **97** could be obtained.
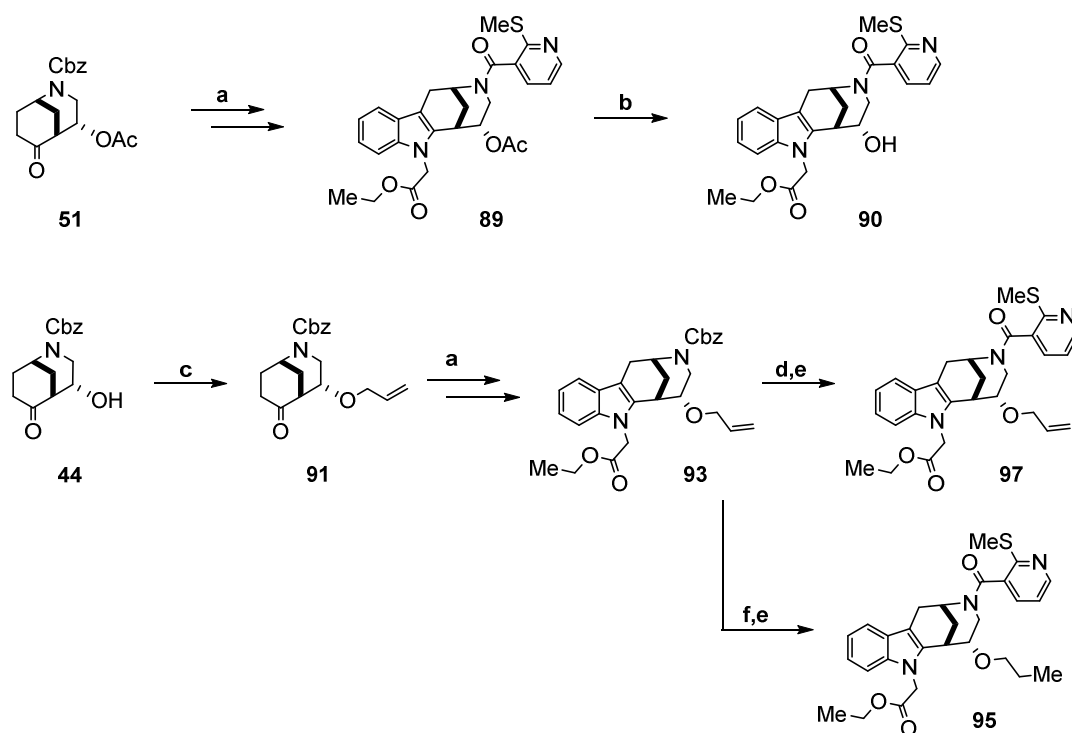
Scheme 6. Synthetic routes for exploring the Glupin R^2 position. **a)** The corresponding steps of the general synthesis of **(+/-)-Glupin-1** were applied (Scheme 4); **b)** LiOH, THF/H$_2$O, then H$_2$SO$_4$, EtOH **c)** Allyl ethyl carbonate, [Pd(PPh$_3$)$_4$], THF, 2.5 h, 80°, 43%; **d)** HBr in AcOH, 30 min, r.t., 79%; **e)** 2-(methylthio)nicotinic chloride, NEt$_3$, CH$_2$Cl$_2$, 12 h, R.T; **f)** H$_2$, Pd/C, EtOH, r.t., 93%.

Alcohol **89** showed a two-fold decrease in activity compared to **(+/-)-Glupin-1** (Table 11, entry 3). *O*-Propyl and *O*-allyl analogues displayed some loss of activity but remained highly potent (entries 4 and 5). The acetyl analogue (**89**) retained the same potency as **(+/-)-Glupin-1**.

Table 11. SAR Analysis of the R^2 position.
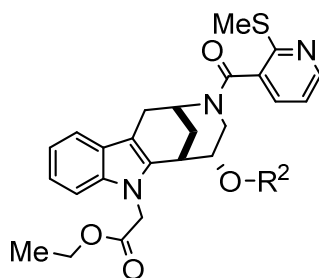
Entry	R^2(cpd)	Activity[a]	Entry	R^2(cpd)	Activity
1[b]	Me	0.055 ± 0.017	4	^{n}Pr (**95**)	0.087 ± 0.015
2	Ac (**89**)	0.053 ± 0.023	5	Allyl (**97**)	0.12 ± 0.02
3	H (**90**)	0.13 ± 0.05			

[a] Activities given as $IC_{50}(\mu M) \pm SD$ ($n \geq 3$). HCT 116 cell line; [b] Entry 1 corresponds to (+/-)-**Glupin-1**.

The high potencies of these analogues suggested that position R^2 might be tolerable to change and, therefore, would represent a suitable position for attaching the molecule to a solid phase or fluorophore via a linker.

4.4.4. SAR analysis for position R^3.

The initial 25-fold increase of activity observed by changing the methyl amide moiety of **1** (Table 3, entry 1) to the ethyl ester of (+/-)-**Glupin-1**, encouraged me to further explored this position. I envisioned that this increase could be explained if the carboxylic acid was the actual active compound. In that case, the hydrolysis of the ester would readily afford the active compound in the cell. Consequently, the free carboxylic acid analogue **98** was synthesised from (+/-)-**Glupin-1** by simple hydrolysis and its activity was measured. Free acid **98** showed very low activity compared to both **1** (Figure 17) and (+/-)-**Glupin-1** (Table 12, entry 2). Nevertheless, the activity drop could be explained by decreased permeability, a common issue with free carboxylic acids.[87] If the permeability was, however, not the issue, then the free acid would have a much lower affinity. If so, a potential hydrolysis of the ethyl ester of (+/-)-**Glupin-1** in cells would be deleterious to the activity. Hence, the non-hydrolyzable pivaloyl ester analogue (**99**) was synthesised. Glupin analogue **99**, however, displayed a significant loss of potency (entry 3). It was then decided to synthesise a series of different esters to study this position. The different groups in R^3 were introduced in the same fashion as for the Glupin synthesis, by alkylating the indole. Subsequent steps of Cbz deprotection and amide formation afforded the Glupin analogues (Scheme 7).
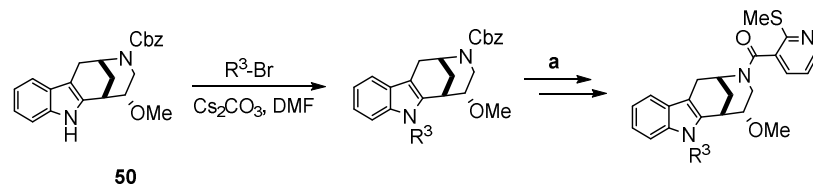
Scheme 7. Synthesis of the different R^3 Glupin analogues.**a)**The corresponding steps of the general synthesis of **(+/-)-Glupin-1** were applied (Scheme 4)

Introduction or removal of a carbon atom of the ester alkyl chain resulted in similar potencies to Glupin-1 (entries 4 and 5). The bigger phenyl group did, however, result in a 4-fold drop in activity (entry 6).The distance between the indole ring and the ester moiety was then explored. When this distance was altered from **(+/-)-Glupin-1**, the result was a strong decrease in potency. Loss of the methylene bridge gave almost no activity (entry 7) while adding methylene groups progressively decreased the activity from IC_{50}s of 8 to 22 µM (entries 8 and 9). The introduction of the heterocycle furan by Dr. Karageorgis also resulted in a great activity loss, which deterred me from exploring further heterocycles at this position (entry 10).

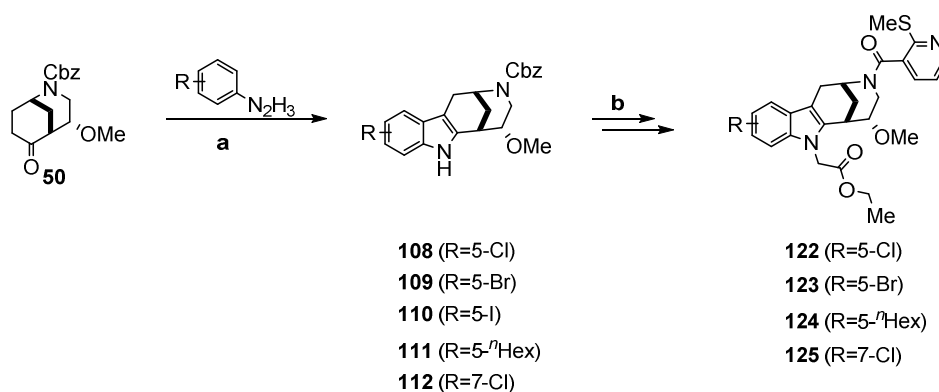**Table 12.** SAR Analysis of the R^3 position.

Entry	R^3 (cpd)	Activity[a]	Entry	R^3 (cpd)	Activity
1[b]	-CH$_2$CO$_2$Et	0.055 ± 0.017	7	-CO$_2$Et (**103**)(**GK**)	28 ± 2
2	-CH$_2$CO$_2$H (**98**)	10.0 ± 4.0	8	-(CH$_2$)$_2$CO$_2$Et (**104**)(**GK**)	8.4 ± 3.6
3	-CH$_2$CO$_2^t$Bu (**99**)(**GK**)	0.19 ± 0.06	9	-(CH$_2$)$_3$CO$_2$Et (**105**)(**GK**)	22 ± 5
4	-CH$_2$CO$_2$Me (**100**)(**GK**)	0.089 ± 0.032	10	(**106**)(**GK**)	6.7 ± 2.4
5	-CH$_2$CO$_2^n$Pr (**101**)(**GK**)	0.093 ± 0.035	11	-H (**107**)	>30
6	-CH$_2$CO$_2$Ph (**102**)(**GK**)	0.22 ± 0.08			

GK: Synthesised by Dr. Karageorgis; [a] Activities given as IC_{50}(µM) $\pm$ SD (n $\geq$ 3). HCT 116 cell line; [b] Entry 1 corresponds to **(+/-)-Glupin-1**.

The analysis of position R^3 did not reveal a significantly more potent compound. The presence of an ester seemed to be essential for high activities and only small changes were tolerated at this position.

4.4.5. SAR analysis of position R^4

To conclude the SAR analysis of the Glupin family the phenyl ring of the indole was explored. To introduce diversity in this part, a variety of phenyl hydrazines were included in the Glupin synthesis. The Fischer indole synthesis is a robust method for the construction of the indole ring and, unless the phenyl hydrazine bears strong electron withdrawing substituents, the reaction should take place. It should be noted that the use of meta substituted phenyl hydrazines would most often lead to a mixture of 4- and 6- substituted indoles with most likely similar polarities. Preparing analogues at this position proved to be a considerable task, since the diversity was introduced at an early step of the synthesis.

108 (R=5-Cl)
109 (R=5-Br)
110 (R=5-I)
111 (R=5-^{n}Hex)
112 (R=7-Cl)

122 (R=5-Cl)
123 (R=5-Br)
124 (R=5-^{n}Hex)
125 (R=7-Cl)

Scheme 8. Use of different phenyl hydrazines for the SAR analysis of the R^4 position. **a)** AcOH, 120º; **b)** The corresponding steps of the general synthesis of (+/-)-**Glupin-1** were applied (Scheme 4).

Several commercial phenyl hydrazines were reacted with ketone **44** to yield the indole products with high yields. Commercially available 4-Cl, Br, I, *n*-Hex and 2-Cl-hydrazines were used in this step (Scheme 8). The resulting indoles were taken through the Glupin synthesis, with no modifications in the general procedure, to arrive at the Glupin analogues. For the 5-iodo analogue, however, I encountered stability issues and the final Glupin class member could not be isolated. With these analogues, the presence of halogens and an alkyl chain on position 5 was

explored for the Glupins. To compare the indole substitutions of positions 5 and 7, one analogue with a 7-Cl substituent on the indole was also synthesised. To further explore the indole ring, the commercially available 5-carboxy phenyl hydrazine was used (Scheme 9). In this case the reaction afforded a variety of side-products and the crude product could only be purified to a certain extent by chromatography (compound **126**). Nevertheless, it was successfully used further in the synthesis of the Glupin analogues. Carboxylic acid **126** was reacted with ethanol to introduce the ester functionality and with morpholine in the presence of the carboxylic acid-activating reagent TBTU to introduce the bulkier heterocyclic amide on indole position 5. Both reactions proceeded with high yields to afford the ester **127** and the amide **128**, which were subjected to the remaining Glupin synthesis to obtain the corresponding Glupin analogues functionalised at the 5 indole position **130** and **131** (Scheme 9).
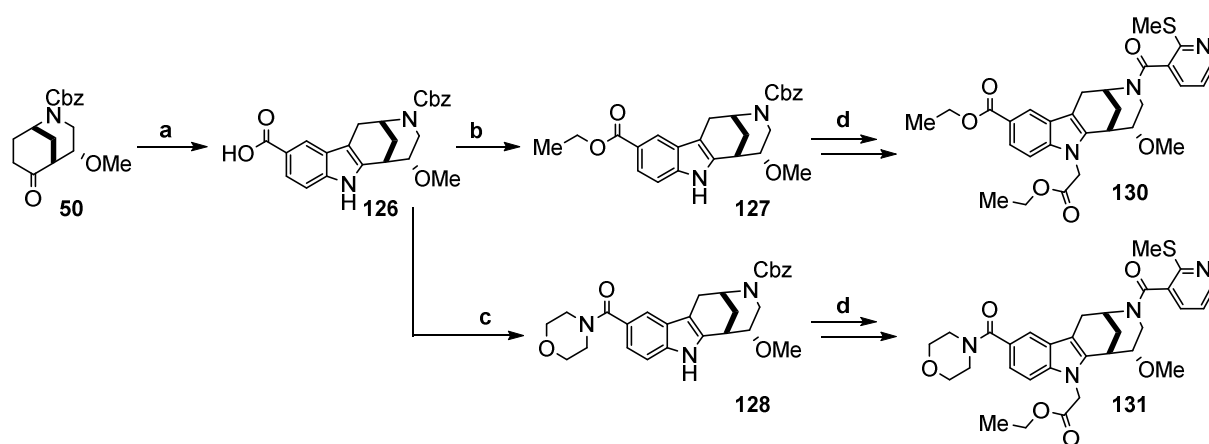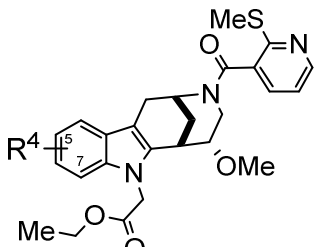

Scheme 9. Amide and ester functionalisation of indole position 5.**a)** 4-hydrazinebenzoic acid, AcOH, 120º; **b)** H_2SO_4, EtOH, r.t., 3 h, 65%; **c)** Morpholine, TBTU, DMF, r.t., 1h, 82%; **d)** The corresponding steps of the general synthesis of **(+/-)-Glupin-1** were applied (Scheme 4).
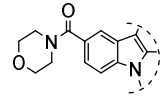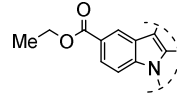
To rapidly introduce different functionalities on the indole ring, the introduction of a triflate that could undergo cross coupling reactions was planned. I envisioned a protected phenol that could be transformed into the triflate at the last step. For this purpose, following a reported procedure, a *N*-Boc protected phenol hydrazine was synthesised from the iodophenol by Dr. Karageorgis (Scheme 10).[88] The protected hydrazine was successfully employed for the synthesis of the indole ring. As expected, the acidic conditions of the reaction removed the Boc protecting group as well, to afford the phenol intermediate **133**. The phenol moiety of this intermediate was protected with a silyl group before the indole could be *N*-alkylated. The resulting *O*-silyl protected *N*-alkylated indole was carried through the Glupin synthesis and finally deprotected to afford phenol **136**, which was readily converted into the methylated analogue **137**.
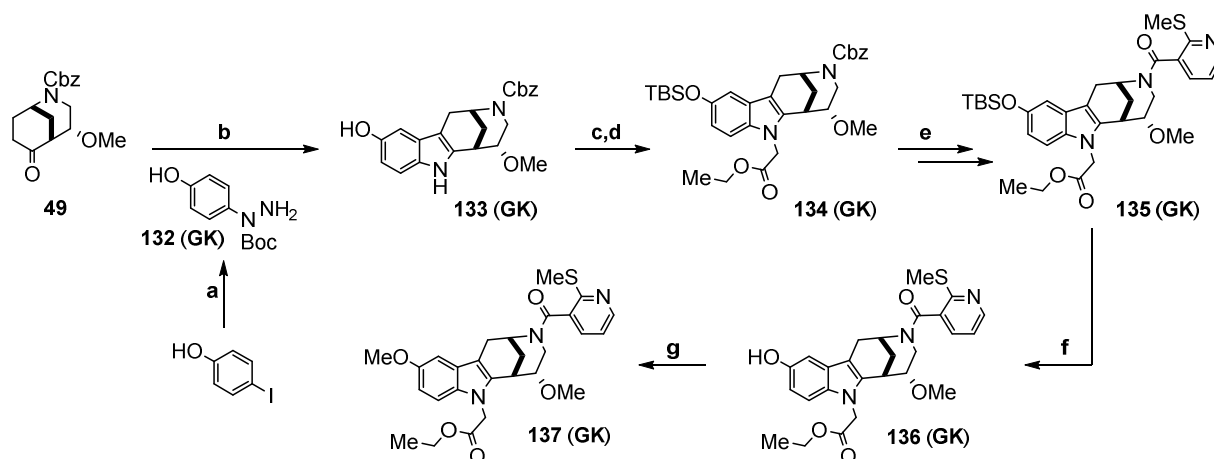
Scheme 10. Introduction of hydroxy and alkoxy groups on the 5-indole position. **GK**: Synthesised by Dr. Karageorgis. **a)**NHBocNH$_2$, CuI, Cs$_2$CO$_3$, 1,10-phenantroline, DMF, 80°, 22 h; **b)** AcOH, 120°, 1.5 h; **c)** TBS chloride, tol. r.t.; **d)** BrCH$_2$CO$_2$Et, Cs$_2$CO$_3$, DMF, 24 h., r.t.; **e)** The corresponding steps of the general synthesis of **(+/-)-Glupin-1** were applied (Scheme 4); **f)** TBAF, THF, 2 h., r.t., 3 h, 16% over the 6 steps from **49**; **g)** KOH, MeI, DMSO, 4 h., R. T., 65%.

Instead of exploring further analogues of the R^4 position, I decided to test the available compounds in our assay (Table 13). To my surprise, the introduction of a small chlorine atom on indole position 5 already led to a 25-fold activity drop (entry 2). Accordingly, the bulkier 5-ethyl ester and 5-morpholine amide analogues led to complete inactivity (entries 6 and 7). Substitution at position 7 of the ring, however, had a much smaller deleterious effect on the activity (entry 3). It is noteworthy that, although the 5-methoxy analogue (**137**) displayed the expected extensive activity drop, the phenol group (**136**) remained highly potent (entry 4). Nevertheless, the general drop in activity for these positions deterred me from further exploring any more substitutions on this part of the scaffold.

Table 13. SAR Analysis of the R^4 position.

Entry	R^4	Activity[a]	Entry	R^4(cpd)	Activity
1[b]	H	0.055 ± 0.017	6	(**131**)	>30
2	5-Cl (**122**)	1.4 ± 0.2	7	(**130**)	>30
3	7-Cl (**125**)	0.21 ± 0.09	8	5-*n*-Hex (**124**)	t.b.d.
4	5-OH (**136**) (**GK**)	0.10 ± 0.06	9	(-)-5-Br (**123**)	4.7 ± 0.8
5	5-OMe (**137**) (**GK**)	4.22 ± 3.46	10	(+)-5-Br (**123**)	>30

GK: Synthesised by Dr. Karageorgis; [**a**] Activities given as $IC_{50}(\mu M) \pm SD$ ($n \geq 3$). HCT 116 cell line; [**b**] Entry 1 corresponds to (**+/-)-Glupin-1**.

I subsequently attempted to introduce a heteroatom in the indole ring. For this purpose, 2-hydrazinopyridine was reacted with **50**, but the reaction did not proceed due to the poor electron density of the heteroaromatic hydrazine. To bypass this problem an electron rich halogen that would donate electron density and allow the Fischer indole synthesis to take place was introduced.[89-90] The halogen could then be eliminated by reductive conditions, as used for the Cbz deprotection step. However, the reaction with 2-bromo-5-hydrazinopyridine afforded a very complicated mixture of products in my Fischer indole conditions and it was not pursued further (Scheme 11).
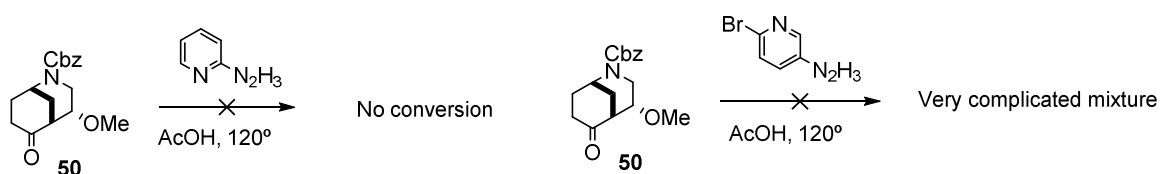
Scheme 11. Attempts on introducing a pyridine ring on R^4.

After revision of the complete SAR study, **(+/-)-Glupin-1**was selected as the lead candidate for further biological studies. Consequently, I set out to separate the racemic mixture and explore the individual activity of the enantiomers.

4.5. (+) and (-) Glupin-1

The racemate **(+/-)-Glupin-1** was successfully separated into both enantiomers by chromatography on a chiral preparative HPLC column (see Experimental Part). The specific optical rotations and the bioactivities of both enantiomers were then measured. **(+)-Glupin-1** was found to be the more potent enantiomer with an 80-fold difference in activity compared to **(-)-Glupin-1** (Table 14). Furthermore, I could confirm the difference of activity between the enantiomers of the Glupin class with another member of the Glupin class, analogue **123** (Table 13, entries 9 and 10). For analogue **123** one of the enantiomers was weakly potent while the other was completely inactive. However, in contrast with Glupin-1, the dextrorotatory enantiomer of **123** was the less active one.

Table 14. Activity values of (+/-), (+) and (-)-Glupin-1.

Glupin-1	(+)	(-)	(+/-)
IC_{50} (nM)	4.2 ± 2.5	336.1 ± 65.8	11.8 ± 1.8

MDA-MB 231 cells, n=3, representative graph shown, mean $\pm$ SEM.
Assay performed by Melanie Schwalfenberg.

Most often, the enantiomers of chiral bioactive compounds present different affinities towards their target, which is due to the chiral three-dimensional environment of the protein binding site. The Glupin class possesses two chiral carbon atoms that conform the asymmetric morphan bicycle and there is a further chiral carbon atom in the morphan scaffold due to a tertiary carbon atom. Consequently, the structural difference between both enantiomers is very high (Figure 18) which translates into a high activity difference between enantiomers. To the best of my knowledge, the enantiomer (+)-Glupin-1 is one of the most potent glucose uptake inhibitors known and the only reported inhibitor with a chiral natural product-like structure.
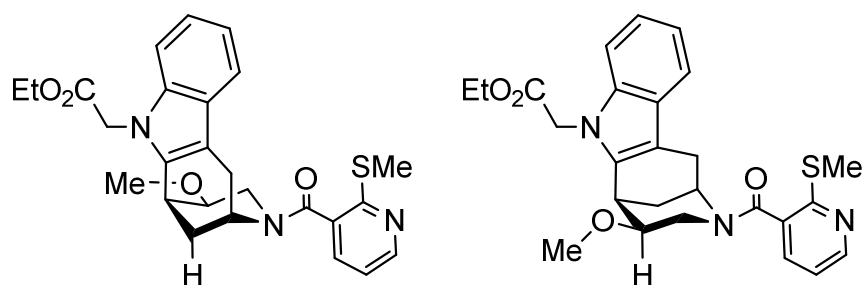
**Figure 18.** Structural representation of both Glupin-1 enantiomers.

4.6. Absolute Configuration of (+)-Glupin-1

In order to fully characterise the structure of the Glupin scaffold, the absolute configuration of all three stereocenters was identified. The strategy was based on the reported determination of the absolute configuration of a morphan compound, similar to the intermediate **44** of the Glupin synthesis by use of chiral NMR auxiliaries.[84, 91] The Glupin analogue **90** was chosen based on its free alcohol moiety and its high potency (IC$_{50}$ = 0.13 µM ± 0.05) for introduction of a the mandelic acid NMR auxiliary (Scheme 12). Nevertheles, the resulting diastereomeric mixture could not be separated.
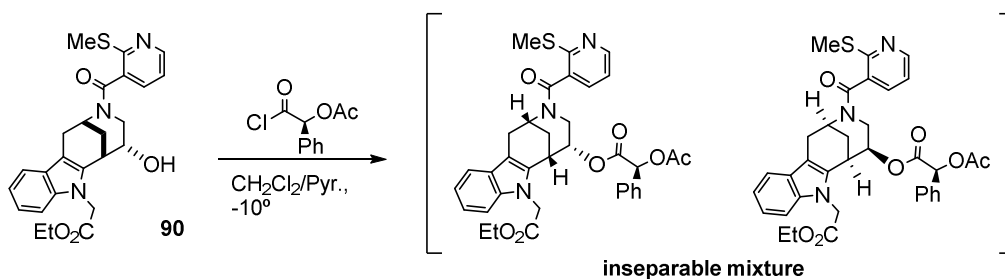
Scheme 12. Introduction of the chiralmandelate auxiliary at a late stage.

The NMR auxiliary was hence introduced at an earlier stage of the Glupin synthesis. The acetyl mandelic acid was converted into the acyl chloride and reacted with intermediate **48** of the Glupin synthesis (Figure 19a).
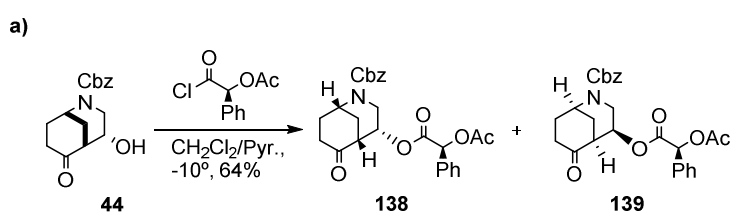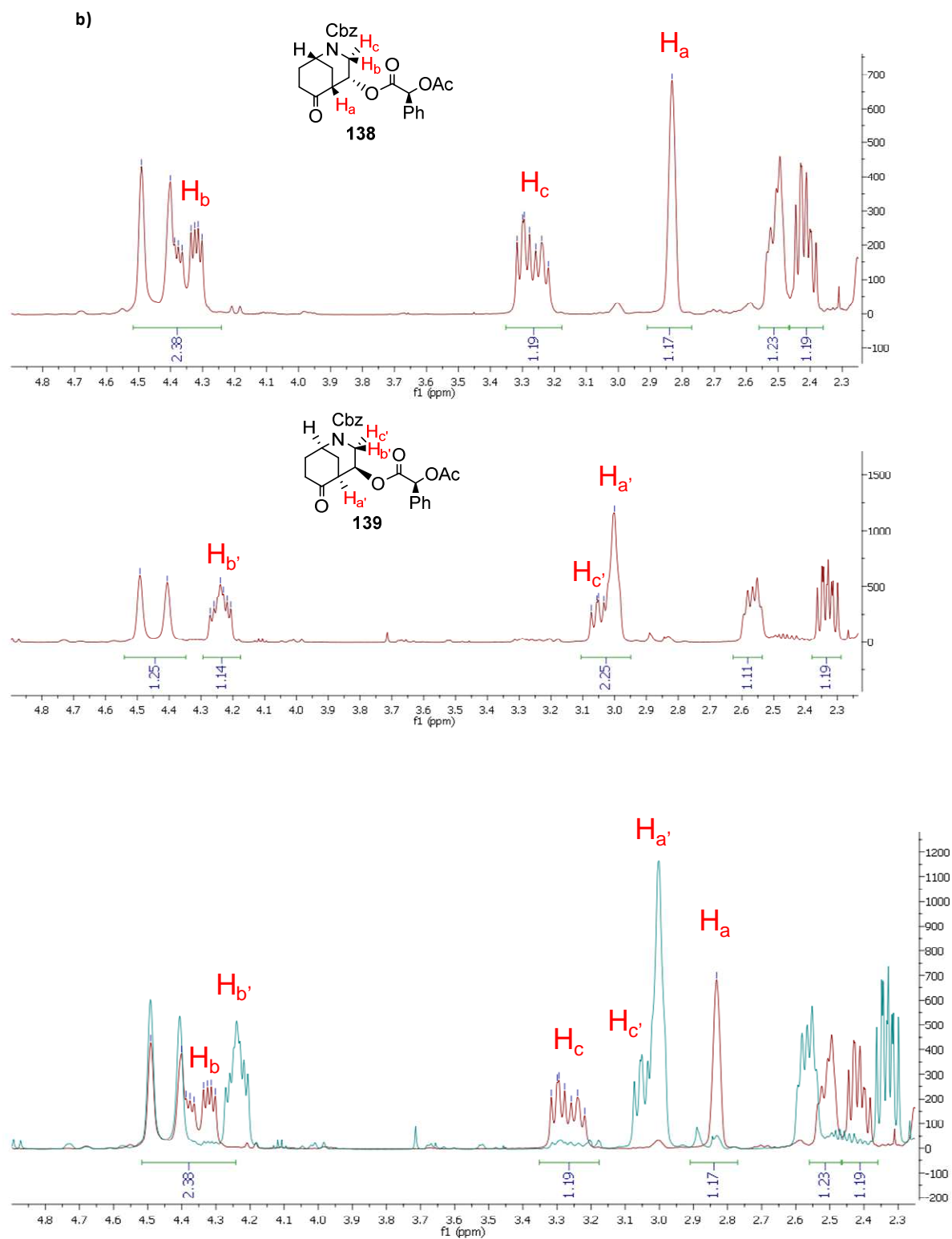
Figure 19. a) Introduction of the chiral mandelate auxiliary on 48. **b)** ¹H NMR comparison of both diastereoisomers.

The resulting mixture proved separable and afforded both diastereoisomers as pure compounds (**138** and **139**). The ^{1}H NMR spectra from both compounds were analysed, and based on the shift of the neighbouring protons to the mandelic auxiliary (Figure 19b) the absolute configuration of all centres could be determined (Figure 20). The shifts observed in the NMR spectra were in agreement with the ones reported in the literature by Bonjoch *et al*. The basis of the use of this auxiliary is that in solution it presents a more stable conformation in which the methine-, the carbonyl- and the acetyl-group are in a *syn* coplanar disposition (as drawn in figure 20), hence the phenyl ring of the auxiliary shields the protons situated in closer proximity. The phenyl ring from the auxiliary shielded different protons of the two diastereoisomers. For **138** the proton in α to the carbonyl was shielded (2.83 ppm in contrast with 3.00 ppm from **139**) and for **139** the methylene group α to the amide was shielded (3.05 and 4.24 ppm in contrast with 3.22-3.30 and 4.35 ppm for **138**).
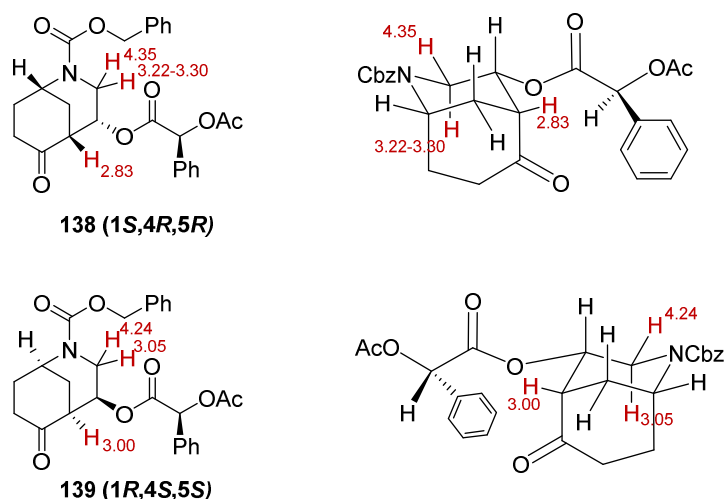

Figure 20. Determination of the absolute configuration of intermediate 48. The δ (ppm) of the corresponding protons are shown in red.

Once the structures of both morphan diastereoisomers were determined, they were taken through the synthesis separately to arrive at the corresponding Glupin analogues. **142** and **143** (Scheme 13) could only be isolated with a mixture of starting material (**140** and **141**) and an unidentified impurity. As such they were submitted for Cbz removal conditions. The conditions used to remove the Cbz protecting group, removed as well the benzylic acetyl group of the mandelic auxiliary. Consequently, the chiral carbon atom of the mandelic auxiliary was lost and the two compounds became enantiomers rather than diastereoisomers. This result would enable me to compare the activity of their respective Glupin analogues in a much more reliable manner.

The crude products of the hydrogenation were directly subjected to the last step of the Glupin synthesis.
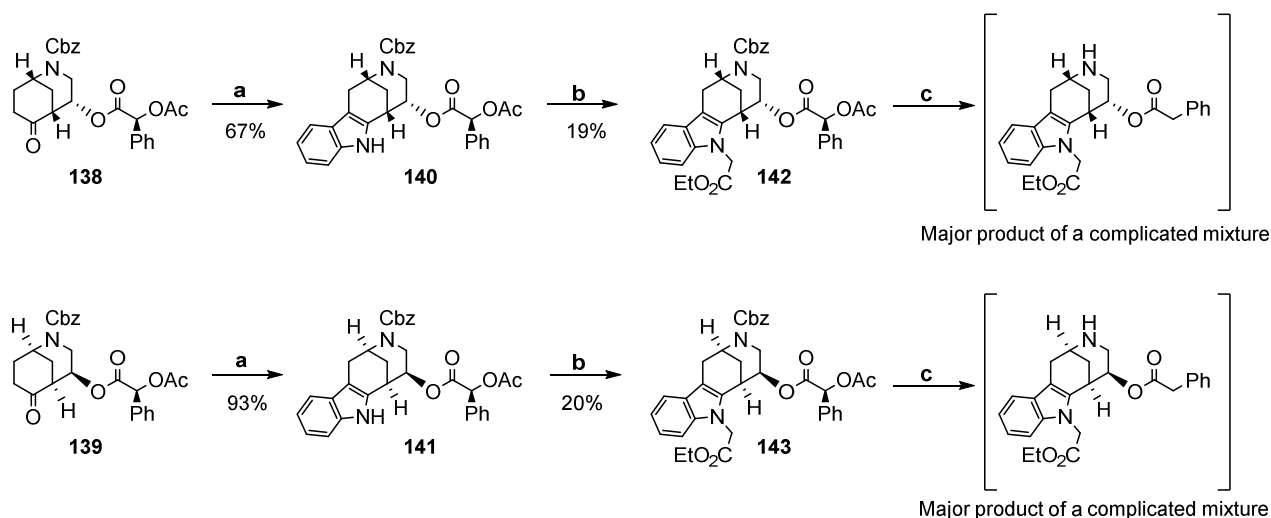
Scheme 13. Synthesis of the mandelate-glupin analogues. **a)** PhN_2H_3, AcOH, reflux, 1.5 h; **b)** $BrCH_2CO_2Et$, Cs_2CO_3, DMF, 6 h, r.t.; **c)** H_2, Pd/C, EtOH, 5 h, r.t.

Finally, the 2-methylthionicotinoyl group was introduced and both compounds, **144** and **145**, were isolated. The activities of both compounds, with their structure known, were measured. Analogue **145** with chiral carbon atoms 2R, 5S and 6R, was found to be ca. 30 times more potent than its enantiomer **144** (Scheme 14).
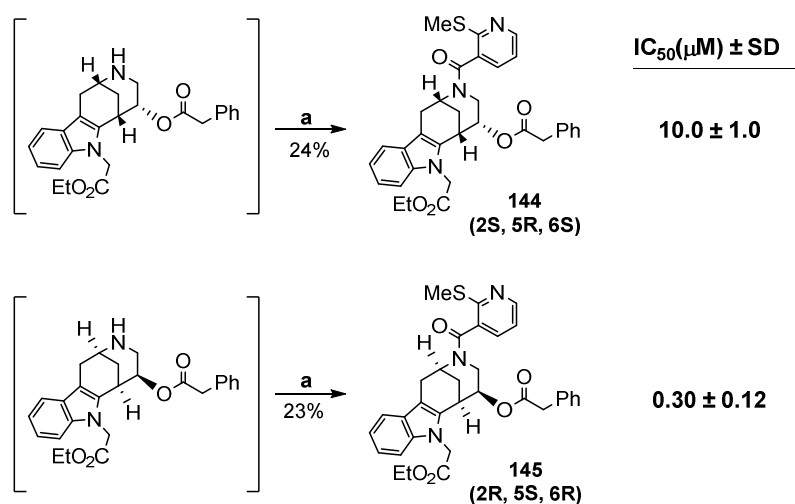

Scheme 14. Activity measure of the enantiopure Glupin analogues **144** and **145**. **a)** 2-(methylthio)nicotinic chloride, NEt_3, CH_2Cl_2, 12 h, r.t. Yields are for the last 2 steps combined.

Finally, I extrapolated the absolute configuration of the three chiral centres of the more active enantiomer **145** into the more active Glupin-1 enantiomer **(+)-Glupin-1**. Finally, with the complete structural information of **(+)-Glupin-1**, the chemical study of the novel glucose uptake inhibitor was considered sufficiently explored for the boundaries of this doctoral thesis.

4.7. Synthesis of the Chemical Probes Based on Glupin-1

In order to confirm the GLUT transporters as the target of the Glupins, an affinity chromatography target engagement assay was envisioned. This method is based on the use of a compound bound to a solid phase by a linker, that upon incubation with a cell lysate, the affinity of the compound with a protein enriches the solid phase with such protein. Among other methods, the chemical probe can be bound to the solid phase by an amide bond. Consequently, a free-amine chemical probe based on Glupin-1 was synthesised. The linker of choice was a diamine-PEG.

Based on the Glupin SAR, the R^2 position was deemed to be the most suitable as the linker attachment point. Since acetylation had been successful on this position, I decided to install the dielectrophile bromoacetyl bromide that will potentially be attacked on the carbonyl by alcohol **44** and a later stage on the bromide by a amine-based linker in an S_N2 reaction. Reaction between **44** and bromoacetyl bromide under the acetylation conditions was successful with moderate yield (Scheme 15a). However, under the Fischer indole conditions the bromide was displaced by an acetic acid group affording compound **148**. Consequently, alternative routes were explored.
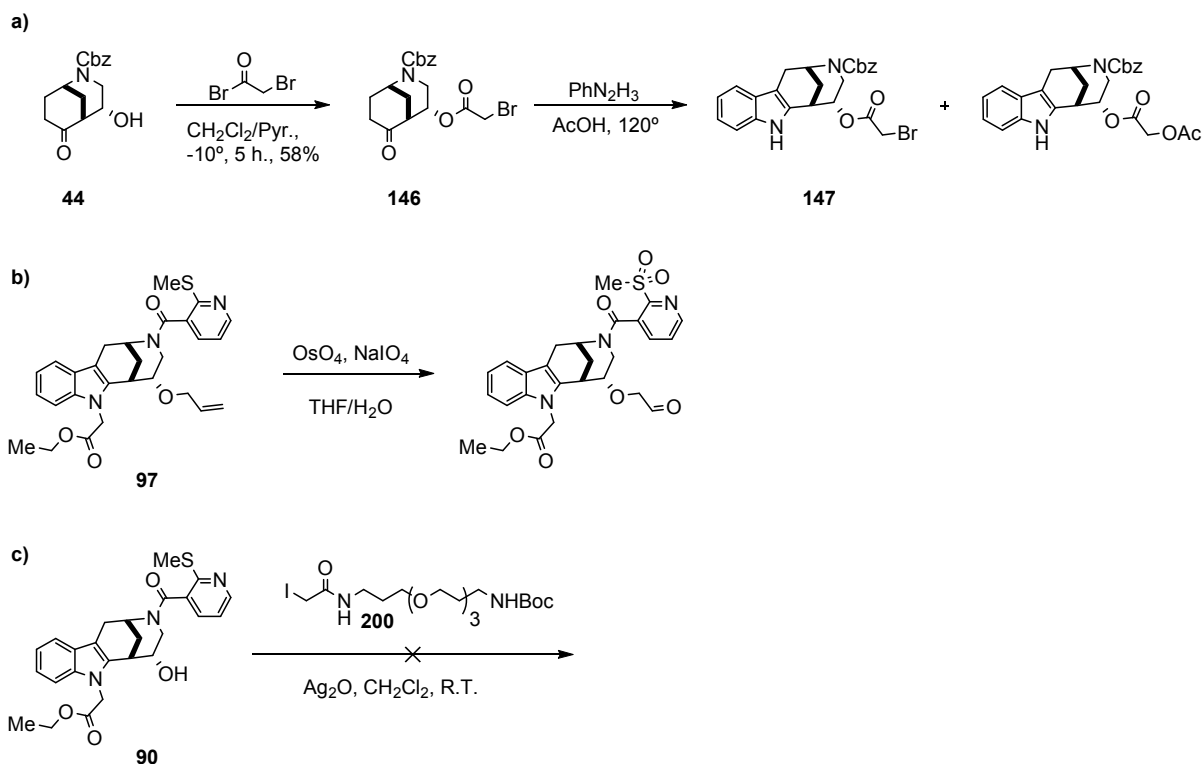
Scheme 15. Linker attachment attempts.

Based on allyl containing analogue **97**, a coupling by reductive amination was envisioned. Therefore the synthesis of the aldehyde from the allyl residue was attempted from compound **97** by an oxidative olefin cleavage. Unfortunately, the reaction also promoted the sulfur oxidation (Scheme 15b). I then switched to the functionalisation of the Glupin analogue **90**, once more this analogue displayed the properties that I was looking for. It offered a clear nucleophile on position R^2 with a very high potency and hence could be coupled with a linker. My first attempt to introduce a linker on the hydroxyl group of **90** was the use of modified iodide-PEG linker with silver oxide to activate the iodide, however the S_N2 reaction did not take place (Scheme 15c).

Since the alkyl iodide electrophile did not work, I turned to a more reactive electrophile; an acyl chloride coupled with a PEG-linker. On this account, the phosgene analogue, 4-nitrobenzoyl chloride was reacted *in situ* with **90** and with the diamine-monoBoc-protected PEG linker (Scheme 16a). The Boc-protected active probe (**138**) was tested and showed the expected strong potency with an IC_{50} of 0.083 µM (± 0.026).
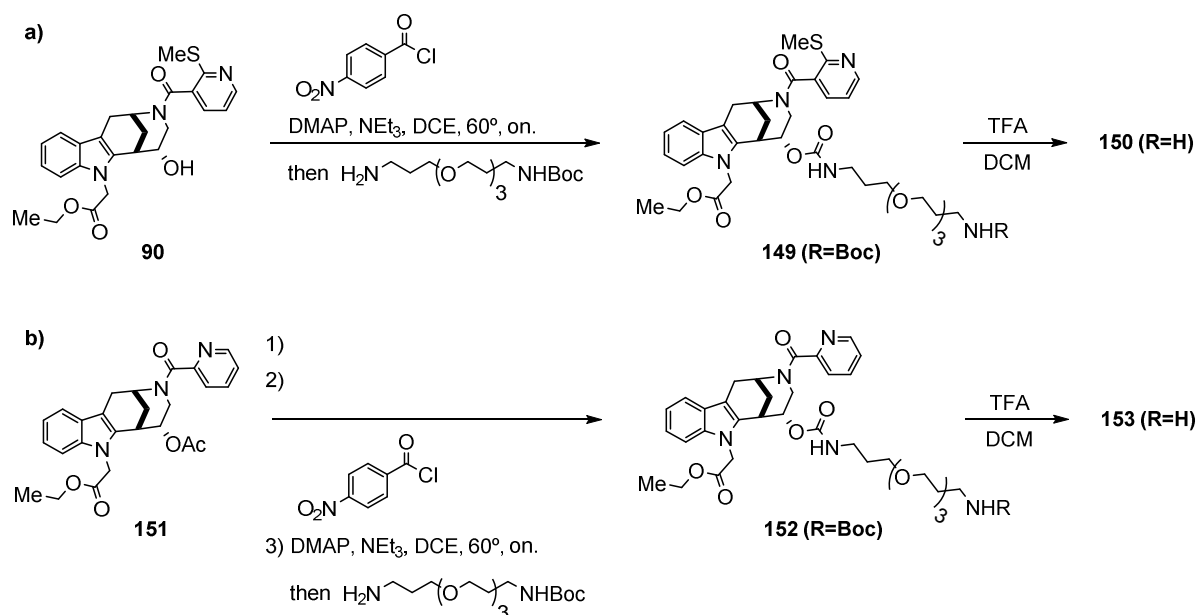
Scheme 16. Synthesis of the glupin active and inactive probes (a) and b) respectively).

The use of an active probe in a pull-down experiment is normally complemented with an inactive probe that will unmask any unselective binding. The inactive probe needs to be very similar in structure to the parent compound whilst being inactive. In the design of the inactive probe I focused on the SAR table of position R^1 that had provided inactive or very weakly active analogues with small changes. Particularly, I envisioned the use of the picolinoyl group (see section 4.4.2., Table10, entry 13) as the base for the inactive probe. The inactive probe was synthesised as described for the active one (Scheme 16b).

With the active and inactive probe in hand, the pull-down experiments were performed by Melanie Schwalfenberg. The active probe was used and the gel was developed with GLUT-1 antibody. When Glupin-1 was used to compete out the active probe, the GLUT-1 band had the expected lower intensity. This result was not observed when glut inhibitor BayGLUT-1 was used. Nevertheless, when only the beads were used in a control experiment the band for GLUT-1 had a similar intensity suggesting that the interaction observed between the active probe and GLUT-1 was unspecific binding. The inactive probe was also used in a pull-down result. The inactive GLUT-1 band detected displayed a lower intensity, suggesting a direct interaction with GLUT-1. Nevertheless, the unspecific binding observed prompted the pursue different target engagement experiments.

The free amine at the linker of both probes allowed for a simple coupling with a solid phase as is necessary in the pull-down experiment. Furthermore, the free amine can be used to couple, for example, molecular dyes. Considering again the use of the probes for target identification, Beate

Schölermann set to establish a BRET (Bioluminescence Resonance Energy Transfer) assay that would show the direct interaction in vivo of the active Glupin probe and the GLUT transporter (expressed with a bioluminescent dye). The basis of this experiment is to detect an energy transfer between a bioluminescent protein (typically luciferase) and a chemical dye when both entities are close in space. Should the energy transfer be detected, the molecule bound to the chemical dye is considered to bind effectively the target protein coupled with the bioluminescent protein. For this purpose, a GLUT-1-luciferase construct was developed in-house and the free-amine active probe was coupled with a TAMRA dye (Scheme 17).
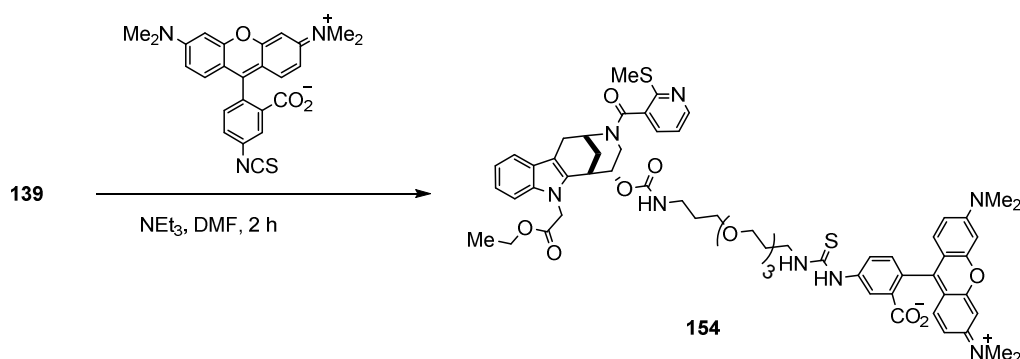
Scheme 17. Synthesis of the Tamra-glupin-1 probe.

4.8. Biological Characterization of Glupin-1

Some biological assays were performed to characterise the behaviour of Glupin-1 in cells. The work was performed by Melanie Schwalfenberg unless otherwise stated.

4.8.1. [^{3}H]-Glucose uptake

The activity of **(+/-)-Glupin-1** was confirmed by the [^{3}H]-radiolabeled glucose assay. This assay represents the most reliable assay for the measurement of glucose uptake. The results confirmed the high potency with an IC$_{50}$ value of 8 nM in MDA-MB 231 cells.

4.8.2. Glucose uptake across tissues

The ability of **(+/-)-Glupin-1** to inhibit the glucose uptake was checked for different cell lines. The compound show very high potencies in all mammalian cell lines tested but did not so for Kc167 a cell line with *Drosophila* origin (Table 15). The IC$_{50}$s were all in the low nM range for the Resazurin assay (Figure 9) performed in a low-throughput manner.

Table 15. (+/-)-Glupin-1 was active in the low nMrange in all mammalian cell lines tested.

Cell line	Origin	IC$_{50}$/nM
HCT 116	Human colon cancer	5 ± 1(57 ± 17)[a]
MDA-MB 231	Human breast cancer	15 ± 4
Hela	Human cervical cancer	22 ± 2
CHO	Chinese hamster ovary	4 ± 3
Kc167	*D. melanogaster* embryo	Not active

Assay performed by Melanie Schwalfenberg. Values derived from low-throughput Resazurin-based assay, n≥3, mean +/- SEM; [a] Value from medium-throughput screen, n=12, mean ± SEM.

4.8.3. Cell proliferation of MDA-MB 231

Since the MDA-MB 231 cell line has a high demand of glucose, the addition of Glupin-1 should inhibit the cell proliferation. Both enantiomers were tested using three different glucose concentrations; 25 mM, 5mM and no glucose. A concentration-dependent sensitivity towards glupin-1 was identified (Table 16). The most potent enantiomer; (+)-Glupin-1, strongly impaired cell proliferation, while the less potent enantiomer; (-)-Glupin-1, also affected cell proliferation although with a lower activity.

Table 16. Proliferation of MDA-MB 231 cells upon compound treatment.

	25 mMGlc	5 mMGlc	0 mMGlc
(+)-Glupin-1	170 ± 157	3 ± 3	1 ± 1
(-)-Glupin-1	2519 ± 916	470 ± 216	46 ± 1

Assay performed by Melanie Schwalfenberg, 48h, MDA-MB 231 cells; Activities given as IC$_{50}$ (nM) ± S.D, n=2;Glc=Glucose

Interestingly, when the MDA-MB 231 cells were starved from glucose for 48 hours the cell growth was only mildly impaired (around 70 % of the DMSO control) in contrast to the impaired cell growth caused by (+)-Glupin-1 treatment. This result suggests that either (+)-Glupin-1 has off-target effects that affect the cell proliferation, or that the cells differ in their

metabolic behaviour depending on whether glucose is present in the media rather than whether glucose is taken up.

4.8.4. Changes in metabolites upon glupin-1 treatment

Since Glupin-1 impeded the glucose uptake, a change in the concentration of the metabolites was to be expected. For example, a decrease in the glycolysis metabolites would suggest a down-regulation of the glycolythic patwhay which would be in agreement with a decreased glucose uptake. The changes in the metabolite concentrations upon compound treatment were measured by Dr. Magnus Sellstedt (Table 17). Molt 16 cells in medium with 11.1 mM glucose and 2 mM glutamine were treated with Glupin-1 (50 nM) and the metabolite concentrations were checked after 24 hours. The metabolites that were significantly altered are shown in Table 16. The decrease in the fructose-6-phosphate and lactic acid clearly proved a decreased glycolytic function. Furthermore, glycerol-3-phosphate which is synthesised from the glycolysis metabolite DHAP also presented a sharp concentration decrease. The same pattern was observed for the citric acid intermediates; citric acid, isocitric acid and malic acid, which were all extensively reduced. The increase in aspartic acid metabolite can be explained by the switch of the cells to the Glutamine as the main nutrient source. Glutamine is then used to fuel the TCA while generating aspartate. Nevertheless, an aspartic acid increase could also come from an increased gluconeogenesis activty, a pathway in which aspartate is an intermediate metabolite as part of the urea cycle. Both pathways point to a reduced glucose metabolism. Finally, the decrease in UDP-*N*-acetylglucosamine was not surprising since it forms part of the glucose sensing mechanism. UDP-*N*-acetylglucosamine is involved in the regulation of multiple cellular processes through protein glycosylation and it is known to be downregulated under glucose depravation.

Table 17. Significantly altered metabolites upon Glupin-1 treatment.

Citricacid	-2.240
Isocitricacid	-1.709
Lacticacid	-1.358
Glycerol-3-phosphate	-1.116
Ribitol/Arabitol	-1.085
UDP-N-Acetylglucosamine	-0.941
Malicacid	-0.790
Beta-alanine	-0.734

Fructose-6-phosphate	-0.467
4-Aminobutyric acid	-0.324
Octadecanoicacid	-0.066
Asparticacid	0.932

Log2-fold values (p = 0.05, biological duplicates). Molt16 cells with 50 nM of (+/-)-Glupin-1 for 24 h compared to DMSO controls. Assay performed by Dr. Magnus Sellstedt.

4.8.5. Inhibition of aminoacid starvation-induced autophagy

In glucose depravation conditions, many cancer cells turn to autophagy as a rescue mechanism, a way to maintain the required energy levels under low nutrient sources. It is therefore expected of a glucose uptake inhibitor to promote the initiation of the autophagy pathway. In our group it was found that when analogues of the Glupin compound class are present, autophagy (promoted by aminoacid starvation) was inhibited. This apparently contradictory results could be explained if the autophagy process were to need some glucose present to activate. If the glucose level does not reach a minimum, it is possible that there is insufficient energy to promote the autophagy process. In the presence of (+)-Glupin-1 the IC_{50} for autophagy inhibition was of 0.14 µM ± 0.05. However, when the autophagy was induced by Rapamycin, Glupin-1 failed to inhibit it, most likely because the cells still have the amino acid nutrient source (Table 18). The autophagy-related assays were run by COMAS, Dr. Luca Laraia and Marjorie Carnero Corrales.

**Table 18.** Inhibition of Aminoacid Starvation-Induced Autophagy.

Cmpd	Autophagy Inhibition (Aa starvation)	Autophagy Inhibition (Rapamycin Induced)	Glucose Uptake Inhibition
(+)-Glupin-1	0.14 µM ± 0.05	> 10 µM	-
BayGLUT-1	0.86 µM ± 0.27	4.4 µM ± 3.3	1.4 µM ± 0.6

Values given as IC_{50}s, in MCF7 cells with EBSS media after 3 h.

4.8.6. (+)-Glupin-1 reduces lipid droplet formation

Since **(+)-Glupin-1** seems to have a widespread effect on the cell metabolism, it was decided to check for an interaction with the lipid metabolism. In fact, when MDA-MB 231cells were treated with **(+)-Glupin-1** in a high caloric diet (400 µM of oleic acid) the lipid droplet formation was dose dependently inhibited (Figure 21). The less active enantiomer did not interact with the lipid formation, and when the cells were pre-fed with oleic acid, the compound

did not show any effect on the lipid droplet concentration. Hence, **(+)-Glupin-1** does not interact with the already formed lipid droplets but rather inhibits their synthesis. The mechanism by which it occurs has yet to be explored but it could be explained by a reduction in uptake and esterification of lipids and/or by an increase in the ß-ketoester route. The assay was run by Dr. Kirsten Tschapalda.
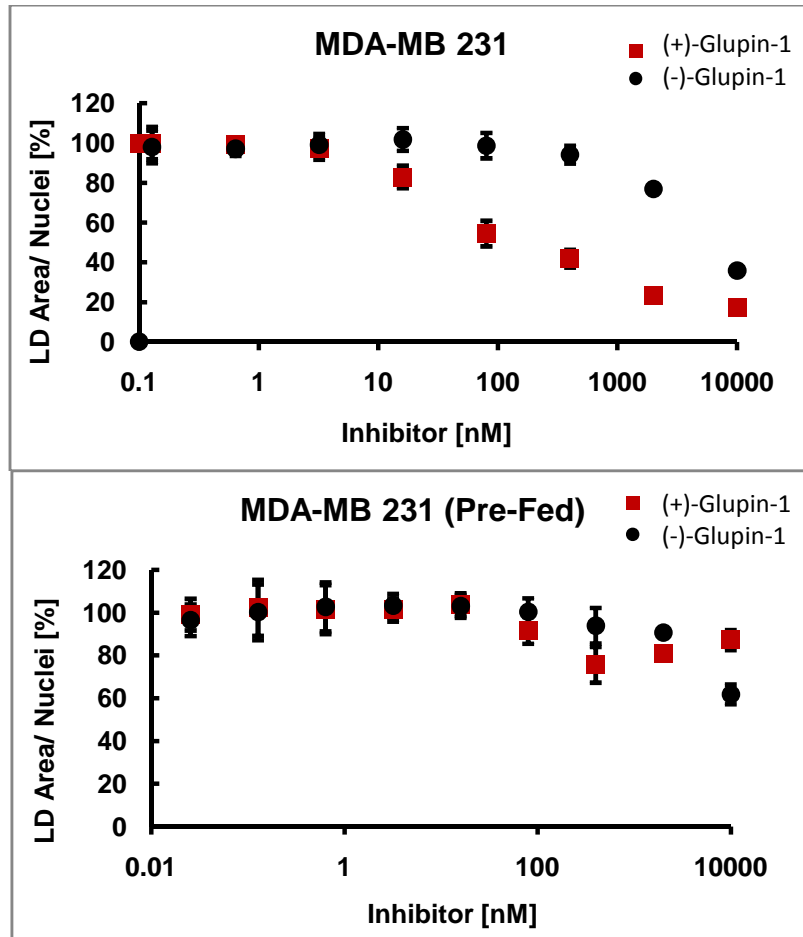
Assay run by Dr. Kirsten Tschapalda. MDA-MB 231 cells, 48 h. Lipid Droplets stained with Bodipy 493/503.

Figure 21. Inhibition of lipid droplet formation.

Splicing Inhibition

5. Introduction

5.1. The Splicing Process

The splicing process refers to the mechanism by which the premature messenger RNA (pre-mRNA), which is the direct product of the DNA transcription process, is converted into a mature messenger RNA (mRNA)ready to be translated into proteins by the ribosomes. The pre-mRNA contains RNA sequences that will later be part of the mRNA; the exons, and sequences that are spliced out and will not be part of the mRNA; the introns. Removing the introns and linking the exons together is the main function of the splicing process.

At a molecular level, this process takes place by two trans-phosphoesterification reactions. In the first step, the 2´-OH of the branching point nucleotide attacks the 5´ splicing site and releases the 5´exon (Figure 22a and b). Then in the second step, the released 5´exon attacks the 3´splicing site, generating the mature mRNA and releasing the intron as a lariat with the branching point forming phosphoester bonds on the 2', 3' and 5' positions. The splicing and branching sites are conserved sequences complementary to the interacting partners necessary for the splicing process.
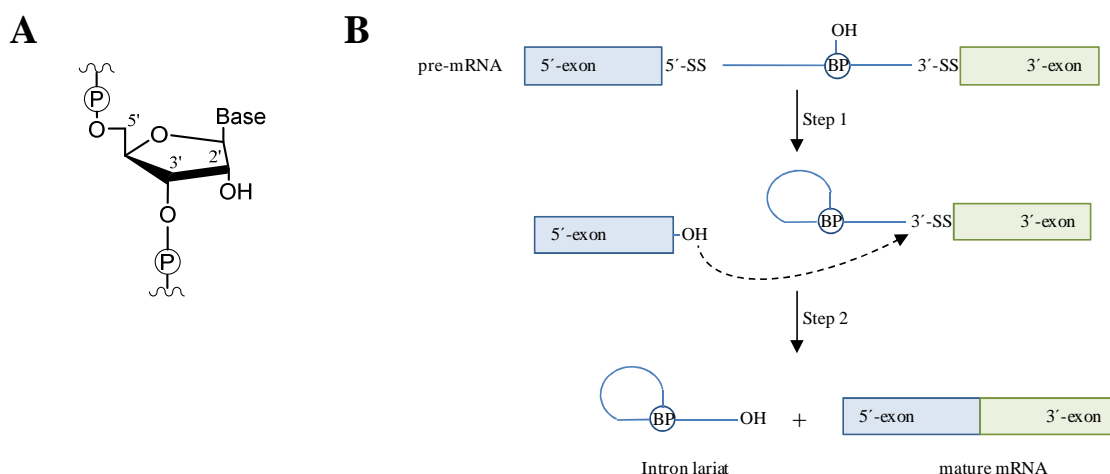

Figure 22. a) RNA schematic structure. **b)** Scheme of the splicing process. In the first step, the BP (branching point) attacks the 5´-SS (5´splicing site) releasing then the 5´-exon. In the second

step, the 5´-exon attacks the 3´-SS, releasing the intron as a lariat and generating the mature RNA (5´-exon-3´-exon).

RNA splicing is an almost ubiquitous process in all living organisms. In prokaryotes, as the ribosomal machinery is in direct contact with the RNA transcript, the splicing process is almost non-existing. Therefore, there is mostly a direct one-to-one correlation between the bases at the DNA and the bases at the mRNA. In eukaryotes, in the other hand, the higher the organism is, the higher is the presence of intron sequences in the genes.[93] Many genes can be spliced in more than one way, leading to different proteins. This process is referred to as alternative splicing and is a highly conserved evolutionary tool by which the encoded DNA information is extensively expanded.[94] In this way, the same gene transcript can lead to different proteins depending on the splicing pattern. An example of the alternative splicing is the above mentioned pyruvate kinase (see section 2.3.2.). The normal spliced form, the PKM1, is replaced in proliferative tissues and tumours by the PKM2 upon selection of a different 5´-exon of the same gene.[56] Misregulation of the alternative splicing has been shown to promote or contribute to many cancer processes, e.g. cancer metabolism, angiogenesis and metastasis.[95]

In conclusion, splicing allows for a tighter control of protein synthesis. Alternative splicing generates extensive possibilities from the same genes in quantity, in synthesis time point and in the function of the translated protein. Besides the gene pool variations offered by the alternative splicing, this process has the evolutionary implication of a "simple" generation of new proteins. The conserved exons, often important protein domains, are recombined into different genes, generating "protein analogues" with the same catalytic domains but different characteristics, as functions, localisation, regulation, etc.

5.2. The Spliceosome

Despite the chemical simplicity of the splicing process (two consecutive trans-esterification reactions) at the molecular biology level, this process requires the participation of numerous proteins and ribonucleoproteins, the use of great quantities of ATP as well as a myriad of protein-protein, protein-RNA and RNA-RNA interactions. The complete ensemble that catalyses this complex process, is called the Spliceosome.[96]

5.2.1. The spliceosome ribonucleoproteins: the snRNPs

The Spliceosome is a multimegadalton complex with a highly dynamic structure and composition. A great number of proteins take part in this process, however, its most

characteristic constituents are the small nuclear ribonucleoproteins (snRNPs). The snRNPs have a non-coding RNA nucleic acid sequence, the small nuclear RNA (snRNA), coupled with a RNA-binding protein sequence. The snRNA sequence is needed to interact with the messenger RNA as in the case of the ribosome subunits. There are five units of snRNPs: U1, U2, U4, U5 and U6. The U1 snRNPs is a complementary sequence of the 5´-splicing site. It recognizes and stabilizes the 5´SS but needs to be displaced in order to activate the B complex of the spliceosome (Figure 23). The U2 recognizes the branching point and contributes to moving the branching point towards the 5´SS at the expense of ATP. The U2 also interacts with the U6 upon its recruitment. The U5 snRNP interacts with the last two nucleotides of the exons that will be bound together forming the mature mRNA, and hence contributes to move the 5´SS towards the 3´SS. The U6 interacts with the 3´ end of the intron and gets recruited by the U2 subunit. The U4 is mainly responsible from stabilising the U6 subunit and also needs to be displaced in order to activate the B complex (Figure 23).[97]

5.2.2. The spliceosome cycle

The snRNPs are recruited to the spliceosome at different stages and promote the corresponding structural changes and pre-mRNA interactions necessary for each stage (Figure 28). Although more evidence is still needed, it is believed that the spliceosome complex acts as a ribozyme(RNA molecules capable of acting as enzymes). As such, the actual catalytic interactions that promote both trans-esterifications are with the snRNA, particularly the sequences from the U2 and the U6.[98-99]
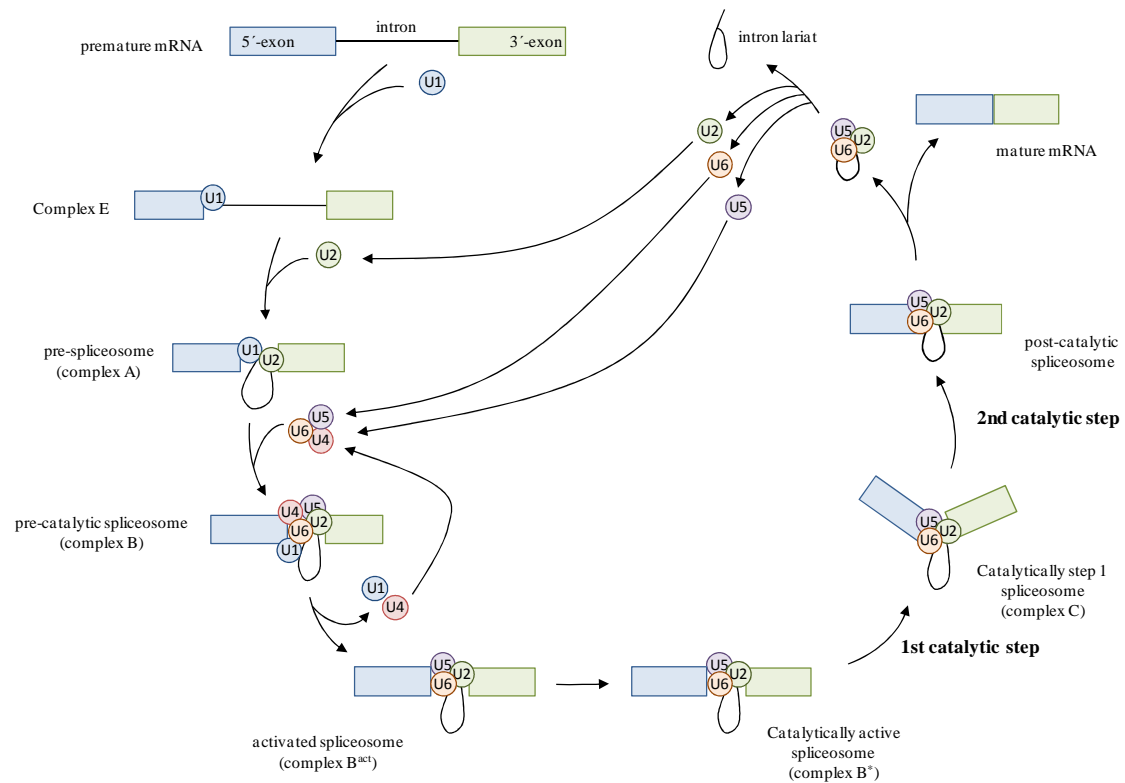
Figure 23. The spliceosome cycle and spliceosome complex stages upon recruitment of the snRNPs. The recruitment and release of proteins and ATP has been omitted for clarity.

The spliceosome cycle starts with the interaction of the pre-mRNA with the U1 snRNP unit, forming complex E. U2 is then recruited and a structural change pulls up the 3´SS to the 5´SS, forming complex A. The rest of the snRNPs are then recruited to obtain the pre-catalytic complex B, which gets activated upon displacement of the subunits U1 and U4 (complex B^{act}). Recruitment of other proteins yield the substrate for the first catalyzed trans-esterification reaction, the catalytically active complex B*. The 2´OH of a nucleotide at the branching point attacks the 5´SS to for a lariat and release the 5´-exon and yield complex C. Finally, complex C promotes the attack of the free 5´-exon to the 3´SS and releases all products; the mature mRNA, the intron lariat and the remaining snRNPs which are recycled back to the splicing process.

5.2.3. The spliceosome structure

Due to the highly dynamic and complex structure of the spliceosome, currently the whole spliceosome can only be observed by electron microscopy (EM). The snRNP and other spliceosome constituents have been thoroughly studied by NMR and X-ray crystallography. These high-resolution structures have hence helped to identify structural features of the whole spliceosome assembly.[100] The heterogeneity of the spliceosome has made obtaining high

resolution structuresa very challenging task (Figure 24). Furthermore, the stability of the spliceosome complexes does often not resist the sample preparation techniques needed for the cryo-EM studies, which remains to be the most promising method to study this dynamic and complex macrostructure.[101-102]
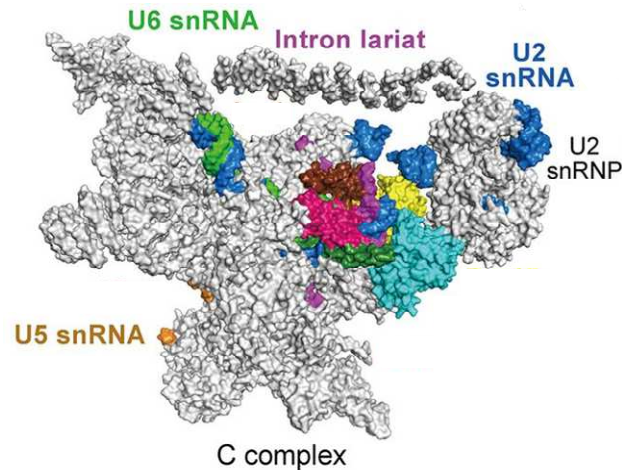

Figure 24. Catalytically activated C complex in the step 2 of the Saccharomyces cerevisae yeast. Adapted from Yan *et al.*[103]

Recent advances in these techniques have enabled researchers to obtain high-resolution images like the one obtained by Yan *et al*. with a 7Å resolution of a catalytically activated C complex of Saccharomyces cerevisae.[103] Nevertheless, additionalstructural information needs to be uncovered in the many spliceosome stages.

5.3. Splicing Inhibition

Since a lot of the splicing process remains to be uncovered, the use of small molecules that target the splicing machinery has gained a lot of importance. The ability to stabilize spliceosome complexes with small molecules continues to hold a great potential in the study of this complex macrostructure, particularly for structural and functional studies. Furthermore, inhibition of the splicing process may help discover novel spliceosome complexes that have yet to be identified. Nevertheless, there are currently only a handful of splicing inhibitors, and more molecules are needed to halt the process at the different stages. Furthermore, novel splicing inhibitors also hold a great potential as drug leads in many of the cancers where splicing has been reported to play an important role.[104-105]

The families of the natural products FR901463 and Pladienolides were identified as potent splicing inhibitors when their cytotoxicities against several tumor cell lines were assayed. The synthesis of chemical analogues led to optimized compounds: Spliceostatin A and pladienolide analogue E7107 (Figure 25).[106-107] The target of these compounds was identified as the splicing factor 3b (SF3B), which is part of the U2 snRNP, the compounds destabilize the interaction between U2 snRNP and the pre-mRNA, stalling the splicing process. The natural product garcinol, a known histone acetyl transferase inhbitor, was also reported to inhibit the splicing process at an A-like complex stage.[108] Psoromic acid and some derivatives, were identified in an *in vitro* splicing inhibiting assay by Lürhman and coworkers, and reported to stall the process at a B-like stage.[109]
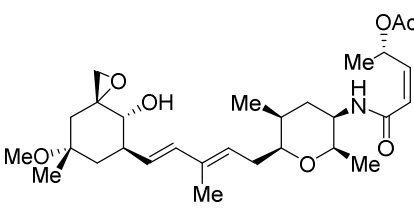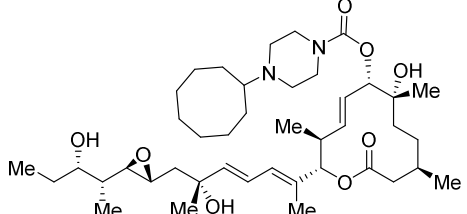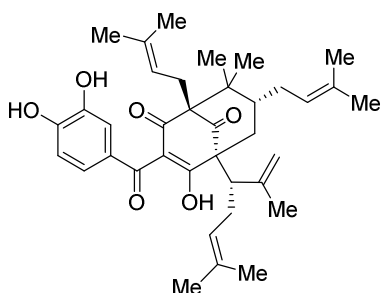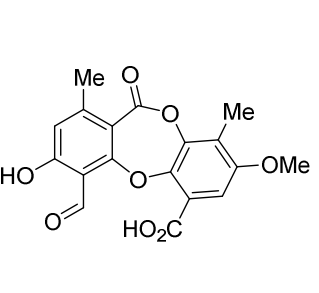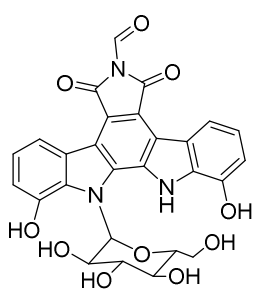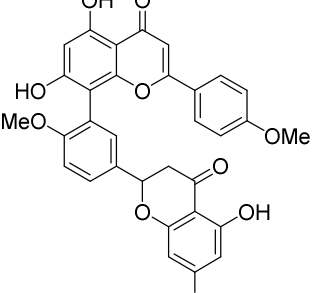

Compound	Spliceostatin A	E7107
Stalled Complex	A	A
Potency (IC$_{50}$)	low nM	low nM
Ref.	106	107

Compound	Garcinol	Psoromic Acid
Stalled Complex	A	B/C
Potency (IC$_{50}$)	50μM	56 μM
Ref.	108	109

Compound	NB-506	Isoginkgetin
Stalled Complex	pre-spliceosome assembly	A
Potency (IC$_{50}$)	50-100 μM	~30 μM
Ref.	110	111

Figure 25. Structure of some splicing inhibitors with the spliceosome complex stalled and the inhibition potencies.

Targeting the kinases and phosphatases involved in splicing has also been shown to stall the process. For example, the serine rich proteins (SR proteins), which are involved in the identification of the splicing sites, have been indirectly targeted by inhibiting the activity of known SR protein kinases like Clk/Sty (cdc2-like kinase 1), SRPK 1, SRPK 2 (SR protein-specific kinase-1) and topoisomerase I. The topoisomerase I inhibitor, NB-506 was shown to prevent pre-spliceosome complexes by inhibiting the phosphorylation of the splicing factor SF2/ASF (Figure 25).[110] Another natural product identified as a splicing inhibitor is the biflavonoid isoginketin. This natural product stalls the A complex of the spliceosome, most likely by preventing PRP28 phosphorylation by the SRPK 2 kinase.[111]

In conclusion, the identification of novel splicing inhibitors still holds a great potential for structural and functional studies of the spliceosome machinery and, perhaps most interestingly in drug development.

6. Aims of the Project

The obtention of structural information or mechanistic insight of the highly complex machinery, the Spliceosome, continues to be a challenging task. However, the identification of novel small molecule inhibitors of this machinery is a powerful tool for this purpose.

It is the aim of this project to chemically explore an identified splicing inhibitor that had been discovered in a HTS assay in this group. The inmediate objective is to validate this compound as a splicing inhibitor. At a later stage, a library of compounds would be established to accomplish a reliable SAR analysis.

The final objective of the project is the identification of the mode of action of a potential splicing inhibitor.

The project was carried out as a collaboration with the group of Professor Lürhmann, particularly with Dr. Anzhalika Sidarovich. The biological experiments were run at the group of Professor Lürhmann.

7. Results and Discussion

7.1. Assay and Compound Class Identification

Identification of compounds with splicing inhibiting activity has mainly been achieved through cell-based assays. Consequently, until recently there was a high need for establishing an in vitro assay that would eliminate all the cell associated restrictions, such as the high costs, high maintenance and complex procedures. Furthermore, there were few existing inhibitors of the splicing process that would target the splicing process at the pre-mRNA stage.[106-108] In 2012, a collaboration between our group and that ofProfessor Lührmann reported a high-throughput in vitro assay that allowed the identification of novel splicing inhibitors.[109] The HTS assay was based on the early incorporation of a specific protein into the spliceosome complex that is only required after the step 1 of the splicing process. By monitoring the presence of this protein in a spliceosome assembled in vitro, the inability to assemble, to activate or to catalyse the splicing step 1, upon compound treatment, could be identified. The monitored protein was a FLAG-tagged version of the DEAD box ATPase Abstrakt, which is specific of the C complex of the spliceosome. This protein, stably expressed in HeLa cells, was detected with anti-FLAG antibody coupled to a horse radish peroxidase (HRP). HeLa nuclear extract was incubated with inmobilized pre-mRNA before washing and checking the HRP fluorescence. If the splicing process was not inhibited, the FLAG-tagged protein would be incorporated, immobilised and detected by the luminescent reaction catalysed by the HRP. On the other hand, if the compound assayed has splicing inhibiting activity, the FLAG-tagged protein would not be incorporated to the spliceosome and the luminescence would hence decrease (Figure 26).
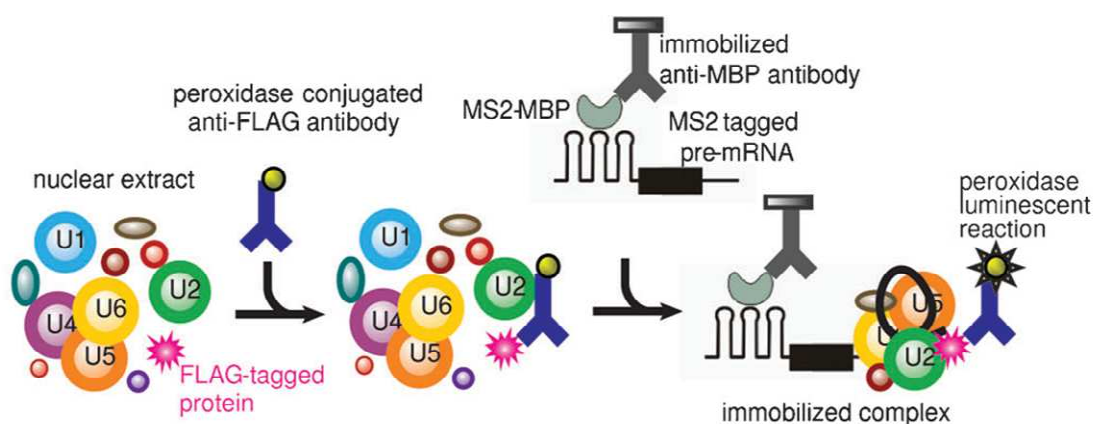

Figure 26. Assay for the identification of splicing inhibitors. Adapted from Samatov et al. (2012).[109]

The assay was run for a library of over 170,000 compounds screened at 50 µM and the assay hits were validated in an in vitro splicing assay with ^{32}P-labelled pre-mRNA in HeLa nuclear extract. Several novel splicing inhibitor scaffolds were identified, including the above mentioned Psoromic and Norstistic acids,[109] or **cp028** (Figure 27). **Cp028** was selected to be further studied in a collaboration between our group and Professor Lürhmann´s. The biological assays run in this project were performed by Dr. Anzhalika Sidarovich. **Cp028** was found to significantly inhibit the splicing process at 50 µM after 60 min and to completely stop it at 150 µM (Figure 28a). A dose dependent study was performed and the IC_{50} of **cp028** was determined as 54 ± 4 µM. DMSO was used as negative control at different incubation time points (0, 2, 10 and 60 min). Without any compound treatment the splicing process was still ongoing at 60 minutes, since a faint pre-mRNA band could still be detected. After 60 minutes the bands of the mature mRNA and the intron lariat (two of the splicing products) were clearly observed. Consequently, 60 minutes was chosen as the reaction time and **cp028** was assayed in different concentrations (from 10 to 175 µM) with 60 minutes of incubation time. At 50 µM compound treatment, the bands for mature mRNA and for the intron lariat became very faint. At higher compound concentrations the pre-mRNA band becomes bigger until 150/175 µM where all the nucleic acid accumulated at the pre-mRNA and no conversion to the splicing products could be observed.

Cp028 contains a strong Michael acceptor, which is commonly viewed as a pan assay interference compound (PAIN).[112] However, the aim of this project was to identify a small molecule tool to study the splicing process in vitro and thus the potential promiscuity of the compound may not be detrimental.
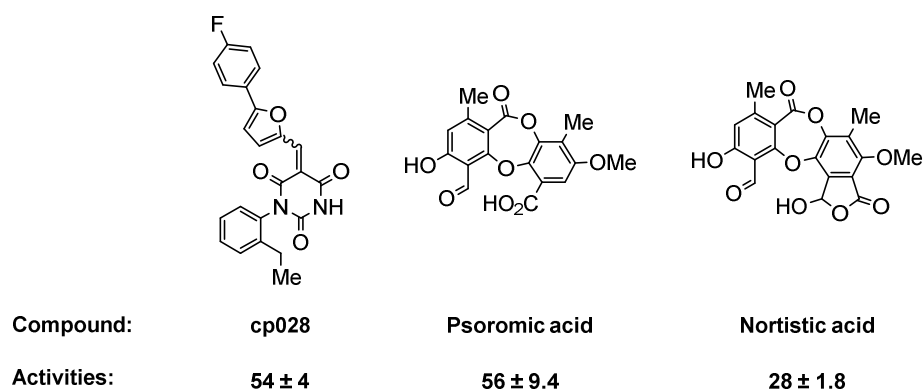

Compound:	cp028	Psoromic acid	Nortistic acid
Activities:	54 ± 4	56 ± 9.4	28 ± 1.8

Figure 27. Examples of identified splicing inhibitors in the HTS. Activities shown as IC_{50} (µM)$\pm$ S.D. (n $\geq$ 3).

84

A titration assay was run by Dr. Anzhalika Sidarovich to determine the content or stage at which the spliceosome complex was stalled by this novel inhibitor (Figure 28b).On the DMSO lane (negative control) the different stages of the spliceosome, according to the different time points, can be seen. After 2 minutes, the main complex formed was the initial **A** complex, at 10 min complexes **B** and **C** started to appear and after 60 minutes the spliceosome showed a mixture of complexes albeit with most of the splicing process having been completed already. When **cp028** was assayed at 60 min, a difference with the dmso control could be detected around 50 µM. This result was in accordance with the splicing activity detected before (Figure 28a). In this titration assay,**cp028** was found to promote the formation of complexes that ran very close to the A and B bands (Figure 28b). The process was therefore stalled somewhere in between complexes A and B. For future references the stalled identified complex was referred to as B^{028}.
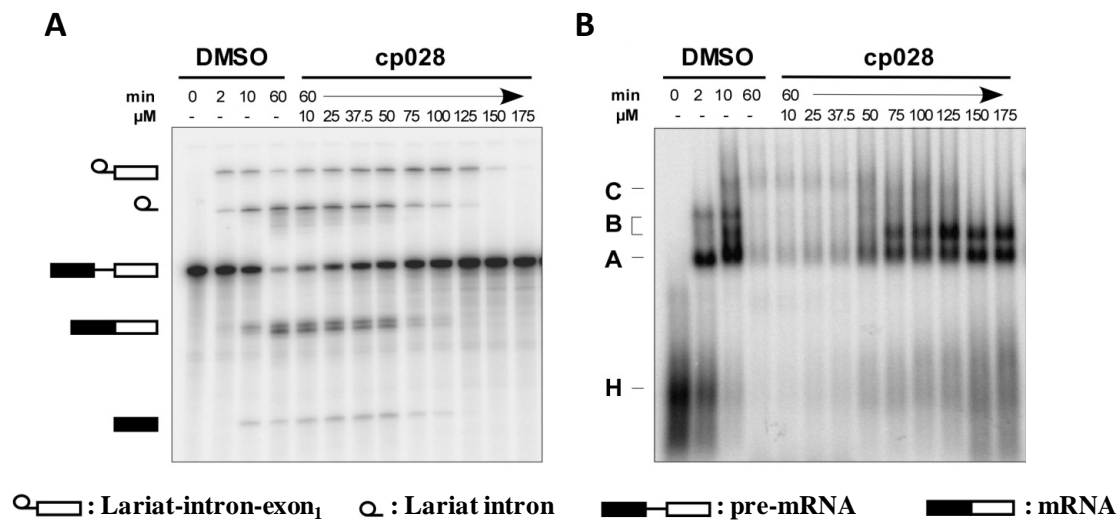

Figure 28.a) Dose-dependent inhibition of the splicing complex by **cp028** (14 % denaturing PAGE). **b)** Titration of the stalled spliceosome with **cp028** at different concentrations (1.5 % native agarose gel).

Due to, among other things, the lack of efficient inhibitors, the splicing process is still not fully understood and much remains to be investigated. Development of new compounds, such as **cp028**, that enable the study of other splicing stages is a powerful tool in the study of the spliceosome. B^{028} represents a novel stage of the splicing process that could be identified and isolated. Consequently, I was encouraged to further study the effects and pursue the class of compounds represented by **cp028**.

7.2. Synthetic Route for Cp028 and Analogues

The characterisation of the novel B^{028} spliceosome stage encouraged me to build small library of analogues in order to establish a SAR analysis around the **cp028**core. The synthetic route was designed based on similar compounds present in the literature.[113-114] A convergent route in which an aldehyde-barbituric acid condensation would represent the final step of the synthesis, was envisioned (Scheme 18). The barbituric core could be built from the urea that in turn could be synthesized from the commercially available aniline. Furthermore, the phenyl-furfural aldehyde could be synthesised in a cross coupling reaction with the commercially available 5-bromofurfural and 4-fluorophenylboronic acid.
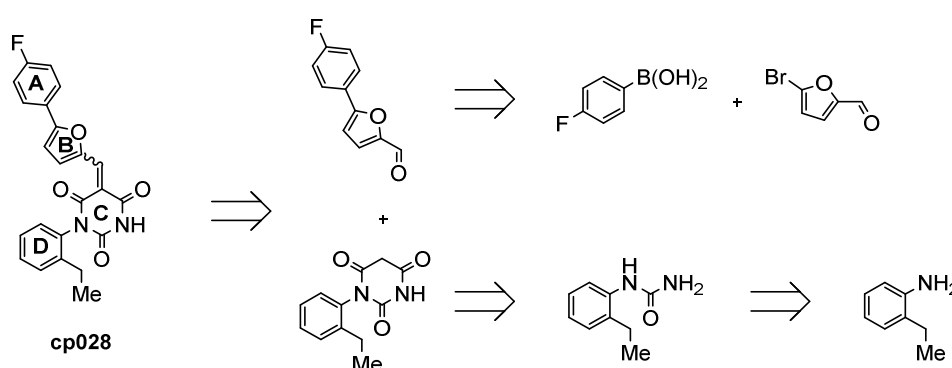
Scheme 18. Retrosynthesis for **cp028**.

This route would allow for an easy introduction of modifications in both halves. Specifically, ring **A**could be readily modified with a set of diverse aryl boronic acids. According to the proposed retrosynthesis **cp028** was synthesised in 4 steps with an overall yield of 26% (Scheme 19). Commercially available 2-ethyl aniline was transformed into the urea with potassium isocyanate.[115] Subsequently, the barbituric ring was constructed with diethyl malonate in refluxing ethanol in the presence on sodium metal to afford **157**. Finally, compound **157** was condensed in refluxing ethanol with aldehyde **160,** which was readily obtained by Suzuki cross coupling of 5-bromofurfural and the corresponding fluorophenylboronic acid.
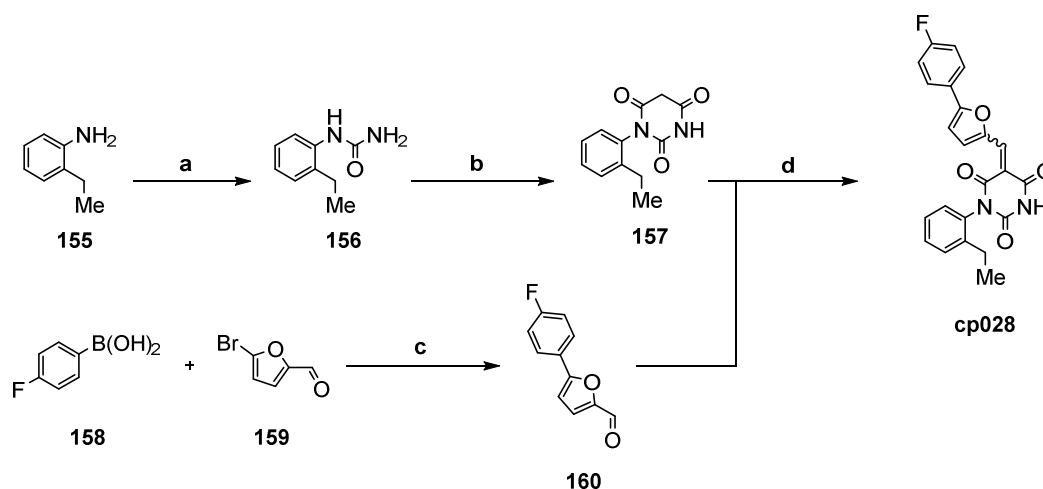
Scheme 19. Synthesis of **cp028**; **a)** KNCO, AcOH/H$_2$O, 4 h, r.t., 62%;**b)** Diethyl malonate, Na, EtOH, 80º, 12 h, 53%;**c)**Pd(OAc)$_2$, K$_2$CO$_3$, NBnMe$_3$Br, 16 h, r.t., 98%;**d)** EtOH, 80º, 12 h, 78%.

The synthesised batch for **cp028** was tested in vitro in the ^{32}P assay (Figure 29). The compound showed interference with the spliceosome as expected, and in a similar potency to the commercial batch. At 150 µM the main band is the pre-mRNA, although faint lariat and mature mRNA can be seen.
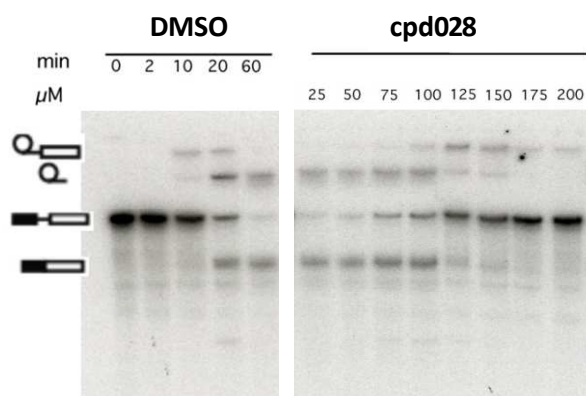
Figure 29. Validation of the splicing activity of the synthesised batch of **cp028**. 14% denaturing PAGE;**cp028**ran with t = 60min; [a]: Synthesised batch; Assay performed by Dr. Anzhalika Sidarovich.

7.3. 1st SAR Round of Cp028 Analogues

With the established synthesis in hand, I set to out to create a small library around the **cp028**core.

7.3.1. Potential covalent inhibitor

First, I decided to explore if the Michael acceptor moiety was essential for the splicing inhibition activity, as it would be for a covalent inhibitor. Compound **161** was hence synthesised from **cp028** by simple reduction of the α,ß-unsaturated barbituric core with sodium borohydride (Figure 30a). Compound **161** has lost its Michael acceptor and cannot, therefore, be attacked by a nucleophile anymore.
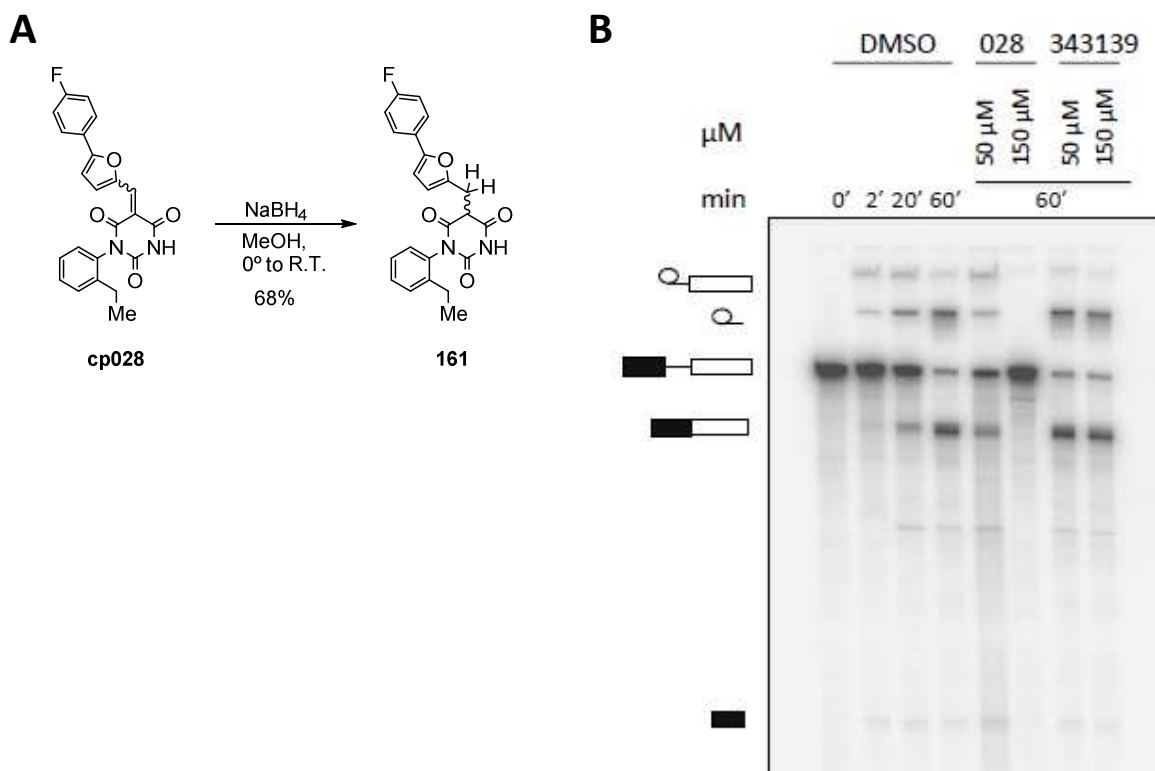

Figure 30. a) Reduction of the α,ß-unsaturated barbituric electrophile; **b)** Activity assay gel for compound 161. Lanes 028 = **cp028**; Lanes 343139 = **161**; 14 % denaturing PAGE. Compounds ran at 50 µM after 60 min of incubation. Assay performed by Dr. AnzhalikaSidarovich.

When compound **161** was assayed for splicing activity, a great loss of potency was observed (Figure 30b). In the gel, **cp028**(lanes 028) showed the expected significant band of the pre-mRNA at 50 µM and the complete accumulation of this band at 150 µM, while the **161** (lanes 343139) displayed a faint pre-mRNA band in both cases (in the range of the DMSO t_{60} band) and accumulation on the splicing product bands (the mature m-RNA and the intron lariat). Since the structural difference between **cp028**and **161**, although not negligible, is not too great, the

significant loss in activity found for the reduced analogue strongly suggested that **cp028** was acting as a covalent inhibitor.

7.3.2.SAR analysis for the synthesised analogues

For the study of the ring **A** of **cp028** a series of aryl boronic acids were introduced into the general synthetic route of **cp028** (Scheme 19). First the corresponding arylfurfurals were synthesised by Suzuki cross coupling and subsequently the condensation with the barbituric acid **157** afforded the final analogues (Figure 31). For two examples, **173** and **174** the phenyl aldehydes were directly condensated with the barbituric core to explore the need of the furan ring for activity.
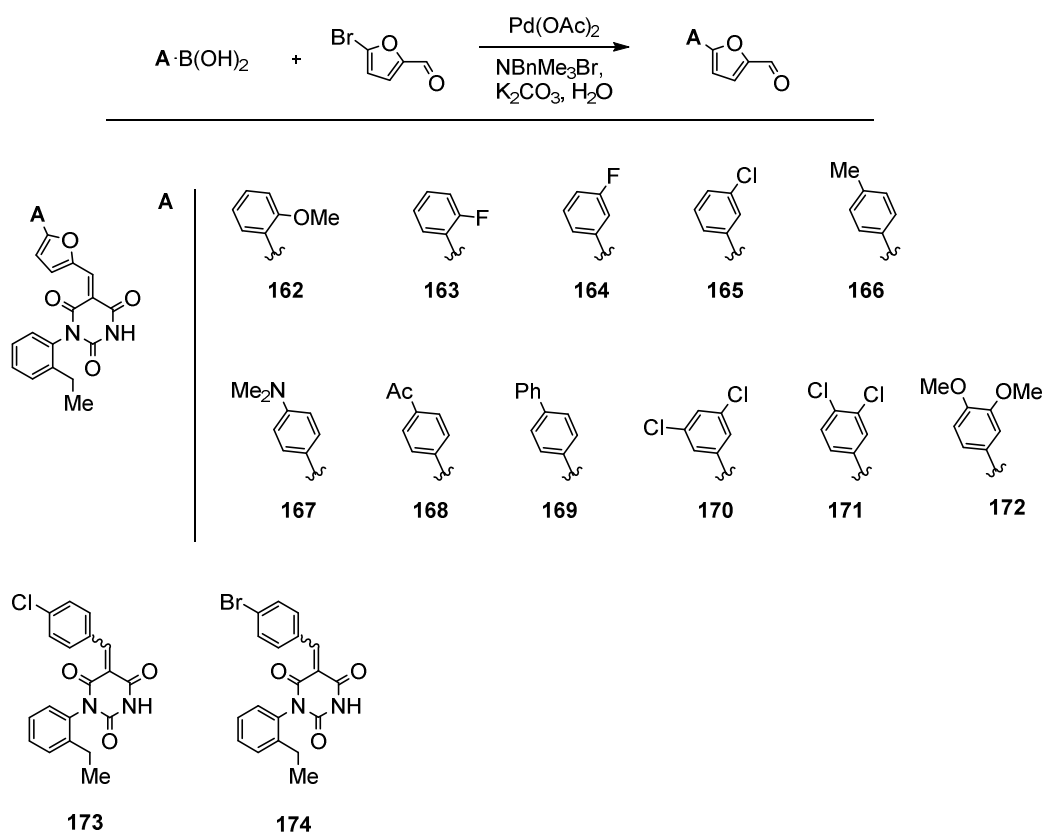
Figure 31. Synthesis of a set of **cp028** analogues.

The synthesised analogues were submitted to the ^{32}P splicing test to determine their activities (Figure 32). The assayed compounds can be compared to the DMSO as negative control and to the **cp028** at 50 and 150 µM (lanes: 028, original, 50µM and 028, original, 150µM).
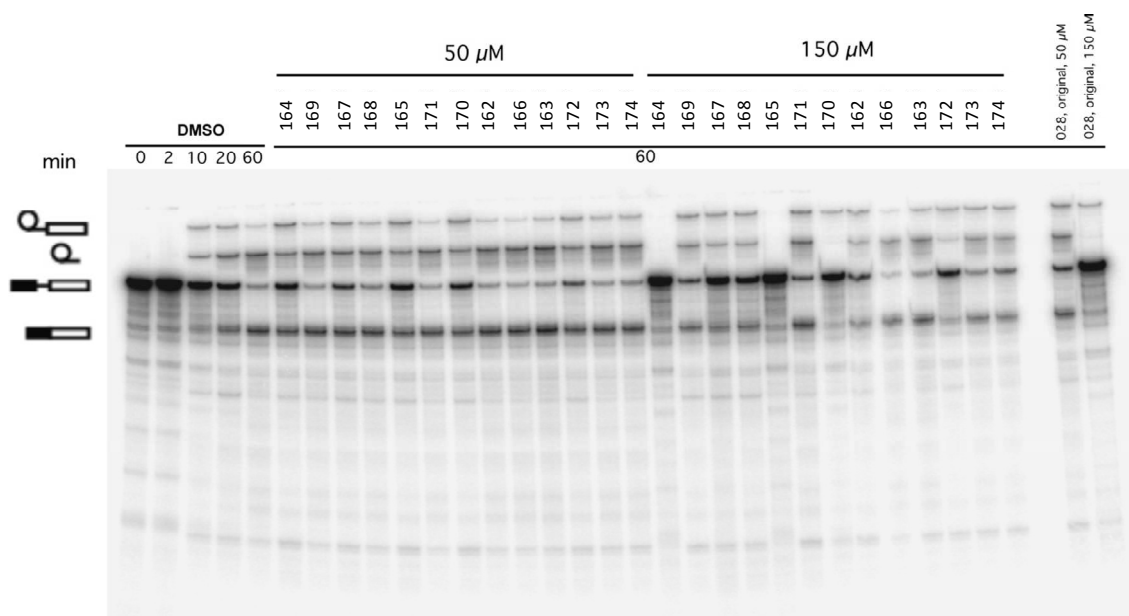
Figure 32. Splicing inhibiting activities of the synthesised analogues at 50 and 150 µM. 14 % denaturing PAGE.Compounds ran with t = 60min. Assay performed by Dr. Anzhalika Sidarovich.

In order to obtain more reliable activity information, the gel was submitted to software quantification to obtain residual splicing activity values for both 50 and 150 µM concentrations of compound treatment. For this purpose the free software Image J was used. The band selected for the quantification was the pre-mRNA band, but the results obtained for the intron lariat band were in accordance to the pre-mRNA band. The results were plotted in a table for an easy visual comparison (Figure 33).
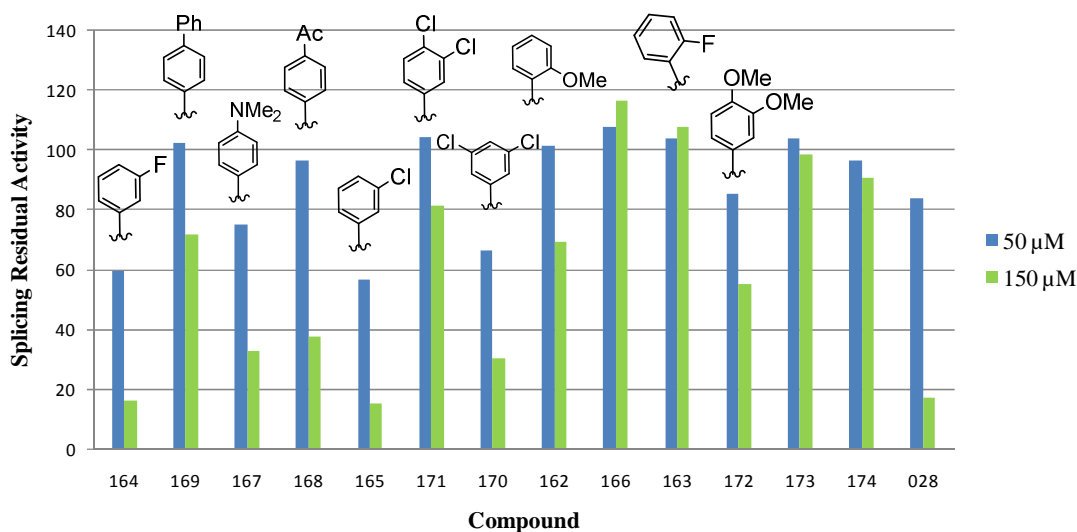
Figure 33. Splicing residual activities for the synthesised analogues of **cp028**. Values normalized to 0% = DMSO t(0 min) and 100% = DMSO t(60 min); The values were obtained from the pre-mRNA band with the ImageJ software.

The information withdrawn from this plot was carefully interpreted. The activity values extracted from the gel with the software allowed for a more precise comparison than simple observation, nevertheless a significant statistical value cannot be obtained and consequently comparison between close values could not be adequately done, for example between analogues **164** and **165**. However, considerable differences in activities were used to gain structural-activity-relationship insight.

Firstly, the removal of the furan ring (ring **B)** of analogues **173** and **174** resulted in almost a complete loss of activity (Figure 33). When comparing the 50 µM value for the *para*-fluoro substitution on **cp028** and the *meta*-fluoro and -chloro substitutions on **164** and **165** I learned that *meta* substitution had a slight positive effect compared to the *para* substitution of the ring **A** in **cp028**. Compound **170** containing two chlorine substitutions on the *meta* positions did, however, displayed a slightly decreased potency. **171** on the other hand, with a *m,p*-dichloro substitution, displayed a much more significant loss in activity, pointing to the deleterious effect of the substitution on the *para* position. This was in accordance with the *para* substitutions of compounds **167**, **168**, and **169** that displayed much lower activities. Furthermore, compound **166** with *p*-Me did not show any activity at all. Substitution on the *ortho* position had a strong detrimental effect on the activities as demonstrated by analogues **162** and **163**. Due to the

commercial availability of this compound class, the rest of the SAR was performed from a purchased set of analogues, where substitution of the **D** ring was mainly explored.

7.3.3. SAR analysis for the commercial set of analogues

In order to obtain further SAR insight a set of commercial analogues was purchased from ChemDiv (Figure 34). The Michael acceptor character on the barbituric core was maintained throughout. Different substitutions patterns were introduced on the **D** ring in analogues **175** to **185.** To check if ring **A** was essential for activity, compounds **188** and **189** were purchased. Compounds **190**, **191** and **192** were purchased to check the effect of aryl disubstituted ureas coupled with loss of the ring **A**.
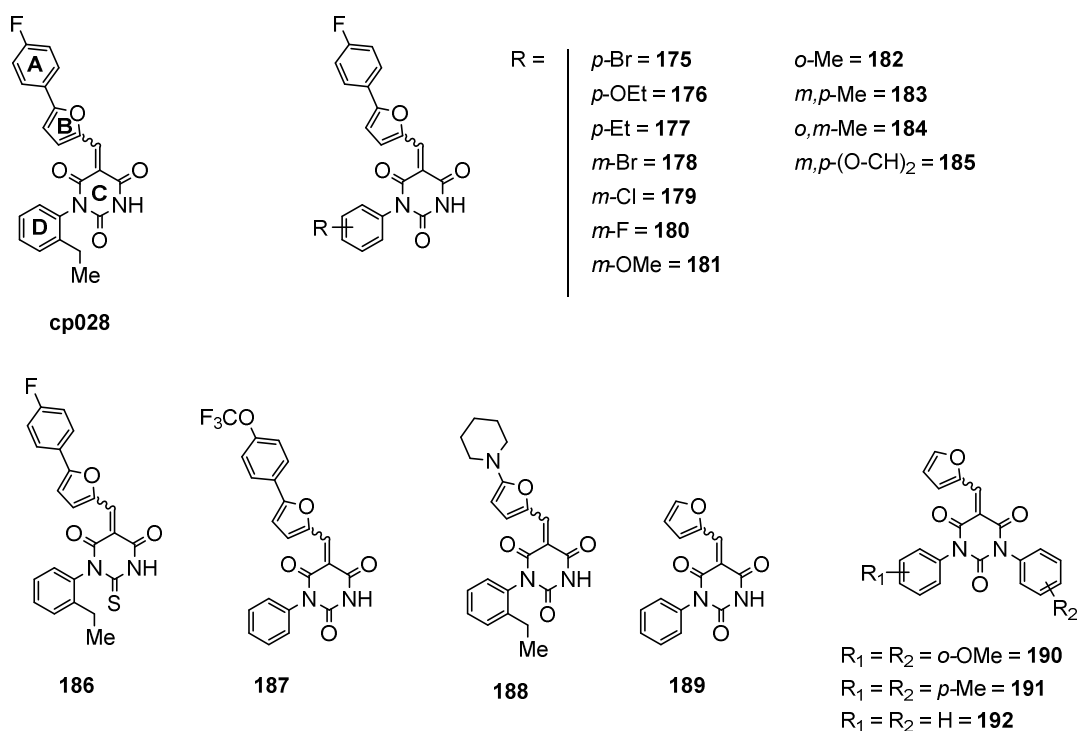
Figure 34. Commercial set of analogues of **cp028**.

The activities of the purchased compounds were also assayed by the in vitro splicing assay (Figure 35) and the activity values were obtained by software quantification of the pre-mRNA band on the gel (Figure 36), although at simple observation many changes in activity could already be identified.
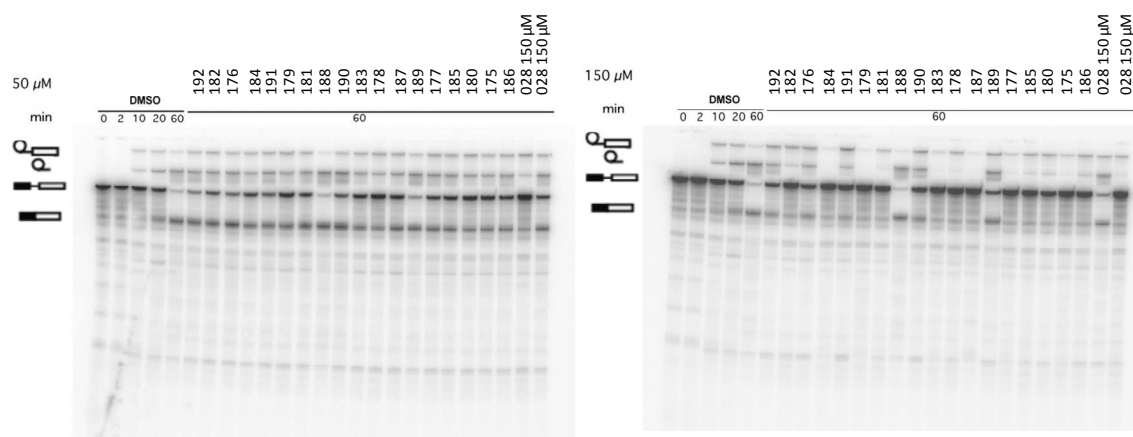
Figure 35. Splicing inhibiting activities of the commercial analogues at 50 and 150 µM. 14 % denaturing PAGE; compounds ran with t = 60min. Assay performed by Dr. AnzhalikaSidarovich.

Here, the activity of **cp028** was lower than in previous experiments, however the data could be used to compare the compounds within each set. When the fluorophenyl group (ring **A**) was exchanged by a piperidine on **188**, it resulted in almost complete inactivity (Figure 36). Complete removal of this ring also resulted in a significant potency loss, as observed for compound **189**.In this series, many analogues displayed very similar potencies to **cp028**. Nevertheless, compounds **178** and **179**, that contained *meta* substitutions of halogens Cl and Br on the ring **D**, seemed to display slightly better activities, particularly when the band for 50 µM concentration was observed. Interestingly, compound **191**, a disubstituted urea lacking the ring **A,** maintained the high potency of **cp028**, but similar compounds like **190** and **192** showed a considerable loss of activity. For ring **D**, *para* substitution seemed to be in the same range of potency as the original *ortho*, as seen for the ethyl substitution on **177** and **cp028**and for the bromine substitution on **175** and **178**.
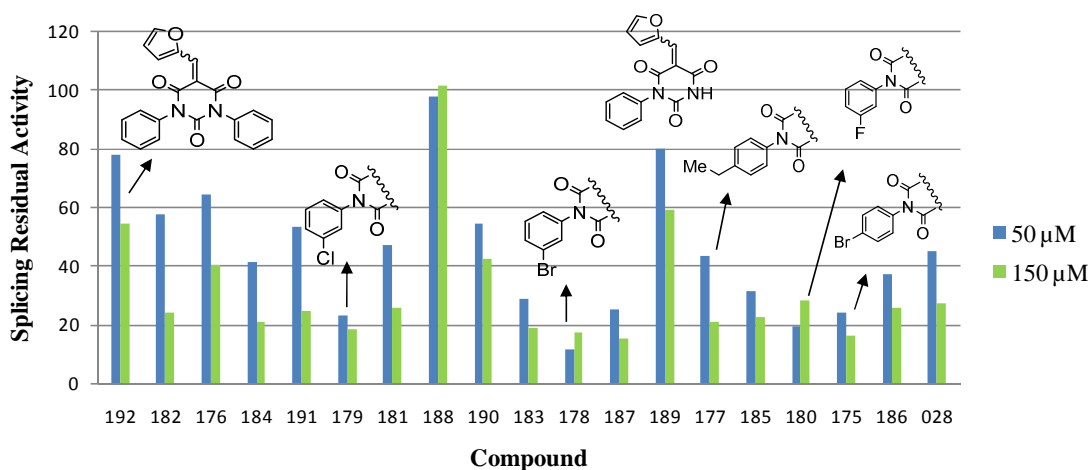
Figure 36. Splicing residual activities for the purchased analogues of **cp028**. Values normalized to 0% = DMSO t(0 min) and 100% = DMSO t(60 min); The values were obtained from the pre-mRNA band on the gel on Figure 30 with the ImageJ software.

For this set of analogues some SAR data could be withdrawn based on the calculated activities. Introduction of a halogen on the **D** ring and possibly on the *meta* position, was found to increase the activity of the **cp028** and was therefore selected for the next SAR round.

In conclusion, the SAR data obtained for this scaffold so far was not very powerful but some insight was gained. The substitution on *meta* position of the ring **A** displayed better potencies, the same was observed for ring **D** but to a lesser extent. Removal of rings **A** or **B**, had a detrimental effect on potency leading to inactive or very weakly active splicing inhibitors. Taken altogether, these results suggest that **cp028** does not inhibit the splicing process by indiscriminately reacting with the proteins but rather an affinity for one or multiple binding pockets is needed before the compound is, most probably, attacked and covalently bound.

7.4. 2nd SAR Round of Cp028 Analogues

Based on the data obtained for the initial round of synthesised and purchased analogues, a second round of analogues was synthesised combining the identified most active substitutions. This would potentially lead to higher potencies for this compound class. Four compounds were synthesised following the same synthetic route (Scheme 19). Since the changes on ring **D** did not seem to have a strong effect, it was not further explored. Instead, the presumably most potent substitution pattern, the *m*-Br (**178**, Figure 34) was used for the synthesis of all four

compounds, and combined with different **A** rings (Figure 37a). Besides chloro and bromo, OCF$_3$ was introduced on the *meta* position to determine the potency. Although expected to display a lower activity due to the substituted *para* position, **195** was also submitted for the splicing inhibiting in vitro assay. The *m*-Br urea intermediate was synthesised according to the reported procedure by Laudien et al.,[115] and the necessary aldehydes were synthesised in the same fashion as the general synthesis for **cp028**.
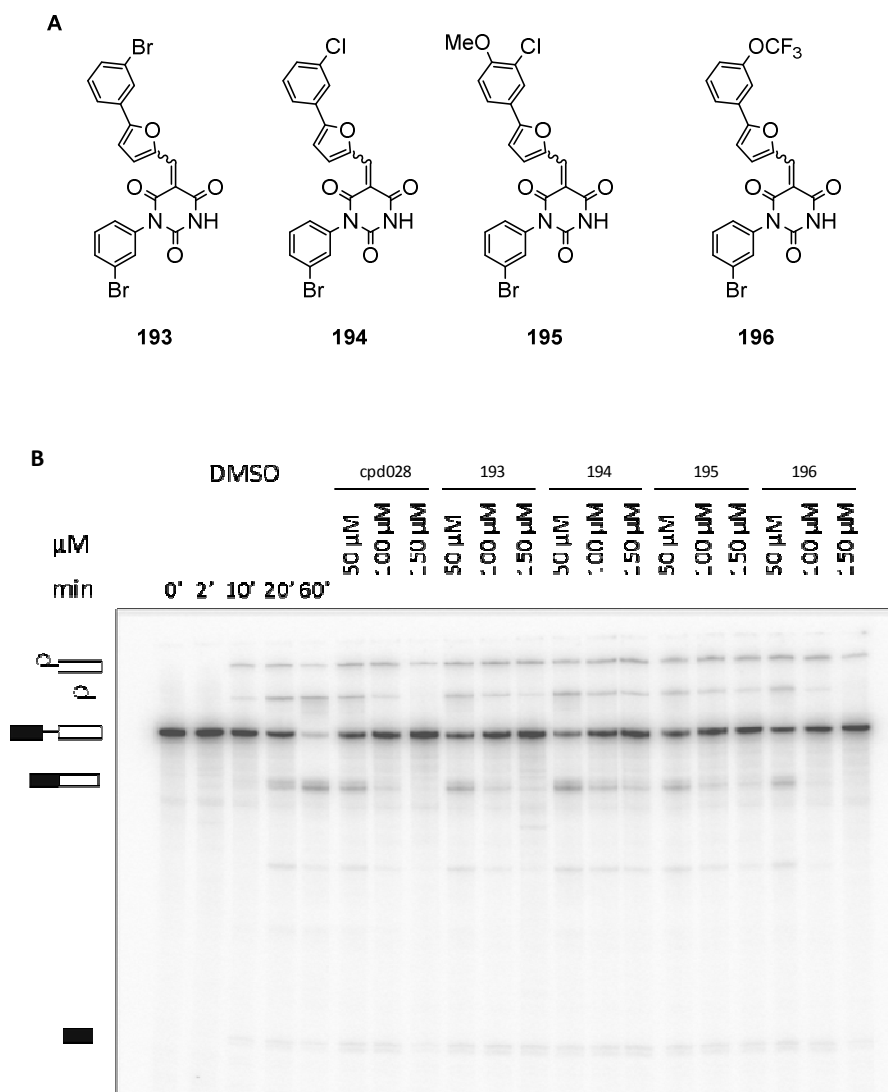
Figure 37. a) Synthesised analogues for the 2nd SAR round. **b)** Splicing inhibiting activities of the 2nd SAR round at 50 and 150 µM. 14 % denaturing PAGE; compounds ran with t = 60min. Assay performed by Dr. AnzhalikaSidarovich.

Compound **193** and **194** did, however, not show the expected higher activities than the **cp028** (Figure 38). Both analogues displayed lower potency easily identified in the intron lariat band of

the gel (Figure 37b). **195** did show the expected lower activity. The combination of a *m*-trifluoromethoxy group on ring **A** and the *m*-bromo group on ring **D** (**196**), displayed a slightly higher activity than **cp028**. Overall, the activity changes were not significant after the second round of SAR and it was decided not to pursue any further SAR studies.

To further explore this class of compounds as splicing inhibitors, **cp028** remained the compound of choice. The potency of other analogues was in the same range and thus did not warrant a change in the compound of choice to further study effects on the splicing process.
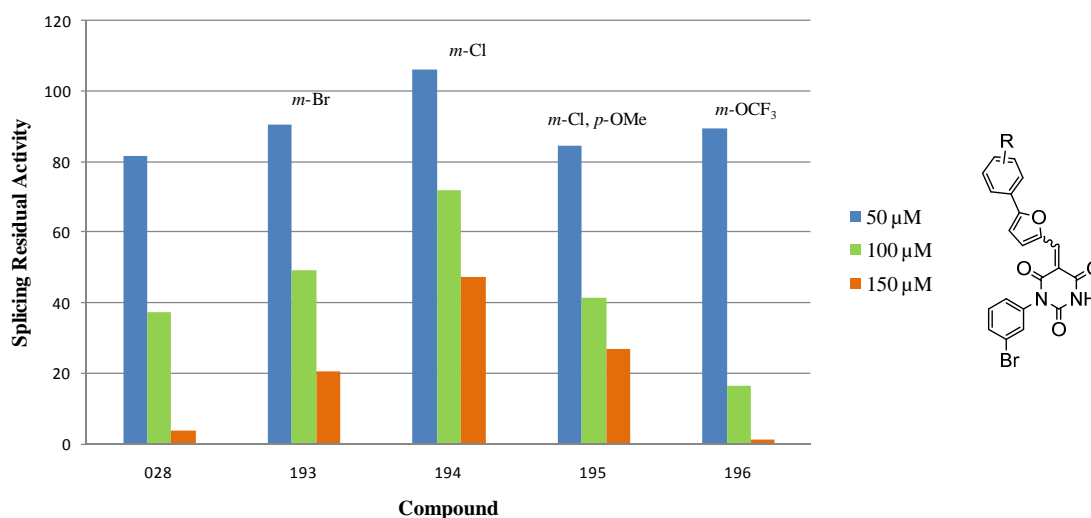
Figure 38. Splicing residual activities for the 2nd round of synthesised analogues. Values normalized to 0% = DMSO t(0 min) and 100% = DMSO t(60 min); The values were obtained from the intron lariat band from the gel on Figure 15 with the ImageJ software.

7.5. Target Identification of Cp028

The splicing process occurs in the cell nucleus and a wide set of proteins is involved. Although many of the protein players have been identified, much remains to be explored. The use of compounds that inhibit this process is a powerful tool to identify key players of the splicing machinery by identifying their targets. In my case, **cp028** stalled the process, presumably by targeting one or multiple enzymes that are required for the splicing process. It was therefore of high interest to me to identify the target(s) of our novel splicing inhibitor.

7.5.1. Synthesis of chemical probes based on cp028

The manageable nuclear proteome compared to the whole cell encouraged me to attempt a "pull-down" approach to identify the target(s). Furthermore, **cp028** bound, most likely,

covalently to its target(s), which would simplify the "pull-down" approach even further. The use of covalent inhibitors allows for a more stringent wash of pull-down beads and consequently the results usually contain a lower background and lower unspecific binding. For the purpose of performing a pull-down assay, I set out to synthesise active and inactive chemical probes based on the **cp028** scaffold.
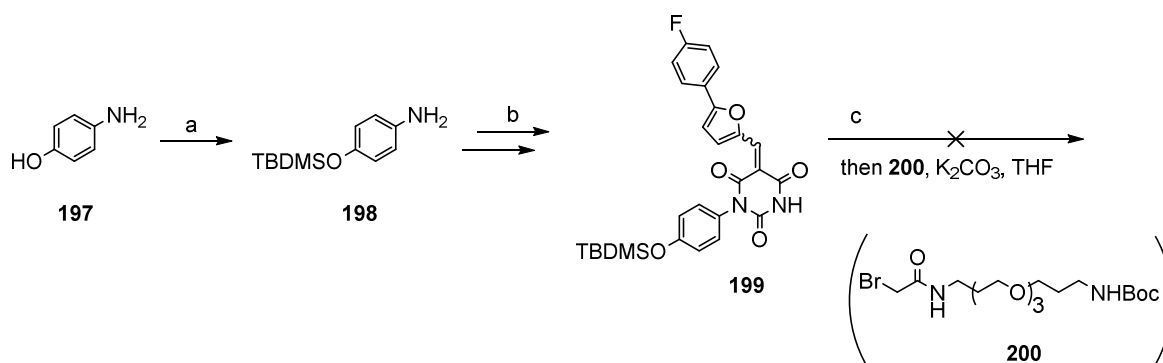
Scheme 20. Synthesis attempts to a **cp028** probe (1). **a)** TBDMS-Cl, imidazole, THF, r.t., 66%; **b)**The corresponding steps of the **cp028** synthesis were taken (Scheme 2); **c)** TBAF, THF, r.t.

Initally, the 4-position of the **D** ring was selected as a linker attachment point. This position was shown not to significantly alter the potency when substituted. Furthermore, it was easily accessible from the commercial aniline. Hence, 4-amiphenol was used as a starting material and upon silyl protection of the phenol, the general synthetic route towards **cp028** was applied to yield **199** (Scheme 20). Unfortunately, attempts to alkylate the phenolic position, after silyl deprotection, were not successful.

The NH position of the urea was then explored. It was known from the SAR analysis that the functionalisation of that position did not necessarily damage the activity of the compound (see analogue **191**, Figures 34 and 36). As a trial, this position was methylated in an efficient manner by methyl iodide in DMF at 85º using sodium hydride as a base (Scheme 21a).
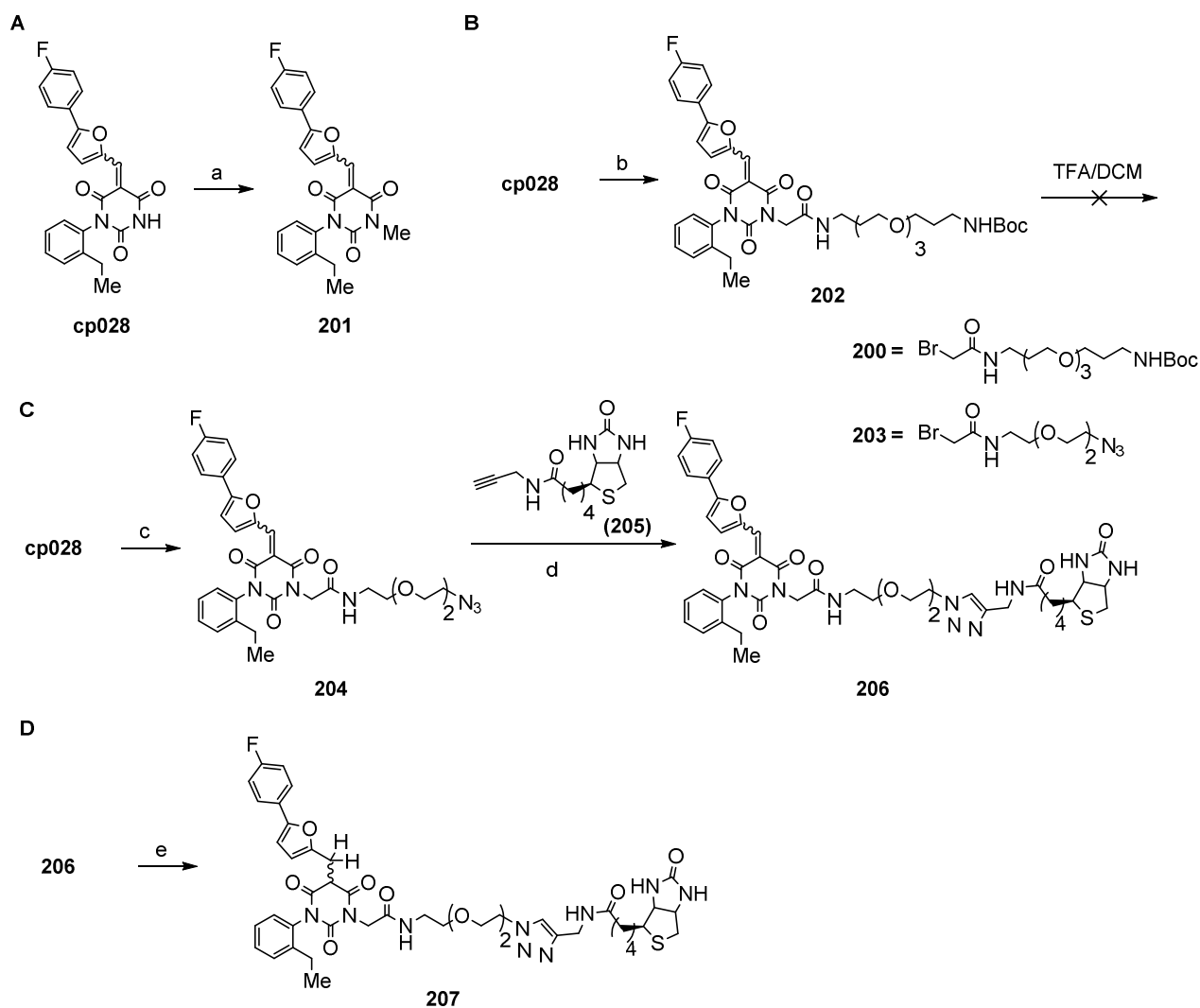
Scheme 21. Synthesis attempts to a **cp028** probe (2). a) MeI, NaH, DMF, 85°, 2h, 69%; b) 200, NaH, DMF, 85°, 16 h, 43%; c) 203, NaH, DMF, 85°, 16h, 19%; d) CuSO$_4$.5H$_2$O, sodium ascorbate, tBuOH/H$_2$O, r.t., 20 h, 10.4%. e) NaBH$_4$, MeOH, 0 °C to r.t., 3 h, 8%. Compounds 203 and 205 were provided by Dr. Andrei Ursu.

Since the alkylation reaction was successful, I then introduced the iodide PEG linker **200** with the same conditions but a large excess of the linker had to be used to achieve a good conversion towards **202** (Scheme 21b). However, when attempting to remove the Boc group, the compound displayed stability problems and the free amine could not be isolated. The probe designed was to carry a biotin group at the end of the linker which added extra steps to this route. Due to the very poor solubility, after each step the compounds had to be purified by preparative-HPLC and in consequence the yields dropped, making it very difficult to continue the synthesis on such a small scale. It was therefore decided to install an azide-bearing linker that would later react with an alkyne-bearing biotin in a copper catalyzed cycloaddition. **Cp028** was then alkylated with azide **203** and subsequently reacted with alkyne-biotin conjugate to afford the active probe **206**

(Scheme 21c). In order to obtain the inactive probe, the active one was readily reduced following the procedure for compound **161** (Scheme 21d).

With both chemical probes in hand, the compounds´ ability to inhibit the splicing process was checked (Figure 39).The difference in activity between both probes is easily noticeable when I observe the intron lariat band: in the case of the active probe this band disappeared at concentrations higher than 100 µM while in the inactive probe this band was still present until 450/500 µM. As expected, the active probe lost some activity compared to **cp028**. This loss in activity can be observed when the control band of **cp028** at 175 µM is compared with the 200 µM band of the active probe. In the first, there was no splicing products while in the second, a faint lariat intron-exon$_1$ band was still noticeable. The potency of the active probe was, however, considered to be enough to be used in target identification experiments.
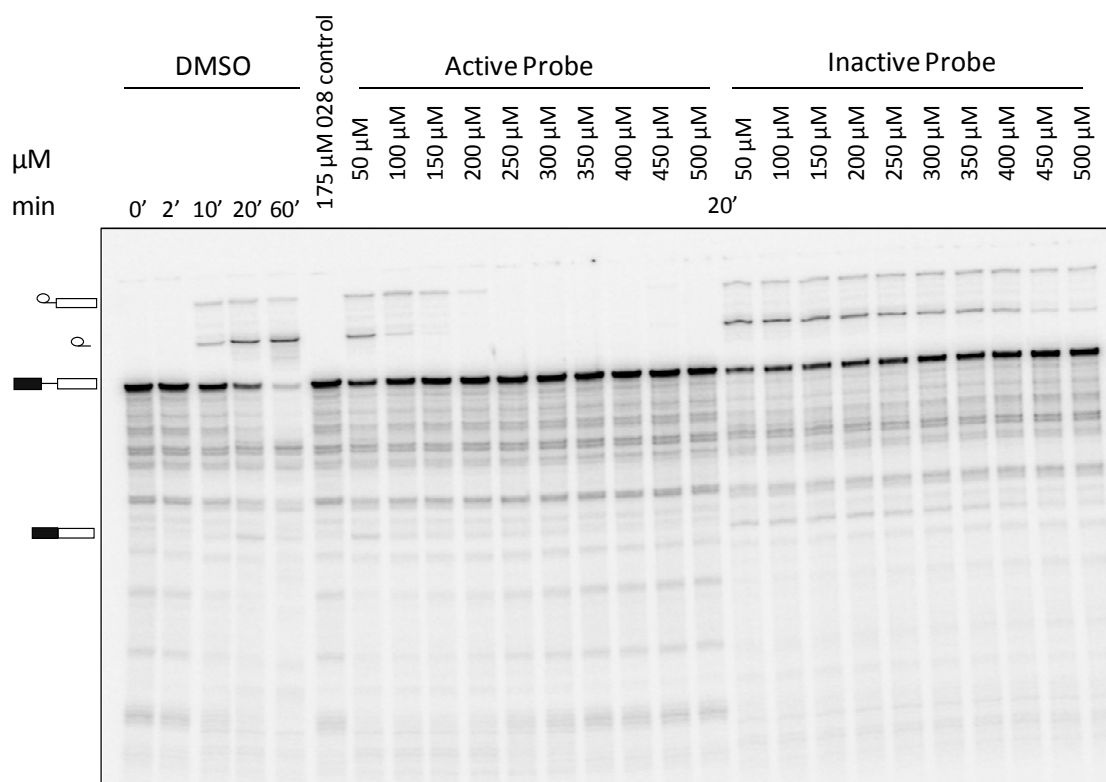

Figure 39. Splicing inhibiting activities of the **cp028**-based chemical probes. 14 % denaturing PAGE; compounds ran with t = 20min. Active Probe = S54, Inactive Probe = S55; Assay performed by Dr. Anzhalika Sidarovich.

7.5.2.Affinity-based proteomics

With the probes in hand, an affinity-based proteomics assay (pull-down assay) with the nuclear extract of HeLa cells was performed. Initially, streptavidin-agarose solid support was used. The inactive probe was incubated with the nuclear extract and washed with a range of salt concentrations but the background intensity was considered too high to identify any targets (Figure 40a). Consequently, magnetic Dyna-beads were tried to try to lower the background (unselective binding of proteins to the beads). However, the magnetic beads afforded a very high background as well (Figure 40b). The resulting gels of the Dyna-beads pull-downs were submitted for mass spectrometry analysis. None of the identified protein was significantly more present when the active probe was used.
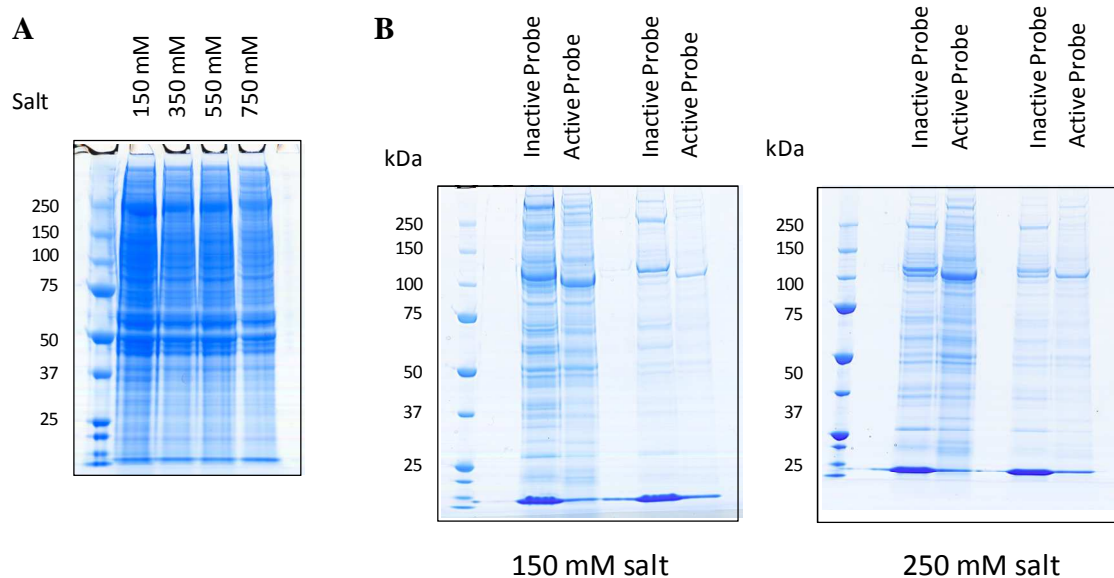
Figure 40. a) Pull-down with inactive probe with agarose streptavidin beads at different salt concentrations. **b)** Pull-down with active and inactive probes with Dyna-magnetic beads at different salt concentrations. Experiments performed by Anzhalika Sidarovich.

The pull-down experiments needed to be further explored and optimized before reaching any conclusions on the mass spectrometry data. At the same time a different approach for target identification was envisioned and it will be discussed in the following section.

7.5.3.Targeting kinases involved in the splicing process

The spliceosome complex at which **cp028** stalled the process is a stage where the next catalysed step has been identified to require several kinases.[110, 116] Furthermore, the structure of **cp028** with a sequence of hydrogen-donor and acceptor on the barbituric core led me to speculate that

it may be a kinase inhibitor. Consequently, a panel of potential kinase targets was selected for commercial screening. The compound was tested in an activity Z´-LYTE assay (the ability to phosphorylate a FRET-peptide is assayed) or in a Lanthascreen binding assay (the ability to displace a known inhibitor coupled to a FRET emissor is assayed) (Table 19). In the case of the activity assay, the ATP concentration was set to the Km apparent value (with the exception of NEK2 where it was set to 100 µM). The potential interference of the FRET pairs (donor: coumarin, acceptor: Fluorescein) was monitored, as well as the interference with the development reaction of the Z´-LYTE assay.

Table 19. Examples of the kinase panel assayed for **cp028**.

Kinase	ATPconc.	Technology	Z'	Inhibition (%)
AKT2 (PKB beta)	Km app	ZLYTE	0.85	92
CDK2/cyclin A	Km app	ZLYTE	0.79	Re5
CLK1	Km app	ZLYTE	0.78	82
CLK2	Km app	ZLYTE	0.8	47
CLK3	Km app	ZLYTE	0.86	87
DYRK1A	Km app	ZLYTE	0.92	22
DYRK1B	Km app	ZLYTE	0.9	62
DYRK3	Km app	ZLYTE	0.85	94
DYRK4	Km app	ZLYTE	0.95	48
GSK3A (GSK3 s)	Km app	ZLYTE	0.93	92
GSK3B (GSK3 beta)	Km app	ZLYTE	0.9	93
MAP2K6 (MKK6)	100	ZLYTE	0.9	97
NEK2	Km app	ZLYTE	0.53	90
PRKACA (PKA)	Km app	ZLYTE	0.87	31
SRPK1	Km app	ZLYTE	0.88	85
SRPK2	Km app	ZLYTE	0.55	72
STK23 (MSSK1)	Km app	ZLYTE	0.85	95
CDK11 (Inactive)	n.a.	LanthaScreen	0.76	85
DYRK2	n.a.	LanthaScreen	0.54	16
PRKACB (PRKAC beta)	n.a.	LanthaScreen	0.86	2

cp028 concentration: 50 µM;Inhibition (%) values n=2; In red are the inhibition activity values over 80%;n.a.: not applicable; Assay outsourced to a company.

Several enzymes of the panel selected were inhibited by **cp028** (Table 19). Interestingly, several of the kinases found were recently identified as part of the Kinase Cysteinome.[117] The kinase cysteinome is a computer generated group that comprises the kinases that posses a cysteine residue close to the active site of the enzyme that upon interaction with covalent inhibitor may impair the enzymatic function. Since, as established before, the highly electrophilic character of **cp028** is essential for the splicing inhibiting activity, it is very likely that the compound impaired the function of these spliceosome-related enzymes in such a way.

The kinases that were inhibited over 60% were further assayed to determine the IC_{50} values in a concentration range of 2.5 nM to 50 µM (Table 20). Interestingly, from the thirteen kinases submitted to dose-dependent studies four of them displayed IC_{50}s below 1 µM; AKT2, DYRK3, MAP2K6 and NEK2. CDK11 displayed 1.15 µM in the binding assay.

Table 20. IC_{50} determination on selected kinases.

Kinase	ATP conc.	IC50 (µM)
AKT2 (PKB beta)	Km app	0.731
CLK1	Km app	28.2
CLK3	Km app	7.58
DYRK3	Km app	0.294
DYRK3	100	0.611
GSK3A (GSK3 alpha)	Km app	4.26
GSK3B (GSK3 beta)	Km app	2.68
MAP2K6 (MKK6)	100	0.646
NEK2	Km app	0.588
SRPK1	Km app	13.9
SRPK2	Km app	16.4
STK23 (MSSK1)	Km app	2.59
CDK11 (Inactive)	-	1.15

Kinases AKT2, GSK3A, GSK3B, MAP2K6 and NEK2 were identified as members of the Kinase Cysteinome previously described. AKT2 is knwon to phosphorylated the nuclear splicing factor, SRp40,[118] that is required for the binding of the U1 snRNP to the downstream 5´splice site.[119] DYRK3 is known to phosphorylate the SR proteins (serine and arginine rich proteins), which are involved in the RNA splicing.[120] The MAP2K6 (or MKK6) is not only involved in the p38-MAPK pathway that modulates transcription[121] but is also known to interact directly with the splicing factor hnRNP A1 (heterogeneus nuclear ribonucleoprotein).[122] The NEK2 kinases interacts with several splicing factors including SRSF1 and induces the phosphorylation of endogenous SR proteins.[123] Finally, the CDK11 kinase was shown to directly promote the pre-mRNA splicing.[124] It should be noted that the activity values against these kinases is in a different range than the one needed for inhibiting the splicing process. Besides an expected potency drop going from binding/inhibiting kinase assays to the complex in vitro lysate experiments, this effect could also be due to a high promiscuity of the **cp028**. The strong electrophilic character of the dicarbonyl michael acceptor moiety may react indiscriminately with many products resulting in the need for high compound concentrations to efficiently target one or several of these kinases. It is also possible that the responsible target(s) for stalling the splicing process are not among this kinase targets and that **cp028** has a much

lower affinity towards those ones. These kinases would now need to be validated with cell biological assays to confirm their role in the splicing process.

7.6. Characteriazation of the stalled B^{028} spliceosome complex.

Compound **cp028** promoted the formation of stalled B-like spliceosome complex. This complex, named B^{028}, discovered in the group of Prof. Lürhmann, was identified as anovel stage of the spliceosome cycle. The stalled complex is an intermediate complex between the pre-catalytic spliceosomal B complex and the activated B^{act} complex (Figure 23). Studies performed on the stalled complex sheds new light into the snRNPs rearrangements prior to the activation of the spliceosome. This data can be found in the manuscript by Dr. Sidarovich *et al.*[125]

8. Summary of the Thesis

The fact that almost all tumours have increased glucose uptake rates has been known for almost a century, since Nobel laureate Otto Warburg discovered this behaviour. The increase glucose uptake is believed to fuel the anabolic pathways needed for the characteristic rapid cellular growth. Furthermore, this cancer behaviour, known as the Warburg effect, is postulated to have other evolutionary advantages over the healthy surrounding tissues. Despite, the ubiquitous character of the Warburg effect, there has yet to be a treatment that targets the upregulated glucose uptake rates. This is mainly due to the lack of compounds that efficiently target the glucose metabolism and in particular the glucose transporters. This notion has inspired the work of this thesis, in the identification and chemical characterization of novel scaffolds that efficiently inhibit the glucose uptake.

Several scaffolds were identified by means of an automated assay established in the COMAS facilities (Dortmund) by Melanie Schwalfenberg. The assay allowed for the screening of over a hundred thousand compounds, and was based on the uptake of a non-hydrolysable glucose analogue, 2-deoxyglucose. The molecules that were found to significantly inhibit the glucose uptake were grouped into classes according to their structure. The class represented by triazole **5** was further investigated. Several close analogues were purchased and tested in the glucose uptake assay. Triazole **5** was found to be a singleton since no other analogues were found to posses significant activity and further research on this class was hence discontinued.

Another scaffold indentified was the Glupin class. This scaffold was identified as a fusion of tryptamine and morphan. Both this moieties are very present in nature, but the fused Glupin scaffold has, to the best of my knowledge, not yet been detected in nature. In contrast to the more present sp^2-rich drugs, the pursue of more "natural" scaffolds like the Glupins offer a higher success of bioactivity. The Glupin scaffold identified was assayed as a racemic a mixture, which further encouraged me to pursue the synthesis and characterisation of this class.

The synthetic route was envisioned through the synthesis of a ketomorphan ring that would allow for the construction of the indole ring. The morphan bicycle was achieved with an acid-catalysed diastereoselective intramolecular aldol reaction, reported by Bonjoch *et al.* The route required the use of a the protecting group Cbz and afforded the racemic Glupin compounds.
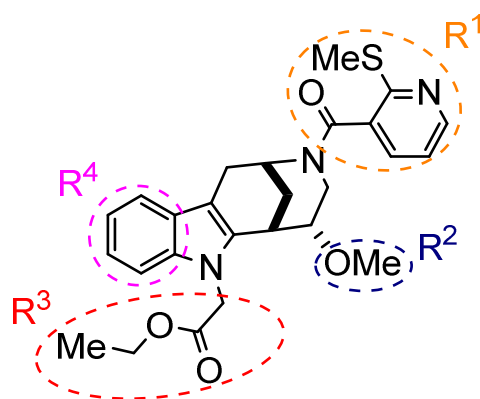
Figure 41. The Glupin analogue **(+/-)**-Glupin-1 and areas selected for modifications.

With the established synthetic route, a library of Glupins was synthesised to generate a structure-activity-relationship analysis. Variations from Glupin-1 (Figure41) were introduced in positions R^1 to R^4 to create a library of over 50 compounds. (+/-)-Glupin-1 was identified as the most potent analogue with an IC_{50} of 50 nM.

The racemic mixture (+/-)-Glupin-1 was separated and the isolated enantiomers displayed an 80-fold difference in activity. **(+)-Glupin-1** was identified as the most potent enantiomer with activities in the single digit nanomolar range. The absolute configuration of the three chiral carbon atoms present in the Glupin class were unambiguously assigned by the use of the chiral derivatising agent, (-)-mandelic acid. The introduction of this agent afforded a diastereomeric mixture that was separated and taken through the Glupin synthesis to obtain two enantiomeric Glupin analogues. The activities of these two enantiomers allowed me to assign the absolute configurations of **(+)-Glupin-1.**
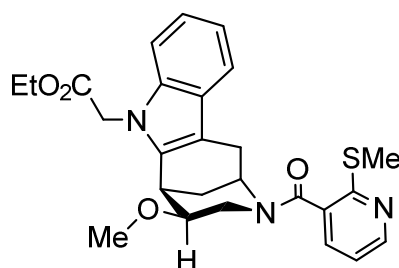
(+)-Glupin-1

Based on the SAR analysis, R^2 was selected for the synthesis of a Glupin-based chemical probe. The active probe retained a very high activity and was hence used in an affinity-based chromatography assay to identify the Glupin target. Nevertheless, the target could not be identified due to unselective binding of the probe.

(+)-Glupin-1 was further characterised with several biological experiments including proliferation and autophagy inhibition assays, as well as the detection of changes in the glycolytic metabolites resulting from treatment with Glupin-1.

(+)-Glupin-1 has met the expectations envisioned for this project. The compound was identified from an extensively characterised Glupin library. With activities in the low nM range **(+)-Glupin-1** joins a short list of potent glucose uptake inhibitors. The absolute configuration of all chiral carbon atoms could be determined. Finally, Glupin-based chemical probes were synthesised, and the chemical work of this thesis was biologically further studied in a collaborative effort.

The process by which pre-mature messenger RNA is transformed into a mature from ready to be translated is performed by one of the most complex machineries identified in the cells, the spliceosome. The process involves numerous proteins and ribonucleproteins that join to form a complex. This complex goes through a series of stages, each with a different function and composition. The study of this complex has been a challenging task, particularly in the structural biology field. However, the use of compounds that stalled the process at different stages has helped the characterisation of the spliceosome.

In an in-vitro assay developed in-house, several scaffolds that could inhibit the splicing process were identified, among them was compound **cp028**. This inhibitor was found to stalled the splicing process at a previously unknown stage, B^{028}.

Cp028 was successfully validated as a splicing inhibitor. A synthesis was established based on similar reported compounds. A SAR analysis was performed by means of the synthesis and by purchasing some commercially available compounds.
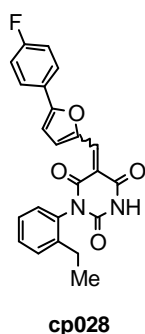
cp028

The library constructed around **cp028** was assayed as splicing inhibitors by an *in vitro* pre-mRNA splicing assay by Dr. Sidarovich. While the compounds provided insightful SAR information, only one of them displayed a higher activity. Compound **196** was to found to be slightly more active than **cp028** as a splicing inhibitor.

In the interest of discovering the mode-of-action, active and inactive probes were synthesised based on the SAR information. Nevertheless, the information obtained in the affinity-based chromatography assays run by Dr. Sidarovich were not conclusive and no protein(s) could be validated as the target(s). However, when **cp028** was assayed against a series of splicing-related kinases, several of them were found to be very sensitive to the compound, with activities below 1 μM. These kinases represent potential key targets in the splicing inhibiting process.

Cp028 was characterised by the chemical work presented in this thesis. A library was created in an attempt to generate more potent analogues. While one analogue displayed a higher activity the increased potency was only slightly higher, remaining the low micromolar range.

9. Experimental Part: Glucose Uptake Inhibition

General Information:

All reactions involving air- or moisture-sensitive reagents or intermediates were carried out in flame-dried glassware under an argon atmosphere. Dry solvents (DMSO, THF, toluene, MeOH, DMF) were used as commercially available. Analytical thin-layer chromatography (TLC) was performed on Merck silica gel aluminum plates with F-254 indicator. Compounds were visualized by irradiation with UV light or potassium permanganate staining. Column chromatography was performed using silica gel Merck 60 (particle size 0.040-0.063 mm). ^{1}H-NMR and ^{13}C-NMR were recorded on a Bruker DRX400 (400 MHz), Bruker DRX500 (500 MHz) and INOVA500 (500 MHz) at 300 K using $CDCl_3$, MeOD or $(CD_3)_2SO$ as solvents. All resonances are reported relative to TMS. Spectra were calibrated relative to solvent's residual proton and carbon chemical shift: CDCl3 (δ=7.26 ppm for ^{1}H NMR and δ=77.16ppm for ^{13}C NMR); (CD3)2SO: δ=2.50 ppm for ^{1}H NMR and δ=39.52 ppm for ^{13}C NMR); MeOD (δ=3.31 ppm for ^{1}H NMR and δ = 49.00ppm for^{13}C NMR). Multiplicities are indicated as: bs (broadened singlet), s (singlet), d (doublet), t (triplet), q (quartet), quin (quintet),m (multiplet); and coupling constants (J) are given in Hertz (Hz). In the NMR spectra where rotameric mixtures are present, the proton signals that split are given as fractions (e.g. 0.5H) so as to easily differentiate which signals split due to the mixture and which don´t. High resolution mass spectra were recorded on a LTQ Orbitrap mass spectrometer coupled to an Acceka HPLC-System (HPLC column: Hypersyl GOLD, 50 mm × 1 mm, particle size 1.9 μm, ionization method: electron spray ionization). Preparative HPLC separations were carried out using a reversed-phase C18 column (RP C18, flow 20.0 mL/min, solvent A: 0.1% TFA in water, solvent B: 0.1% TFA in Acetonitrile, from 10 % B to 100 % B) (some prepHPLC runs were done without TFA).ChiralAll other chemicals and solvents were purchased from Sigma-Aldrich, Fluka, TCI, Acros Organics, ABCR and AlfaAesar. Unless otherwise noted, all commercially available compounds were used as received without further purifications.Amine**56**was synthesised according to the literature procedure.[84] The compounds not included in the experimental part were purchased and used directly.

9.1. Synthesised Compounds

Benzyl (2,2-diethoxyethyl)(1,4-dioxaspiro[4.5]decan-8-yl)carbamate (43):
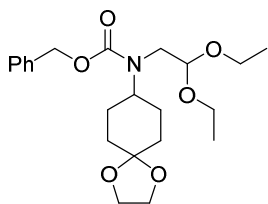
To a solution of amine **56** (10g, 36.58mmol) in MeCN (0,155M), K$_2$CO$_3$ (10.11g, 73.16mmol) and benzyl chloroformate (10.44mL, 73.16mmol) were added at room temperature. The mixture was allowed to stir at room temperature for 12h. Then the solvent was evaporated and the remaining oil was partitioned between brine and DCM. The aqueous phase was extracted twice with DCM and the organic phases were combined. Solvents were removed *in vacuo* to afford the crude product that was further purified by chromatography (2 to 30% ethyl acetate/DCM) to yield compound **43** as a colourless oil (11.18g, 75%). 1H NMR (CDCl$_3$, 400MHz) (rotameric mixture 1:1):δ 1.12 (m, 6H), 1.59-1.78 (m, 8H), 1.88 (m, 2H), 3.25-3.73 (m, 7H), 3.92 (s, 4H), 4.53 (bs, 0.5H), 4.70 (bs, 0.5H), 5.14 (s, 2H), 7.28-7.38 (m, 5H). 13C NMR HRMS: calc. for [M+H]$^+$ C$_{22}$H$_{34}$NO$_6$: 408.23806, found. 408.23844.

(+/-)-Benzyl-4-hydroxy-6-oxo-2-azabicyclo[3.3.1]nonane-2-carboxylate (44):
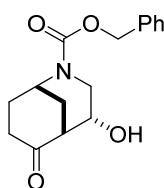
A solution of carbamate **43** (11.18 g, 27.43 mmol) in a mixture of THF (180 mL, 0.15 M) and 10% aqueous HCl (365 mL, 0.075 M) was stirred at room temperature for 3h. The mixture was extracted with DCM and the solvents removed *in vacuo*. The crude product (6.98 g, 88%) contains around 15% of the *syn* diasteroisomer but is pure enough to continue the synthesis. **^{1}H NMR (CDCl$_3$, 400 MHz)** (NMR Spectra shows a 1:1.5 mixture of rotamers plus some *syn* diasteroisomer, data given for the mayor diasteroisomer)**:** 1.91-2.24 (m, 4H), 2.40-2.61 (m, 2H), 2.79 (bs, 1H), 2.88 (t, *J*= 12.3, 1H), 3.01-3.04 (m, 1H), 3.92-4.02 (m, 1H), 4.29 (dd, *J* =13.3, 6.1 Hz, 0.6H), 4.37 (dd, *J*=13.5, 6.1 Hz, 0.4H), 4.52 (bs, 0.4H), 4.63(bs, 0.6H), 5.15 (s, 2H), 7.35 (m, 5H). **^{13}C NMR (CDCl$_3$, 100 MHz):** δ 27.7, 28.7, 29.5, 30.0, 36.9, 38.4, 38.5, 43.7, 44.0, 46.1, 46.3, 49.4, 49.6, 67.6, 67.9, 128.0, 128.1, 128.2, 128.3, 128.7, 136.5, 136.6, 155.5, 212.5, 213.4 **HRMS:** calc. for [M+H]$^+$ C$_{16}$H$_{20}$NO$_4$:290.13868, found:290.13906

(+/-)-Benzyl (2R,5R,6S)-5-hydroxy-1,2,4,5,6,7-hexahydro-3H-2,6-methanoazocino[5,4-b]indole-3-carboxylate (45):
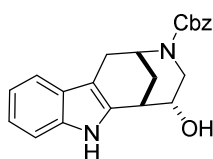
A solution of carbamate **43** (0.558 g, 1.369 mmol) in a mixture of THF (9.1mL, 0.15M) and 10% aqueous HCl (18.3 mL, 0.075M) was stirred at room temperature for 3h before adding phenyl hydrazine (0.135mL, 1.369 mmol). The mixture was extracted with DCM and the solvents removed *in*
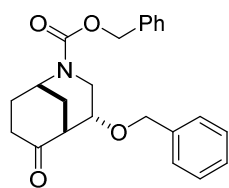
vacuo. Crude product **45** was purified by chromatography (10 to 50% ethyl acetate/DCM) to yield **45** (0.347 g, 70%) as an orange foamy solid. **^{1}H NMR (CDCl$_3$, 400 MHz)** (NMR spectrum shows a 1:1 mixture of rotamers): δ 1.99-2.08 (m, 2H), 2.48-2.59 (m, 1H), 2.81 (t, *J*=18.5 Hz, 1H), 3.08-3.17 (m, 1H), 3.29 (d, *J*=2.3 Hz, 1H), 4.00-4.17 (m, 2H), 4.74 (s, 0.5H), 4.82 (s, 0.5H), 5.13 (d, *J*=4.1 Hz, 1H), 5.19 (s, 1H), 7.11 (t, *J*=7.4 Hz, 1H), 7.17 (t, *J*=8.4 Hz, 1H), 7.30-7.41 (m, 6H), 7.45-7.49 (m, 1H), 7.99 (d, *J*=12.4 Hz, 1H). **HRMS:** calc. for [M+H]$^+$ C$_{22}$H$_{23}$N$_2$O$_3$: 363.17032, found: 363.17027

(+/-)-Benzyl (2R,5R,6S)-5-hydroxy-7-methyl-1,2,4,5,6,7-hexahydro-3H-2,6-methanoazocino[5,4-b]indole-3-carboxylate (46):
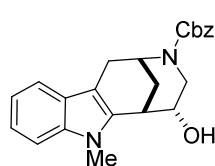
To a solution of compound **45** (72.6 mg, 0.20 mmol) in DMF (3 mL, 0.07 M), methyl iodide (37.5 µL, 0.60 mmol), potassium carbonate (83 mg, 0.60 mmol) and tetrabutyl ammoniun (37.0 mg, 0.10 mmol) were added and the mixture was allowed to stir at 90º for 5 hours. The mixture was extracted with DCM and the solvents were removed *in vacuo.* The crude product was purified by chromatography (10% ethyl acetate/DCM) to afford pure **46** (26.4 mg, 35%) as an orange oil. **^{1}H NMR (CDCl$_3$, 400 MHz)** (NMR spectrum shows a 1:1mixture of rotamers): δ 1.92-2.04 (m, 2H), 2.54-2.64 (m, 1H), 2.81 (t, *J*=18.2 Hz, 1H), 3.11-3.20 (m, 1H), 3.45 (s, 1H), 3.74 (s, 3H), 3.98-4.10 (m, 2H), 4.74 (s, 0.5H), 4.781 (s, 0.5H), 5.16 (d, *J*=16.6 Hz, 2H), 7.11 (t, *J*=7.3 Hz, 1H), 7.21 (t, *J*=7.6 Hz, 1H), 7.30-7.41 (m, 6H), 7.47 (t, *J*=8.70 Hz, 1H). **HRMS:** calc. for [M+H]$^+$ C$_{23}$H$_{25}$N$_2$O$_3$: 377.18597, found: 377.18631

(+/-)-Benzyl (2R,5R,6S)-7-(2-ethoxy-2-oxoethyl)-5-hydroxy-1,2,4,5,6,7-hexahydro-3H-2,6-methanoazocino[5,4-b]indole-3-carboxylate (47):
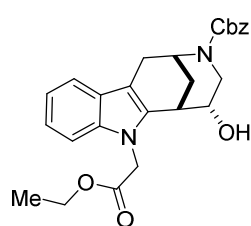
To a solution of **45** (30 mg, 0.083 mmol) in DMF, ethyl 2-bromoacetate (27.5 µL, 0.249 mmol) and potassium carbonate (34.4 mg, 0.249 mmol) were added. The mixture was allowed to stir at 90º for 12 h. The mixture was extracted with DCM and washed with a mixture of H$_2$O/BRINE (1:1). The crude product was purified by chromatography (20 to 50% E.A./DCM) to afford the product **47** in a mixture with the starting material (28.2 mg,34%) as a colorless oil. **HRMS:** calc. for [M+H]$^+$ C$_{26}$H$_{28}$N$_2$O$_5$: 448.19982, found: 448.19965

(+/-)-Benzyl (1S,4R,5R)-4-(benzyloxy)-6-oxo-2-azabicyclo[3.3.1]nonane-2-carboxylate (48):

To a solution of **44** (30 mg, 0.104 mmol) in a mixture of DCM/Hex. (1:1, 0.8mL, 0.15M), triflic acid (0.008 mmol) and Benzyl 2,2,2-trichloroacetimidate (52.5 mg, 0.208 mmol) were added at 0º and the mixture was allowed to reach room temperature while stirring. After 4 h the reaction

was quenched with H_2O and extracted with DCM. The solvents were removed *in vacuo* and the crude product was purified by chromatogrpahy (0 to 5% E.A./DCM) to yield **48** (22.9 mg, 58%). **¹H NMR (CDCl₃, 600 MHz)** (NMR spectrum shows a 1:1mixture of rotamers): δ 1.90-2.00 (m, 3H), 2.12-2.22 (m, 1H), 2.37-2.59 (m, 2H), 3.00-3.17 (m, 2H), 3.58 (m,1H), 4.32 (dd, *J*=13.6, 7.1 Hz, 0.5H), 4.40-4.42 (m,1H), 4.51 (bs, 0.5H), 4.60-4.65 (m, 2H), 5.10-5.15 (m, 2H), 7.34-7.38 (m, 5H). **HRMS:** calc. for [M+H]⁺ $C_{23}H_{25}NO_4$: 379.17836, found. 379.17795

(+/-)-Benzyl (1S,4R,5R)-6-oxo-4-((tetrahydro-2 h.-pyran-2-yl)oxy)-2-azabicyclo[3.3.1]nonane-2-carboxylate (49):
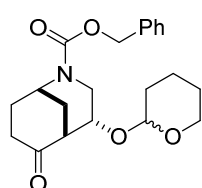
To a solution of 3,4-dihydro-2*H*-pyran (DHP) (11.4 µL, 0.125 mmol) and PPTS (2.1 mg, 0.0083 mmol) in DCM (0.6mL, 0.14M), **44** (24.1 mg, 0.083 mmol) was added and the mixture was allowed to stir at room temperature for 2 hours. The solvents were removed *in vacuo* and the crude product was purified by chromatography (30% ethyl acetate/DCM) to give pure product **49** (29.8 mg, 96%) as a colourless oil. **¹H NMR (CDCl₃, 400 MHz)** (NMR spectrum shows a very complicated signal pattern, due to a rotameric mixture and a diastereoisomeric mixture): δ 1.25 (t, *J*=7.13 Hz, 1H), 1.48-1.83 (m, 6H), 1.98-2.05 (m, 3H), 2.17-2.30 (m, 1H), 2.42-2.60 (m, 2H), 3.01 (bs, 1H), 3.21-3.29 (m, 1H), 3.44-3.53 (m, 1H), 3.78-4.51 (m, 3H), 4.65-4.91 (m, 1H), 5.17 (s, 2H), 7.36-7.46 (m, 5H). **HRMS:** calc. for [M+H]⁺ $C_{21}H_{28}NO_5$: 374.19620, found: 374.19764

(+/-)-Benzyl 4-methoxy-6-oxo-2-azabicyclo[3.3.1]nonane-2-carboxylate (50):
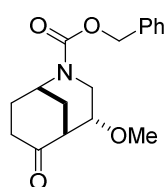
To a solution of ketone **44** (3.0g, 10.37 mmol) in DCM (72 mL, 0.145 M), silver oxide (12.01 g, 51.84 mmol) and methyl iodide (3.23 mL, 51.85 mmol) were added and the mixture was allowed to stir at room temperature for 48 h protected from the light. The mixture was filtered through Celite and solvents were removed *in vacuo*. The crude was purified by chromatography (8 to 50% ethyl acetate/DCM) to obtain **50** (isolated with 10% of the *syn* diasteroisomer) (2.01 g, 64%) as a colorless oil and starting material **44** (0.690 g, 23% recovery). **¹H NMR (CDCl₃, 700 MHz)** (NMR spectrum shows a 1:1mixture of rotamers plus the *syn* diasteroisomer impurity, data given for the mayor diasteroisomer): δ 1.92-2.05 (m, 3H), 2.13-2.23 (m, 1H), 2.35-2.58 (m, 2H), 3.07-3.20 (m, 2H), 3.30-3.39 (m, 3H), 3.60 (m,1H), 4.30 (dd, *J*=13.6, 7.1 Hz, 0.5H), 4.39-4.42 (m,1H), 4.51 (bs, 0.5H), 5.13-5.18 (m, 2H), 7.32-7.36 (m, 5H). **¹³C NMR (CDCl₃, 100 MHz):** δ29.8, 30.4, 30.5, 30.8, 39.0, 44.3, 44.4, 44.9, 46.9, 47.3, 56.6, 56.7, 67.5, 67.6, 75.4, 75.6, 128.0, 128.1, 128.2 128,6 136.4, 136.5, 155.4, 155.5, 209.2, 209.3. **HRMS:** calc. for [M+H]⁺ $C_{17}H_{22}NO_4$: 304.15433, found. 304.15450.

(+/-)-Benzyl 4-acetoxy-6-oxo-2-azabicyclo[3.3.1]nonane-2-carboxylate (51):
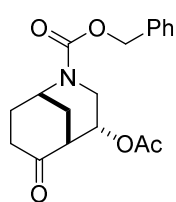
To a solution of compound **44** (2.0 g, 6.91 mmol) in pyridine (40 mL, 0.175 M) a solution of acetyl chloride (1.5 mL, 20.73 mmol) in DCM (40 mL, 0.175 M). was added dropwise at -10°, and the mixture was stirred at this temperature for 3 hours. The mixture was then washed with a saturated solution of copper sulfate (8X) to remove the pyridine. The solvents were coevaporated with toluene and the crude was then purified by chromatography (5 to 20% ethyl acetate/DCM) to yield product **51** (with ~15% of the *syn* diasteroisomer) (1.6 g, 69%) as a light brown oil.**^{1}H NMR (CDCl$_3$, 400 MHz)** (NMR Spectra shows a 1:1 mixture of rotamers, data given for the mayor diasteroisomer)**:**δ1.97-2.06 (m, 6H), 2.16-2.28 (m, 1H), 2.36-2.54 (m, 1H), 2.59-2.65 (m, 1H), 3.00 (s, 1H), 3.23 (t, *J*=12.0 Hz, 1H), 4.27-4.36 (m, 1H), 4.45 (s, 0.44H), 4.55 (s, 0.56H), 5.06-5.21 (m, 3H), 7.36 (m, 5H). **^{13}C NMR (CDCl3, 100 MHz):** δ 21.0, 29.6, 30.4, 30.5, 30.7, 37.0, 38.9, 43.8, 43.9, 44.2, 44.4, 47.1, 47.2, 67.7, 68.0, 128.1, 128.2, 128.4, 128.6, 128.7, 136.3, 155.4, 169.9, 208.4, 208.6. **HRMS:** calc. for [M+H]$^+$ C$_{18}$H$_{22}$NO$_5$: 332.14925, found. 332.14977.

(+/-)-Benzyl 5-acetoxy-1,2,4,5,6,7-hexahydro-3H-2,6-methanoazocino[5,4-b]indole-3-carboxylate (52):
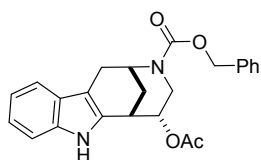
To a solution of ketone **51** (1.0 g, 3.02 mmol) in acetic acid (20.1 mL, 0.15 M), phenyl hydrazine hydrochloride (0.437 g, 3.02 mmol) was added and the solution was stirred and refluxed for 1.5 h. The reaction was quenched with sodium bicarbonate (saturated aqueous solution), the mixture was extracted with DCM, solvents were removed *in vacuo* and the crude was purified by chromatography (3 to 15% ethyl acetate/DCM) to yield compound **52** (0.927 g, 76%) as a light orange foamy solid) (as the pure *anti* diasteroisomer). The crude product can be further used to continue the synthesis. **^{1}H NMR (CDCl$_3$, 400 MHz)** (rotameric mixture 1:1.5)**:** δ 2.07-2.16 (m, 5H), 2.67-2.87 (m, 2H), 3.09-3.17 (m, 1H), 3.38 (m, 1H), 4.08-4.21 (m, 1H), 4.78 (s, 0.4H), 4.86 (m, 0.6H), 5.05-5.12 (m, 1H), 5.14-5.21(m, 2H), 7.12 (t, *J*=7.4 Hz, 1H), 7.17-7.21 (m, 1H), 7.29-7.41 (m, 6H), 7.49 (t, *J*=8.4 Hz, 1H), 7.86 (s, 1H). **HRMS:** calc. for [M+H]$^+$ C$_{24}$H$_{25}$N$_2$O$_4$: 405.18088, found. 405.18110.

(+/-)-Benzyl 5-acetoxy-7-(2-ethoxy-2-oxoethyl)-1,2,4,5,6,7-hexahydro-3H-2,6-methanoazocino[5,4-b]indole-3-carboxylate (53):
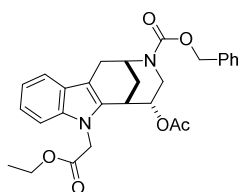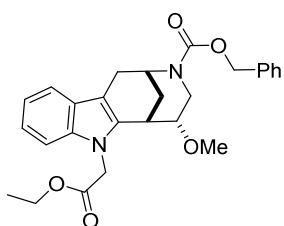
To a solution of compound **52** (0.927g,2.30 mmol) in DMF (13.5 mL, 0.17 M), caesium carbonate (0.75g, 6.90 mmol) and ethyl 2-bromoacetate (0.254 mL, 6.90 mmol) were added and the mixture allowed to stir at room temperature for 2 h. The mixture was then partitioned between DCM and brine/H_2O (1:1). The aqueous phase was extracted with DCM (5X), solvents were removed *in vacuo* and the crude product was purified by chromatography (1to 5% ethyl acetate/DCM) to yield compound **53** (1.13 g, 85%) as a light orange oil.**^{1}H NMR (CDCl$_3$, 500 MHz)**: δ 1.25 (t, *J*=7.1 Hz, 3H), 2.03-2.15 (m, 5H), 2.68-2.89 (m, 2H), 3.09-3.25 (m, 1H), 3.34-3.42 (m, 1H), 4.10-4.25 (m, 3H), 4.79-4.89 (m, 3H), 5.08-5.22 (m, 3H), 7.11-7.15 (m, 1H), 7.20-7.22 (m, 2H), 7.30-7.51 (m, 6H).**^{13}C NMR (CDCl$_3$, 100 MHz):**δ14.3, 21.2, 27.8, 28.2, 29.4, 29.8, 30.6, 30.6. 30.9, 31.1, 41.1, 44.8, 44.9, 61.8, 67.5, 67.7, 71.4, 71.6, 109.0, 110.5, 110.7, 118.6, 119.9, 122.1, 126.8, 127.8, 128.0, 128.1, 128.3, 132.9, 136.7, 137.3, 155.5, 168.8, 170.0 **HRMS:** calc. for [M+H]+ $C_{28}H_{31}N_2O_6$: 491.21766, found. 491.21961.

(+/-)-Benzyl 5-methoxy-1,2,4,5,6,7-hexahydro-3H-2,6-methanoazocino[5,4-b]indole-3-carboxylate (57):
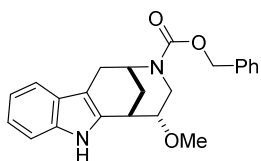
To a solution of ketone **50** (2.0 g, 6.59 mmol) in acetic acid (44.0 mL, 0.15 M), phenyl hydrazine hydrochloride (0.953g, 6.59mmol) was added and the solution was stirred and refluxed for 1.5 h. The reaction was quenched with sodium bicarbonate (saturated aqueous solution), the mixture was extracted with DCM, solvents were removed *in vacuo* and the crude product was purified by chromatography (3 to 15% ethyl acetate/DCM) to yield compound **57** (as the pure *anti* diasteroisomer) (1.74 g, 74%) as an orange solid. **^{1}H NMR (CDCl$_3$, 400 MHz):** δ 2.02-2.11 (m, 2H), 2.54 (dt, *J*=23.5, 11.7 Hz, 1H), 2.81 (t, *J*=18.0 Hz, 1H), 3.11 (ddd, *J*=16.8, 7.4, 5.8 Hz, 1H), 3.34 (m, 1H), 3.40 (s, 3H), 3.55 (td, *J*=10.3, 5.7 Hz, 1H), 4.13 (dd, *J*=12.5, 5.1 Hz, 0.5H), 4.29 (dd, *J*=12.7, 5.3 Hz, 0.5H), 4.79 (d, *J*=28.4 Hz, 1H), 5.18 (d, *J*=19.3 Hz, 2H), 7.09 (t, *J*=7.4 Hz, 1H), 7.15 (td, *J*=6.8, 1.2 Hz, 1H), 7.31-7.58 (m, 7H), 7.95 (d, *J*=12.6 Hz, 1H). **^{13}C NMR (CDCl3, 100 MHz):** δ 27.8, 28.2, 30.1, 30.5, 32.5, 32.9, 42.3, 42.4, 45.4, 56.9, 67.3, 67.5, 77.7, 78.0, 109.1, 109.4, 111.0, 118.0, 118.1, 119.4, 121.6, 126.95, 127.00, 127.97, 128.03, 128.1, 128.2, 128.6, 128.7, 132.7, 132.8, 136.1, 136.9, 137.0, 155.7 **HRMS:** calc. for [M+H][+] $C_{23}H_{25}N_2O_3$: 377.18597, found. 377.18728.

(+/-)-Benzyl 7-(2-ethoxy-2-oxoethyl)-5-methoxy-1,2,4,5,6,7-hexahydro-3H-2,6-methanoazocino[5,4-b]indole-3-carboxylate (58):

To a solution of compound **57** (1.5 g, 3.98 mmol) in DMF (23.4 mL, 0.17 M), caesium carbonate (3.89 g, 11.94 mmol) and ethyl 2-bromoacetate (1.32 mL, 11.94 mmol) were dissolved and the mixture was allowed to stir at room temperature for 2 h. The mixture was then partitioned between DCM and brine/H_2O (1:1). The aqueous phase was extracted with DCM (5X), solvents were removed *in vacuo* and the crude was purified by chromatography (1 to 5% ethyl acetate/DCM) to yield an orange oil as product **58** (1.62 g, 88%). **^{1}H NMR (CDCl$_3$, 400 MHz)** (with small impurity of the ethyl 2-bromoacetate): δ 1.24 (t, *J*=7.12 Hz, 3H), 1.97-2.07 (m, 2H), 2.57 (t, *J*=11.8 Hz, 0.5H),2.64 (t, *J*=11.6 Hz, 0.5H), 2.80 (d, *J*=16.8, 0.5H), 2.84 (d, *J*=16.9 Hz, 0.5H), 3.16 (td, *J*=5.5, 16.1 Hz, 1H), 3.34 (d, *J*=9.2 Hz, 3H), 3.40 (s, 1H), 3.54-3.59 (m, 1H), 4.13-4.33 (m, 3H), 4.77-4.84 (m, 2H), 5.08-5.16(m, 1H), 5.17 (s, 1H), 5.21 (s, 1H), 7.10 (s, 1H), 7.18-7.21 (m, 2H), 7.31-7.48 (m, 6H). **^{13}C NMR (CDCl$_3$, 100 MHz):** δ14.3, 27.9, 28.2, 30.6, 30.9, 31.7, 31.8, 41.6, 41.7, 45.0, 45.2, 56.8, 56.9, 61.2, 61.4, 67.3, 67.5, 68.3, 78.3, 78.7, 108.9, 109.5, 109.8, 118.1, 118.2, 119.4, 121.6, 126.6, 126.7, 127.9, 128.0, 128.1, 128.2, 128.6, 128.7, 134.0, 134.1, 136.9, 137.1, 137.2, 155.6, 169.5, 169.6, 169.8 **HRMS:** calc. for [M+H]$^+$ $C_{27}H_{31}N_2O_5$: 463.22275, found. 463.22269.

(+/-)-Ethyl 2-(5-methoxy-1,2,3,4,5,6-hexahydro-7H-2,6-methanoazocino[5,4-b]indol-7-yl)acetate (59):
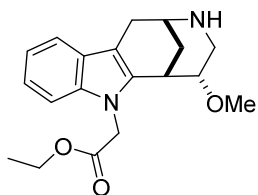
To a solution of compound **58** (1.0g, 2.16mmol) in ethanol (14.4 mL, 0.15 M), Pd/C (0.108 mg, 50 mg/mmol) was added and the atmosphere was changed to hydrogen gas (1atm). After 5 h. the mixture was filtered through Celite, solvents were removed *in vacuo* and submitted to chromatography (5% MeOH/DCM) to yield compound **59** as a white solid (0.610 g, 86%).**^{1}H NMR (CDCl$_3$, 600 MHz):** δ 1.25 (t, *J*=7.13 Hz, 3H), 2.00 (ddd, *J*=2.3, 3.8, 12.6 Hz, 1H), 2.16 (dt, *J*=3.0, 12.6 Hz, 1H), 2.55 (t, *J*=11.1 Hz, 1H), 2.81 (d, *J*=17.0 Hz, 1H), 3.06 (dd, *J*=4.5, 11.6 Hz, 1H), 3.19 (dd, *J*=6.0, 16.9 Hz, 1H), 3.30 (s, 3H), 3.39 (m, 1H), 3.53-3.56 (m, 2H), 3.60 (dt, *J*=4.4, 10.4 Hz, 1H), 4.12-4.24 (m, 2H), 4.79 (d, *J*=18.0 Hz, 1H), 5.11 (d, *J*=18.0 Hz, 1H), 7.1 (ddd, *J*=1.2, 6.6, 7.8 Hz, 1H), 7.18 (td, *J*=1.2, 6.6 Hz, 1H), 7.20 (d, *J*=8.0 Hz, 1H), 7.49 (d, *J*=7.8 Hz, 1H). **^{13}C NMR (CDCl$_3$, 100 MHz):** δ 14.2, 29.1, 32.1, 32.2, 42.2, 44.8, 45.6, 56.5, 61.2, 76.9, 77.2, 77.4, 78.9, 108.8, 110.4, 118.1, 119.2, 121.3, 126.5, 135.1, 137.0, 169.5 **NOESY:** To confirm the *anti* configuration between the methylene bridge and the methoxy group a NOESYexperiment was performed. NOE interactions are shown

below (for simplicity only one enantiomer has been drawn). **HRMS:** calc. for $[M+H]^+$ $C_{19}H_{25}N_2O_3$: 329.18597, found. 329.18658.
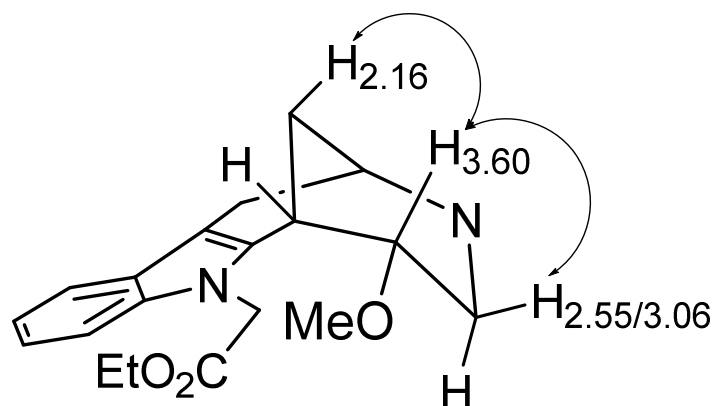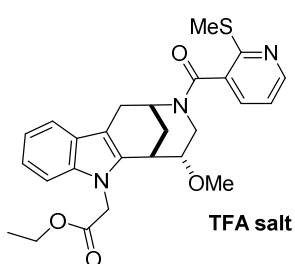

Figure 42. Proton coupling detected by NOESY experiment

(+/-)-Ethyl 2-(5-methoxy-3-(2-(methylthio)nicotinoyl)-1,2,3,4,5,6-hexahydro-7H-2,6-methanoazocino[5,4-b]indol-7-yl)acetate (TFA salt) ((+/-)-Glupin-1:):
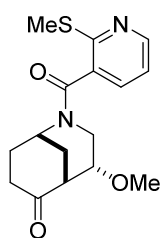

To a solution of compound **59** (50.0 mg, 0.152 mmol) in DCM (0.8 mL, 0.2 M), triethylamine (0.0254 mL, 0.182 mmol) and 2-(methylthio)nicotinoyl chloride (28.5 mg, 0.152 mmol) were dissolved and the mixture was allowed to stir overnight at room temperature. The mixture was washed with water and brine, solvents were removed *in vacuo* and the crude product was purified by chromatography (1.5% MeOH/DCM) or by preparative HPLC (10% to 50% ACN/H_2O with 0.1% TFA) to yield compound **(+/-)-Glupin-1** (38.6 mg, 53%) as the TFA salt: **^{1}H NMR (CDCl$_3$, 500 MHz):** δ 1.22-1.27 (m, 3H), 1.94-2.33 (m, 2H), 2.60-2.66 (m, 4H),2.83-3.10 (m, 1.5H),3.18 (s, 1.5H), 3.30-3.36 (m, 1H), 3.42 (s, 1.5H), 3.48 (s, 1H), 3.69-3.84 (m, 1H), 4.01 (bs,0.5H), 4.10-4.26 (m, 2H), 4.79 (dd, *J*=18.0, 14.4 Hz, 1H), 4.89 (dd, *J*=4.9, 12.9 Hz, 0.5H), 5.03 (d, *J*=18.0 Hz, 0.5H), 5.15 (d, *J*=18.0 Hz, 0.5H), 5.44 (bs, 0.5H), 7.06-7.23 (m, 4H), 7.44-7.52 (m, 2H), 7.73 (bs, 1H), 8.51 (d, *J*=3.8 Hz, 0.5H), 8.57 (d, *J*=3.8 Hz, 0.5H). **^{13}C NMR (CDCl$_3$, 100 MHz):**δ13.3, 13.5, 14.3, 31.5, 31.9, 32.3, 43.3, 45.0, 45.1, 49.4, 57.1, 61.5, 78.1, 79.2, 109.0, 109.1, 118.2, 118.3, 119.4, 119.6, 121.9, 126.6, 133.8, 133.9, 134.1, 137.2, 137.3, 149.5, 149.6, 167.4, 169.4, 169.5. **HRMS:** calc. for $[M+H]^+$ $C_{26}H_{30}N_3O_4S$: 480.19515, found. 480.19559. After chiral separation (see Chiral Separation) specific optical rotations were measured for both enantiomers (not as the TFA salt): (+)-Glupin-1 $[\alpha]_D$= + 10.7° ± 3.4; (-)-Glupin-1 $[\alpha]_D$= - 10.0° ± 1.0

(+/-)-4-methoxy-2-(2-(methylthio)nicotinoyl)-2-azabicyclo[3.3.1]nonan-6-one (60):

To a solution of compound **50** (0.046 g, 0.152 mmol) in ethanol (1.0 mL, 0.15 M), Pd/C (15 mg, 100 mg/mmol) was added. The atmosphere was then changed to hydrogen gas and the mixture was allowed to stir for 2 hours. The mixture was then filtered through celite and the solvents were removed *in vacuo*. The crude product was redissolved in DCM (2.0 mL, 0.08 M) and triethylamine (64μL, 0.456 mmol) and 2-(methylthio)nicotinoyl chloride (57 mg, 0.304 mmol) were added. The mixture was allowed to stir overnight, solvents were removed *in vacuo* and the the crude product was purified by prepHPLC to yield compound **60** (17 mg, 35%) as white solid. The product has very low solubility and was charaterised only by HRMS. **HRMS:** calc. for [M+H]$^+$ C$_{16}$H$_{21}$N$_2$O$_3$S: 321.12674, found: 321.12960

Benzyl methyl(1,4-dioxaspiro[4.5]decan-8-yl)carbamate (61):
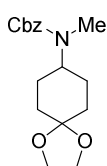
To a solution of N-methyl-1,4-dioxaspiro[4.5]decan-8-amine(0.625 g, 3.65 mmol) in acetonitrile (24 mL, 0.155 M), potassium carbonate (1.0 g, 7.30 mmol) and benzylchloroformate (1.0 mL, 7.30 mmol) were added. The mixture was allowed to stir overnigthbefore evaporating the solvents. The mixture was redissolved in DCM and washed with brine, solvents were removed *in vacuo* and the crude product was purified by chromatography (0 to 7% ethyl acetate/DCM) to yield compound **61** (0.624 g, 56%). The product was further used without characterization at this point.

Benzyl methyl(4-oxocyclohexyl)carbamate (62):
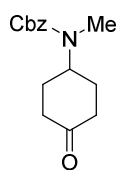
A solution of compound **61** (0.563 g, 1.843 mmol) in a mixture of 10% HCl aqueous solution (25 mL, 0.075M) and THF (12 mL, 0.15M) was allowed to stir for 3 hours. The mixture was then extracted with DCM and the solvents were removed *in vacuo*. Crude product was purified by chromatography (30 to 50% ethyl acetate/DCM) to yield compound **62**(0.460 g, 95%) as a colorless oil. **¹H NMR (CDCl₃, 500 MHz):** δ 1.85 (m, 2H), 1.99-2.03 (m, 2H), 2.41-2.48 (m, 4H), 2.82 (s, 3H), 4.35-4.55 (m, 1H), 5.16 (s, 2H), 7.30-7.35 (m, 1H), 7.36 (d, *J*=4.4 Hz, 3H). **¹³C NMR (CDCl₃, 100 MHz):** δ 28.5, 39.9, 52.9, 67.4, 128.0, 128.2, 128.6, 136.8, 156.2, 209.7 **HRMS:** calc. for [M+H]$^+$ C$_{15}$H$_{20}$NO$_3$: 262.14377, found: 262.14392

(+/-)-Benzyl methyl(2,3,4,9-tetrahydro-1H-carbazol-3-yl)carbamate (63):

Compound **62** (0.665 g, 86%) was synthesized as described for compound **57**. **¹H NMR (CDCl₃, 500 MHz):** δ 1.99-2.11 (m, 2H), 2.78-2.99 (m, 7H), 4.49-4.61 (m, 1H), 5.16-5.21 (m, 2H), 7.08 (t, *J*=7.3 Hz, 1H), 7.13 (t, *J*=7.2 Hz, 1H), 7.27-7.43 (m, 7H), 7.79 (bs, 1H). **¹³C NMR**
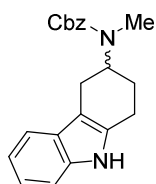
(CDCl₃, 100 MHz): δ 23.0, 24.1, 27.3, 28.8, 52.6, 67.2, 108.8, 110.6, 117.8,119.5, 121.5, 128.0, 128.1, 128.6, 132.7, 136.4, 137.1, 156.4 **HRMS:** calc. for $[M+H]^+$ $C_{21}H_{23}N_2O_2$: 335.17540, found: 335.17557

## (+/-)-Ethyl 2-(3-(((benzyloxy)carbonyl)(methyl)amino)-1,2,3,4-tetrahydro-9H-carbazol-9-yl)acetate (65):
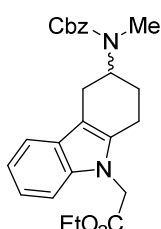
Compound **65** (0.370 g, 71%) was synthesized as described for compound **58**. **¹H NMR (CDCl₃, 400 MHz):** δ1.25 (t, *J*=7.1 Hz, 3H), 2.00-2.17 (m, 2H), 2.78-3.00 (m, 7H), 4.19 (q, *J*=7.1 Hz, 2H), 4.45-4.60 (m, 1H), 4.72 (s, 2H), 5.18 (2, 2H), 7.06-7.13 (m, 1H), 7.16-7.18 (m, 2H), 7.29-7.41 (m, 5H), 7.43 (d, *J*=7.7 Hz, 1H). **ESI:** calc. for $[M+H]^+$ $C_{25}H_{29}N_2O_4$: 420.2, found: 421.2; calc. for $[M+Na]^+$ $C_{25}H_{28}N_2O_4$: 443.2, found: 443.2

(+/-)-Ethyl 2-(3-(methylamino)-1,2,3,4-tetrahydro-9H-carbazol-9-yl)acetate (65):

To a solution of compound **64** (0.304 g, 0.748 mmol) in ethanol (7.5 mL, 0.1 M), Pd/C (38 mg, 50mg/mmol) and ammonium formate (0.236 g, 3.739 mmol) were added. The mixture was allowed to stir at reflux for 2 h. The mixture was then filtered through celite and solvents were removed *in vacuo*, the crude product was then purified by chromatography (5 to 20% MeOH/DCM) to yield compound **65** (0.165 g, 66%) as a formate salt. **¹H NMR (CDCl₃, 600 MHz):** δ 1.25 (t, *J*=7.1 Hz, 3H), 2.07-2.14 (m, 1H), 2.39-2.41 (m, 1H), 2.67 (s, 3H), 2.75-2.89 (m, 3H), 3.22 (dd, *J*=14.6, 4.9 Hz, 1H), 3.25-3.30 (m, 1H), 3.48 (s, 1H), 4.19 (1, *J*=4.2 Hz, 2H), 4.70 (q, *J*=17.7 Hz, 2H), 7.08-7.11 (m, 1H), 7.17 (d, *J*=4.0 Hz, 2H), 7.45 (d, *J*=7.8 Hz, 1H).**¹³C NMR (CDCl₃, 100 MHz):** δ 14.3, 20.3, 25.2, 26.7, 31.2, 44.8, 55.5, 61.8, 106.9, 108.6 ,118.1, 119.9, 121.9, 127.2, 134.0, 137.3, 168.8 **HRMS:** calc. for $[M+H]^+$ $C_{16}H_{21}N_2O_2$:273.15975, found: 273.15998
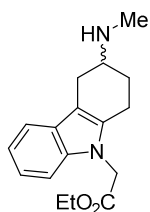
## (+/-)-Ethyl 2-(3-(N-methyl-2-(methylthio)nicotinamido)-1,2,3,4-tetrahydro-9H-carbazol-9-yl)acetate (66):
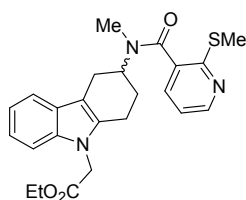
Compound **66** (0.032 g, 67%) was synthesized as described for **(+/-)-Glupin-1**. **¹H NMR (CDCl₃, 500 MHz)** (rotameric mixture 1:2.3): δ 1.22-1.28 (m, 3H), 2.05-2.27 (m, 2H), 2.53-2.71 (m, 3H), 2.77-3.10 (m, 5H), 3.15 (s, 1.3H), 2.77-3.10 (m, 5H), 3.15 (s, 1.3H), 3.47 (s, 0.7H), 3.78-3.94 (m, 0.7H), 4.15-4.23 (m, 2H), 4.65 (s, 1H), 4.74-4.79 (m, 1H), 5.13-5.19 (m, 0.3H), 6.98-7.12 (m, 4H), 7.41-7.49 (m, 2H), 8.14-8.26 (m, 0.3H), 8.41-8.49 (m, 0.7H). **HRMS:** calc. for $[M+H]^+$ $C_{23}H_{26}N_3O_3S$: 424.16894, found: 424.16896

Substituted nicotinic acid derivatives:

Compounds with 2-substituted nicotinic acid can give rise to very complicated spectra. The purity was determined by the NMR spectra of the starting material of the final reaction, the free amine (compound **9**). However, the formation of the amide bond and 2-substitution of the nicotinic acid can give rise to rotamers and atropoisomers, respectively. This can be seen in the NMR spectra of the final products. In some cases, due to very complicated spectra, only ^{1}H spectra are given. This is noticeable at the 78 ppm area of the ^{13}C spectra, where 4 signals can be seen for the same carbon (instead of the normal 1 signal per carbon). Purity was checked by HPLC, and was in all cases over 95% before submitting the compounds for biological activity measurement. Some signals are given as fractions of protons and some apparent coupling constants are given in cases were clearly the signal splitting is due to rotamers/atropoisomers and not because of actual coupling between ^{1}H nuclei (i.e. values over 30 Hz). Furthermore, when easily determined the ratio of the rotamers was given, but for simplification the integrals of the NMR spectra was given 0.5H/0.5H (instead of e.g. 0.46H/0.54H).

(+/-)-Ethyl 2-(3-(2-chloronicotinoyl)-5-methoxy-1,2,3,4,5,6-hexahydro-7H-2,6-methanoazocino[5,4-b]indol-7-yl)acetate (67):
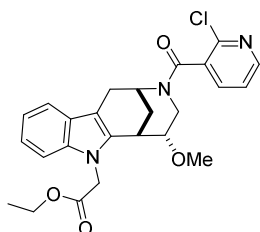
To a solution of 2-chloronicotinic acid (17.3 mg, 0.110 mmol) in toluene (1.6 mL, 0.067 M), freshly distilled oxalyl chloride (11.3 µL, 0.132 mmol) and a drop of DMF were added. The solution was stirred at reflux for 1 h., then solvents were removed *in vacuo* and the crude product was redissolved in DCM (0.25 mL, 0.55 M). The solution was canulated to a solution of compound **59** (30 mg, 0.091mmol) and triethylamine (15.2 µL, 0.110 mmol) in DCM (0.25 mL, 0.37 M). The mixture was allowed to stir at room temperature overnight. The organic phase was then washed with water and brine, solvents were removed *in vacuo* and the crude was purified by chromatography (3% MeOH/DCM). Pure compound **67** (39.0mg, 82%) was isolated as a colourless oil.**^{1}H NMR (CDCl$_3$, 500 MHz)** (rotameric mixture)**:** δ 1.22-1.27 (m, 3H), 1.93-2.29 (m, 2H), 2.60 (dd, *J*=10.9, 12.7 Hz, 0.4H), 2.69 (dd, *J*=13.8, 23.8 Hz, 0.6H), 2.78-2.90 (m, 0.6H), 2.96-3.01 (m, 1H), 3.10-3.22 (m, 1.4H), 3.28-3.36 (m, 1H), 3.40-3.42 (m, 1.6H), 3.48 (s, 1H), 3.62-3.78 (m, 1H), 3.98 (s, 0.6H), 4.11-4.24 (m, 2H), 4.81 (dd, *J*=10.3, 25.7 Hz, 1H), 4.90 (dd, *J*=5.3, 12.8 Hz, 0.6H), 5.03 (dd, *J*=7.6, 18.0 Hz, 0.4H), 5.14 (dd, *J*=7.2, 18.1 Hz, 0.6H), 5.43 (s, 0.4H), 7.09-7.15 (m, 1H), 7.19-7.23 (m, 2H), 7.29-7.43 (m, 1.4H), 7.48-7.53 (m, 0.6H), 7.60-7.73 (m, 1H), 8.42-8.49 (m, 1H).**^{13}C NMR (CDCl$_3$, 100 MHz):** δ 14.2, 14.4, 18.8, 19.5, 20.5, 22.7, 26.9, 27.7, 27.7, 27.9, 28.4, 28.9, 29.1, 30.1, 30.3, 31.2, 31.5, 31.8, 32.1, 32.3, 33.7, 36.1, 38.7, 39.1, 41.4, 42.9, 42.9, 44.0, 44.9, 44.9,

45.1, 49.0, 49.3, 56.9, 56.9, 57.0, 57.0, 61.4, 77.8, 78.2, 78.7, 78.9, 108.5, 108.9, 108.9, 109.0, 109.5, 109.7, 117.9, 118.1, 118.2, 118.4, 119.5, 121.8, 122.8, 122.8, 123.0, 126.2, 126.4, 126.4, 132.4, 132.7, 132.8, 133.2, 133.5, 133.7, 134.0, 136.4, 136.5, 136.6, 137.1, 137.1, 137.1, 137.2, 146.6, 146.9, 147.1, 147.2, 150.0, 150.1, 150.1, 150.2, 165.2, 165.3, 165.4, 165.6, 169.2, 169.3, 169.3, 169.4 **HRMS:** calc. for $[M+H]^+$ $C_{25}H_{27}N_3O_4Cl$: 468.16846, found: 468.16951.

(+/-)-Ethyl 2-(5-methoxy-3-(2-(trifluoromethyl)nicotinoyl)-1,2,3,4,5,6-hexahydro-7H-2,6-methanoazocino[5,4-b]indol-7-yl)acetate (68):
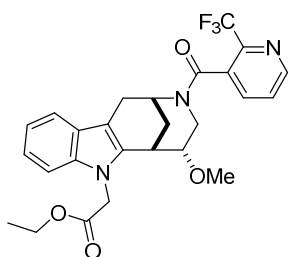
To a solution of compound **59** (20 mg, 0.030 mmol) in DMF (0.06M, 0.5mL), TBTU (CAS: 125700-67-6) (31.0 mg, 0.098 mmol), 2-trifluoromethylnicotinic acid (17.4 mg, 0.092 mmol) and DIPEA (54 µL, 0.305 mmol) were added. The mixture was allowed to stir for 3 h. The crude product was purified directly by preparative HPLC (10% to 50% ACN/H_2O) to yield compound **68** (13.5 mg, 35%).[1]**H NMR (CDCl$_3$, 500 MHz)** (rotameric mixture)**:** δ 1.21-1.26 (m, 3H), 1.90-1.93 (m, 0.5H), 1.96-1.98 (m, 0.2H), 2.08-2.15 (m, 1.3H), 2.61 (dd, *J*=12.8, 10.8 Hz, 0.4H), 2.66 (dd, *J*=12.8, 10.7 Hz, 0.2H), 2.77-2.83 (m, 0.8H), 2.87-2.92 (m, 0.8), 3.02-3.09 (m, 0.5H), 3.12-3.15 (m, 1.5H), 3.20 (dd, *J*=12.8, 4.9 Hz, 0.5H), 3.29-3.36 (m, 0.5H), 3.40-3.42 (m, 1.5H), 3.45-3.50 (m, 1H), 3.55 (dt, *J*=10.3, 4.4 Hz, 0.3H), 3.62-3.66 (m, 0.5H), 3.91-3.93 (m, 0.5H), 4.11-4.24 (m, 2H), 4.77 (dd, *J*=18.0, 5.5 Hz, 0.5H), 4.81 (dd, *J*=18.1, 4.4 Hz, 0.5H), 4.92 (dd, *J*=12.9, 5.0 Hz, 0.5H), 5.01 (dd, *J*=18.0, 12.1 Hz, 0.5H), 5.14 (dd, *J*=18.1, 8.1 Hz, 0.5H), 5.39-5.40(m, 0.2H), 5.44 (m, 0.3H), 7.10-7.15 (m, 1H), 7.19-7.23 (m, 2H), 7.43 (d, *J*=7.8 Hz, 0.4H), 7.48 (d, *J*=7.8 Hz, 0.2H), 7.50-7.54 (m, 0.8H), 7.58 (dd, *J*=7.9, 4.8 Hz, 0.2H), 7.60 (dd, *J*=7.8, 4.7 Hz, 0.2H), 7.64-7.65 (m, 0.6H), 7.75-7.76 (m, 0.3H), 7.82 (dd, *J*=7.8, 1.1 Hz, 0.3H), 8.76 (ddd, *J*=9.9, 4.6, 1.0 Hz, 0.5H), 8.81-8.82 (m, 0.5H).[13]**C NMR (CDCl$_3$, 100 MHz):** δ 14.2, 14.2, 26.6, 26.9, 27.8, 28.4, 29.9, 30.4, 30.4, 31.5, 31.7, 31.9, 32.0, 32.3, 38.6, 39.0, 42.8, 43.0, 44.7, 44.9, 44.9, 45.2, 49.0, 49.1, 56.8, 56.8, 56.9, 57.0, 61.3, 61.4, 61.4, 61.4, 77.7, 78.2, 78.2, 78.7, 108.4, 108.7, 108.8, 108.9, 109.0, 109.1, 109.4, 109.7, 117.9, 118.1, 118.2, 118.4, 119.6, 119.6, 119.6, 120.4, 120.5, 120.7, 120.7, 121.8, 122.0, 122.1, 122.1, 122.2, 122.3, 123.8, 123.9, 126.9, 126.2, 126.2, 126.4, 126.4, 126.5, 126.6, 131.3, 131.4, 131.8, 131.8, 133.4, 133.6, 134.0, 134.1, 135.4, 135.4, 135.5, 136.0, 137.1, 137.1, 137.2, 142.7, 142.9, 143.1, 143.1, 143.3, 143.3, 143.5, 143.6, 143.6, 143.7, 143.8, 149.8, 149.9, 150.0, 165.3, 165.4, 165.6, 165.8, 169.1, 169.3, 169.4 **HRMS:** calc. for $[M+H]^+$ $C_{26}H_{27}N_3O_4F_3$: 502.19482, found: 502.19439.b

(+/-)-Ethyl 2-(5-methoxy-3-(2-(phenylthio)nicotinoyl)-1,2,3,4,5,6-hexahydro-7H-2,6-methanoazocino[5,4-b]indol-7-yl)acetate (69):
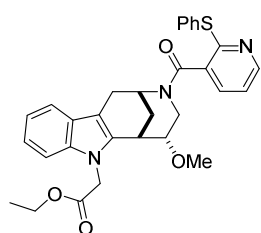
Compound **69** (6.5mg, 39%) was synthesised as described for compound **67**. **^{1}H NMR (CDCl$_3$, 500 MHz)** (rotameric mixture): δ 1.25 (dt, *J*=11.0, 7.1 Hz, 3H), 1.99 (bs, 0.5H), 2.12-2.13 (m, 0.5H), 2.22 (bs, 0.5H), 2.41 (bs, 0.5H), 2.64-3.20 (m, 4H), 3.34 (dd, *J*=17.2, 6.0 Hz, 0.5H), 3.42 (s, 2H), 3.49 (d, *J*=2.9 Hz, 1H), 3.73-3.86 (m, 1H), 4.11 (bs, 0.5H), 4.13-4.24 (m, 2H), 4.80 (dd, *J*=22.7, 18.0 Hz, 1H), 4.93 (dd, *J*=12.9, 5.0 Hz, 0.5H), 5.03 (d, *J*=18.0 Hz, 0.5H), 5.16 (d, *J*=18.1 Hz, 0.5H), 5.46 (bs, 0.5H), 7.07-7.14 (m, 1.5H), 7.16 (dd, *J*=7.0, 5.0 Hz, 0.5H), 7.19-7.23 (m, 2H), 7.37-7.58 (m, 7H), 8.37 (dd, *J*=4.8, 1.8 Hz, 0.5H), 8.44 (dd, *J*=4.8, 1.6 Hz, 0.5). **^{13}C NMR (CDCl$_3$, 100 MHz):** δ 14.2, 28.4, 30.1, 31.4, 31.8, 32.2, 39.0, 42.8, 44.9, 44.9, 49.1, 56.9, 61.3, 61.4, 77.9, 79.1, 108.8, 108.9, 109.0, 109.7, 118.0, 118.3, 119.5, 120.6, 121.7, 121.7, 126.3, 126.5, 128.7, 128.8, 129.2, 129.2, 132.2, 133.8, 134.0, 134.1, 134.4, 137.1, 137.1, 150.2, 155.0, 166.9, 166.9, 169.2, 169.4 **HRMS:** calc. for [M+H]$^+$ C$_{31}$H$_{32}$N$_3$O$_4$S: 542.21080, found: 542.21115

(+/-)-Ethyl 2-(5-methoxy-3-(2-(propylthio)nicotinoyl)-1,2,3,4,5,6-hexahydro-7H-2,6-methanoazocino[5,4-b]indol-7-yl)acetate (70):
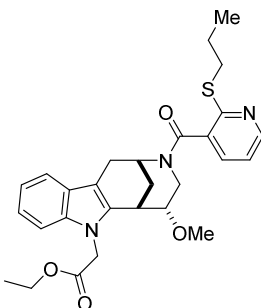
Compound **70** (16.5 mg, 53%) was synthesised as described for compound **67**.**^{1}H NMR (CDCl$_3$, 500 MHz)** (rotameric mixture): δ 0.93-1.06 (m, 3H), 1.24 (dd, *J*=7.2, 15.5 Hz, 3H), 1.62-1.79 (m, 2H), 1.94-2.37 (m, 2H), 2.58-2.88 (m, 2H), 3.02-3.36 (m, 5H), 3.41-3-47 (m, 3H), 3.64-4.00 (m, 1H), 4.10-4.24 (m, 2H), 4.79 (t, *J*=17.8 Hz, 1H), 4.91 (dd, *J*=5.0, 12.8 Hz, 0.6H), 5.03 (d, *J*=18.0 Hz, 0.4H), 5.15 (d, *J*=18.1 Hz, 0.6H), 5.43 (s, 0.4H), 7.02 (bs, 0.4H), 7.09-7.14 (m, 1.6H), 7.18-7.23 (m, 2H), 7.36-7.52 (m, 2H), 8.44 (dd, *J*=1.66, 4.9 Hz, 0.4H), 8.50 (dd, *J*=1.7, 4.9 Hz, 0.6H).**^{13}C NMR (CDCl$_3$, 100 MHz):** δ 13.8, 14.3, 22.9, 27.0, 28.4, 31.3, 31.9, 32.0, 32.1, 32.3, 39.2, 42.9, 45.0, 49.1, 57.0, 57.0, 61.5, 61.5, 77.9, 109.1, 118.1, 119.3, 119.6, 121.8, 121.8, 126.4, 126.6, 133.6, 133.9, 134.2, 137.2, 137.2, 149.5, 167.3, 169.4, 169.6 **HRMS:** calc. for [M+H]$^+$ C$_{28}$H$_{34}$N$_3$O$_4$S: 508.22645, found: 508.22657.

(+/-)-Ethyl 2-(3-(2-bromonicotinoyl)-5-methoxy-1,2,3,4,5,6-hexahydro-7H-2,6-methanoazocino[5,4-b]indol-7-yl)acetate (71):

To a solution of compound **59** (10 mg, 0.030 mmol) in DMF (0.06 M, 0.5 mL), TBTU (CAS: 125700-67-6) (15.6 mg, 0.049 mmol), 2-bromonicotinic acid (9.3 mg, 0.046 mmol) and DIPEA (19 µL, 0.105 mmol) were added and the mixture was allowed to stir for 3 h. Crude product was
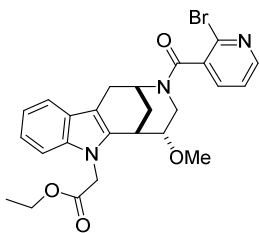
then purified directly by preparative HPLC (10% to 50% ACN/H$_2$O) to yield compound **71** (6.0 mg, 39%).**^{1}H NMR (CDCl$_3$, 700 MHz)** (rotameric mixture): δ 1.22-1.26 (m, 3H), 1.93 (s, 0.4H), 2.00 (d, *J*=11.9 Hz, 0.4H), 2.11 (m, 0.6H), 2.21 (d, *J*=13.2 Hz, 0.3H), 2.35 (d, *J*=12.8 Hz, 0.4H), 2.60 (dd, *J*=10.9, 12.7 Hz, 0.4H), 2.67-2.73 (m, 0.6H), 2.79 (dd, *J*=10.8, 12.6 Hz, 0.3H), 2.87 (d, *J*=17.2 Hz, 0.4H), 3.03-3.11 (m, 1H), 3.15-3.17 (m, 0.7H), 3.23 (s, 0.7H), 3.27-3.35 (m, 0.9H), 3.40-3.42 (m, 1.3H), 3.49 (m, 1H), 3.62-3.65 (m, 0.3H), 3.71 (dt, *J*=4.6, 10.3 Hz, 0.4H), 3.82-3.85 (m, 0.3H), 3.95-3.99 (m, 0.6H), 4.11-4.23 (m, 2H), 4.77-4.83 (m, 1H), 4.89-4.93 (m, 0.5H), 5.02 (dd, *J*=12.0, 18.0 Hz, 0.5H), 5.14 (dd, *J*=11.1, 18.1 Hz, 0.5H), 5.43 (m, 0.5H), 7.09-7.23 (m, 3H), 7.32-7.44 (m, 1H)7.49-7.53 (m, 1H), 7.59-7.66 (m, 1H), 8.40-8.47 (m, 1H).**^{13}C NMR (CDCl$_3$, 100 MHz):** δ 14.2, 26.6, 27.8, 28.0, 28.4, 29.7, 29.9, 30.3, 31.2, 31.5, 31.8, 32.1, 32.3, 38.6, 39.1, 42.9, 43.0, 44.1, 44.9, 44.9, 44.9, 44.9, 44.9, 45.2, 49.1, 49.4, 56.9, 56.9, 57.0, 57.0, 61.3, 61.4, 61.4, 77.7, 78.2, 78.7, 78.9, 108.5, 108.9, 108.9, 109.0, 109.0, 109.5, 109.7, 117.9, 118.1, 118.2, 118.3, 119.5, 121.8, 121.8, 121.8, 126.2, 126.2, 126.4, 126.4, 133.5, 133.7, 134.0, 135.3, 135.6, 135.7, 135.7, 135.8, 135.9, 136.1, 136.5, 137.1, 137.1, 137.2, 138.1, 138.4, 138.6, 150.3, 150.3, 150.4, 165.9, 166.0, 166.0, 166.3, 169.2, 169.3, 169.3, 169.4 **HRMS:** calc. for [M+H]$^+$ C$_{25}$H$_{27}$N$_3$O$_4$Br:512.11795, found: 512.11821. Calc. for [M+H]$^+$ C$_{25}$H$_{27}$N$_3$O$_4$^{81}Br: 514.11590, found: 514.11590

(+/-)-Ethyl 2-(5-methoxy-3-(2-methoxynicotinoyl)-1,2,3,4,5,6-hexahydro-7H-2,6-methanoazocino[5,4-b]indol-7-yl)acetate (72):
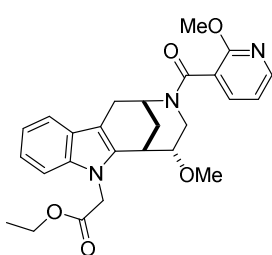
To a solution of 2-methoxynicotinic acid (16.8 mg, 0.091 mmol) in toluene (1.6 mL, 0.067 M), freshly distilled thionyl chloride (27.2μL, 0.385mmol) and a drop of DMF were added. The solution was stirred at reflux for 1h. The solvents were then removed *in vacuo* and the crude product was redissolved in DCM (0.25 mL, 0.55 M). The solution was canulated to a solution of compound **59** (30 mg, 0.091 mmol) and triethylamine (15.2 µL, 0.110 mmol) in DCM (0.25 mL, 0.37 M). The mixture was allowed to stir at room temperature overnight. The organic phase was then washed with water and brine, solvents were removed *in vacuo* and the crude product was purified by chromatography (3% MeOH/DCM). Pure compound **72** (39.0 mg, 92%) was isolated as a colourless oil. **^{1}H NMR (CDCl$_3$, 500 MHz):** δ 1.24 (q, *J*=7.0 Hz, 3H), 1.90-1.96 (m, 0.8H), 2.09-2.17 (m, 1.2H), 2.55-3.14 (m, 3H), 3.18 (d, *J*=16.3 Hz, 1.2H), 3.27-3.36 (m, 1H), 3.41 (s, 1.8H), 3.46 (s, 1H), 3.60-3.71 (m, 1H), 3.87 (s, 0.4H), 4.01 (s, 0.6H), 4.10 (d, *J*=21.9 Hz, 2H), 4.14-4.24 (m, 2H), 4.79 (dd, *J*=14.6, 18.0 Hz, 1H), 4.88-4.93 (m, 0.6H), 5.04 (d, *J*=17.9 Hz, 0.4H), 5.15 (dd, *J*=5.4, 18.0 Hz, 0.6H), 5.42 (s, 0.4H), 6.96-7.23 (m, 4H), 7.41-7.54 (m, 1H),

7.60-7.68 (m, 1H), 8.21 (dd, *J*=1.9, 5.1 Hz, 0.4H), 8.27 (dd, *J*=1.9, 5.1 Hz, 0.6H).**^{13}C NMR (CDCl$_3$, 100 MHz):** δ 14.3, 27.6, 28.4, 30.4, 30.6, 31.2, 31.7, 31.9, 32.2, 32.4, 38.8, 39.1, 42.9, 44.9, 45.0, 48.9, 49.1, 49.1, 54.3, 54.5, 57.0, 61.5, 78.1, 78.4, 79.1, 79.3, 109.0, 109.1, 117.2, 117.3, 117.4, 118.1, 118.3, 119.6, 120.7, 121.8, 126.4, 134.1, 137.2, 137.4, 147.2, 147.4, 166.2, 169.4, 169.5 **HRMS:** calc. for [M+H]$^+$ C$_{26}$H$_{30}$N$_3$O$_5$: 464.21800, found: 464.21828.

(+/-)-Ethyl 2-(3-(2-ethoxynicotinoyl)-5-methoxy-1,2,3,4,5,6-hexahydro-7H-2,6-methanoazocino[5,4-b]indol-7-yl)acetate (73):
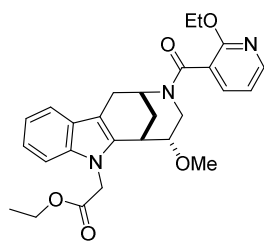
Compound **73** (35 mg, 80%) was synthesized as described for compound **67**. **^{1}H NMR (CDCl$_3$, 500 MHz)** (rotameric mixture): δ 1.25 (t, *J*=7.2 Hz, 3H), 1.43-1.53 (m, 3H), 1.90-1.97 (m, 0.8H), 2.11-2.22 (m, 1.2H), 2.54-3.15 (m, 3H), 3.19 (d, *J*=3.7 Hz, 1.2H), 3.24-3.34 (m, 0.8H), 3.39-3.41 (d, *J*=7.8 Hz, 1.8H), 3.47 (s, 1.2H), 3.60-3.72 (m, 1H), 4.03 (s, 0.6H), 4.10-4.31 (m, 2.4H), 4.41-4.53 (m, 1H), 4.54-4-63 (m, 0.6H), 4.76-4.85 (m, 1H), 4.88-4.94 (m, 0.6H), 5.04 (dd, *J*=7.9, 18.0 Hz, 0.4H), 5.15 (dd, *J*=8.0, 18.1 Hz), 5.42 (s, 0.4H), 6.92-7.03 (m, 1H), 7.08-7.13 (m, 1H), 7.20 (m, 2H), 7.43 (dd, *J*=7.7, 18.4 Hz, 0.6H), 7.49 (d, *J*=7.7 Hz, 0.4H), 7.58-7.68 (m, 1H), 8.17 (m, 0.4H), 8.24 (d, *J*=3.8 Hz, 0.6H).**^{13}C NMR (CDCl$_3$, 100 MHz):** δ 14.3, 14.4, 14.4, 14.8, 15.0, 18.9, 19.6, 20.6, 22.7, 27.6, 27.8, 27.8, 28.4, 29.0, 29.2, 30.1, 30.6, 31.2, 31.5, 31.7, 32.1, 32.2, 32.3, 38.7, 38.1, 41.4, 42.8, 42.9, 44.2, 44.7, 45.0, 48.7, 48.9, 56.8, 56.9, 57.0, 57.1, 61.4, 62.8, 62.8, 62.9, 63.0, 78.2, 78.3, 79.0, 79.1, 108.9, 109.0, 109.0, 109.2, 109.7, 110.0, 116.8, 116.9, 117.1, 117.2, 118.0, 118.1, 118.2, 118.3, 119.5, 120.7, 120.8, 120.9, 121.3, 121.8, 126.4, 126.4, 126.5, 126.6, 133.6, 134.0, 134.3, 134.3, 137.2, 137.2, 137.3, 137.4, 138.1, 147.3, 147.4, 158.6, 158.8, 159.0, 159.1, 166.3, 166.4, 167.0, 169.4, 169.5 **HRMS:** calc. for [M+H]$^+$ C$_{27}$H$_{32}$N$_3$O$_5$: 478.23365, found: 478.23391.

(+/-)-Ethyl 2-(3-(2-fluoronicotinoyl)-5-methoxy-1,2,3,4,5,6-hexahydro-7H-2,6-methanoazocino[5,4-b]indol-7-yl)acetate (74):
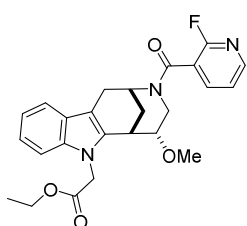
To a solution of compound **59** (20 mg, 0.061 mmol) in DMF (0.06 M, 0.5 mL), TBTU (CAS: 125700-67-6) (31.0 mg, 0.098 mmol), 2-fluoronicotinic acid (13.0 mg, 0.091 mmol) and DIPEA (27 µL, 0.153 mmol) were added and the reaction was allowed to stir at room temperature for 3 h. The crude product was then purified directly by preparative HPLC (10% to 50% ACN/H$_2$O) to yield compound **74** (5.4 mg, 20%).[1]**H NMR (CDCl$_3$, 500 MHz)** (rotameric mixture 1:1.3): δ 1.23-1.26 (m, 3H), 1.97-2.00 (m, 1H), 2.10-2.21 (m, 1H), 2.62-2.80 (m, 1H), 2.90 (d, *J*=17.2 Hz, 1H), 3.10-3.22 (m, 2H), 3.33 (dd, *J*=17.3, 6.1 Hz, 0.44H), 3.41 (s, 2H), 3.48-3.49 (m, 1H), 3.66 (bs, 1H), 4.08 (bs, 0.56H), 4.12-4.24 (m, 2H), 4.80 (dd, *J*=19.2, 18.1 Hz, 1H), 4.87 (bs, 0.56H), 5.04 (d, *J*=18.0 Hz, 0.44H), 5.14 (d, *J*=18.1 Hz, 0.56H), 5.39 (bs, 0.44H), 7.10-7.13 (m, 1H), 7.19-7.23 (m, 2H), 7.27-7.29 (m, 0.44H),7.33-7.35 (m, 0.56H), 7.44 (bs, 0.56H), 7.50 (d, *J*=7.8 Hz, 0.44H), 7.87-7.92 (m, 1H), 8.28 (dd, *J*=4.8, 1.6 Hz, 0.44H), 8.33 (dd, *J*=4.8, 1.5 Hz, 0.56H)). **^{13}C NMR (CDCl$_3$, 100 MHz):** δ 14.3, 27.6, 30.5, 32.0, 32.2, 43.4, 45.0, 45.0, 49.3, 57.0, 57.1, 61.5, 61.5, 78.1, 78.9, 109.1, 109.7, 118.2, 118.3, 119.3, 119.5, 119.6, 119.7, 121.9, 122.2, 122.2, 126.4, 126.5, 133.9, 134.2, 137.2, 137.3, 140.1, 148.9, 149.0, 149.1, 149.1, 157.8, 157.9, 159.1, 159.3, 163.9, 164.0, 169.3, 169.5 **HRMS:** calc. for [M+H]$^+$ C$_{25}$H$_{27}$N$_3$O$_4$F: 452.19801, found: 452.19813.

(+/-)-Ethyl 2-(5-methoxy-3-(2-morpholinonicotinoyl)-1,2,3,4,5,6-hexahydro-7H-2,6-methanoazocino[5,4-b]indol-7-yl)acetate (75):
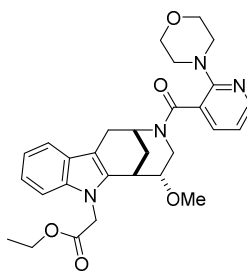
Compound **75** (11.3 mg, 73%) was synthesised as described for compound **67**. **^{1}H NMR (CDCl$_3$, 500 MHz)** (rotameric mixture): δ 1.22-1.27 (m, 3H), 1.98-2.28 (m, 2H), 2.55-2.69 (m, 1H), 2.82 (dd, *J*=30.5, 17.3 Hz, 0.5H), 2.92-2.97 (m, 0.5H), 3.12-3.18 (m, 2H), 3.26-3.91 (m, 13H), 4.10-4.24 (m, 2H), 4.76-4.83 (m, 1.3H), 4.93 (dd, *J*=12.6, 4.8 Hz, 0.2H), 5.03 (dd, *J*=18.0, 6.0 Hz, 0.5H), 5.13 (dd, *J*=18.0, 6.4 Hz, 0.5H), 5.37 (d, *J*=30.2 Hz, 0.5H), 6.87-7.00 (m, 1H), 7.07-7.16 (m, 1H), 7.17-7.24 (m, 2H), 7.40 (d, *J*=7.8 Hz, 0.3H), 7.46-7.51 (m, 1H), 7.55-7.61 (m, 0.7H), 8.27 (ddd, *J*=9.8, 4.9, 1.5 Hz, 0.5H), 8.34-8.35 (m, 0.5H). **^{13}C NMR (CDCl$_3$, 100 MHz):** δ 14.3, 27.3, 27.9, 27.9, 28.5, 30.6, 31.2, 31.6, 31.8, 32.0, 32.1, 32.3, 38.5, 39.4, 42.8, 42.9, 44.3, 44.8, 44.9, 45.0, 45.0, 48.6, 49.0, 49.5, 49.8, 49.9, 50.0, 56.9, 56.9, 57.0, 57.1, 61.5, 61.5, 66.9, 67.0, 67.1, 78.2, 78.5, 78.9, 79.2, 108.8, 108.9, 109.0, 109.1, 109.1, 109.3, 109.6, 116.0, 116.5, 116.6, 116.7, 118.0, 118.1, 118.2, 118.2, 119.6, 119.7, 119.9, 121.9, 121.9, 122.0, 122.9, 122.9, 123.4,

126.3, 126.3, 126.4, 126.5, 133.6, 133.8, 133.8, 134.4, 137.2, 137.2, 137.2, 169.3, 169.5 **HRMS:** calc. for $[M+H]^+$ $C_{29}H_{35}N_4O_5$: 519.26020, found: 519.26056.

(+/-)-Ethyl 2-(5-methoxy-3-(2-pivalamidonicotinoyl)-1,2,3,4,5,6-hexahydro-7H-2,6-methanoazocino[5,4-b]indol-7-yl)acetate (77):
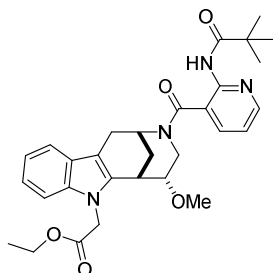
To a solution of compound **59** (20 mg, 0.061 mmol) in DMF (0.06 M, 0.5 mL), TBTU (CAS: 125700-67-6) (31.0mg, 0.098mmol), 2-pivalamidonicotinic acid (20.2 mg, 0.091 mmol) and DIPEA (27 µL, 0.153 mmol) were added and the mixture was allowed to stir for 3 h. The crude product was then purified directly by preparative HPLC (10% to 50% ACN/H_2O) to yield compound **77** (3.2 mg, 10%). The compound was characterised only by HRMS measurement. U-HPLC chromatogram showed a purity above 95%. **HRMS:** calc. for $[M+H]^+$ $C_{30}H_{37}N_4O_5$: 533.27585, found: 533.27488

(+/-)-Ethyl 2-(5-methoxy-3-picolinoyl-1,2,3,4,5,6-hexahydro-7H-2,6-methanoazocino[5,4-b]indol-7-yl)acetate (78):
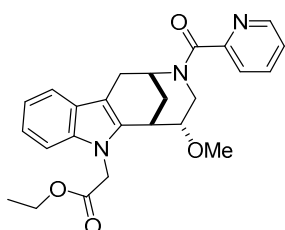
To a solution of picolinic acid (13.5 mg, 0.110 mmol) in toluene (1.6 mL, 0.067 M), freshly distilled thionyl chloride (27.2 µL, 0.385 mmol) and a drop of DMF were added. The solution was allowed to stirred at reflux for 1h. The solvents were then removed *in vacuo* and the crude product redissolved in DCM (0.25 mL, 0.55 M). The solution was canulated to a solution of compound **59** (30 mg, 0.0913 mmol) and triethylamine (15.2 µL, 0.110 mmol) in DCM (0.25 mL, 0.37 M). The mixture was allowed to stir at room temperature overnight. The organic phase was then washed with water and brine, solvents were removed *in vacuo* and the crude product was purified by chromatography (2% MeOH/DCM). Pure compound **78** (25.7 mg, 65%) was isolated as a colourless oil. **^{1}H NMR (CDCl$_3$, 500 MHz)** (rotameric mixture): δ 1.24 (q, *J*=7.2 Hz, 3H), 1.92 (dt, *J*=2.6, 12.7 Hz, 0.6H), 2.10 (dt, *J*=2.5, 13.0 Hz, 0.4H), 2.10-2.24 (m, 1H), 2.65 (dd, *J*=10.9, 12.6 Hz, 0.6H), 2.86 (dd, *J*=12.3, 13.6 Hz, 0.4H), 2.93-3.00 (m, 1H), 3.06-3.11 (m, 0.6H), 3.22 (s, 1.2H), 3.33 (dd, *J*=6.1, 17.3 Hz, 0.4H), 3.40 (s, 1.8H), 3.48 (m, 1H), 3.69-3.73 (m, 0.7H), 3.80-3.85 (m, 0.7H), 4.10-4.24 (m, 2H), 4.41 (bs, 0.6H), 4.80 (dd, *J*=15.3, 18.0 Hz, 1H), 4.87 (dd, *J*=4.9, 12.9 Hz, 0.6H), 5.06 (d, *J*=18.0Hz, 0.4H), 5.16 (d, *J*=18.1 Hz, 0.6H), 5.38 (bs, 0.4H), 7.08-7.12(m, 1H), 7.17-7.22 (m, 2H), 7.38 (dd, *J*=5.3, 6.9 Hz, 0.4H), 7.43 (dd, *J*=5.2, 7.1 Hz, 0.6H), 7.46 (d, *J*=7.8 Hz, 0.6H), 7.50 (d, *J*=7.8 Hz, 0.4H), 7.63 (d, *J*=7.9 Hz, 0.4H), 7.65 (d, *J*=7.8 Hz, 0.6H), 7.85 (t, *J*=7.9 Hz, 0.4H), 7.89 (t, *J*=7.7 Hz, 0.6H), 8.59 (d, *J*=4.6 Hz, 0.4H), 8.68 (d, *J*=4.6 Hz, 0.6H). **^{13}C NMR (CDCl$_3$, 100 MHz)** (rotameric mixture): δ 14.3, 27.4, 28.5, 30.4, 31.2, 32.0, 32.3, 39.4, 43.4,

44.6, 45.0, 48.6, 56.8, 57.0, 61.4, 78.1, 78.7, 108.97, 108.98, 109.3, 109.7, 118.2, 118.3, 119.5, 121.69, 121.71, 123.5, 124.0, 124.7, 124.8, 126.4, 126.6, 134.3, 137.2, 138.1, 138.3, 147.6, 148.1, 153.8, 154.4, 167.2, 167.5, 1690.4, 169.6 **HRMS:** calc. for $[M+H]^+$ $C_{25}H_{28}N_3O_4$: 434.20743, found: 434.20535.

**(+/-)-Ethyl 2-(5-methoxy-3-nicotinoyl-1,2,3,4,5,6-hexahydro-7H-2,6-methanoazocino[5,4-b]indol-7-yl)acetate (79):**
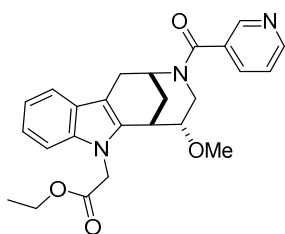
To a solution of nicotinic acid (13.5 mg, 0.110 mmol) in toluene (1.6 mL, 0.067 M) freshly distilled thionyl chloride (27.2 µL, 0.385 mmol) and a drop of DMF were added.The solution was then stirred at reflux for 1h. The solvents were then removed *in vacuo* and the crude product was redissolved in DCM (0.25 mL, 0.55 M). The solution was canulated to a solution of compound **9** (30 mg, 0.0913 mmol) and triethylamine (15.2 µL, 0.110 mmol) in DCM (0.25 mL, 0.37 M). The mixture was allowed to stir at room temperature overnight. The organic phase was then washed with water and brine, solvents were removed *in vacuo* and the crude product was purified by chromatography (2% MeOH/DCM). Pure compound **79** (35 mg, 88%) was isolated as a colourless oil. **^{1}H NMR (CDCl$_3$, 500 MHz)** (rotameric mixture): δ 1.23 (m, 3H), 1.95 (d, *J*=12.4 Hz, 0.6H), 2.04 (d, *J*=12.7 Hz, 0.6H), 2.13 (s, 0.8H), 2.64 (t, *J*=9.5 Hz, 0.6H), 2.86-2.96 (m, 1.4H), 3.16 (dd, *J*=5.6, 17.0 Hz, 0.6H), 3.19 (s, 1.2H), 3.33 (dd, *J*=5.9, 17.4 Hz, 0.4H), 3.41 (s, 1.8H), 3.49 (d, *J*=2.6 Hz, 1H), 3.53-3.55 (m, 0.4H), 3.59-3.72 (m, 1H), 4.11-4.24 (m, 2H), 4.27 (bs, 0.6H), 4.77-4.87 (m, 1.6H), 5.02 (d, *J*=18.0 Hz, 0.4H), 5.14 (d, *J*=18.1 Hz, 0.6H), 5.38 (bs, 0.4H), 7.10-7.13 (m, 1H), 7.19-7.23 (m, 2H), 7.39-7.52 (m, 2H), 7.79 (d, *J*=7.5 Hz, 0.4H), 7.88 (d, *J*=7.5 Hz, 0.6H), 8.67-8.76 (m, 2H). **^{13}C NMR (CDCl$_3$, 100 MHz)** (rotameric mixture): δ 14.3, 26.8, 27.5, 29.4, 30.5, 30.8, 31.3, 38.3, 42.3, 43.9, 44.5, 48.2, 56.0, 60.5, 77.0, 77.9, 107.7, 108.1, 108.7, 117.1, 117.3, 118.7, 120.9, 123.0, 123.2, 125.3, 125.5, 132.1, 131.6, 132.8, 133.2, 134.6, 134.9, 136.1, 136.2, 145.7, 145.8, 148.8, 148.9, 166.6, 168.3, 168.5 **HRMS:** calc. for $[M+H]^+$ $C_{25}H_{28}N_3O_4$: 434.20743, found: 434.20705.

(+/-)-Ethyl 2-(3-isonicotinoyl-5-methoxy-1,2,3,4,5,6-hexahydro-7H-2,6-methanoazocino[5,4-b]indol-7-yl)acetate (80):
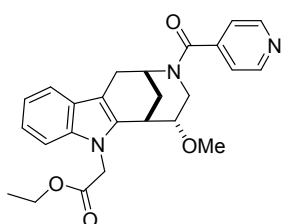
To a solution of compound **59** (10 mg, 0.030 mmol) in DMF (0.06 M, 0.5 mL), TBTU (CAS: 125700-67-6) (15.6 mg, 0.049 mmol), isonicotinic acid (5.7 mg, 0.046 mmol) and DIPEA (19 µL, 0.105 mmol) were dissolved and the mixture was allowed to stir for 3 h. The mixture was then purified directly by preparative HPLC (10% to 50% ACN/H_2O) to yield compound **80** (4 mg, 31%).**^{1}H NMR (CDCl$_3$, 500 MHz)** (rotameric mixture): δ 1.25 (td, *J*=3.8, 7.1 Hz, 3H), 1.98-2.19 (m, 2H), 2.66 (dd, *J*=10.9, 12.7 Hz, 0.5H), 2.85-2.97 (m, 1H), 3.17 (dd, *J*=5.9, 17.1 Hz, 0.5H), 3.19 (s, 1.2H), 3.35 (td. *J*=5.8, 11.7 Hz, 1H), 3.41 (s, 1.8H), 3.51 (s, 1H), 3.64-3.68 (m, 1H), 4.07 (bs, 0.7H), 4.11-4.24 (m, 2.5H), 4.77-4.83 (m, 1.5H), 5.00 (d, *J*=18.0 Hz, 0.4H), 5.13 (d, *J*=18.0 Hz, 0.6H), 5.35 (bs, 0.3H), 7.11-7.16 (m, 1H), 7.20-7.24 (m, 2H), 7.45 (d, *J*=7.8 Hz, 0.6H), 7.50 (d, *J*=7.8 Hz, 0.4H), 7.62 (d, *J*=5.2 Hz, 1H), 7.68 (d, *J*=4.9 Hz, 1H), 8.78 (bs, 1H), 8.86 (bs, 1H).**^{13}C NMR (CDCl$_3$, 100 MHz)** (rotameric mixture)**:** δ14.3, 27.9, 28.6, 30.2, 31.4, 31.8, 32.2, 39.4, 43.6, 44.9, 45.0, 45.6, 49.3, 57.1, 57.2, 61.6, 77.9, 78.8, 108.4, 109.2, 109.5, 118.1, 118.3, 119.8, 122.1, 122.2, 122.9, 123.2, 126.2, 126.4, 133.4, 133.8, 137.2, 137.3, 145.5, 145.9, 149.4, 166.1, 169.2, 169.4 **HRMS:** calc. for $[M+H]^+$ $C_{25}H_{28}N_3O_4$: 434.20743, found: 434.20660

(+/-)-Ethyl 2-(5-methoxy-3-(pyrimidine-5-carbonyl)-1,2,3,4,5,6-hexahydro-7H-2,6-methanoazocino[5,4-b]indol-7-yl)acetate (81):
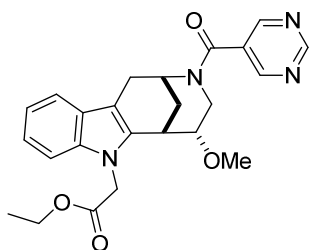
To a solution of pyrimidine-5-carboxylic acid (11.3 mg, 0.091 mmol) in toluene (1.6 mL, 0.067 M), freshly distilled thionyl chloride (23.1 µL, 0.319 mmol) and a drop of DMF were added. The solution was allowed to stir at reflux for 1h. The solvents were then removed *in vacuo* and the crude product was redissolved in DCM (0.25 mL, 0.55 M). The solution was canulated to a solution of compound **59** (30 mg, 0.091 mmol) and triethylamine (15.2 µL, 0.110 mmol) in DCM (0.25 mL, 0.37 M). The mixture was allowed to stir at room temperature overnight. The organic phase was washed with water and brine, solvents were removed *in vacuo* and the crude product was purified by chromatography (2% MeOH/DCM). Pure compound **81** (9.0 mg, 23%) was isolated as a colourless oil. **^{1}H NMR (CDCl$_3$, 400 MHz)** (rotameric mixture 1:1.5): δ 1.25 (t, *J*=7.0 Hz, 3H), 1.99-2.15 (m, 2H), 2.66 (t, *J*=11.7 Hz, 0.6H), 2.88-2.95 (m, 1H), 3.01 (t, *J*=10.4, 0.4H), 3.19-3.24 (m, 2H), 3.51-3.57 (m, 1.4H), 3.60-3.72 (m, 1H), 4.11-4.25 (m, 2.6H), 4.77-4.87 (m, 1.6H), 5.02 (d, *J*=18.0 Hz, 0.4H), 5.14 (d, *J*=18.1 Hz, 0.6H), 5.38 (bs, 0.4H), 7.11-7.16 (m, 1H), 7.19-7.22 (m, 2H), 7.46 (d, *J*=7.8 Hz, 0.6H), 7.54 (d, *J*=7.6 Hz, 0.4H), 8.80 (s, 0.8H), 8.88 (s,

1.2H), 9.26 (s, 0.4H), 9.32 (m, 0.6H). **HRMS:** calc. for $[M+H]^+$ $C_{24}H_{27}N_4O_4$: 435.20268, found: 435.20259.


(+/-)-Ethyl 2-(5-methoxy-3-(thiophene-2-carbonyl)-1,2,3,4,5,6-hexahydro-7H-2,6-methanoazocino[5,4-b]indol-7-yl)acetate (82):
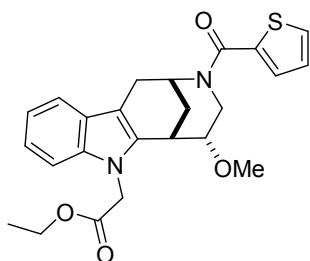
To a solution of compound **59** (20 mg, 0.061 mmol) in DCM (0.09 M, 0.667 mL), triethylamine (10.5 µL, 0.076 mmol) and thiophene-2-carbonyl chloride (6.52 µL, 0.061 mmol) were added and the mixture was allowed to stir overnight at room temperature. The solvents were then removed *in vacuo* and the crude product was purified by chromatography (1% MeOH/DCM) to yield compound **82** (26.5 mg, 98%) as a colourless oil. **^{1}H NMR (CDCl$_3$, 500 MHz)** (rotameric mixture): δ 1.26 (t, *J*=7.1 Hz, 3H), 1.78 (bs, 1H), 2.00-2.07 (m, 2H), 2.62 (bs, 0.6H), 2.95 (d, *J*=15.1 Hz, 1.4H), 3.25-3.37 (m, 4H), 3.48 (d, *J*=3.0 Hz, 1H), 3.62 (bs, 1H), 4.12-4.25 (m, 2H), 4.81 (d, *J*=18.0 Hz, 2H), 5.12 (bs, 1H), 7.08 (m, 1H), 7.11-7.14 (m, 1H), 7.19-7.24 (m, 2H), 7.35 (bs, 1H), 7.47-7.50 (m, 2H). **^{13}C NMR (CDCl$_3$, 100 MHz)** (rotameric mixture): δ 14.3, 22.8, 27.8, 29.2, 32.2, 41.5, 45.0, 57.0, 61.5, 78.1, 109.0, 118.2, 119.6, 121.8, 126.5, 126., 128.7, 134.3, 137.2, 137.7, 164.0, 169.5 **HRMS:** calc. for $[M+H]^+$ $C_{24}H_{27}N_2O_4S$: 439.16860, found: 439.16819

(+/-)-Ethyl 2-(5-methoxy-3-(6-methyl-2-(methylthio)nicotinoyl)-1,2,3,4,5,6-hexahydro-7H-2,6-methanoazocino[5,4-b]indol-7-yl)acetate (83):
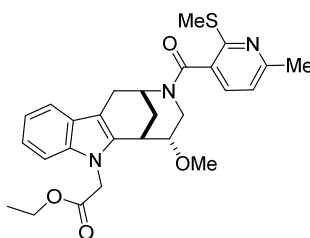
Compound **83** (72mg, 71%) was synthesized as described for compound **84** using 2-chloro-6-methylnicotinic acid (CAS: 30529-70-5) as a starting material and following the procedure for compound **67** to obtain the chloride derivative (the crude product is enough to be used for the amide formation). Compound **83** was purified by preparative HPLC (10% to 50% ACN/H$_2$O) and isolated as the TFA salt. **^{1}H NMR (CDCl$_3$, 400 MHz)** (rotameric mixture 1:1): δ 1.22-1.27 (m, 3H), 1.96 (d, *J*=11.6 Hz, 1H), 2.10-2.20 (m, 1H), 2.55 (s, 2H), 2.67 (s, 2H), 2.76-3.09 (m,2H), 3.19 (s, 1.5H), 3.29-3.39 (s, 1.5H), 3.47 (d, *J*=3.0 Hz, 1H), 3.69 (bs, 0.5H), 4.04 (bs, 0.5H), 4.10-4.26 (m, 2H), 4.80 (dd, *J*=18.0, 13.2 Hz, 1H), 4.88 (dd, *J*=12.9, 4.9 Hz, 0.5H), 5.03 (d, *J*=18.0 Hz, 0.5H), 5.14 (d, *J*=18.0 Hz, 0.5H), 5.43 (bs, 0.5H), 6.94 (d, *J*=7.7 Hz, 0.5H), 7.02 (d, *J*=7.7 Hz, 0.5H), 7.09-7.16 (m, 1H), 7.18-7.23 (m, 2H), 7.38 (d, *J*=6.5 Hz, 0.5H), 7.48 (dd, *J*=27.7, 7.6 Hz, 1.5H), 9.35 (bs, 1H). **^{13}C NMR (CDCl$_3$, 100 MHz):** δ 13.5, 13.7, 24.0, 28.4, 30.2, 31.4, 31.9, 32.2, 39.5, 43.5, 45.0, 49.5, 57.1, 57.1, 61.5, 78.1, 79.1, 108.8, 109.0, 109.1, 109.6, 118.1, 118.4, 119.3, 119.7, 121.9, 126.4, 126.6, 128.6, 133.8, 134.1, 134.8, 137.2, 137.3,

154.7, 159.1, 159.1, 159.6, 167.9, 169.4, 169.6 **HRMS:** calc. for $[M+H]^+$ $C_{27}H_{32}N_3O_4S$: 494.21080, found: 494.21134

(+/-)-Ethyl 2-(3-(5-bromo-2-(methylthio)nicotinoyl)-5-methoxy-1,2,3,4,5,6-hexahydro-7H-2,6-methanoazocino[5,4-b]indol-7-yl)acetate (84):
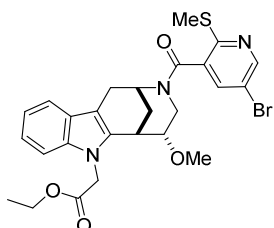
To a solution of compound **87** (80 mg, 0.322 mmol) in toluene (4.6 mL, 0.07 M), freshly distilled thionyl chloride (82 µL, 1.129 mmol) and a drop of DMF were added. The mixture was allowed to stir at reflux for 1 h. The solvents were then evaporated and the crude product was redissolved in DCM (1.5 mL, 0.11 M). To this solution, compound **59** (55 mg, 0.167 mmol) and triethylamine (70 µL, 0.501 mmol) were added, the mixture was then allowed to stir overnight at room temperature. The crude product was washed with NaHCO$_3$ (saturated aqueous solution) and the solvents were then evaporated. The crude product was purified by flash chromatography (15% ethyl acetate/DCM) to give compound **84** (66 mg, 71%) as a colorless oil. **^{1}H NMR (CDCl$_3$, 400 MHz)** (rotameric mixture 1:1): δ 1.22-1.27 (m, 3H), 1.97 (d, *J*=11.2 Hz, 0.5H), 2.12-2.32 (m, 1.5H), 2.53-2.61 (m, 4H), 2.79-2.94 (m, 1H), 3.11 (dd, *J*=17.0, 5.7 Hz, 1H), 3.21 (s, 1.5H), 3.28-3.35 (m, 1H), 3.41 (s, 1.5H), 3.48 (d, *J*=3.2 Hz, 1H), 3.67 (bs, 0.5H), 4.00 (bs, 0.5H), 4.10-4.26 (m, 2H), 4.76-4.89 (m, 1.5H), 5.03 (d, *J*=17.9 Hz, 0.5H), 5.15 (d, *J*=18.0 Hz, 0.5H), 7.10-7.15 (m, 1H), 7.18-7.24 (m, 2H), 7.47-7.59 (m, 2H), 8.50 (d, *J*=2.2 Hz, 0.5H), 8.56 (d, *J*=2.2 Hz, 0.5H).**^{13}C NMR (CDCl$_3$, 100 MHz):** δ 12.1, 12.3, 13.2, 27.4, 28.7, 29.1, 30.5, 30.8, 31.2, 38.1, 41.9, 43.9, 48.1, 55.9, 55.9, 60.3, 76.9, 78.0, 107.7, 107.9, 108.6, 114.7, 117.0, 117.2, 118.5, 118.5, 120.7, 125.2, 125.4, 131.0, 131.5, 132.7, 133.0, 134.5, 135.1, 136.1, 136.1, 149.3, 153.7, 164.3, 164.5, 168.1, 168.3 **HRMS:** calc. for $[M+H]^+$ $C_{26}H_{29}N_3O_4{}^{81}BrS$: 560.10362,found: 560.10518

(+/-)-Ethyl 2-(5-methoxy-3-(2-(methylthio)-4-(trifluoromethyl)nicotinoyl)-1,2,3,4,5,6-hexahydro-7H-2,6-methanoazocino[5,4-b]indol-7-yl)acetate (85):
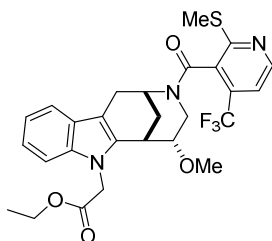
Compound **85** (80 mg, 73%) was synthesized as described for compound **84** using 2-chloro-4-(trifluoromethyl)nicotinic acid (CAS: 590371-81-6) as the starting material and following the procedure for compound **67** to obtain the chloride derivative (crude product is pure enough to be used for the amide formation). Compound **85** was purified by preparative HPLC (10% to 50% ACN/H$_2$O) and isolated as the TFA salt.**^{1}H NMR (CDCl$_3$, 400 MHz)** (rotameric mixture 1:2.3): δ 1.22-1.27 (m, 3H), 1.90 (ddt, *J*=26.3, 12.7, 2.5 Hz, 0.3H), 2.06-2.15 (m, 1H), 2.26 (dt, *J*=13.1, 3.6 Hz, 0.3H), 2.52 (s, 1H), 2.65-2.62 (m, 3H), 2.81-2.87 (m, 0.7H), 3.01-3.09 (m, 0.7H), 3.12-3.23 (m, 3H), 3.28-

3.35 (m, 1H), 3.42 (d, J=4.9 Hz, 1H), 3.47-3.50 (m, 1H), 3.52-3.64 (m, 0.3H), 3.76-4.00 (m, 0.7H), 4.11-4.26 (m, 2H), 4.80 (t, J=16.4 Hz, 1H), 4.94-5.00 (m, 0.3H), 5.04 (d, J=17.9 Hz, 0.7H), 5.15 (dd, J=18.0, 2.7 Hz, 0.3H), 5.48 (bs, 0.7H), 7.09-7.18 (m, 1H), 7.20-7.24 (m, 2.3H), 7.27-7.31 (m, 0.7H), 7.48 (dd, J=12.9, 7.8 Hz, 0.3H), 7.54 (dd, J=11.4, 7.8 Hz, 0.7H), 8.66 (t, J=4.7 Hz, 0.7H), 8.64-8.71 (m, 0.3H). **^{13}C NMR (CDCl$_3$, 100 MHz):** δ 13.5, 13.7, 13.9, 14.0, 14.1, 14.4, 26.7, 26.9, 27.1, 28.3, 30.1, 30.2, 30.6, 31.9, 32.0, 32.1, 32.5, 32.6, 39.0, 39.1, 43.1, 43.8, 45.1, 45.1, 49.6, 49.7, 57.1, 57.1, 57.2, 61.6, 77.9, 78.0, 78.4, 79.5, 109.0, 109.0, 109.1, 109.2, 109.3, 109.8, 109.9, 115.1, 115.1, 115.6, 118.3, 118.5, 119.6, 119.7, 119.7, 121.9, 126.5, 126.7, 126.8, 133.8, 134.0, 134.4, 137.3, 137.4, 150.0, 150.1, 150.1, 151.5, 158.4, 158.9, 159.2, 159.4, 163.9, 164.0, 169.4, 169.5, 169.6, 169.6 **HRMS:** calc. for [M+H]$^+$ C$_{27}$H$_{29}$N$_3$O$_4$F$_3$S:548.18254, found: 548.18209

(+/-)-Ethyl 2-(5-methoxy-3-(2-(methylthio)-5-(trifluoromethyl)nicotinoyl)-1,2,3,4,5,6-hexahydro-7H-2,6-methanoazocino[5,4-b]indol-7-yl)acetate (86):
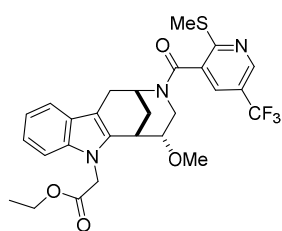
Compound **86** (76 mg, 84%) was synthesized as described for compound **84** using 2-chloro-5-(trifluoromethyl)nicotinic acid (CAS: 280566-45-2) as a starting material and following the procedure for compound **67** to obtain the chloride derivative (crude product is pure enough to be used for the amide formation).**^{1}H NMR (CDCl$_3$, 400 MHz)** (rotameric mixture 1:1)**:** δ 1.23-1.28 (m, 3H), 1.98 (d, J=12.2 Hz, 0.5H), 2.15-2.32 (m, 1.5H), 2.58-2.67 (m, 4H), 2.95-3.13 (m, 2H), 3.20 (s, 1.5H), 3.26-3.36 (m, 1H), 3.42 (s, 1.5H), 3.49 (d, J=3.2 Hz, 1H), 3.67-3.73 (m, 0.5H), 3.95 (bs, 0.5H), 4.11-4.26 (m, 2H), 4.81 (dd, J=18.0, 13.4 Hz, 1H), 4.89 (dd, J=12.9, 4.9 Hz, 0.5H), 5.03 (d, J=17.9 Hz, 0.5H), 5.15 (d, J=18.0 Hz, 0.5H), 5.42 (bs, 0.5H), 7.10-7.17 (m, 1H), 7.19-7.24 (m, 2H), 7.51 (dd, J=19.1, 7.7 Hz, 1H), 7.62 (bs, 0.5H), 7.67 (bs, 0.5H), 8.69 (d, J=1.2 Hz, 0.5H), 8.76 (d, J=1.2 Hz, 0.5). **^{13}C NMR (CDCl$_3$, 100 MHz):** δ 13.2, 13.4, 14.3, 28.5, 29.8, 30.3, 31.6, 31.9, 32.3, 39.2, 43.2, 45.0, 45.0, 49.3, 57.0, 61.4, 78.1, 79.2, 108.8, 109.0, 109.1, 109.7, 118.2, 118.3, 119.6, 121.9, 122.3, 125.0, 126.3, 126.5, 130.1, 130.8, 131.1, 133.7, 134.1, 137.2, 137.3, 146.2, 146.2, 161.1, 165.6, 165.7, 169.3, 169.4 **HRMS:** calc. for [M+H]$^+$ C$_{27}$H$_{29}$N$_3$O$_4$F$_3$S: 548.18254, found:548.18391

5-bromo-2-(methylthio)nicotinic acid (87):
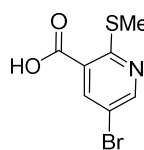
To a solution of 5-bromo-2-chloronicotinic acid (CAS: 29241-65-4) (100mg, 0.423 mmol) in a mixture of in dioxane (1 mL, 0.4 M) and water (0.4 mL, 1.0 M), sodium thiometoxide (75 mg, 1.06 mmol) was added and the mixture was allowed to stir in a sealed tube at 120º overnigth. The mixture was then acidify with citric acid (20% aqueous solution) to pH 3-4 and extracted with ethyl acetate. The crude product was purified by flash chromatography (2 to 10% MeOH/DCM) to give product **87** (50 mg, 48%) as a white solid. **^{1}H NMR (DMSO-d6, 400 MHz):** δ 2.42 (s, 3H), 8.30 (d, J=2.4 Hz, 1H), 8.78 (d, J=2.4 Hz, 1H), 13.71 (bs,.1H). **HRMS:** calc. for [M+H]$^+$ $C_7H_7NO_2BrS$: 247.93754, found: 247.93714. Calc. for [M+H]$^+$ $C_7H_7NO_2{}^{81}BrS$: 249.93475, found: 249.93549

(+/-)-Ethyl 2-(5-acetoxy-1,2,3,4,5,6-hexahydro-7H-2,6-methanoazocino[5,4-b]indol-7-yl)acetate (88):
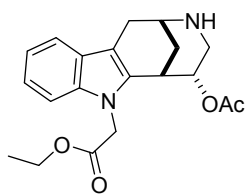
Compound **88** (72%, white solid) was synthesised as described for compound **59**. **^{1}H NMR (CDCl$_3$, 400 MHz):** δ 1.26 (t, J=7.1 Hz, 3H), 2.01 (s, 3H), 2.06 (d, J=14.0 Hz, 1H), 2.21 (d, J=12.6 Hz, 1H), 2.67 (t, J=11.3 Hz, 1H), 2.80 (bs, 1H), 2.85 (d, J=17.1 Hz, 1H), 2.99 (dd, J=4.7, 12.0 Hz, 1H), 3.22 (dd, J=6.2, 17.2 Hz, 1H), 3.41 (s, 1H), 3.54 (s, 1H), 4.12-4.26 (m, 2H), 4.87 (s, 2H), 5.08 (dt, J=4.5, 9.2 Hz, 1H), 7.13-7.17 (m, 1H), 7.20-7.26 (m, 2H), 7.54 (d, J=7.7 Hz, 1H).). **^{13}C NMR (CDCl$_3$, 100 MHz):** δ14.2, 21.1, 28.8, 31.1, 33.0, 42.1, 44.7, 45.2, 61.5, 72.7, 108.8, 111.4, 118.4, 119.5, 121.7, 126.7, 134.1, 137.0, 168.8, 170.0 **HRMS:** calc. for [M+H]$^+$ $C_{20}H_{25}N_2O_4$: 357.18088, found. 357.18259

(+/-)-Ethyl 2-(5-acetoxy-3-(2-(methylthio)nicotinoyl)-1,2,3,4,5,6-hexahydro-7H-2,6-methanoazocino[5,4-b]indol-7-yl)acetate (89):
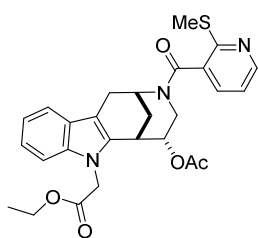
Compound **89** (71%, white solid) was synthesised as described for compound **(+/-)-Glupin-1**. **1H NMR (CDCl$_3$, 400 MHz)** (rotameric mixture)**:** δ 1.25 (t, J=7.12 Hz, 3H), 1.94-2.00 (m, 2H), 2.08 (s, 1H), 2.11-2.19 (m, 1H), 2.27 (bs, 1H), 2.59-2.66 (m, 3H), 2.75-3.09 (m, 3H), 3.33-3.38 (m, 1H), 3.50 (dd, J=2.8, 15.0 Hz, 1H), 4.12-4.24 (m, 2H), 4.71-4.90 (m, 2H), 5.01-5.24 (m, 1H), 5.47 (s, 1H), 7.07-7.24 (m, 4H), 7.47-7.51 (m, 1H), 7.56 (d, J=7.71 Hz, 1H), 8.38-8.54 (m, 1H). **^{13}C NMR (CDCl$_3$, 100 MHz)**(rotameric mixture)**:** δ 13.3, 13.4, 14.2, 21.0, 21.1, 27.1, 28.4, 30.3, 30.8, 30.9, 31.4, 42.8, 44.8, 61.8, 71.0, 71.8, 109.0, 109.1, 110.4, 118.4, 118.6, 119.4, 120.0, 120.0, 122.3, 122.3, 126.5, 126.7, 130.7, 131.2, 132.8, 132.9, 134.0, 134.3, 137.2, 149.6, 156.0, 167.3, 167.4, 168.7, 169.8, 169.8 **HRMS:** calc. for [M+H]$^+$ $C_{27}H_{30}N_3O_5S$: 508.19007, found. 508.19232

(+/-)-Ethyl 2-(5-hydroxy-3-(2-(methylthio)nicotinoyl)-1,2,3,4,5,6-hexahydro-7H-2,6-methanoazocino[5,4-b]indol-7-yl)acetate (90):
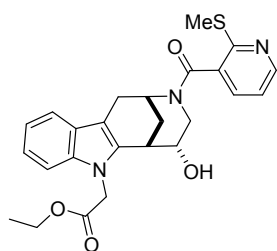
To a solution of compound **89** (0.39 g, 0.786 mmol) in a mixture of THF (0.07 M)/H_2O (0.16 M), LiOH (0.110 g, 4.61 mmol) was dissolved. The mixture was allowed to stir for one hour and then taken to pH~3 with HCl 1M. The mixture was extracted with DCM (3x) and the solvents were removed *in vacuo*. The crude product was then redissolved in EtOH (0.1 M) and sulphuric acid was added (8 M). The mixture was allowed to stir overnight at room temperature. The mixutre was then neutralized with Na_2CO_3 and extracted with DCM. After evaporation of the solvents, the crude product was purified by preparative HPLC (10% to 50% ACN/H_2O with 0.1% TFA) to yield compound **90** (53%) as a light yellow solid. **^{1}H NMR (CDCl$_3$, 400 MHz)** (rotameric mixture)**:** δ 1.28 (td, *J*=2.6, 7.1 Hz, 3H), 1.94-2.12 (m, 1H), 2.19-2.35 (m, 1H), 2.58-2.65 (m, 3H), 3.02 (bs, 2H), 3.26-3.36 (m, 1H), 3.44-3.47 (m, 1H), 4.00-4.11 (m, 1H), 4.21 (qd, *J*=3.5, 7.2 Hz, 2H), 4.68 (dd, *J*=5.3, 13.4 Hz, 0.4H), 4.84-5.07 (m, 4H), 5.44 (bs, 0.6H), 7.06-7.24 (m, 4H), 7.46 (bs, 1H), 7.54 (dd, *J*=7.8, 15.1 Hz, 1H), 8.50 (dd, *J*=1.5, 5.1 Hz, 0.6H), 8.57 (dd, *J*=1.4, 4.9 Hz, 0.4H). **^{13}C NMR (CDCl$_3$, 100 MHz)** (rotameric mixture)**:** δ 13.4, 13.5, 14.3, 28.4, 30.3, 31.5, 33.5, 33.6, 42.4, 42.9, 45.1, 49.1, 62.1, 62.3, 69.4, 70.1, 109.0, 109.1, 118.3, 118.6, 119.5, 120.1, 120.2, 122.3, 122.4, 126.5, 126.8, 132.8, 133.3, 134.1, 134.5, 137.3, 137.5, 149.4, 149.5, 156.1, 167.2, 167.3, 170.2, 170.6 **HRMS:** calc. for [M+H]$^+$ C$_{25}$H$_{28}$N$_3$O$_4$S: 466.17950, found. 466.17937

(+/-)-Benzyl 4-(allyloxy)-6-oxo-2-azabicyclo[3.3.1]nonane-2-carboxylate (91):
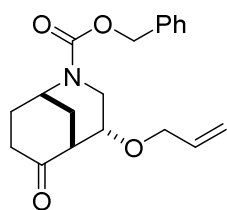
To a solution of compound **44** (0.103 g, 0.356 mmol) in THF (1.8 mL, 0.2 M), allyl ethylcarbonate (CAS number: 1469-70-1) (0.120 mL, 0.712 mmol) and a solution of Pd(PPh$_3$)$_4$ (0.021 mg, 0.018 mmol) in THF (1.8 mL; 0.01M) were added. The mixture was allowed to stir at 80° for 2.5 h. The mixture was then filtered through Celite and the solvents were removed *in vacuo*. The crude product was purified by chromatography (1 to 5% ethyl acetate/DCM) to obtain compound **91** (50.7 mg, 43%) as colorless oil. **^{1}H NMR (CDCl$_3$, 400 MHz)** (rotameric mixture 1:1): δ 1.88-2.06 (m, 3H), 2.15-2.27´(m, 1H), 2.42-2.61 (m, 2H), 3.06 (bs, 1H), 3.15-3.23 (m, 1H), 3.76 (td, *J*=11.5, 5.9 Hz, 1H), 3.94-4.03 (m, 1H), 4.14-4.21 (m, 1H), 4.34 (ddd, *J*=20.9, 14.4, 7.5 Hz, 1H), 4.42(bs, 0.5H), 4.51 (bs, 0.5H), 5.14-5.20 (m, 3H), 5.25 (d, *J*=17.3 Hz, 1H), 5.85 (ddd, *J*=22.7, 10.9, 5.8 Hz, 1H), 7.31-7.38 (m, 5H). **HRMS:** calc. for [M+H]$^+$ C$_{19}$H$_{24}$NO$_4$: 330.16998, found: 330.17035

**(+/-)-Benzyl 5-(allyloxy)-1,2,4,5,6,7-hexahydro-3H-2,6-methanoazocino[5,4-b]indole-3-carboxylate (92):**
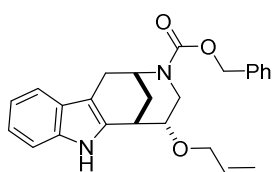
Compound **92** (35 mg, 73%) was synthesized as described for compound **52** and isolated with a 10% impurity. **^{1}H NMR (CDCl$_3$, 400 MHz)** (rotameric mixture 1:1): δ 1.98-2.09 (m, 2H), 1.98-2.09 (m, 2H), 2.54 (dd, *J*=12.0, 11.2, 0.5H), 2.60 (t, *J*=8.0 Hz, 0.5H), 2.78 (d, *J*=16.8 Hz, 0.5H), 2.83 (d, *J*=17.0 Hz, 0.5H), 3.07-3.13 (m, 1H), 3.32-3.33 (m, 1H), 3.69 (ddd, *J*=15.5, 10.7, 4.8 Hz, 1H), 4.03-4.10 (m, 2H), 4.23 (dd, *J*=12.6, 5.3 Hz, 0.5H), 4.74 (bs, 0.5H), 4.81 (bs, 0.5H), 5.12-5.20 (m, 3.5H), 5.27 (dd, *J*=17.3, 6.5 Hz, 1H), 5.90 (ddd, *J*=22.6, 10.7, 5.5 Hz, 1H), 7.07-7.10 (m, 1H), 7.14-7.18 (m, 2H), 7.30-7.36 (m, 3H), 7.41 (d, *J*=4.2 Hz, 2H), 7.45 (dd, *J*=15.8, 7.8 Hz, 1H), 7.92 (bs, 0.5H), 7.96 (bs, 0,5H). **^{13}C NMR (CDCl$_3$, 100 MHz):** δ 21.2, 21.6, 27.8, 28.2, 30.2, 30.6, 33.0, 33.2, 42.6, 42.7, 67.3, 67.5, 67.0, 70.0, 75.5, 75.8, 109.2, 109.5, 111.0, 111.1, 117.2, 118.0, 118.1, 119.4, 121.6, 125.4, 127.0, 127.0, 128.0, 128.1, 128.1, 128.2, 128.4, 128.6, 128.7, 129.2, 132.8, 132.9, 135.0, 136.2, 136.9, 137.0, 138.0, 155.7, 155.7 **HRMS:** calc. for [M+H]$^+$ C$_{25}$H$_{27}$N$_2$O$_3$: 403.20162, found: 403.20132

(+/-)-Benzyl 5-(allyloxy)-7-(2-ethoxy-2-oxoethyl)-1,2,4,5,6,7-hexahydro-3H-2,6-methanoazocino[5,4-b]indole-3-carboxylate (93):
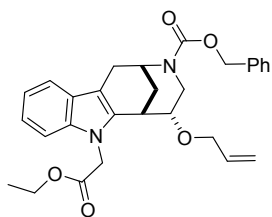
Compound **93** (0.150 mg, 85%) was synthesized as described for compound **53**. **^{1}H NMR (CDCl$_3$, 400 MHz)** (rotameric mixture 1:1): δ 1.24 (t, *J*=6.9 Hz, 3H), 1.97-2.07 (m, 2H), 2.59-2.70 (m, 1H), 2.8890 (t, *J*=17.9 Hz, 1H), 3.12-3.20 (m, 1H), 3.40 (d, *J*=3.0 Hz, 1H), 3.67-3.73 (m, 1H), 3.97-4.27 (m, 5H), 4.75-4.77 (m, 1H), 4.81-4.82 (m, 1H), 5.13-5.30 (m, 5H), 5.81-5.90 (m, 1H), 7.08-7.11 (m, 1H), 7.13-7.21 (m, 2H), 7.31-7.37 (m, 3H), 7.41 (d, *J*=4.3 Hz, 2H), 7.46 (dd, *J*=11.0, 8.0 Hz, 1 H). **^{13}C NMR (CDCl$_3$, 100 MHz):** δ 14.3, 30.7, 31.0, 32.0, 32.0, 42.0, 42.1, 45.1, 45.1, 45.2, 61.4, 67.3, 67.5, 70.2, 70.4, 76.3, 76.6, 108.9, 109.6, 109.9, 117.4, 117.5, 118.2, 118.3, 119.5, 121.7, 126.7, 126.7, 128.0, 128.1,128.1, 128.2, 128.6, 128.7, 134.1, 134.1, 134.6, 134.6, 136.9, 137.2, 155.6, 169.5, 169.6 **HRMS:** calc. for [M+H]$^+$ C$_{29}$H$_{33}$N$_2$O$_5$: 489.23840, found: 489.23778

**(+/-)-Ethyl 2-(5-propoxy-1,2,3,4,5,6-hexahydro-7H-2,6-methanoazocino[5,4-b]indol-7-yl)acetate (94):**
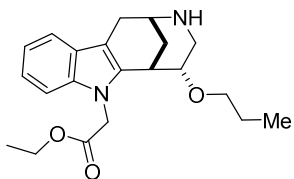
Compound **94** (0.041 mg, 93%) was synthesized as described for compound **59**. **¹H NMR (CDCl₃, 400 MHz):** δ 0.87 (t, *J*=7.4 Hz, 3H), 1.26 (t, *J*=7.1 Hz, 3H), 1.54 (dq, *J*=14.1, 7.0 Hz, 3H), 1.97-2.18 (m, 2H), 2.53 (d, *J*=13.6 Hz, 1H), 2.74 (t, *J*=11.5 Hz, 1H), 3.22-3.48 (m, 6H), 4.04-4.07 (m, 1H), 4.13-4.25 (m, 2H), 4.78 (d, *J*=18.0 Hz, 1H), 5.14 (d, *J*=18.0 Hz, 1H), 7.08-7.24 (m, 3H), 7.46-7.51 (m, 1H). **¹³C NMR (CDCl3, 100 MHz):** δ 10.7, 14.3, 23.2, 25.4, 28.9, 31.3, 40.4, 44.9, 46.5, 61.6, 71.7, 74.8, 108.4, 109.0, 118.5, 119.9, 122.2, 126.2, 133.7, 137.2, 169.3 **HRMS:** calc. for [M+H]⁺ C₂₁H₂₈N₂O₃: 357.21727, found: 357.21660

(+/-)-Ethyl 2-(3-(2-(methylthio)nicotinoyl)-5-propoxy-1,2,3,4,5,6-hexahydro-7H-2,6-methanoazocino[5,4-b]indol-7-yl)acetate (95):
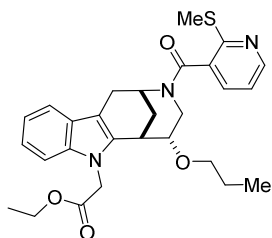
Compound **95** (0.022 g, 39%) was synthesized as described for **(+/-)-Glupin-1**. **¹H NMR (CDCl₃, 700 MHz)** (rotameric mixture 1:1): δ 0.8 (t,*J*=7.4 Hz, 1H), 0.91 (t, *J*=7.4 Hz, 2H), 1.25 (q, *J*=7.1 Hz, 4H), 1.41-1.46 (m, 1H), 1.51-1.60 (m, 2H), 1.94-2.33 (m, 2H), 2.56-2.66 (m, 3H), 3.05-3.34 (m, 2H), 3.46 (s, 1.5H), 3.48 (s, 1H), 3.57 (dd, *J*=15.5, 7.0 Hz, 0.5H), 3.76 (bs, 0.5H), 3.99 (s, 0.5H), 4.13-4.24 (m, 2H), 4.78 (dd, *J*=23.4, 18.0 Hz, 1H), 4.86 (dd, *J*=12.9, 4.9 Hz, 0.5H), 5.16 (d, *J*=18.0 Hz, 0.5H), 5.27 (d, *J*=18.1 Hz, 0.5H), 5.42 (s, 0.5H), 7.05-7.23 (m, 4H), 7.41-7.52 (m, 2H), 8.48 (d, *J*=4.8 Hz, 0.5H), 8.54 (d, *J*=4.8 Hz, 0.5H). **¹³C NMR (CDCl₃, 100 MHz):** δ 10.7, 10.8, 13.3, 13.4, 14.3, 23.1, 23.4, 28.5, 304, 31.7, 32.4, 32.6, 42.9, 45.0, 45.0, 51.0, 61.5, 71.8, 71.3, 108.9, 109.0, 109.7, 118.1, 118.2, 118.4, 119.3, 119.5, 119.6, 121.8, 121.8, 126.5, 126.7, 133.7, 134.2, 134.5, 137.2, 137.2, 149.2, 149.3, 161.3, 161.4, 166.8, 166.9, 169.5, 169.6 **HRMS:** calc. for [M+H]⁺ C₂₈H₃₃N₃O₄S:508.21918, found: 508.22645

(+/-)-Ethyl 2-(5-(allyloxy)-1,2,3,4,5,6-hexahydro-7H-2,6-methanoazocino[5,4-b]indol-7-yl)acetate (96):
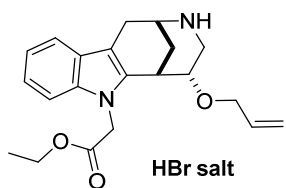
Compound **96** (0.050 g, 79%) was synthesized as described for compound **119**.**¹H NMR (CDCl₃, 400 MHz)** (rotameric mixture 1:1): δ1.25 (t, *J*=7.1 Hz, 3H), 2.14 (d, *J*=12.5 Hz, 1H), 2.61 (d, *J*=13.8 Hz, 1H), 2.76-2.84 (m, 1H), 3.34 (d, *J*=2.7 Hz, 2H), 3.43 (d, *J*=10.6 Hz, 1H), 3.50 (d, *J*=2.2 Hz, 1H), 4.06 (d, *J*=5.5 Hz, 2H), 4.12-4.24 (m, 4H), 4.79 (d, *J*=18.0 Hz, 1H), 5.07 (d, *J*=18.0 Hz, 1H), 5.21 (d, *J*=10.4 Hz, 1H), 5.25 (dd, *J*=17.2, 1.2 Hz, 1H), 5.83 (ddd, *J*=22.7, 10.9, 5.7 Hz, 1H), 7.13-7.16 (m, 1H), 7.21-7.25 (m, 2H), 7.51 (d,

J=7.8 Hz, 1H), 9.47 (bs, 2H). **^{13}C NMR (CDCl$_3$, 100 MHz):** δ 14.3, 25.0, 28.5, 31.1, 40.2, 45.0, 46.8, 61.7, 71.1, 73.8, 108.1, 109.1, 118.4, 118.6, 120.0, 122.4, 126.0, 133.2, 133.7, 137.3, 169.2 **HRMS:** calc. for [M+H]$^+$ C$_{21}$H$_{27}$N$_2$O$_3$: 355.20162, found: 355.20058

(+/-)-Ethyl 2-(5-(allyloxy)-3-(2-(methylthio)nicotinoyl)-1,2,3,4,5,6-hexahydro-7H-2,6-methanoazocino[5,4-b]indol-7-yl)acetate (97):
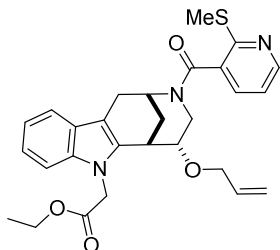

Compound **97** (0.039 g, 61%) was synthesized as described for **(+/-)-Glupin-1**. **^{1}H NMR (CDCl$_3$, 500 MHz)** (rotameric mixture 1:1): δ 1.24 (q, J=6.9 Hz, 3H), 1.94-2.33 (m, 2.5H), 2.59-2.65 (m, 4H), 2.79-3.07 (m, 1.5H), 3.30-3.35 (m, 1H), 3.45-3.47 (m, 1.5H), 3.82 (bs, 1.5H), 4.00 (bs, 0.5H), 4.06 (dd, J=12.6, 5.6 Hz, 0.5H), 5.02-5.11 (m, 1.5H), 5.19-5.29 (m, 1.5H), 5.42 (s, 0.5H), 5.71 (qd, J=11.1, 5.7 Hz, 0.5H), 5.89 (ddd, J=22.5, 10.7, 5.5 Hz, 0.5H), 7.04 (dd, J=7.1, 5.2 Hz, 0.5H), 7.09-7.14 (m, 1.5H), 7.18-7.23 (m, 2H), 8.47 (dd, J=4.8, 1.3 Hz, 0.5H), 8.53 (dd, J=4.8 Hz, 0.5H). **^{13}C NMR (CDCl$_3$, 100 MHz):** δ 13.1, 13.3, 14.3, 28.4, 31.7, 32.3, 32.5, 42.8, 45.0, 45.0, 49.0, 51.0, 61.5, 61.5, 70.4, 70.5, 76.2, 109.0, 109.0, 117.4, 117.8, 118.2, 118.4, 119.2, 119.6, 119.6, 121.8, 121.8, 126.4, 126.6, 133.6, 134.0, 134.2, 134.4, 134.5, 137.1, 137.2, 149.4, 149.4, 166.9, 167.0, 169.4, 169.5 **HRMS:** calc. for [M+H]$^+$ C$_{28}$H$_{32}$N$_3$O$_4$S: 506.21080, found: 506.21021

(+/-)-2-(5-methoxy-3-(2-(methylthio)nicotinoyl)-1,2,3,4,5,6-hexahydro-7H-2,6-methanoazocino[5,4-b]indol-7-yl)acetic acid (98):
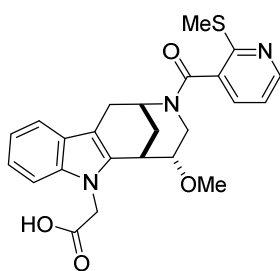

To a solution of **(+/-)-Glupin-1** (5.0 mg, 0.010 mmol) in THF (0.14 mL, 0.07 M) and H$_2$0 (60 μL, 0.16M), LiOH (1.5 mg, 0.06 mmol) was added. The mixture was allowed to stir for 1 hour. The mixture was then taken to pH 2 with HCl 1M and extracted with DCM. The crude product was purified by chromatography (due to the amount of crude product the chromatograpy was performed on a Pasteur pipette, 1 to 5% MeOH/DCM) to obtain product **98** (2.1 mg, 47%) as a solid. The compound purity was checked by uHPLC (> 95%) and characterized only by HRMS. **HRMS:** calc. for [M+H]$^+$ C$_{24}$H$_{26}$N$_3$O$_4$S: 452.16385, found: 452.16381

(+/-)- (5-methoxy-1,2,4,5,6,7-hexahydro-3H-2,6-methanoazocino[5,4-b]indol-3-yl)(2-(methylthio)pyridin-3-yl)methanone (107):
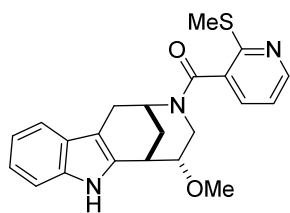
To a solution of compound **107** (100 mg, 0.266 mmol) in EtOH (2.7 mL, 0.1 M), ammonium formate (84 mg, 1.328 mmol) and Pd/C (13 mg, 50mg/mL) were added. The mixture was refluxed for 1.5h. The solvents were removed *in vacuo* and the crude product was redissolved in DCM (2.9 mL, 0.1M). To this solution triethylamine (80.6 μL, 0.579 mmol) and 2-(methylthio)nicotinoyl chloride (54.2 mg, 0.289 mmol) were added and the mixture was allowed to stir overnight at room temperature. The organic phase was washed with sodium bicarbonate (saturated aqueous solution) and the solvents were removed *in vacuo*. The crude product was purified by chromatography to yield compound **107** (92 mg, 81%) as a white foamy solid. **HRMS:** calc. for [M+H]$^+$ C$_{22}$H$_{24}$N$_3$O$_2$S: 394.15837, found: 394.15833; calc. for [M+Na]$^+$ C$_{22}$H$_{23}$N$_3$O$_2$NaS: 416.14032, found: 416.14028

(+/-)-Benzyl 10-chloro-5-methoxy-1,2,4,5,6,7-hexahydro-3H-2,6-methanoazocino[5,4-b]indole-3-carboxylate (108):
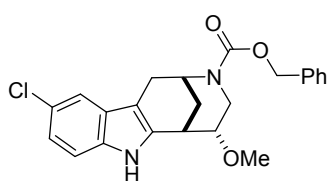
Compound **108** (0.104 g, 73%) was synthesized as described for compound **109**, using 4-chlorophenylhydrazine chloride (CAS: 1073-70-7). **¹H NMR (CDCl₃, 400 MHz)** (rotameric mixture 1:1)**:** δ 2.00-2.08 (m, 2H), 2.50 (dt, *J*=23.6, 11.8 Hz, 1H), 2.76 (t, *J*=17.6 Hz, 1H), 3.05 (dt, *J*=16.6, 5.1 Hz, 1H), 3.31-3.33 (m, 1H), 3.40 (d, *J*=8.2 Hz, 3H), 3.54 (dd, *J*=9.2, 4.3 Hz, 1H), 4.14 (dd, *J*=12.8, 5.2 Hz, 0.5H), 4.30 (dd, *J*=12.7, 5.2 Hz, 0.5H), 4.75 (bs, 0.5H), 4.83 (bs, 0.5H), 5.19 (d, *J*=18.9 Hz, 2H), 7.08 (d, *J*=8.6, 1.8 Hz, 1H), 7.18 (d, *J*=8.6 Hz, 1H), 7.35-7.42 (m, 6H), 8.09 (d, *J*=10.9 Hz, 1H). **¹³C NMR (CDCl₃, 100 MHz):** δ27.6, 28.0, 30.0, 30.3, 42.3, 42.3, 45.2, 56.9, 67.4, 67.6, 77.4, 77.5, 77.9, 108.9, 109.2, 111.9, 112.0, 117.5, 117.6, 121.6, 125.0, 128.0, 128.0, 128.1, 128.2, 128.6, 128.7, 134.3, 134.4, 134.4, 136.8, 136.8, 155.6 **HRMS:** calc. for [M+H]$^+$ C$_{23}$H$_{24}$N$_2$O$_3$Cl: 411.14700, found: 411.14757. Calc. for [M+H]$^+$ C$_{23}$H$_{24}$N$_2$O$_3$^{37}Cl: 413.14405, found: 413.14456

(+/-)-Benzyl 10-bromo-5-methoxy-1,2,4,5,6,7-hexahydro-3H-2,6-methanoazocino[5,4-b]indole-3-carboxylate (109):
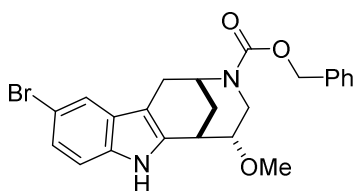
To a solution of compound **50** (0.300 g, 0.99 mmol) in glacial acetic acid (6.6 mL, 0.15 M), 4-bromophenylhydrazine chloride (CAS: 622-88-8) (0.221 g, 0.99 mmol) was added and the mixture was stirred and refluxed for 1 hour. The mixture was then neutralised with sodium bicarbonate (saturated aqueous solution) and extracted with ethyl acetate. The crude product was purified by chromatography (3% ethyl acetate/DCM) to obtain compound **109** (0.378 g, 84%) as an orange foamy solid. **^{1}H NMR (CDCl$_3$, 400 MHz)** (rotameric mixture 1:1): δ 1.96-2.09 (m, 2H), 2.47 (dt, J=23.4, 11.8 Hz, 1H), 2.75 (t, J=17.8 Hz, 1H), 3.04 (dt, J=16.6, 6.6 Hz, 1H), 3.31-3.34 (m, 1H), 3.39 (d,J=3.5 Hz, 3H), 3.54 (td, J=10.1, 5.6 Hz, 1H), 4.13 (dd, J=12.8, 5.6 Hz, 0.5H), 4.13 (dd, J=12.6, 5.3 Hz, 0.5H), 4.74 (bs, 0.5H), 4.82 (bs, 0.5H), 5.18 (d, J=18.5 Hz, 2H), 7.16 (d, J=8.6 Hz, 1H), 7.22 (dd, J=8.6, 1.8 Hz, 1H), 7.31-7.41 (m, 5H), 7.57 (d, J=5.8 Hz, 1H), 8.00 (d, J=12.9 Hz, 1H). **^{13}C NMR (CDCl$_3$, 100 MHz):** δ 27.6, 27.0, 30.0, 30.4, 32.6, 33.0, 42.3, 42.3, 45.2, 57.0, 57.0, 67.4, 67.6, 77.4, 77.5, 77.9, 108.9, 109.2, 112.4, 112.7, 120.7, 120.8, 124.3, 128.0, 128.1, 128.2, 128.3, 128.6, 128.7, 134.2, 134.3, 134.7, 136.8, 136.8, 155.6 **ESI**: calc. [M+H$^+$]: C$_{23}$H$_{24}$N$_2$O$_3$Br: 455.0, found 455.0; calc. [M+H$^+$]: C$_{23}$H$_{24}$N$_2$O$_3$^{81}Br: 457.0, found 457.0

**(+/-)-Benzyl 10-iodo-5-methoxy-1,2,4,5,6,7-hexahydro-3H-2,6-methanoazocino[5,4-b]indole-3-carboxylate (110):**
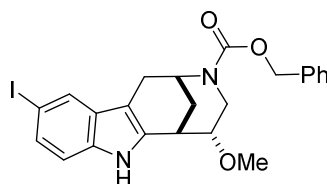
Compound **110** (0.250 g, 54%) was synthesized as described for compound **109**, using 4-iodophenylhydrazine (CAS: 13116-27-3). **^{1}H NMR (CDCl$_3$, 400 MHz)** (rotameric mixture 1:1)**:** δ 1.99-2.12 (m, 2H), 2.51 (dt, J=23.8, 11.7 Hz, 1H), 2.76 (t, J=17.6 Hz, 1H), 3.03 (dd, J=16.9, 5.3 Hz, 1H), 3.32 (d, J=6.2 Hz, 1H), 3.39 (d, J=15.3 Hz, 3H), 3.54 (dt, J=9.8, 5.0 Hz, 1H), 4.16 (dd, J=12.5, 5.1 Hz, 0.5H), 4.32 (dd, J=12.3, 5.5 Hz, 0.5H), 4.76 (bs, 0.5H), 4.84 (bs, 0.5H), 5.22 (d, J=19.3 Hz, 2H), 7.02 (dd, J=8.4, 3.6 Hz, 1H), 7.41 (dd, J=27.2, 4.2 Hz, 6H), 7.86 (s, 1H), 8.27 (d, J=6.6 Hz, 1H). **^{13}C NMR (CDCl$_3$, 100 MHz):** δ27.5, 27.9, 29.8, 30.2, 32.3, 32.6, 42.2, 42.2, 45.1, 56.8, 56.9, 67.3, 67.5, 77.4, 77.8, 82.6, 108.3, 108.6, 112.9, 126.7, 126.8, 127.9, 128.1, 128.2, 128.5, 128.6, 129.4, 129.4, 129.5, 133.6, 133.7, 135.1, 136.6, 136.7, 155.5 **HRMS:** calc. for [M+H]$^+$ C$_{23}$H$_{24}$N$_2$O$_3$I: 503.08261, found: 503.08331

(+/-)-Benzyl 10-hexyl-5-methoxy-1,2,4,5,6,7-hexahydro-3H-2,6-methanoazocino[5,4-b]indole-3-carboxylate (111):
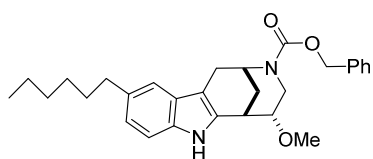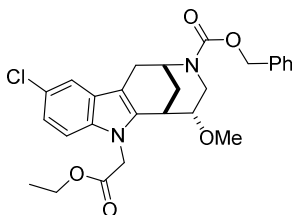

Compound **111** (0.220 g, 48%) was synthesized as described for compound **109**, using 4-*n*-hexylphenylhydrazine chloride (CAS: 823-85-8) as the starting material. **¹H NMR (CDCl₃, 400 MHz)** (rotameric mixture 1:1)**:** δ 0.88-0.92 (m, 3H), 1.27-1.39 (m, 6H), 1.61-1.70 (m, 2H), 1.96-2.10 (m, 2H), 2.56 (quin, *J*=11.4 Hz, 1H), 2.69 (t, *J*=17.0 Hz, 2H), 2.80 (t, *J*=17.0 Hz, 1H), 3.09 (dt, *J*=16.7, 6.4 Hz, 1H), 3.30-3.33 (m, 1H), 3.40 (d, *J*=2.1 Hz, 3H), 3.54 (td, *J*=10.5, 5.0 Hz, 1H), 4.12 (dd, *J*=12.4, 5.4 Hz, 0.5H), 4.29 (dd, *J*=12.5, 5.4 Hz, 0.5H), 4.75 (bs, 0.5H), 4.82 (bs, 0.5H), 5.18 (d, *J*= 19.2 Hz, 2H), 6.99 (d, *J*=8.2 Hz, 1H), 7.23 (t, *J*=8.5 Hz, 2H), 7.30-7.39 (m, 3H), 7.42 (d, *J*=4.2 Hz, 2H), 7.84 (d, *J*=12.9 Hz, 1H). **¹³C NMR (CDCl₃, 100 MHz):** δ 14.3, 22.8, 27.8, 28.2, 29.3, 30.2, 30.6, 32.0, 32.6, 33.0, 36.3, 42.3, 42.4, 45.5, 56.8, 67.3, 67.5, 77.7, 78.1, 108.8, 109.1, 110.7, 110.7, 117.1, 117.2, 122.5, 127.1, 127.1, 128.0, 128.0, 128.1, 128.2, 128.6, 128.7 ,132.8, 132.9, 134.0, 134.1, 134.6, 136.9, 137.0, 155.7 **HRMS:** calc. for [M+H]⁺ C₂₉H₃₇N₂O₃: 461.27987, found: 461.28035

**(+/-)-Benzyl 8-chloro-5-methoxy-1,2,4,5,6,7-hexahydro-3H-2,6-methanoazocino[5,4-b]indole-3-carboxylate (112):**
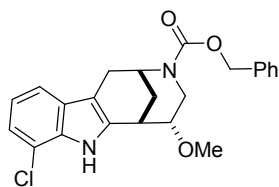
Compound **112** (0.220 g, 48%) was synthesized as described for compound **109**, using 6-chlorophenylhydrazine hydrochloride (CAS:823-85-8).**¹H NMR (CDCl₃, 400 MHz)** (rotameric mixture 1:1)**:** δ 2.04 (d, *J*=12.1 Hz, 2H), 2.60 (quin, *J*=11.4 Hz, 1H), 2.86 (t, *J*=17.9 Hz, 1H), 3.12 (dt, *J*=16.4, 4.8 Hz, 1H), 3.38-3.44 (m, 4H), 3.57 (bs, 1H), 4.22 (dd, *J*=12.0, 4.7 Hz, 0.5H), 4.39 (dd, *J*=12.5, 4,9 Hz, 0.5H), 4.81 (bs, 0.5H), 4.90 (bs, 0.5H), 5.26 (d, *J*=18.1 Hz, 2H), 7.06 (t, *J*=7.7 Hz, 1H), 7.19 (d, *J*=7.5 Hz, 1H), 7.30-7.47 (m, 6H), 8.38 (bs, 0.5H), 8.42 (bs, 0.5H). **¹³C NMR (CDCl₃, 100 MHz):** δ27.7, 28.1, 29.9, 30.3, 32.4, 32.7, 42.0, 42.1, 45.0, 56.7, 56.8, 67.2, 67.4, 77.3, 77.7, 110.0, 110.3, 116.2, 116.3, 116.5, 116.6, 120.0, 120.8, 127.8, 127.9, 128.0, 128.1,128.3, 128.4, 128.5, 128.6, 133.2, 133.5, 133.6, 136.7, 136.8, 155.5 **HRMS:** calc. for [M+H]⁺ C₂₃H₂₄N₂O₃Cl: 411.14700, found: 411.14752. Calc. for [M+H]⁺ C₂₃H₂₄N₂O₃³⁷Cl: 413.14405, found: 413.14436
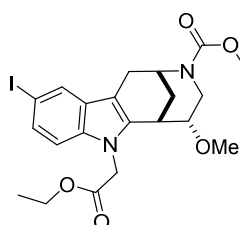
(+/-)-Benzyl 10-chloro-7-(2-ethoxy-2-oxoethyl)-5-methoxy-1,2,4,5,6,7-hexahydro-3H-2,6-methanoazocino[5,4-b]indole-3-carboxylate (113):

Compound **113** (0.253 g, 88%) was synthesized as described for compound **53**. Compound **113** was isolated with a small impurity of the ethyl 2-bromoacetate, as an orange oil **^{1}H NMR (CDCl3, 400 MHz)** (rotameric mixture 1:1): δ 1.24 (t, *J*=7.1 Hz, 3H), 1.95-2.07 (m, 2H), 2.56 (dt, *J*=25.3, 11.8 Hz, 1H), 2.76 (t, *J*=16.6 Hz, 1H), 3.10 (ddd, *J*=15.5, 8.6, 5.9 Hz, 1H), 3.35 (d, *J*=4.7 Hz, 3H), 3.38 (sept, *J*=4.5 Hz, 1H), 4.11-4.22 (m, 2,5H), 4.33 (dd, *J*=12.6, 5.0 Hz, 0.5H), 4.74-4.79 (m, 1.5H), 4.84 (bs, 0.5H), 5.09 (dd, *J*=21.1, 18.3 Hz, 1H), 5.19 (d, *J*=14.6 Hz, 2H), 7.09-7.14 (m, 2H), 7.31-7.42 (m, 6H). **^{13}C NMR (CDCl3, 100 MHz):** δ 14.3, 27.78, 28.0, 30.4, 30.7, 31.8, 31.9, 41.6, 41.7, 45.0, 45.1, 56.8, 57.0, 61.4, 67.3, 67.5, 68.3, 77.4, 78.2, 78.6, 109.3, 109.6, 110.0, 117.7, 117.8, 121.7, 125.2, 127.6, 127.7, 127.9, 128.0, 128.1, 128.2, 128.6, 128.7, 135.5, 135.6, 136.8, 155.5, 169.0, 169.1 **HRMS:** calc. for [M+H]$^+$ $C_{27}H_{30}N_2O_5Cl$: 497.18378, found: 497.18455 Calc. for [M+H]$^+$ $C_{27}H_{30}N_2O_5{}^{37}Cl$: 499.18083, found: 499.18182

(+/-)-Benzyl 10-bromo-7-(2-ethoxy-2-oxoethyl)-5-methoxy-1,2,4,5,6,7-hexahydro-3H-2,6-methanoazocino[5,4-b]indole-3-carboxylate (114):
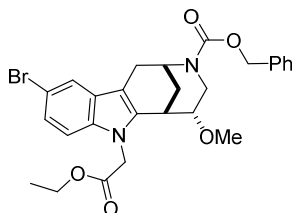
Compound **114** (0.240 g, 84%) was synthesized as described for compound **53**. Compound **114**was isolated with a small impurity of the ethyl 2-bromoacetate, as an orange oil.**^{1}H NMR (CDCl$_3$, 400 MHz)** (rotameric mixture 1:1): δ 1.25 (t, *J*=7.1 Hz, 3H), 1.94-2.05 (m, 2H), 2.51-2.63 (m, 1H), 2.77 (t, *J*=17.0 Hz, 1H), 3.05-3.13 (m, 1H), 3.35 (d, *J*=4.8 Hz, 3H), 3.39 (d, *J*=2.8 Hz, 1H), 3.54-3.59 (m, 1H), 4.12-4.27 (m, 2.5H), 4.34 (dd, *J*=12.5, 4.9 Hz, 0.5H), 4.76-4.80 (m, 1.5H), 4.85 (bs, 0.5H), 5.09 (t, *J*=19.5 Hz, 1H), 5.21 (d,*J*=14.8 Hz, 2H), 7.07 (d, *J*=8.7 Hz, 1H), 7.26 (dd, *J*=8.6, 1.9 Hz, 1H), 7.33-7.43 (m, 5H), 7.59 (d, *J*=3.7 Hz, 1H). **^{13}C NMR (CDCl$_3$, 100 MHz):** δ 14.0, 14.1, 27.5, 27.8, 30.2, 30.5, 31.6, 31.7, 41.5, 41.6, 44.8, 44.9, 56.7, 56.8, 60.9, 61.3, 67.1, 67., 368.1, 77.4, 78.0, 78.3, 109.0, 109.3, 110.4, 112.5, 120.6, 124.0, 127.8, 127.8, 127.9, 128.0, 128.1, 128.2, 128.4, 128.5, 135.3, 135.4, 135.8, 136.7, 155.3, 168.7, 168.8 **HRMS:** calc. for [M+H]$^+$ $C_{27}H_{30}N_2O_5Br$: 541.13326, found: 541.13476. Calc. for [M+H]$^+$ $C_{27}H_{30}N_2O_5{}^{81}Br$: 543.13121, found: 543.13278

(+/-)-Benzyl 10-iodo-7-(2-ethoxy-2-oxoethyl)-5-methoxy-1,2,4,5,6,7-hexahydro-3H-2,6-methanoazocino[5,4-b]indole-3-carboxylate (115):

Compound **115** (0.253 g, 88%) was synthesized as described for compound **53**. Compound **115** was isolated with a small impurity of the ethyl 2-bromoacetate, as an orange oil **^{1}H NMR** **(CDCl$_3$, 400 MHz)** (rotameric mixture 1:1): δ 1.24 (t, J=7.1 Hz, 3H), 1.93-2.01 (m, 2H), 2.56 (dt, J=25.9, 11.8 Hz, 1H), 2.76 (t, J=16.9 Hz, 1H), 3.04-3.12 (m, 1H), 3.34 (d, J=4.7 Hz, 3H, 3.38 (d, J=2.6 Hz, 1H), 3.56 (dq, J=14.0, 4.6 Hz, 1H), 4.11-4.23 (m, 2.5H), 4.33 (dd, J=12.6, 5.0 Hz, 0.5H), 4.74-4.79 (m, 1.5H), 4.84 (bs, 0.5H), 5.08 (t, J=19.5 Hz, 1H), 5.20 (d, J=14.6 Hz, 2H), 6.98 (d, J=9.8 Hz, 1H), 7.31-7.43 (m, 6H), 7.79 (d, J=3.4 Hz, 1H). **^{13}C NMR (CDCl$_3$, 100 MHz):** δ 14.1, 14.2, 27.5, 27.9, 30.2, 30.6, 31.5, 31.6, 41.5, 41.6, 44.8, 56.7, 56.8, 61.3, 61.6, 63.8, 67.1, 67.4, 77.4, 78.0, 78.4, 82.7, 108.8, 109.1,111.0, 126.9, 127.0, 127.8, 127.9, 127.9, 128.0, 128.4, 128.5, 129.0, 129.6, 143.9, 135.0, 136.2, 136.7, 155.9, 166.9, 168.8, 168.9 **HRMS:** calc. for [M+H]$^+$ C$_{27}$H$_{30}$N$_2$O$_5$I: 589.11939, found: 589.12160

(+/-)-Benzyl 7-(2-ethoxy-2-oxoethyl)-10-hexyl-5-methoxy-1,2,4,5,6,7-hexahydro-3H-2,6-methanoazocino[5,4-b]indole-3-carboxylate (116):
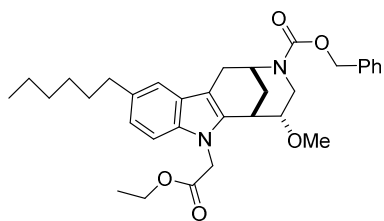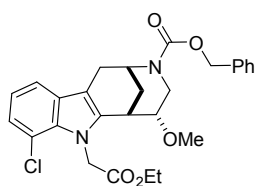
Compound **116** (0.155 g, 72%) was synthesized as described for compound **53** (flash chromatography, 5 to 15% ethyl acetate/petroleum ether). **^{1}H NMR (CDCl3, 400 MHz)** (rotameric mixture 1:1): δ0.89 (t, J=6.9 Hz, 3H), 1.24 (t, J=7.1 Hz, 3H), 1.28-1.36 (m, 6H), 1.63 (dt, J=15.3, 7.5 Hz, 2H), 1.96-2.03 (m, 2H), 2.56-2.65 (m, 1H), 2.69 (t, J=7.7 Hz, 2H), 2.80 (t, J=16.9 Hz, 1H), 3.11-3.17 (m, 1H), 3.33 (d, J=4.9 Hz, 3H), 3.38 (s, 1H), 3.51-3.57 (m, 1H), 4.11-4.24 (m, 2.5H), 4.30 (dd, J=12.9, 4.4 Hz, 0.5H), 4.74-4.78 (m, 1.5H) 4.82 (bs, 0.5H), 5.09 (dd, J=26.6, 18.1 Hz, 1H), 5.18 (d, J=4.4 Hz, 2H), 7.02 (d, J=8.3 Hz, 1H), 7.11 (d, J=8.3 Hz, 1H), 7.25 (d, J=7.8 Hz, 1H), 7.31-7.42 (m, 5H). **^{13}C NMR (CDCl3, 100 MHz):** δ 14.3, 14.3, 22.8, 27.9, 28.2, 29.3, 30.6, 30.9, 31.7, 31.8, 32.0, 32.6, 36.2, 45.0, 45.2, 56.8, 56.9, 61.3, 67.3, 67.5, 78.3, 78.7, 108.6, 109.1, 109.4, 117.4, 117.5, 122.6, 126.7, 126.7, 127.9, 128.0, 128.1, 128.2, 128.6, 128.7, 134.0, 134.1, 134.1, 135.7, 135.7, 136.9, 155.6, 169.6, 160.7 **HRMS:** calc. for [M+H]$^+$ C$_{33}$H$_{43}$N$_2$O$_5$: 547.31665, found: 547.31606

(+/-)-Benzyl 8-chloro-7-(2-ethoxy-2-oxoethyl)-5-methoxy-1,2,4,5,6,7-hexahydro-3H-2,6-methanoazocino[5,4-b]indole-3-carboxylate (117):

Compound **117** (0.155 g, 72%) was synthesized as described for compound **53**. Compound **117** was isolated with a small impurity of the ethyl 2-bromoacetate, as an orange oil **1H NMR (CDCl₃, 400 MHz)** (rotameric mixture 1:1): δ 1.25 (t, *J*=7.1 Hz, 3H), 1.93-2.06 (m, 2H), 2.56-2.68 (m, 1H), 2.79 (t, *J*=17.2 Hz, 1H), 3.08-3.16 (m, 1H), 3.36 (d, *J*=7.7 Hz, 4H), 3.57 (m, 1H), 4.13-4.22 (m, 2.5H), 4.35 (dd, *J*=12.6, 5.0 Hz, 0.5H), 4.79 (bs, 0.5H), 4.86 (bs, 0.5H), 5.21 (d, *J*=14.5 Hz, 2H), 5.33 (dd, *J*=18.4, 9.3 Hz, 1H), 5.48 (bs, 1H), 6.99 (t, *J*=7.7 Hz, 1H), 7.12 (dd, *J*=7.6, 0.6 Hz, 1H), 7.32-7.43 (m, 6H). **¹³C NMR (CDCl₃, 100 MHz):** δ 14.2, 27.6, 27.9, 30.5, 30.8, 31.4, 31.5, 41.4, 41.5, 44.9, 46.6, 56.7, 56.8, 60.9, 6.1, 67.2, 67.4, 68.1, 78.1, 78.5, 110.0, 110.3, 116.3, 116.7, 116.8, 120.0, 123.3, 127.8, 127.9, 128.0, 128.1, 128.5, 128.5, 129.6, 129.6, 132.1, 135.6, 135.7, 136.7, 155.4, 169.6, 169.8, 169.9 **HRMS:** calc. for $[M+H]^+$ $C_{27}H_{30}N_2O_5Cl$: 497.18378, found: 497.18457; calc. for $[M+H]^+$ $C_{27}H_{30}N_2O_5{}^{37}Cl$: 499.18083, found: 499.18175

(+/-)-7-(2-ethoxy-2-oxoethyl)-10-chloro-5-methoxy-2,3,4,5,6,7-hexahydro-1H-2,6-methanoazocino[5,4-b]indol-3-ium bromide (118):
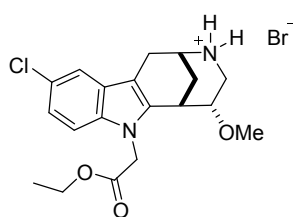
Compound **118** (39.0 mg, 50%) was synthesized as described for compound **119**. **¹H NMR (CDCl₃, 400 MHz):** δ1.25 (t, *J*=7.1 Hz, 3H), 2.10 (d, *J*=12.3 Hz, 1H), 2.54 (d, *J*=13.8 Hz, 1H), 2.70 (dd, *J*=20.6, 11.1 Hz, 1H), 3.23 (s, 2H), 3.36 (s, 3H), 3.43-3.47 (m, 2H), 3.99-4.02 (m, 2H), 4.12-4.24 (m, 3H), 4.75 (d, *J*=18.0 Hz, 1H), 7.11 (d, *J*=8.7 Hz, 1H), 7.16 (dd, *J*=8.7, 1.8 Hz, 1H), 7.45 (d, *J*=1.5 Hz, 1H), 9.46 (bs, 2H).**¹³C NMR (CDCl₃, 100 MHz):** δ 14.3, 24.8, 28.3, 30.9, 40.0, 45.1, 46.7, 57.5, 61.8, 75.7, 61.8, 75.7, 107.8, 110.3, 118.0, 122.6, 125.8, 127.1, 134.7, 135.8, 168.8 **HRMS:** calc. for $[M+H]^+$ $C_{19}H_{24}N_2O_3Cl$: 363.14700, found: 363.14740; calc. for $[M+H]^+$ $C_{19}H_{24}N_2O_3{}^{37}Cl$: 365.14405, found: 365.14441

(+/-)-7-(2-ethoxy-2-oxoethyl)-10-iodo-5-methoxy-2,3,4,5,6,7-hexahydro-1H-2,6-methanoazocino[5,4-b]indol-3-ium bromide (119):
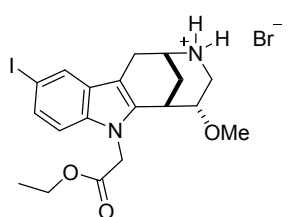
To a solution of compound **115** (253 mg, 0.429 mmol) in acetic acid (1.0 mL, 0.43 M), HBr in acetic acid 33% solution (0.29 mL, 0.420 mmol) was added and the mixture was allowed to stir for 30 min. Water was then added and the aqueous phase was extracted with DCM (5X). Solvents were removed *in vacuo* and the crude product was purified by chromatography (5 to 10% MeOH/DCM) to yield compound **119** (180 mg,

140

78%) as a pasty solid. The product was isolated with 15-20% of an impurity. **^{1}H NMR (CDCl$_3$, 400 MHz)**: δ 1.22 (t, *J*=7.1 Hz, 3H), 2.01-2.09 (m, 1H), 2.54-2.72 (m, 2H), 3.16-3.30 (m, 2H), 3.34-3.48 (m, 2H), 4.01-4.05 (m, 1H), 4.08-4.21 (m, 3H), 4.72 (d, *J*=18.0 Hz, 1H), 4.95 (d, *J*=18.0 Hz, 1H), 6.96 (d, *J*=8.6 Hz, 1H), 7.41 (dd, *J*=8.6, 1.6 Hz, 1H), 7.80 (d, *J*=1.54 Hz, 1H), 9.39 (bs, 2H). **^{13}C NMR (CDCl$_3$,100 MHz):** δ 14.2, 24.6, 28.2, 30.7, 39.7, 44.9, 46.4, 57.4, 61.6, 75.4, 83.2, 107.4, 111.3, 127.2, 128.4, 130.4, 134.2, 136.6, 168.5 **HRMS:** calc. for [M+H]$^+$ C$_{19}$H$_{24}$N$_2$O$_3$I: 455.08261, found: 455.08324

(+/-)-10-hexyl-5-methoxy-7-(2-methoxy-2-oxoethyl)-2,3,4,5,6,7-hexahydro-1H-2,6-methanoazocino[5,4-b]indol-3-ium bromide (120):
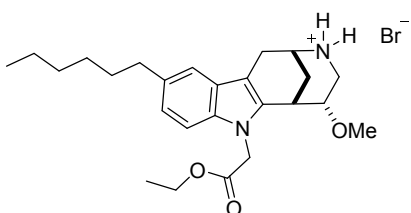
Compound **120** (83.0 mg, 53%) was synthesized as described for compound **119**. **^{1}H NMR (CDCl$_3$, 500 MHz)**: δ 0.86 (t, *J*=6.8 Hz, 3H), 1.22 (t, *J*=7.1 Hz, 3H), 1.26-1.34 (m, 6H), 1.59-1.65 (m, 2H), 2.09 (d, *J*=11.8 Hz, 2H), 2.55 (d, *J*=13.7 Hz, 1H), 2.65-2.76 (m, 3H), 3.28 (s, 1H), 3.34 (s, 3H), 3.40-3.45 (m, 2H), 3.96-4.00 (m, 1H), 4.07-4.21 (m, 3H), 4.73 (d, *J*=18.0 Hz, 1H), 4.97 (d, *J*=18.0 Hz, 1H), 7.02 (d, *J*=8.4 Hz, 1H), 7.09 (d, *J*=8.4 Hz, 1H), 7.25 (d, *J*=10.9 Hz, 1H), 9.87 (bs, 2H). **^{13}C NMR (CDCl$_3$, 100 MHz):** δ 14.3, 22.8, 25.1, 28.5, 29.2, 30.8, 31.9, 32.5, 36.2, 39.7, 45.0, 46.7, 57.4, 61.6, 75.9, 107.8, 108.7, 117.7, 123.3, 126.2, 133.2, 134.6, 135.8, 169.3 **HRMS:** calc. for [M+H]$^+$ C$_{25}$H$_{37}$N$_2$O$_3$: 413.27987, found: 413.27941

(+/-)-8-chloro-7-(2-ethoxy-2-oxoethyl)-5-methoxy-2,3,4,5,6,7-hexahydro-1H-2,6-methanoazocino[5,4-b]indol-3-ium bromide (121):
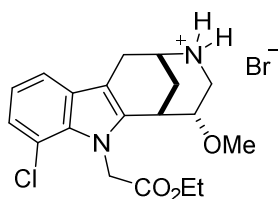
Compound **121** (0.150 g, 65%) was synthesized as described for compound **119**. **^{1}H NMR (MeOD, 400 MHz)**: δ 1.23 (t, *J*=7.1 Hz, 3H), 2.11 (ddd, *J*=14.1, 3.9, 2.1 Hz, 1H), 2.36 (dt, *J*=14.2, 2.8 Hz, 1H), 2.61 (t, *J*=11.7 Hz, 1H), 3.02 (d, *J*=18.0 Hz, 1H), 3.26 (d, *J*=6.2 Hz, 1H), 3.37-3.42 (m, 4H), 3.62-3.63 (m, 1H), 3.90 (dt, *J*=11.2, 4.3 Hz, 1H), 4.09-4.10 (m, 1H), 4.14-4.21 (m, 2H), 5.31 (bs, 2H), 7.02 (t, *J*=7.7 Hz, 1H), 7.12 (dd, *J*=7.7, 0.8 Hz, 1H), 7.41 (dd, *J*=7.8, 0.8 Hz, 1H). **^{13}C NMR (MeOD, 100 MHz):** δ 14.5, 25.4, 29.4, 31.3, 41.0, 47.8, 48.0, 57.9, 62.5, 77.1, 109.8, 117.5, 118.0, 121.5, 124.8, 130.6, 133.9, 136.7, 171.5 **HRMS:** calc. for [M+H]$^+$ C$_{19}$H$_{24}$N$_2$O$_3$Cl: 363.14700, found: 363.14784; calc. for [M+H]$^+$ C$_{19}$H$_{24}$N$_2$O$_3$^{37}Cl: 365.14405, found: 365.14485

(+/-)-Ethyl 2-(10-chloro-5-methoxy-3-(2-(methylthio)nicotinoyl)-1,2,3,4,5,6-hexahydro-7H-2,6-methanoazocino[5,4-b]indol-7-yl)acetate (122):
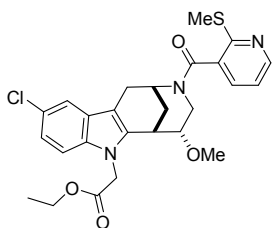
To a solution of compound **118** (39.0 mg, 0.107 mmol) in DCM (1.2 mL, 0.09M), 2-(methylthio)nicotinoyl chloride (20.1 mg, 0.107 mmol) and triethylamine (0.0328 mL, 0.236 mmol) were added. The mixture was allowed to stir overnight at room temperature. The solvents were then removed *in vacuo* and the crude product was purified by preparative HPLC (no TFA was added) to give compound **122** (16.1 mg, 29%). **^{1}H NMR (CDCl$_3$, 400 MHz)** (rotameric mixture 1:1.3): δ 1.24 (q, *J*=7.1 Hz, 3H), 1.93 (d, *J*=11.6 Hz, 0.5H), 2.07-2.32 (m, 1.5H), 2.58 (bs, 2H), 2.64 (s, 2H), 2.88-3.02 (m, 1.5H), 3.12-3.19 (m, 1.5H), 3.31 (ddd, *J*=23.4, 15.1, 5.3 Hz, 1H), 3.41 (s, 1.5H), 3.44 (d, *J*=3.4 Hz, 1H), 3.68-3.80 (m, 1H), 4.00 (bs, 0.5H), 4.10-4.25 (m, 2H), 4.75 (dd, *J*=18.0, 13.6 Hz, 1H), 4.91 (dd,*J*=12.8, 4.9 Hz, 0.5H), 5.00 (d, *J*=18.0 Hz, 0.5H), 5.11 (d, *J*=18.1 Hz, 0.5H), 5.43 (bs, 0.5H), 7.04 (dd, *J*=7.5, 5.0 Hz, 0.5H), 7.09-7.16 (m, 2.5H), 7.41 (bs, 1H), 7.47 (bs, 1H), 8.47 (dd*J*=4.9, 1.7 Hz, 0.5H), 8.54 (dd, *J*=4.9, 1.7 Hz, 0.5H). **^{13}C NMR (CDCl$_3$, 100 MHz):** δ 13.2, 13.3, 14.3, 28.3, 30.2, 31.5, 32.1, 32.4, 42.8, 45.2, 45.2, 46.2, 49.0, 57.1, 57.1, 61.6, 61.6, 78.0, 79.1, 109.6, 110.1, 110.1, 117.8, 118.0, 119.3, 122.0, 125.4, 127.5, 127.7, 133.5, 135.7, 135.7, 135.8, 149.7, 167.3, 167.4, 169.0, 169.2 **HRMS:** calc. for [M+H]$^+$ C$_{26}$H$_{29}$N$_3$O$_4$ClS: 514.15618, found: 514.15692; calc. for [M+H]$^+$ C$_{26}$H$_{29}$N$_3$O$_4$^{37}ClS: 516.15323, found: 516.15420

(+/-)-Ethyl 2-(10-bromo-5-methoxy-3-(2-(methylthio)nicotinoyl)-1,2,3,4,5,6-hexahydro-7H-2,6-methanoazocino[5,4-b]indol-7-yl)acetate (123):
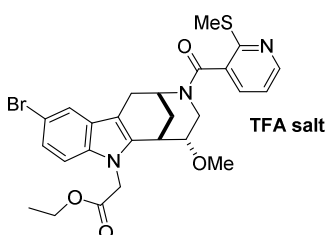
To a solution of compound **114** (50 mg, 0.092 mmol) in acetic acid (0.3 mL, 0.3 M), HBr in acetic acid 33% solution (0.063 mL, 0.092 mmol) was added and the mixture was allowed to stir for 30 min. Water was then added and the aqueous phase was extracted with DCM (5X). Solvents were then removed *in vacuo* and the crude product was redissolved in DCM (0.5 mL, 0.18 M). Triethylamine (0.028 mL, 0.202 mmol) and 2-(methylthio)nicotinoyl chloride (17.3 mg, 0.092 mmol) were added and the mixture was stirred overnight at room temperature. Solvents were then removed *in vacuo* and the crude product was purified by preparative HPLC to give compound **123** (30.9 mg, 60%). **^{1}H NMR (CDCl3, 400 MHz)** (rotameric mixture 1:1.3): δ 1.24 (q, *J*=7.1 Hz, 3H), 1.94 (d, *J*=11.0 Hz, 0.5H), 2.08-2.32 (m, 1.5H), 2.60 (bs, 2H), 2.66 (s, 2H), 2.83-3.03 (m, 1.5H), 3.17 (s, 1.5H), 3.30 (ddd, *J*=23.4, 15.1, 5.4 Hz, 1H), 3.41 (s, 1.5H), 3.45 (d, *J*=3.5 Hz, 1H), 3.68-3.82 (m, 1H), 4.00 (s, 0.5H), 4.09-4.25 (m, 2H), 4.75 (dd, *J*=18.0, 13.7 Hz, 1H), 4.90 (dd, *J*=12.9, 4.9 Hz, 0.5H), 4.99 (d, *J*=180 Hz, 0.5H), 5.11 (d, *J*=18.0 Hz, 0.5H), 5.42 (bs, 0.5H), 7.05-7.10 (m,

1.5H), 7.15 (dd, J=7.2, 5.1 Hz, 0.5H), 7.26-7.28 (m, 1H), 7.46-7.51 (m, 1H), 7.57 (s, 0.5H), 7.63 (s, 0.5H), 7.83 (bs, 1H), 8.50 (dd, J=5.0, 1.7 Hz, 0.5H), 8.57 (dd, J=5.0, 1.7 Hz, 0.5H). ^{13}C NMR (CDCl₃, 100 MHz): δ 13.3, 13.5, 14.3, 28.3, 30.1, 31.4, 32.0, 32.3, 39.4, 43.1, 45.1, 45.1, 49.2, 57.1, 61.4, 61.7, 77.9, 79.0, 110.6, 110.6, 113.0, 119.5, 120.8, 121.0, 124.6, 128.1, 128.3, 133.9, 135.2, 135.5, 136.0, 136.0, 149.6, 167.4, 167.5, 169.0, 169.1 **HRMS:** calc. for [M+H]$^+$ C₂₆H₂₉N₃O₄BrS:558.10567, found: 558.10757; calc. for [M+H]$^+$ C₂₆H₂₉N₃O₄^{81}BrS:560.10362, found: 560.10521After chiral separation (see Chiral Separation) specific optical rotations were measured for both enantiomers (as the TFA salt): (+)-**61**[α]$_D$= - 14.8°; (-)-**61**[α]$_D$= +20.3°

(+/-)-Ethyl2-(10-hexyl-5-methoxy-3-(2-(methylthio)nicotinoyl)-1,2,3,4,5,6-hexahydro-7H-2,6-methanoazocino[5,4-b]indol-7-yl)acetate (124):
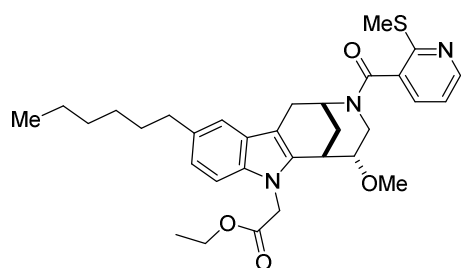
Compound **124** (60.3 mg, 63%) was synthesized as described for compound **122**. ^{1}H NMR (CDCl₃, 500 MHz) (rotameric mixture 1:1.3): δ 0.89 (q, J=6.8 Hz, 3H), 1.24 (dd, J=13.6, 6.9 Hz, 3H), 1.30-1.37 (m, 6H), 1.64 (m, 2H), 1.94 (d, J=9.8 Hz, 0.5H), 1.98 (s, 1.5H), 2.08-2.31 (s, 1.5H), 2.61 (bs, 1.5H), 2.65 (s, 2H), 2.69 (dd, J=16.8, 9.1 Hz, 2H), 3.05-3.16 (m, 2H), 3.31 (td, J=13.1, 4.8 Hz, 1H), 3.40 (s, 1.5H), 3.44 (s, 1H), 3.58-3.87 (m, 1H), 3.99 (bs, 0.5H), 4.10-4.24 (m, 2H), 4.76 (t, J=18.0 Hz, 1H), 4.89 (dd, J=12.8, 5.0 Hz, 0.5H), 5.00 (d, J=18.0 Hz, 0.5H), 5.12 (d, J=18.0 Hz, 0.5H), 5.42 (bs, 0.5H), 7.02-7.05 (m, 1.5H), 7.11 (t, J=6.9 Hz, 1.5H), 7.27 (d, J=30.4 Hz, 1H), 7.40-7.44 (bs, 0.5H), 7.48 (d, J=6.7 Hz, 0.5H), 8.46 (dd, J=4.9, 1.4 Hz, 0.5H), 8.52 (dd, J=4.9, 1.5 Hz, 0.5H). ^{13}**C NMR (CDCl₃, 100 MHz):** δ 13.0, 13.3, 14.2, 14.3, 22.7, 22.8, 28.4, 29.2, 29.2, 31.5, 31.9, 32.2, 32.5, 32.5, 36.2, 39.1, 42.9, 44.9, 45.0, 49.1, 56.9, 61.3, 61.4, 78.0, 79.2, 108.4, 108.6, 108.7, 109.3, 116.5, 117.3, 117.5, 119.2, 122.7, 122.7, 126.4, 126.6, 133.5, 133.9, 134.2, 134.2, 135.7, 135.7, 149.4, 166.9, 167.0, 169.4, 169.6 **HRMS:** calc. for [M+H]$^+$ C₃₂H₄₂N₃O₄S: 564.28905, found: 564.28839

(+/-)-Ethyl 2-(8-chloro-5-methoxy-3-(2-(methylthio)nicotinoyl)-1,2,3,4,5,6-hexahydro-7H-2,6-methanoazocino[5,4-b]indol-7-yl)acetate (125):
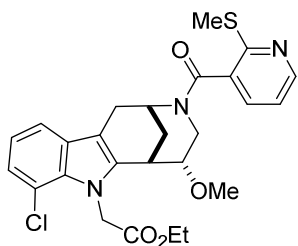
Compound **125** (110 mg, 43%) was synthesized as described for compound **122** but it was purified by chromatography (5 to 50% ethyl acetate/CHCl₃).**¹H NMR (CDCl₃, 600 MHz)** (rotameric mixture 1:1.5): δ 1.14-1.20 (m, 3H), 1.23 (bs, 1H), 1.80 (bs, 0.5H), 1.92 (d, *J*=12.9 Hz, 0.5H), 2.06 (d, *J*=12.6 Hz, 0.5H), 2.12 (bs, 0.5H), 2.31-2.42 (m, 1H), 2.56 (s, 2H), 2.66 (bs, 0.5H), 2.77-2.80 (m, 1H), 2.89-2.99 (m, 0.5H), 3.12 (s, 1H), 3.16-3.19 (m, 1H), 3.36 (m, 2H), 3.62 (d, *J*=15.6 Hz, 2H), 3.86 (s, 0.5H), 4.08-4.18 (m, 2H), 4.64 (dd, *J*=12.7, 4.9 Hz, 0.5H), 5.19-5.33 (m, 2H), 7.01 (dt, *J*=11.3, 7.7 Hz, 1H), 7.11 (dd, *J*=7.5, 2.5 Hz, 1H), 7.20 (bs, 0.4H), 7.26 (dd, *J*=7.4, 4.9 Hz, 0.6H), 7.37 (d, *J*=7.7 Hz, 0.6H), 7.45 (d, *J*=7.7 Hz, 0.4H), 7.64 (bs, 0.4H), 7.76 (d, *J*=6.7 Hz, 0.6H), 8.50 (dd, *J*=4.9, 1.7 Hz, 0.4H), 8.55 (dd, *J*=4.9, 1.7 Hz, 0.6H). **¹³C NMR (CDCl₃, 100 MHz):** δ 12.4, 12.6, 14.1, 14.1, 27.3, 29.6, 30.3, 30.6, 40.1, 41.7, 46.3, 48.2, 56.6, 60.8, 77.3, 109.4, 109.7, 115.4, 117.1, 117.2, 119.5, 119.6, 120.1, 120.1, 122.8, 129.2, 129.4, 130.9, 131.3, 131.6, 133.9, 136.5, 149.4, 149.5, 154.5, 154.6, 165.9, 169.2, 169.3 **HRMS:** calc. for [M+H]⁺ $C_{26}H_{29}N_3O_4ClS$: 514.15618, found: 514.15706; calc. for [M+H]⁺ $C_{26}H_{29}N_3O_4{}^{37}ClS$: 516.15323, found: 516.15425

(+/-)-3-((benzyloxy)carbonyl)-5-methoxy-2,3,4,5,6,7-hexahydro-1H-2,6-methanoazocino[5,4-b]indole-10-carboxylic acid (126):
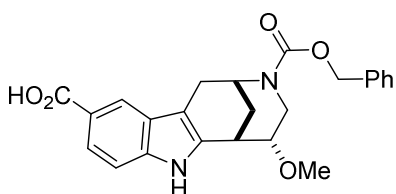
To a solution of compound **50** (0.250 g, 0.824 mmol) in acetic acid (5.5 mL, 0.15 M), 4-hydrazinobenzoic acid (0.125 g, 0.824 mmol) (619-67-0) was added. The mixture was allowed to stir and reflux for 2 h. Water and DCM were then added and the aqueous phase was extracted with DCM (5x). Solvents were then removed *in vacuo* and the crude product was purified by chromatography (1 to 100% ethyl acetate/DCM) to yield compound **126** (0.240 g, 69%) as a very pasty solid. The purified product showed high purity when checked by HPLC but the NMR spectra obtained was very complicated. The product was used further as obtained after chromatography.

(+/-)-3-benzyl 10-ethyl (2R,5R,6S)-7-(2-ethoxy-2-oxoethyl)-5-methoxy-1,2,4,5,6,7-hexahydro-3H-2,6-methanoazocino[5,4-b]indole-3,10-dicarboxylate (127):
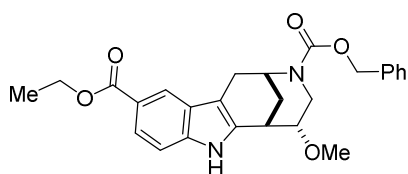

To a solution of compound **126** (0.093 g, 0.221 mmol) in ethanol (2.2 mL, 0.1 M), sulphuric acid (16 μL, 0.014 M) was added. The mixture was allowed to stir at room temperature for 3 h before quenching it with sodium bicarbonate (saturated aqueous solution). The aqueous phase was then extracted with DCM and the solvents were removed *in vacuo*. The crude product was purified by chromatography (1 to 100% ethyl acetate/DCM) to yield compound **127** (65 mg, 65%). Compound was further used in the synthesis without characterisation.

(+/-)-Benzyl 5-methoxy-10-(morpholine-4-carbonyl)-1,2,4,5,6,7-hexahydro-3H-2,6-methanoazocino[5,4-b]indole-3-carboxylate (128):
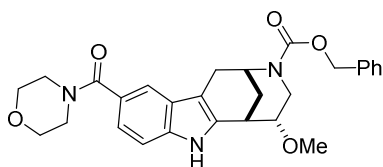

To a solution of compound **126** (0.091 g, 0.216 mmol) in DMF (3.6 mL, 0.06M), TBTU (0.111 g, 0.346 mmol) (125700-67-6) and DIPEA (60.3 μL, 0.346 mmol) were added. The mixture was allowed to stir at room temperature for 5 min before adding morpholine (18.7 μL, 0.216 mmol). The mixture was allowed to stir further for 1 h and partitioned between DCM and brine/water (1:1), the organic phase was washed several time with this mixture and the organic solvents were removed *in vacuo*. The crude product was purified by chromatography (1 to 3% MeOH/DCM) to obtain compound **66** (87 mg, 82%) with a minor impurity (most probably the *syn* diasteroisomer). For analytical purposes some of the product was further purified by preparative HPLC. **^{1}H NMR (CDCl$_3$, 600 MHz)** (rotameric mixture 1:1): δ 1.99-2.09 (m, 2H), 2.44 (dd, *J*=12.2, 11.0 Hz, 0.5H), 2.49-2.52 (m, 0.5H), 2.79 (dd, *J*=29.3, 16.8 Hz, 1H), 3.08 (dd, *J*=17.0, 5.2 Hz, 1H), 3.34 (bs, 0.5H), 3.36 (bs, 0.5H), 3.40 (s, 1H), 3.41 (s, 1H), 3.53-3.58 (m, 1H), 3.72-3.91 (m, 9H), 4.13 (dd, *J*=12.6, 5.3 Hz, 0.5H), 4.28 (dd, *J*=12.6, 5.3 Hz, 0.5H), 4.75 (bs, 0.5H), 4.82 (bs, 0.5H), 5.15 (s, 1H), 5.19 (d, *J*=3.1 Hz, 1H), 7.18-7.19 (m, 1H), 7.29-7.41 (m, 6H), 7.55 (d, *J*=6.2 Hz, 1H), 8.16 (bs, 0.5H), 8.12 (bs, 0.5H). **^{13}C NMR (CDCl$_3$, 100 MHz):** δ 27.6, 28.0, 30.0, 30.3, 32.6, 32.9, 42.3, 45.2, 45.3, 53.6, 57.0, 57.0, 67.1, 67.5, 67.7, 77.5, 77.9, 109.9, 110.2, 111.0, 111.0, 118.0, 118.1, 120.8, 120.9, 125.1, 125.8, 126.6, 126.6, 128.1, 128.1, 128.2 ,128.3, 128.7, 128.8, 134.3, 134.4, 136.7, 136.7, 137.0, 155.8, 155.8, 173.0, 173.1 **ESI:** calc. [M+H$^+$]: C$_{28}$H$_{32}$N$_3$O$_5$: 490.2, found 490.2; calc. [M+H$^+$]: C$_{28}$H$_{32}$N$_3$O$_5$: 521.2, found 521.2

(+/-)-3-benzyl 10-ethyl 7-(2-ethoxy-2-oxoethyl)-5-methoxy-1,2,4,5,6,7-hexahydro-3H-2,6-methanoazocino[5,4-b]indole-3,10-dicarboxylate (129):
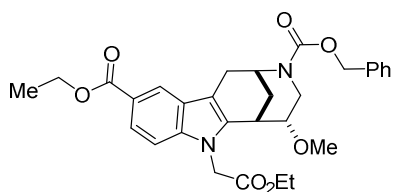
Compound **129** (26 mg, 41%) was synthesized as described for compound **53**. **^{1}H NMR (CDCl$_3$, 500 MHz)** (rotameric mixture 1:1): δ 1.29 (t, *J*=7.2 Hz, 3H), 1.41 (t, *J*=7.1 Hz, 3H), 1.96-2.07 (m, 2H), 2.54 (td, *J*=30.3, 11.8 Hz, 1H), 2.85 (t, *J*=17.4 Hz, 1H), 3.13-3.20 (m, 1H), 3.34 (d, *J*=6.9 Hz, 3H), 3.38 (s, 1H), 3.53-3.59 (m, 1H), 4.11-4.19 (m, 2H), 4.26-4.34 (m, 1H), 4.35-4.43 (m, 2H), 4.77 (bs, 0.5H), 4.79 (s, 0.5H), 4.83 (s, 0.5H), 4.84 (bs, 0.5H), 5.07-5.19 (m, 3H), 7.19 (d, *J*=8.7 Hz, 1H), 7.30-7.42 (m, 5H), 7.90 (d, *J*=8.6 Hz, 1H), 8.22 (d, *J*=6.2 Hz, 1H). **^{13}C NMR (CDCl$_3$, 100 MHz):** δ 14.3, 14.3, 14.6, 27.8, 28.1, 30.4, 30.8, 31.8, 31.9, 41.6, 41.7, 45.0, 45.1, 56.9, 57.0, 60.6, 61.2, 61.6, 67.4, 67.6, 68.3., 78.1, 78.5, 108.6, 110.1, 111.4, 121.0, 121.1, 121.8, 123.2, 126.3, 126.3, 128.0, 128.1, 128.1, 128.3, 128.6, 128.7, 135.5, 135.6, 136.8, 139.8, 155.5, 155.6, 167.9, 169.0, 169.1, 169.8 **HRMS:** calc. for [M+H]$^+$ C$_{30}$H$_{35}$N$_2$O$_7$: 535.24388, found: 535.24388

(+/-)-Ethyl 7-(2-ethoxy-2-oxoethyl)-5-methoxy-3-(2-(methylthio)nicotinoyl)-2,3,4,5,6,7-hexahydro-1H-2,6-methanoazocino[5,4-b]indole-10-carboxylate (130):
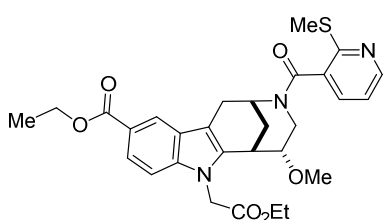
Compound **130** (11 mg, 42%) was obtained as described for **(+/-)-Glupin-1**, without the need to purify the crude product after the Cbz deprotection. **^{1}H NMR (CDCl$_3$, 500 MHz)** (rotameric mixture 1:1): δ 1.24 (dt, *J*=8.9, 7.1 Hz, 3H), 1.42 (dd, *J*=13.2, 7.0 Hz, 3H), 1.95 (bs, 0.5H), 2.07-2.34 (m, 1H), 2.56-2.79 (m, 4H), 2.87-3.11 (m, 1H), 3.18 (s, 1H), 3.31-3.37 (m, 1H), 3.42 (s, 1.5 H), 3.46 (d, *J*=3.2 Hz, 1H), 3.70 (bs, 0.5H), 3.92-4.02 (m, 2.5H), 4.11-4.24 (m, 2H), 4.40 (quin, *J*=6.9 Hz, 2H), 4.82 (t, *J*=17.9 Hz, 1H), 4.91 (dd, *J*=12.9, 4.9 Hz, 0.5H), 5.04 (d, *J*=18.0 Hz, 0.5H), 5.15 (d, *J*=18.1 Hz, 0.5H), 5.45 (bs, 0.5H), 7.07 (dd, *J*=7.3, 5.1 Hz, 0.5H), 7.15 (bs, 0.5H), 7.20 (dd, *J*=8.6, 6.0 Hz, 1H), 7.43-7.50 (m, 1H), 7.91 (dd, *J*=8.6, 1.5 Hz, 1H), 8.21 (bs, 0.5H), 8.27 (bs, 0.5H), 8.49 (dd, *J*=4.9, 1.7 Hz, 0.5H), 8.56 (dd, *J*=5.0, 1.7 Hz, 0.5H). **^{13}C NMR (CDCl$_3$, 100 MHz):** δ 13.2, 13.4, 14.3, 14.6, 28.4, 30.1, 31.4, 32.0, 32.3, 39.3, 42.9, 45.1, 45.2, 49.0, 57.1, 60.8, 60.8, 61.7, 61.7, 77.9, 78.9, 108.8, 119.4, 121.0, 121.2, 121.9, 121.9, 123.4, 126.1, 126.2, 133.8, 135.4, 135.7, 139.8, 149.7, 167.4, 167.9, 168.0, 168.1, 169.1 **HRMS:** calc. for [M+H]$^+$ C$_{29}$H$_{34}$N$_3$O$_6$S: 552.21628, found: 552.21580; Calc. for [M+Na]$^+$ C$_{29}$H$_{33}$N$_3$O$_6$NaS: 574.19823, found: 574.19767

(+/-)-Ethyl 2-(5-methoxy-3-(2-(methylthio)nicotinoyl)-10-(morpholine-4-carbonyl)-1,2,3,4,5,6-hexahydro-7H-2,6-methanoazocino[5,4-b]indol-7-yl)acetate (131):
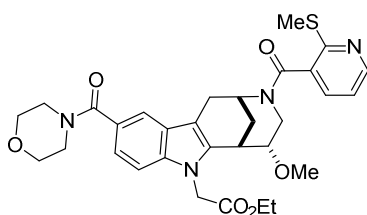
Compound **128** was taken through the Glupin synthetic pathway with no modifications on the procedure. Compound **131** (8 mg, 47 %) was obtained by preparative HPLC to yield a colorless oil. **^{1}H NMR (CDCl$_3$, 500 MHz)** (rotameric mixture 1:1): δ 1.25 (dd, J= 13.3, 7.1 Hz, 3H), 1.93-2.20 (m, 1.5H), 2.48-2.58 (m, 5H), 2.63 (s, 2H), 2.89-3.17 (m, 2.5H), 3.33 (ddd, J=23.4, 15.1, 5.4 Hz, 1H), 3.41 (s, 1.5H), 3.45 (d, J=2.7 Hz, 1H), 3.71 (bs, 7H), 4.01 (bs, 0.5H), 4.12-4.25 (m, 2H), 4.80 (t, J=18.0 Hz, 1H), 4.91 (dd, J=12.9, 5.0 Hz, 0.5H), 5.04 (d, J=18.0 Hz, 0.5H), 5.15 (d, J=18.1 Hz, 0.5H), 5.44 (bs, 0.5H), 7.05 (dd, J=7.5, 5.0 Hz, 0.5H), 7.12 (m, 0.5H), 7.19-7.25 (m, 2H), 7.41-7.47 (m, 1H), 7.58 (bs, 0.5H), 7.63 (bs, 0.5H); 8.47 (dd, J=4.9, 1.7 Hz, 0.5H), 8.53 (dd, J=4.9, 1.7 Hz, 0.5H). **HRMS:** calc. for [M+H]$^+$ C$_{31}$H$_{37}$N$_4$O$_6$S: 593.24283, found: 593.24252; calc. for [M+Na]$^+$ C$_{31}$H$_{36}$N$_4$O$_6$NaS: 615.22478, found: 615.22452

9.2. Determination of the Absolute Configuration of (+) and (-)-Glupin analogues:

9.2.1. Resolution of compound 44:

To a solution of (S)-O-acetyl mandelic acid (7322-88-5) (1.47 g, 7.57 mmol) in DCM (22.3 mL, 0.34M), freshly distilled thionyl chloride (0.60 mL, 8.33 mmol) and two drops of DMF were added. The mixture was allowed to stir at reflux conditions for 2 hours before evaporating the solvents. The crude product was redissolved in DCM (20.0 mL, 0.175M) and added dropwise to a solution of racemic compound **44** (1.0 g, 3.456 mmol) in pyridine (20.0 mL, 0.175 M) kept at -10°. The mixture was allowed to stir at this temperature for 6 hours. The mixture was quenched with a saturated aqueous solution of CuCl$_2$ and washed with this solution until no pyridine remained in the organic phase. The organic phase was finally washed with ammonium chloride saturated solution and with brine before evaporating solvents. The crude product was purified by chromatography (5 to 10% ethyl acetate/DCM) to yield compound **138** (less polar, T$_R$: 2.80 min in a 4.5 min run from 10% MeCN/90% water to 100% MeCN) (0.530g, 34%) and compound **139** (more polar, T$_R$: 2.75 min in a 4.5 min run from 10% MeCN/90% water to 100% MeCN) (0.500g, 31%).
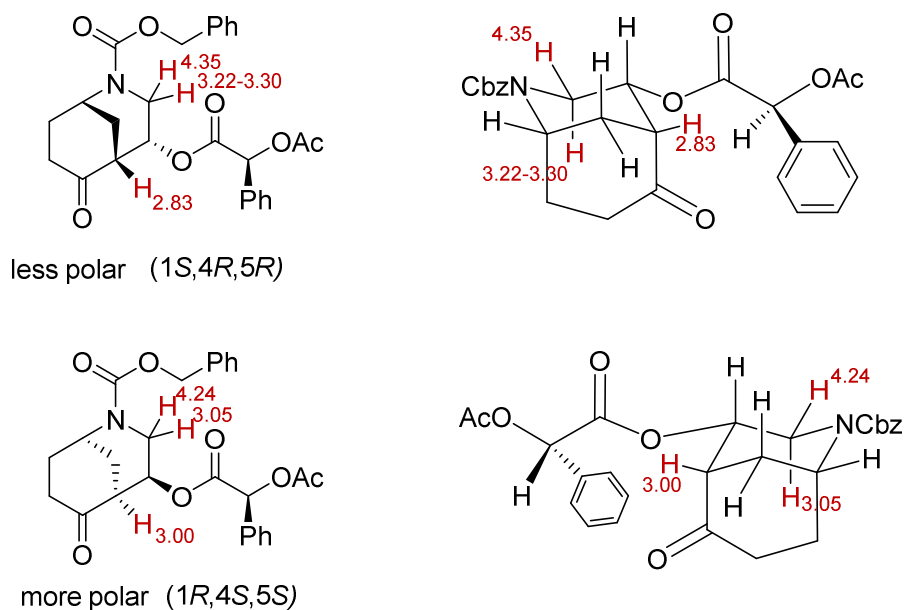
**Figure 43.** [1]H shifts of the neighboring protons of the chiral auxiliary

Benzyl (1S,4R,5R)-4-(2-acetoxy-2-phenylacetoxy)-6-oxo-2-azabicyclo[3.3.1]nonane-2-carboxylate(less polar) (138):

[1]**H NMR (CDCl$_3$, 600 MHz)** (rotameric mixture 1:1): δ 1.94-2.03 (m, 3H), 2.16-2.25 (m, 4H), 2.38-2.45 (m, 1H), 2.49-2.53 (m, 1H), 2.83 (s, 1H), 3.22-3.26 (m, 0.5H), 3.30 (dd, *J*=13.2, 10.3 Hz, 0.5H), 4.35 (ddd, *J*=37.2, 13.6, 7.1 Hz, 0.5H), 4.40 (m, 0.5H), 4.49 (s, 0.5H), 5.09-5.18 (m, 3H), 5.84 (d, *J*=11.5 Hz, 1H), 7.31-7.44 (m, 10H). [13]**C NMR (CDCl$_3$, 100 MHz):** δ 20.7, 29.7, 30.8, 30.5, 38.7, 43.6, 43.7, 44.2, 44.4, 47.1, 67.6, 67.7, 68.9, 69.2, 74.5, 127.5, 128.1, 128.3, 128.6, 128.8, 129.4, 133.0, 133.1, 136.3, 155.6, 167.7, 167.9, 170.4, 170.5, 207.1, 207.2 **HRMS:** calc. for [M+H]$^+$ C$_{26}$H$_{28}$NO$_7$: 466.18603, found: 466.18568

Benzyl (1R,4S,5S)-4-((S)-2-acetoxy-2-phenylacetoxy)-6-oxo-2-azabicyclo[3.3.1]nonane-2-carboxylate(more polar) (139):
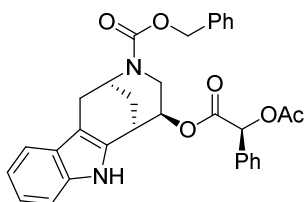
[1]**H NMR (CDCl3, 600 MHz)** (rotameric mixture 1:1): δ 1.96-2.04 (m, 3H), 2.16-2.22 (m, 4H), 2.33 (ddd, *J*=17.8, 11.7, 8.9 Hz, 1H), 2.54-2.59 (m, 1H), 3.00 (bs, 1.5H), 3.05 (dd, *J*=13.3, 10.3 Hz, 0.5H), 4.24 (m, 1H), 4.41 (s, 0.5H), 4.49 (s, 0.5H), 5.08-5.17 (m, 3H), 5.90 (s, 1H), 7.31-7.36 (m, 8H), 7.40-7.41 (m, 2H). [13]**C (CDCl3, 100 MHz):** δ 20.7, 29.6, 30.4, 30.5, 30.7, 38.7, 38.8, 43.3, 43.4, 44.2, 44.3, 47.1, 47.1, 67.6, 67.7, 69.0, 69.2, 74.3, 74.3, 127.7, 128.1, 128.3, 128.3, 128.6, 128.9, 129.4, 133.5, 136.3, 155.3, 155.4, 167.7, 167.8, 170.1, 170.2, 207.4, 207.6 **HRMS:** calc. for [M+H]$^+$ C$_{26}$H$_{28}$NO$_7$: 466.18603, found: 466.18581

Benzyl (2R,5R,6S)-5-((S)-2-acetoxy-2-phenylacetoxy)-1,2,4,5,6,7-hexahydro-3H-2,6-methanoazocino[5,4-b]indole-3-carboxylate(140):
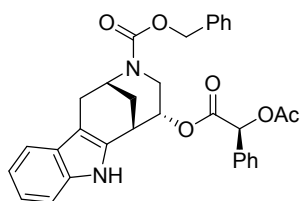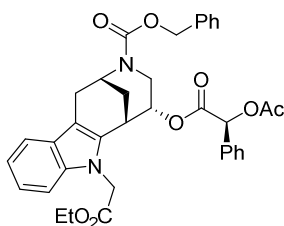

Compound **140** (0.424 mg, 67%) was synthesized as described for compound **57**, starting from compound **138**. **¹H NMR (CDCl₃, 500 MHz)** (rotameric mixture 1:1): δ 2.02-2.06 (m, 1H), 2.10-2.12 (m, 1H), 2.35 (d, *J*=5.2 Hz, 3H), 2.83-2.93 (m, 2H), 3.15-3.21 (m, 1H), 3.69-3.72 (m, 1H), 3.90 (dd, *J*=12.7, 5.7 Hz, 0.5H), 4.03 (dd, *J*=12.8, 5.7 Hz, 0.5H), 4.78 (bs, 0.5H), 4.86 (bs, 0.5H), 4.95-4.99 (m, 1H), 5.13 (s, 1H), 5.16-5.22 (m, 1H), 5.61 (d, *J*=8.6 Hz, 1H), 7.13 (t, *J*=7.5 Hz, 1H), 7.21 (t, *J*=7.6 Hz, 1H), 7.29-7.45 (m, 11H), 7.52 (t, *J*=8.9 Hz, 1H), 9.34 (s, 0.5H), 9.38 (s, 0.5H).**¹³C (CDCl₃, 100 MHz):** δ 21.0, 27.6, 27.9, 29.6, 30.0, 30.9, 31.0, 40.7, 40.8, 45.0, 45.1, 67.4, 67.6, 72.5, 72.7, 75.7, 75.8, 109.0, 109.2, 111.3, 111.3, 118.0, 118.1, 119.2 121.5, 121.5, 126.6, 126.6, 127.4, 127.8, 128.1, 128.1, 128.2, 128.3, 128.6, 128.7, 129.1, 129.8, 129.9, 131.3, 131.4, 132.0, 132.1, 136.2, 136.2 **HRMS:** calc. for [M+H]⁺ C₃₂H₃₁N₂O₆: 539.21766, found: 539.21778

Benzyl (2S,5S,6R)-5-((S)-2-acetoxy-2-phenylacetoxy)-1,2,4,5,6,7-hexahydro-3H-2,6-methanoazocino[5,4-b]indole-3-carboxylate (141):

Compound **141** (0.473 mg, 93%) was synthesized as described for compound **57**, starting from compound **139**. **¹H NMR (CDCl₃, 500 MHz)** (rotameric mixture 1:1): δ 1.98 (t, *J*=14.2 Hz, 1H), 2.08-2.10 (m, 1H), 2.18 (d, *J*=8.5 Hz, 3H), 2.76-2.84 (m, 2H), 3.07 (dd, *J*=17.1, 5.4 Hz, 1H), 3.24 (bs, 0.5H), 3.32 (bs, 0.5H), 4.02 (dd, *J*=12.5, 5.5 Hz, 0.5H), 4.11-4.16 (m, 0.5H), 4.74 (bs, 0.5H), 4.81 (bs, 0.5H), 5.12-5.23 (m, 3H), 5.86 (s, 1H), 6.55 (s, 0.5H), 7.00 (s, 0.5H), 7.07-7.17 (m, 3H), 7.32-7.44 (m, 6H), 7.52-7.68 (m, 5H). **¹³C (CDCl₃, 100 MHz):** δ 20.9, 21.0, 27.6, 28.0, 30.0, 30.4, 31.7, 31.7, 41.1, 41.2, 44.9, 45.0, 67.5, 67.6, 72.1, 72.1, 74.6, 75.0, 109.5, 109.8, 110.9, 118.0, 118.1, 119.4, 121.7, 121.7, 126.5, 126.6, 128.1, 128.1, 128.2, 128.2, 128.3, 128.4, 128.7, 128.7, 129.5, 129.6, 130.1, 130.1, 130.4, 130.6, 133.9, 135.7, 135.8, 136.5, 136.7, 155.4, 155.5, 167.9, 167.9, 171.2, 171.7 **HRMS:** calc. for [M+H]⁺ C₃₂H₃₁N₂O₆: 539.21766, found: 539.21784

Benzyl (2R,5R,6S)-5-(2-acetoxy-2-phenylacetoxy)-7-(2-ethoxy-2-oxoethyl)-1,2,4,5,6,7-hexahydro-3H-2,6-methanoazocino[5,4-b]indole-3-carboxylate (142):

Compound **142** (0.022 mg, 19%) was synthesized as described for compound **58**, starting from compound **140**. Compound **142** was purified by prep-HPLC from a complicated mixture of products and characterized only by HRMS before proceeding with the synthesis. **HRMS:** calc. for [M+H]$^+$ C$_{36}$H$_{37}$N$_2$O$_8$:625.25444, found: 625.25516;calc. for [M+Na]$^+$ C$_{36}$H$_3$N$_2$O$_8$Na: 647.23639, found: 647. 23724

Benzyl (2S,5S,6R)-5-((S)-2-acetoxy-2-phenylacetoxy)-7-(2-ethoxy-2-oxoethyl)-1,2,4,5,6,7-hexahydro-3H-2,6-methanoazocino[5,4-b]indole-3-carboxylate (143):
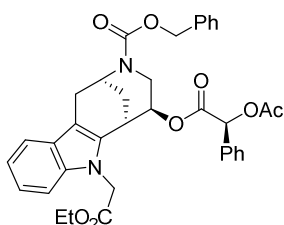
Compound **143** (0.022 mg, 19%) was synthesized as described for compound **58**, starting from compound **141**. Compound **143** was purified by prep-HPLC from a complicated mixture of products and characterized only by HRMS before proceeding with the synthesis. **HRMS:** calc. for [M+H]$^+$ C$_{36}$H$_{37}$N$_2$O$_8$: 625.25444, found: 625.25516;calc. for [M+Na]$^+$ C$_{36}$H$_3$N$_2$O$_8$Na: 647.23639, found: 647. 23724

(2R,5R,6S)-7-(2-ethoxy-2-oxoethyl)-3-(2-(methylthio)nicotinoyl)-2,3,4,5,6,7-hexahydro-1H-2,6-methanoazocino[5,4-b]indol-5-yl 2-phenylacetate (144):
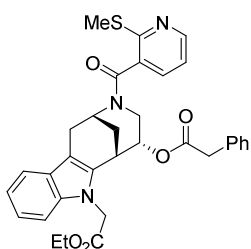
Compound **144** (0.005 mg, 24%) was synthesized starting from compound **142** and submitted to the conditions for the synthesis of compounds **59** and the crude product directly submitted to the conditions of **(+/-)-Glupin-1**. Compound **144** was purified by preparative HPLC from a complicated mixture and was isolated with small impurities of the unalkylated indole analogue and the analogue in which the acetyl group has not been removed. **¹H NMR (CDCl₃, 700 MHz)** (rotameric mixture 1:1): δ 1.21-1.23 (m, 3H), 2.09-2.29 (m, 2H), 2.55-2.63 (m, 3H), 2.76-3.18 (m, 2.5H), 3.36 (ddd, *J*=23.7, 15.2 5.7 Hz, 1H),3.41 (d, *J*=2.44 Hz, 0.5H), 3.45-3.54 (m, 2H), 3.60 (d, *J*=15.0 Hz, 0.5H), 3.66 (d, *J*=15.0 Hz, 0.5H), 4.03 (bs, 0.5H), 4.06-4.17 (m, 2H), 4.34 (d, *J*=23.1 Hz, 2H), 4.73 (dd, *J*=13.0, 5.3 Hz, 0.5H), 5.25 (bs, 0.5H), 5.46 (s, 0.5H), 7.05-7.24 (m, 6H), 7.28-7.55 (m, 5H), 8.47 (dd, *J*=4.9, 1.6 Hz, 0.5H), 8.53 (dd, *J*=4.9, 1.7 Hz, 0.5H). **HRMS:** calc. for[M+H]$^+$ C$_{33}$H$_{34}$N$_3$O$_5$: 584.22137, found: 584.22218

(2S,5S,6R)-7-(2-ethoxy-2-oxoethyl)-3-(2-(methylthio)nicotinoyl)-2,3,4,5,6,7-hexahydro-1H-2,6-methanoazocino[5,4-b]indol-5-yl 2-phenylacetate (145):
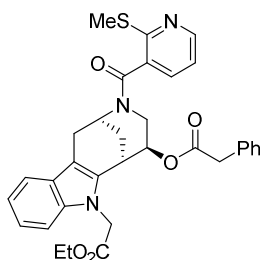
Compound **145** (0.005 mg, 23%) was synthesized starting from compound **143** and submitted to the conditions for the synthesis of compound **59** and the crude product directly submitted to the conditions of **(+/-)-Glupin-1**. Compound **145** was purified by preparative HPLC from a complicated mixture and was isolated with small impurities of the unalkylated indole analogue and the analogue in which the acetyl group has not been removed.**^{1}H NMR (CDCl₃, 700 MHz)** (rotameric mixture 1:1): δ 1.21-1.23 (m, 3H), 2.04-2.29 (m, 2H), 2.55-2.63 (m, 3H), 2.76-3.18 (m, 2.5H), 3.36 (ddd, *J*=23.6, 15.1, 5.7 Hz, 1H),3.41 (d, *J*=2.4 Hz, 0.5H), 3.45-3.54 (m, 2H), 3.60 (d,*J*=15.0 Hz, 1H), 4.03 (bs, 0.5H), 4.06-4.16 (m, 2H), 4.34 (d, *J*=23.5 Hz, 1H), 4.73 (dd, *J*=12.9, 5.3 Hz, 0.5H), 5.25 (bs, 0.5H), 5.46 (s, 0.5H), 7.06-7.24 (m, 6H), 7.28-7.55 (m, 5H), 8.48 (dd, *J*=4.9, 1.6 Hz, 0.5H), 8.53 (dd, *J*=4.9, 1.7 Hz, 0.5H).**HRMS:** calc. for $[M+H]^+$ $C_{33}H_{34}N_3O_5$: 584.22137, found: 584.22197

9.3. Synthesis of the Active Glupin Probre

(+/-)-Benzyl (1S,4R,5R)-4-(2-bromoacetoxy)-6-oxo-2-azabicyclo[3.3.1]nonane-2-carboxylate (146):
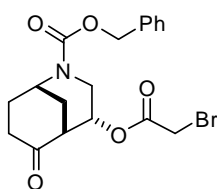
Compound **146** (0.180 g, 58 %) (isolated with 10% of the *syn* diasteroisomer) was synthesised as described for compound **51**. **^{1}H NMR (CDCl₃, 400 MHz)** (rotameric mixture 1:1) (data given for the mayor diasteroisomer): δ 1.92-2.07 (m, 3H), 2.16-2.28 (m, 1H), 2.43-2.64 (m, 2H), 3.03 (s, 1H), 3.23-3.31 (m, 1H), 3.79 (s, 2H), 4.28-4.39 (m, 1H), 4.46 (bs, 0.5H), 4.55 (bs, 0.55H), 5.16 (s, 3H), 7.30-7.37 (m, 5H). **^{13}C NMR (CDCl₃, 100 MHz):** δ 25.5, 29.4, 30.1, 30.3, 30.5, 38.7, 43.4, 44.2, 44.4, 46.8, 46.9, 67.8, 69.6, 69.7, 128.1, 128.2, 128.4, 128.7, 136.3, 155.3, 155.5, 166.2, 207.8, 208.0

tert-Butyl (1-bromo-2-oxo-7,10,13-trioxa-3-azahexadecan-16-yl)carbamate:
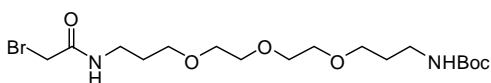
Compound (0.29 g, 54%) was synthesised according to the literature procedure for the chloro analogue.[92]

^{1}H NMR (CDCl₃, 400 MHz): δ 1.44 (s, 9H), 1.72-1.79 (m, 2H), 1.82 (dt, *J*=11.7, 5.9 Hz, 2H), 3.22 (dd, *J*=12.3, 6.1, 2H), 3.42 (dd, *J*=12.1, 5.8 Hz, 2H), 3.54 (t, *J*=6.0 Hz, 2H), 3.58-3.69 (m, 10H), 3.85 (s, 2H), 4.93 (bs, 1H), 7.18 (bs, 1H).

(+/-)-Ethyl 2-(5-(((2,2-dimethyl-4-oxo-3,9,12,15-tetraoxa-5-azaoctadecan-18-yl)carbamoyl)oxy)-3-(2-(methylthio)nicotinoyl)-1,2,3,4,5,6-hexahydro-7H-2,6-methanoazocino[5,4-b]indol-7-yl)acetate (149):
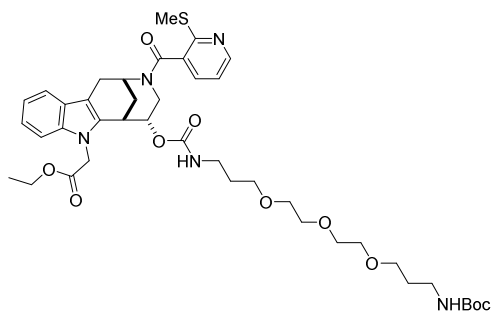
To a solution of compound **90** (30 mg, 0.064 mmol) in DCE (4 mL, 0.016 M), 4-nitrophenyl carbonochloridate (52 mg, 0.258 mmol) (CAS: 7693-46-1), DMAP (24 mg, 0.192 mmol) and triethylamine (18 mL, 0.128 mmol) were added. The mixture was heated to 60° overnight (after 15/20 min everything solubilized). Then tert-butyl (3-(2-(2-(3-aminopropoxy)ethoxy)ethoxy)propyl)carbamate (410 mg, 1.28 mmol) and the mixture was allowed to stir for 5 more hours. Solvents were removed *in vacuo* and the crude product was dissolved in MeCN (1mL) and subjected to preparative HPLC purification. (10% to 50% ACN/H2O with 0.1% TFA). Compound **149** (31.2 mg, 60%) was obtained as a white solid. **^{1}H NMR (CDCl$_3$, 400 MHz)** (rotameric mixture): δ 1.23 (td, J=2.4, 7.1 Hz, 3H), 1.40-1.43 (m, 9H), 1.61-1.83 (m, 4H), 1.95-2.26 (m, 2H), 2.54 (bs, 1.8H), 2.62 (s, 1.2H), 2.70-2.76 (m, 1H), 2.96-3.59 (m, 20H), 4.02 (bs, 0.4H), 4.10-4.22 (m, 2H), 4.66-5.14 (m, 4H), 5.31 (bs, 0.6H), 5.46 (bs, 1H), 7.01-7.23 (m, 4H), 7.42-7.48 (m, 1.4H), 7.54 (d, J=7.5 Hz, 0.6H), 8.44 (dd, J=1.6, 4.9 Hz, 0.6H), 8.51 (dd, J=1.5, 4.9 Hz, 0.4H).). **^{13}C NMR (CDCl$_3$, 100 MHz)** (rotameric mixture):δ 13.1, 13.2, 14.3, 27.1, 28.7, 29.5, 29.7, 30.2, 31.1, 31.3, 31.4, 38.6, 39.2, 39.4, 39.5, 42.4, 44.9, 48.7, 61.7, 69.5, 69.6, 70.23, 70.31, 70.28, 70.49, 70.52, 70.56, 70.61, 71.0, 71.4, 109.0, 110.3, 118.3, 118.6, 119.1, 119.2, 119.9, 122.1, 126.6, 126.8, 130.8, 133.4, 133.5, 133.8, 137.3, 149.7, 155.2, 155.4, 156.1, 156.2, 167.1, 167.3, 169.1, 169.2. **HRMS**: calc. for [M+H]+ C$_{41}$H$_{58}$N$_5$O$_{10}$S: 812.38989, found. 812.39275

(+/-)-1-((7-(2-ethoxy-2-oxoethyl)-3-(2-(methylthio)nicotinoyl)-2,3,4,5,6,7-hexahydro-1H-2,6-methanoazocino[5,4-b]indol-5-yl)oxy)-1-oxo-6,9,12-trioxa-2-azapentadecan-15-aminium (150):
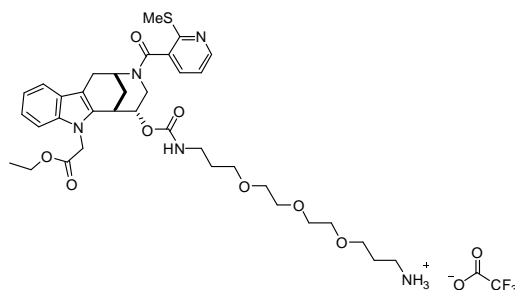
To a solution of compound **149** (30 mg, 0.037 mmol) in DCM (0.07M), TFA (28 μL, 0.555 mmol) was added and the mixture was allowed to stir overnight at room temperature. Solvents were then coevaporated with 3 mL of toluene (3x, without reaching dryness). The crude product was purified by HPLC (10% to 50% ACN/H2O with 0.1% TFA) to yield pure compound **150** (19 mg, 62%) as a TFA salt.Compound **150** has solubility problem and could only be characterised by HRMS. **HRMS:** calc. for $[M+H]^+$ $C_{36}H_{50}N_5O_8S$: 712.33746, found. 712.33903.

9.4. Synthesis of the Inactive Glupin Probe

(+/-)-Ethyl 2-(5-acetoxy-3-picolinoyl-1,2,3,4,5,6-hexahydro-7H-2,6-methanoazocino[5,4-b]indol-7-yl)acetate (151):
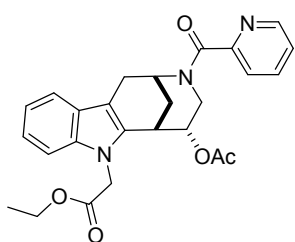
Compound **151** (244mg, 95%) was synthesized as described for compound **89**. Isolated with a 10% of the minor diasteroisomer. Data given for the *anti* diasteroisomer. **^{1}H NMR (CDCl$_3$, 400 MHz)** (rotameric mixture)**:** δ 1.22-1.28 (m, 3H), 1.96-1.99 (m, 2H), 2.07 (s, 1H), 2.11-2.17 (m, 1H), 2.27 (ddt, *J*=25.0, 12.8, 2.9 Hz, 1H), 2.8 (dd, *J*=12.6, 11.1 Hz, 0.5H), 2.98-3.07 (m, 1.5H), 3.10-3.15 (m, 0.5H), 3.34-3.38 (m, 1H), 3.49-3.52 (m, 1H), 3.86 (dd, *J*=12.8, 5.1 Hz, 0.5H), 4.13-4.24 (m, 2H), 4.58 (bs, 0.5H), 4.74 (dd, *J*=12.8, 5.2 Hz, 0.5H), 4.81-4.87 (m, 1.5H), 5.14 (dt, *J*=10.4, 4.7 Hz, 0.5H), 5.25 (dt, *J*=10.5, 5.0 Hz, 0.5H), 5.44 (s, 0.5H), 7.12-7.16 (m, 1H), 7.20-7.25 (m, 2H), 7.32 (dd, *J*=7.9, 5.3 Hz, 0.5H), 7.38 (dd, *J*=7.3, 5.1 Hz, 1H), 7.61 (d, *J*=8.0 Hz, 0.5H), 7.67 (d, *J*=7.8 Hz, 0.5H), 7.75-7.80 (m, 0.5H), 7.83-7.86 (m, 0.5H), 8.57 (d, *J*=4.7 Hz, 0.5H), 8.67 (d, *J*=4.7 Hz, 0.5H). **^{13}C NMR (CDCl3, 100 MHz)** (rotameric mixture): δ 14.3, 14.3, 21.1, 21.2, 28.6, 30.6, 30.9, 30.9, 31.4, 39.0, 42.8, 44.1, 44.8, 44.8, 48.0, 61.8, 61.8, 71.2, 71.9, 109.0, 109.0, 110.5, 110.7, 118.6, 118.7, 120.0, 122.1, 122.2, 122.3, 123.6, 123.8, 124.6, 124.7, 126.7,

126.8, 133.1, 133.2, 137.2, 137.3, 137.3, 148.7, 148.8, 154.1, 154.8, 168.2, 168.3, 168.8, 168.9, 169.8 **HRMS:** calc. for $[M+H]^+$ $C_{26}H_{28}N_3O_5$: 462.20235, found. 462.20193

(+/-)-Ethyl 2-(5-(((2,2-dimethyl-4-oxo-3,9,12,15-tetraoxa-5-azaoctadecan-18-yl)carbamoyl)oxy)-3-picolinoyl-1,2,3,4,5,6-hexahydro-7H-2,6-methanoazocino[5,4-b]indol-7-yl)acetate (152):
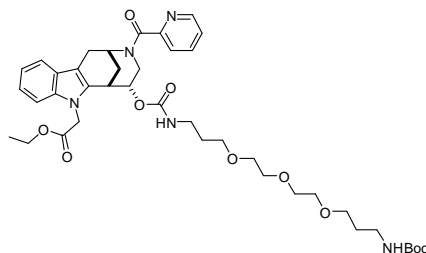

To a solution of compound **151** (0.223g, 0.483mmol) in a mixture of THF (7mL, 0.07M) and H_2O (3mL, 0.16M), LiOH (70mg, 2.90mmol) was added. The mixture was allowed to stir at room temperature for 30 min. The mixture was then taken to pH 2 with HCl 1M and extracted with DCM (3x). The solvents were removed *in vacuo* and the crude product was dissolved in EtOH (4.8 mL, 0.1 M). To this solution sulphuric acid was added (40 µL, 0.014M) and the mixture allowed to stir overnight at room temperature. The mixture was neutralized by sodium bicarbonate saturated aqueous solution and extracted with DCM. From the crude product obtained (0.181mg, 90% crude yield) 50 mg were used to synthesize compound **152** (36.9mg, 41%) as described for compound **149**. **^{1}H NMR (CDCl$_3$, 700 MHz)** (rotameric mixture)**:** δ 1.21-1.26 (m, 3H), 1.40-1.42 (m, 9H), 1.63-1.84 (m, 4H), 1.88-2.16 (m, 2H), 2.23-2.28 (m, 1H), 2.76 (t, *J*=11.5 Hz, 0.5H), 2.97-3.67 (m, 18H), 4.12-4.21 (m, 2H), 4.53-4.64 (m, 1H), 4.69 (dd, *J*=12.8, 5.3 Hz, 0.5H), 4.76 (dd, *J*=21.5, 18.0 Hz, 1H), 4.83-4.99 (m, 2H), 5.02-5.05 (m, 0.5H), 5.13-5.15 (m, 0.5H), 5.33-5.60 (m, 1.5H), 7.10-7.14 (m, 1H), 7.17-7.21 (m, 2H), 7.31 (dd, *J*=7.1, 5.3 Hz, 0.5H), 7.38 (dd, *J*=7.0, 4.9 Hz, 0.5H), 7.50 (dd, *J*=18.8, 7.8 Hz, 1H), 7.60 (d, *J*=7.8 Hy, 0.5H), 7.65 (d, *J*=7.7 Hz, 0.5H), 7.78 (td, *J*=7.8, 1.6 Hz, 0.5H), 7.83 (td, *J*=7.6, 1.4 Hz, 0.5H), 8.56 (d, *J*=4.5 Hz, 0.5H), 8.66 (d, *J*=4.7 Hz, 0.5H). **^{13}C NMR (CDCl$_3$, 100 MHz)** (rotameric mixture): δ 14.3, 27.4, 28.6, 29.5, 29.5, 29.6, 29.7, 30.3, 31.1, 31.2, 31.2, 38.6, 38.6, 38.6, 39.4, 39.4, 42.7, 44.6, 44.8, 44.9, 48.1, 61.7, 61.8, 69.5, 69.6, 69.7, 70.2, 70.2, 70.3, 70.3, 70.4, 70.5, 70.5, 70.5, 70.6, 70.7, 70.7, 71.0, 71.5, 79.0, 79.1, 109.0, 109.0, 110.1, 110.4, 118.5, 118.6, 119.9, 122.0, 123.6, 123.7, 124.6 ,124.6, 126.7, 126.8, 133.5, 133.5, 137.3, 137.3, 148.7, 148.8, 154.2, 154.9, 155.3, 155.5, 156.1, 156.2, 168.2, 169.2, 169.3 **HRMS:** calc. for $[M+H]^+$ $C_{40}H_{56}N_5O_{10}$: 766.40217, found: 766.40418

(+/-)-Ethyl 2-(5-(((3-(2-(2-(3-aminopropoxy)ethoxy)ethoxy)propyl)carbamoyl)oxy)-3-picolinoyl-1,2,3,4,5,6-hexahydro-7H-2,6-methanoazocino[5,4-b]indol-7-yl)acetate (153):
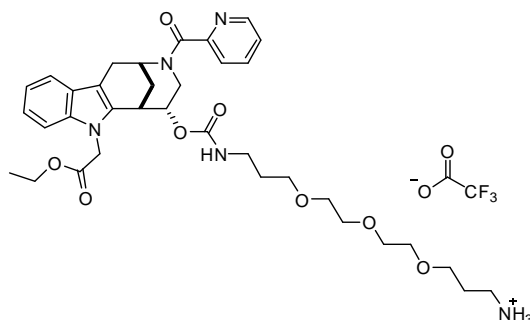
To a solution of compound **152** (14.8 mg, 0.0193 mmol) in DCM (0.07M), TFA (15 µL, 0.193 mmol) was added and the mixture was allowed to stir overnight at room temperature. Solvents were then coevaporated with 3mL of toluene (3x, without reaching dryness). The crude product was purified by HPLC (10% to 50% ACN/H2O with 0.1% TFA) to yield pure compound **153** (12 mg, 80%) as a TFA salt. **HRMS:** calc. for $[M+H]^+$ $C_{35}H_{48}N_5O_8$: 666.34974, found: 666.35019.

(+/-)-2-(6-(dimethylamino)-3-(dimethyliminio)-3H-xanthen-9-yl)-5-(3-(1-((7-(2-ethoxy-2-oxoethyl)-3-(2-(methylthio)nicotinoyl)-2,3,4,5,6,7-hexahydro-1H-2,6-methanoazocino[5,4-b]indol-5-yl)oxy)-1-oxo-6,9,12-trioxa-2-azapentadecan-15-yl)ureido)benzoate (154):
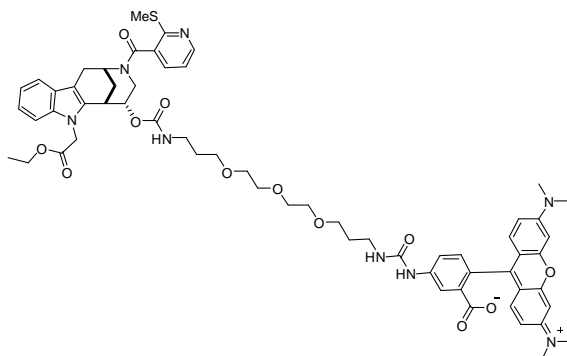
To a solution of compound **149** (8.5 mg, 0.010 mmol) in DMF (0.010 M), triethylamine (1.7 mL, 0.012 mmol) and a solution of TAMRA-isocyanate (CAS: 80724-19-2) (5 mg, 0.011 mmol) in DMF (0.01 M) were added. The mixture was allowed to stir for 2 h. protected from the light. This mixture was directly purified by preparative HPLC (10% to 50% ACN/H₂O) to yield pure compound **154** (3.03 mg, 41%). Compound **154** was only characterised by HRMS. **HRMS:** calc. for $[M+H]^+$ $C_{61}H_{71}N_8O_{11}S_2$: 1155.46782, found. 1155.47189.
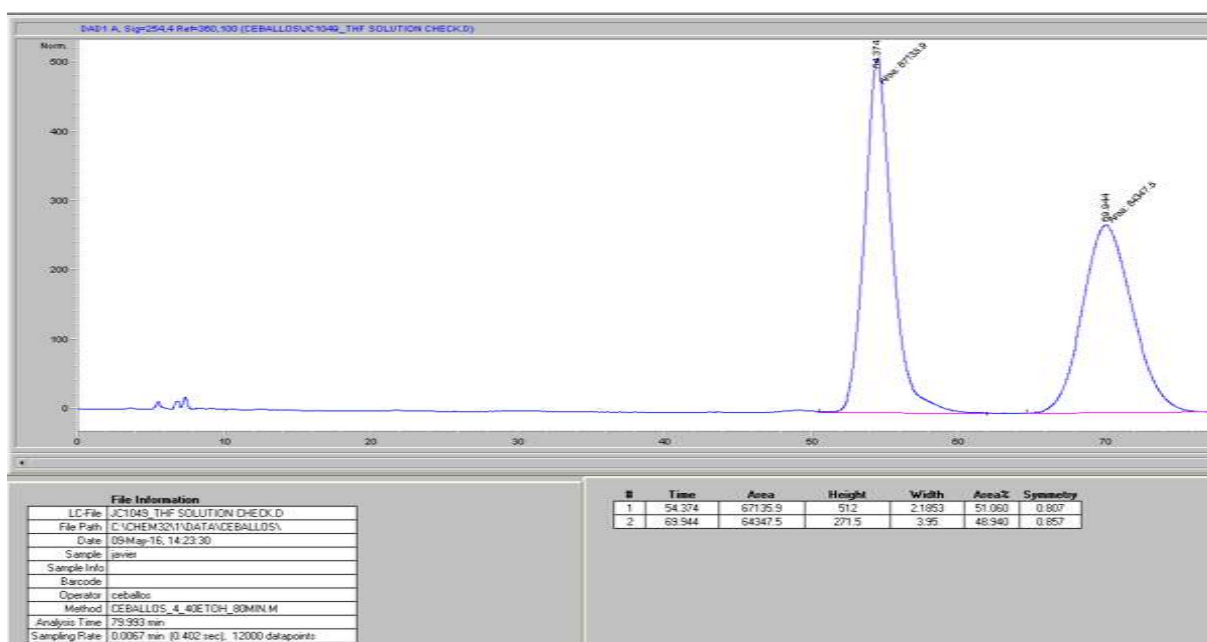
9.5. Chiral Separation:

(+/-)-Glupin-1:

Analytical HPLC Separation:(+/-)-Glupin-1 was submitted to Chiral Analytical HPLC separation. Column: ChiralPak® IC. Eluent: 40% EtOH/60% iso-Hexane. Flowrate: 0.5mL/min. The first enantiomer to exit the column is referred as e1.E_1: T_R=54.4 min. E_2: T_R=69.9 min (see Chiral Chromatograms section).
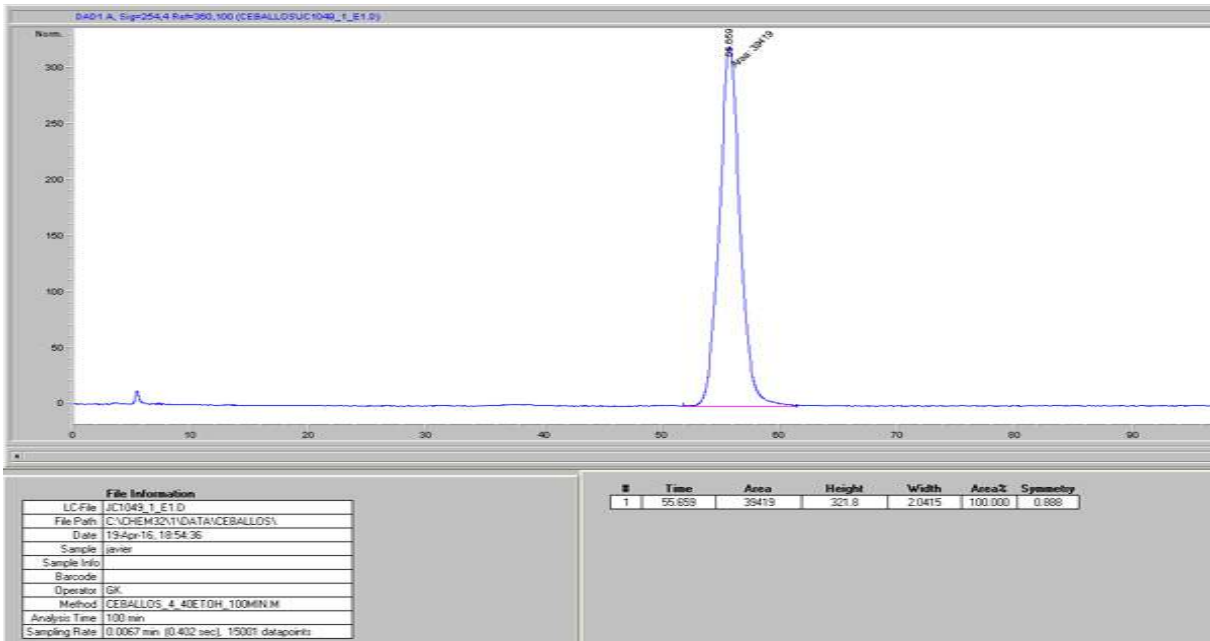
Preparative HPLC Separation: (+/-)-Glupin-1(not as the TFA salt) was submitted to Chiral preparative HPLC separation. Column: ChiralPak® IC. Eluent: 40% EtOH/60% *iso*-Hexane. Flowrate: 4mL/min. The first enantiomer to exit the column is referred as e1.E_1: T_R=45.7 min. E_2: T_R=61. min (see Chiral Chromatogram section).
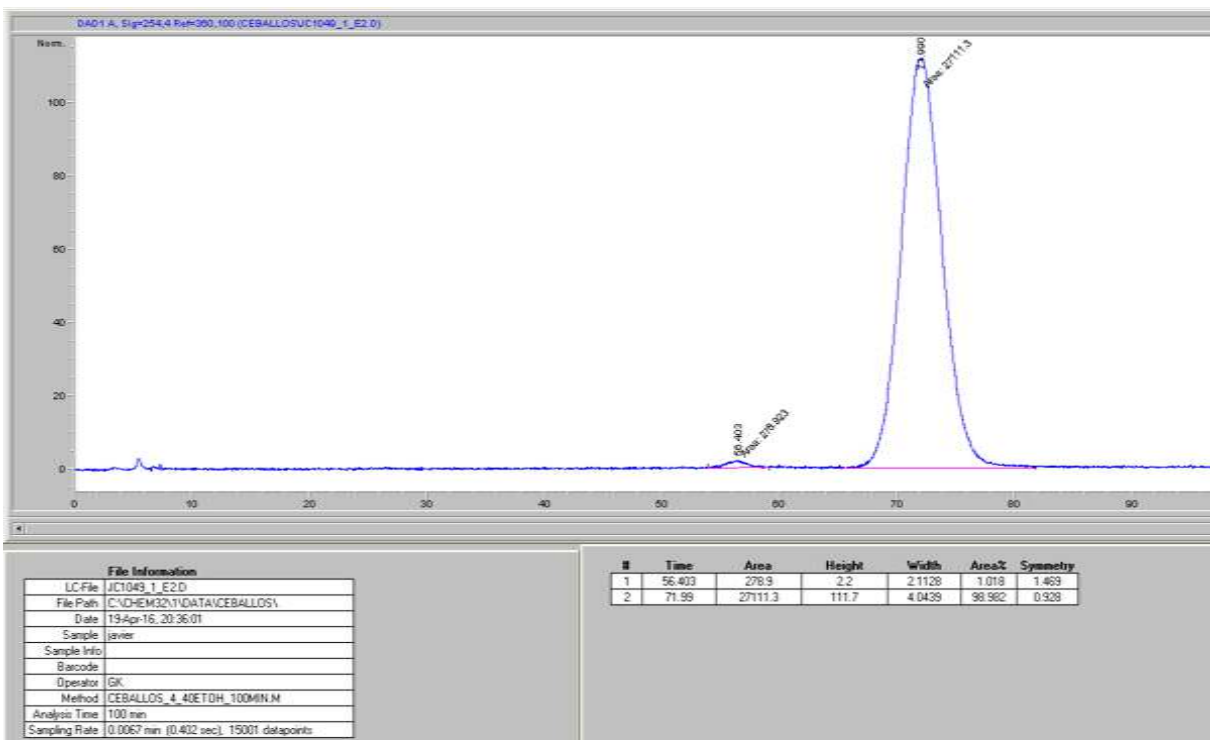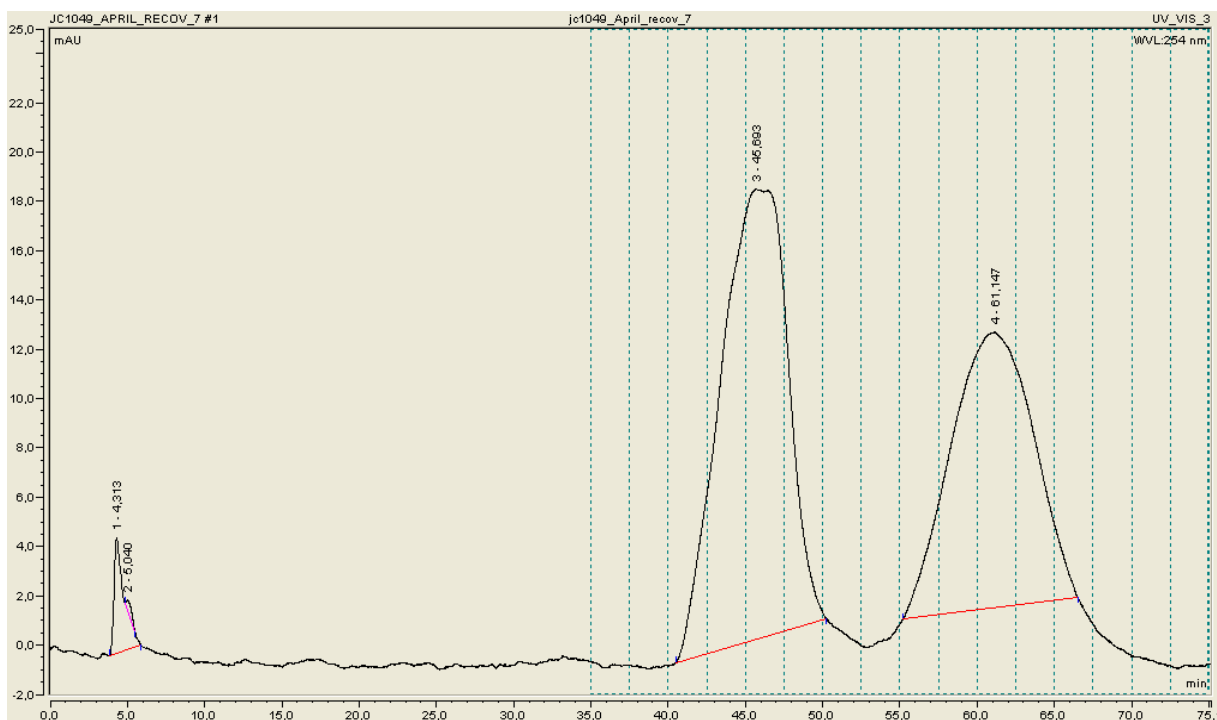
9.6. Chiral Chromatograms:

(+/-)-Glupin-1:

(+)-Glupin-1:

#	Time	Area	Height	Width	Area%	Symmetry
1	55.659	39419	321.8	2.0415	100.000	0.888

File Information

LC-File	JC1049_1_E1.D
File Path	C:\CHEM32\1\DATA\CEBALLOS\
Date	19-Apr-16, 18:54:36
Sample	javier
Sample Info	
Barcode	
Operator	GK
Method	CEBALLOS_4_40ETOH_100MIN.M
Analysis Time	100 min
Sampling Rate	0.0067 min (0.402 sec), 15001 datapoints

(-)-Glupin-1:

#	Time	Area	Height	Width	Area%	Symmetry
1	56.403	278.9	2.2	2.1128	1.018	1.469
2	71.99	27111.3	111.7	4.0439	98.982	0.928

File Information

LC-File	JC1049_1_E2.D
File Path	C:\CHEM32\1\DATA\CEBALLOS\
Date	19-Apr-16, 20:36:01
Sample	javier
Sample Info	
Barcode	
Operator	GK
Method	CEBALLOS_4_40ETOH_100MIN.M
Analysis Time	100 min
Sampling Rate	0.0067 min (0.402 sec), 15001 datapoints

**Preparative Separation of (+) and (-)-Glupin-1:**

# 10.Experimental Part: Splicing Inhibition

General Remarks

All reactions involving air- or moisture-sensitive reagents or intermediates were carried out in flame-dried glassware under an argon atmosphere. Dry solvents (THF, toluene, MeOH, DMF) were used as commercially available. Analytical thin-layer chromatography (TLC) was performed on Merck silica gel aluminium plates. Compounds were visualized by irradiation with UV light or potassium permanganate staining. Column chromatography was performed using silica gel Merck 60 (particle size 0.040-0.063 mm). ^{1}H-NMR and ^{13}C-NMR were recorded on a Bruker DRX400 (400 MHz), Bruker DRX500 (500 MHz) and INOVA500 (500 MHz) at 300 K using CDCl3 or (CD3)2SO as solvents. All resonances are reported relative to TMS. Spectra were calibrated relative to solvent's residual proton and carbon chemical shift: CDCl3 (δ = 7.26 ppm for 1H NMR and δ = 77.16ppm for 13C NMR); (CD3)2SO: δ= 2.50 ppm for 1H NMR and δ= 39.52 ppm for 13C NMR). Multiplicities are indicated as: br s (broadened singlet), s (singlet), d (doublet), t (triplet), q (quartet), quin (quintet), m (multiplet); and coupling constants (J) are given in Hertz (Hz). High resolution mass spectra were recorded on a LTQ Orbitrap mass spectrometer coupled to an Acceka HPLC-System (HPLC column: Hypersyl GOLD, 50 mm × 1 mm, particle size 1.9 μm, ionization method: electron spray ionization). Preparative HPLC separations were carried out using a reversed-phase C18 column (RP C18, flow 20.0 mL/min, solvent A: 0.1% TFA in water, solvent B: 0.1% TFA in Acetonitrile, from 10 % B to 100 % B. All other chemicals and solvents were purchased from Sigma-Aldrich, Fluka, TCI, Acros Organics, ABCR and Alfa Aesar. Unless otherwise noted, all commercially available compounds were used as received without further purifications. Compounds: **187**, **188**, **175**, **178**, **179**, **180**, **177**, **182**, **183**, **184**, **181**, **185**, **186**, **176**, **189**, **192**, **191** and **190** were purchased in ChemDiv and their purity check by HPLC-MS prior to their use. Compounds: **cp028**, **167**, **168**, **172**, **170**, **164**, **166**, **165**, **173**, **174**, **171**, **169, 162** and **163** were synthesized with the general strategy shown in Scheme 22. Starting materials: 2-Ethylaniline and 5-bromo-2-carbaldehyde (5-bromofurfural), and the different boronic acids were purchase in Aldric or Alfa Aesar. Urea **159** and analogue ureas were obtained according to literature procedure by R. Laudien *et al.*[115], ^{1}H NMR of the compound **159**was in accordance with the literature data. Compound **160** and similar aldehydes were obtained in Suzuki coupling conditions reported by Martín-Matute *et al.*[126]Final compounds were synthesized from the ureas such as **156** in two steps as described in the literature by M. Hussein *et al.*[127]. All the **cp028** analogues present really low solubility on all solvents, but chloroform seemed to possess the best solubility value. All analogues present E/Z isomeric mixtures. Furthermore, due to the

conjugated electronic system, all analogues are very colorful and can be seen in chromatography columns and TLCs directly.
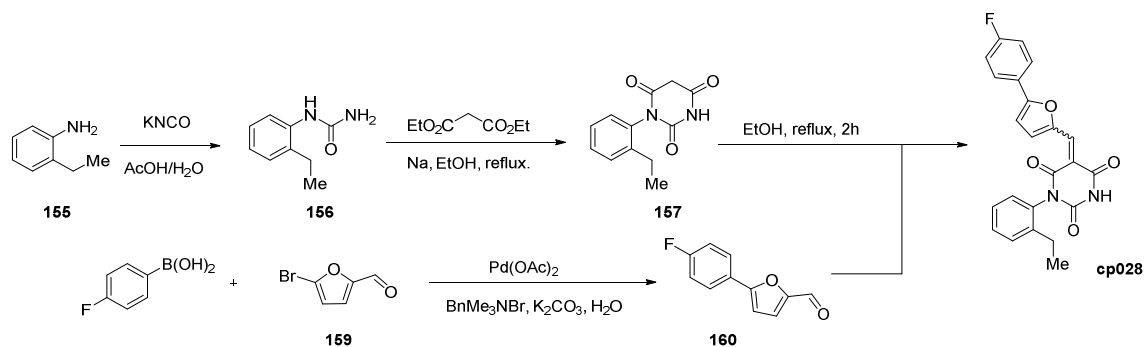

Scheme 22. Synthetic route towards cp028.

### 1-(2-ethylphenyl)pyrimidine-2,4,6(1H,3H,5H)-trione (157):
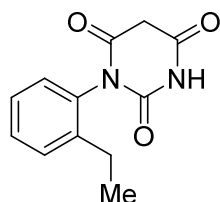
In an oven-dried flask under argon flow, sodium metal (0.21g, 9.14mmol) was placed. Dry ethanol (50mL, 0.18M) was cannulated into the flask and stirred until no more solid was observed. Diethyl malonate (1.39mL, 9.14mmol) was then added, stirred for 5 min and finally urea **156** (1.50g, 9.14mmol) was added. The mixture was stirred at reflux conditions for 16 hours. Solvents were evaporated and the crude was redissolved in NaOH aq. (2M), the mixture was then washed with Ethyl acetate to remove the remaining starting urea. The aqueous phase was then taken to pH 1 with HCl aq. (1M) leading to precipitation of the product. Product **157** (1.13g, 53%) was isolated as a white solid pure enough to continue the synthesis. The product could be recrystallized in a mixture of EtOH/water (1:1) if further purity was needed.**¹H NMR (DMSO, 400 MHz):** δ 1.07 (t, *J*=7.6 Hz, 3H), 2.43 (q, *J*=7.8 Hz, 2H), 3.67 (d, *J*=20.9 Hz, 1H), 3.91 (d, *J*=20.9 Hz, 1H), 7.16 (d, *J*=7.7 Hz, 1H), 7.24-7.28 (m, 1H), 7.35 (m, 2H), 11.50 (s, 1H) **HRMS:** calc. for $[M+H]^+$ $C_{12}H_{13}N_2O_3$: 233.09207, found 233.09211

5-(4-fluorophenyl)furan-2-carbaldehyde (160):
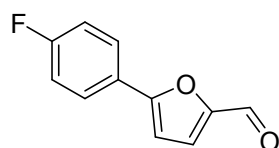
To a solution of 5-Bromofurfural (1.75 g, 10.00 mmol) in water (14 mL, 0.71 M), *p*-fluoroboronic acid (1.40g, 10.00 mmol), potassium carbonate (3.46g, 25.00mmol), benzyltrimethylammoniun bromide (2.30 g, 10.00 mmol) and palladium acetate (0.05 g, 0.2 mmol) were added. The mixture was allowed to stir overnight at room temperature. The aqueous mixture is extracted with ethyl acetate and solvent was evaporated. After purification by flash chromatography (20% ethyl acetate/petroleum ether) compound **160** was isolated as a white solid (1.86 g, 98%).**¹H NMR (CDCl₃, 400 MHz):** δ 6.78 (d, *J*=3.7 Hz, 1H), 7.14 (t, *J*=8.7 Hz, 2H), 7.31 (d, *J*=3.7 Hz, 1H),

7.79-7.84 (m, 2H), 9.65 (s, 1H), in agreement with the literature (Zhang *et al. Bioorg. Med. Chem. Lett.* 2016).
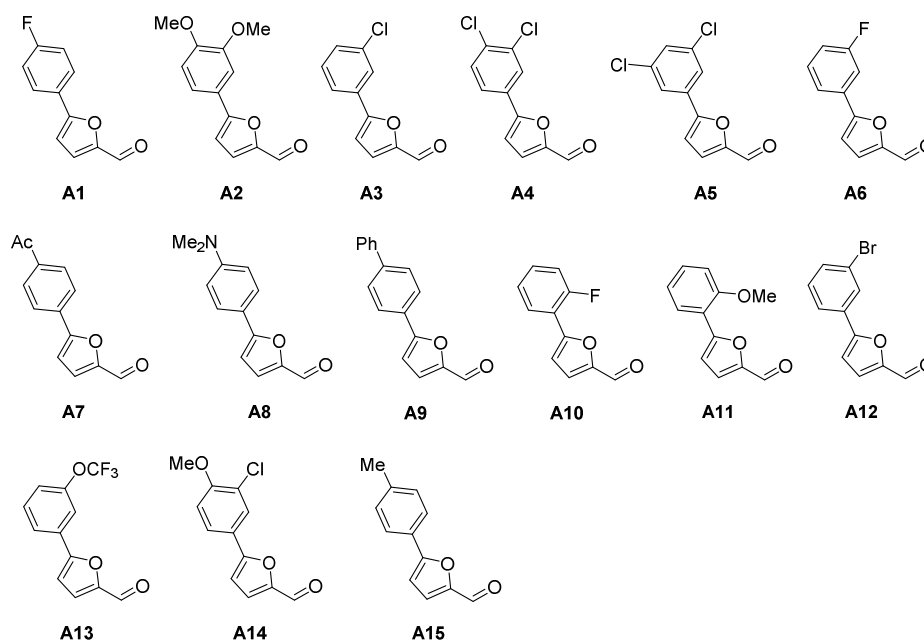
Scheme 23. Aldehydes used for the synthesis of the **cp028** analogues

All aldehydes (A_X) used are all reported in the literature and most of them are commercially available. However, in my case all A_X aldehydes (Scheme 23) were synthesized following the procedure for compound **160**, and checked by ^{1}H NMR spectra (^{1}H NMR spectra are given for those analogues were a ^{1}H NMR spectrum could not be found in the literature, $A_{2,3,6,9}$).Compound A_8.[128]Compound A_7.[129]Compound A_{10}.[130]Compound A_4.[131]CompoundA_5.[132]CompoundA_{11}.[133]

Compound A_2 (95%), **^{1}H NMR (CDCl$_3$, 400 MHz):** δ 3.85 (s, 6H), 6.51 (t, *J*=2.3 Hz, 1H), 6.82 (d, *J*=3.7 Hz, 1H), 6.96 (d, *J*=2.3 Hz, 2H), 7.31 (d, *J*=3.7 Hz, 1H), 9.65 (s, 1H). Compound A_3(87%), **^{1}H NMR (CDCl$_3$, 400 MHz):** δ 6.86 (d, *J*=3.7 Hz, 1H), 7.32 (d, *J*=3.7 Hz, 1H), 7.36-7.41 (m, 2H), 7.69-7.71 (m, 1H), 9.68 (s, 1H). Compound A_6 (80%), **^{1}H NMR (CDCl$_3$, 400 MHz):** δ6.86 (d, *J*=3.7 Hz, 1H), 7.09 (t, *J*=8.3, 2.5 Hz, 1H), 7.32 (d, *J*=3.7 Hz, 1H), 7.42 (td, *J*=8.0, 5.8 Hz, 1H), 7.52 (dt, *J*=9.6, 2.3 Hz, 1H), 7.60 (ddd, *J*=7.8, 1.5, 0.9 Hz, 1H), 9.68 (s, 1H).Compound A_9(74%), **^{1}H NMR (CDCl$_3$, 400 MHz):** δ 6.88 (d, *J*=3.7 Hz, 1H), 7.34 (d, *J*=3.7 Hz, 1H), 7.38 (t, *J*=7.3 Hz, 1H), 7.47 (t, *J*=7.5 Hz, 2H), 7.63 (d, *J*=7.4 Hz, 1H), 7.69 (d, *J*=8.7 Hz, 2H), 7.90 (d, *J*=8.7 Hz, 2H). Compound A_{12} (46%), **^{1}H NMR (CDCl$_3$, 400 MHz):** δ6.86 (d, *J*=3.7 Hz, 1H), 7.30-7.34 (m, 2H), 7.52 (ddd, *J*=8.0, 1.9, 1.0 Hz, 1H), 7.97 (t, *J*=2.0

Hz, 1H), 9.68 (s, 1H).Compound **A₁₃** (76%), **¹H NMR (CDCl₃, 400 MHz):** δ6.89 (d, *J*=3.7 Hz, 1H), 7.24-7.25 (m, 1H), 7.33 (d, *J*=3.7 Hz, 1H), 7.48 (t, *J*=8.0 Hz, 1H), 7.66 (s, 1H), 7.75 (d, *J*=7.8 Hz, 1H), 9.69 (s, 1H). Compound **A₁₄** (44%), **¹H NMR (CDCl₃, 400 MHz):** δ3.96 (s, 3H), 6.74 (d, *J*=3.8 Hz, 3H), 6.74 (d, *J*=3.8 Hz, 1H), 6.99 (d, *J*=8.8 Hz, 1H), 7.31 (d, *J*=3.8 Hz, 1H), 7.71 (dd, *J*=8.6, 2.2 Hz, 1H), 9.63 (s, 1H).

(E/Z)-1-(2-ethylphenyl)-5-((5-(4-fluorophenyl)furan-2-yl)methylene)pyrimidine-2,4,6(1H,3H,5H)-trione (1:1 mixture of E/Z isomers) (cp028):
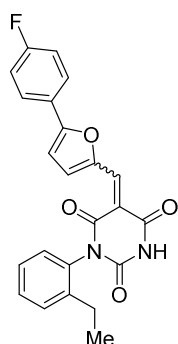
To a solution of barbituric acid **157** (0.069 g, 0.263 mmol) in EtOH (3.3 mL, 0.08 M), aldehyde **160** (0.050 g, 0.263 mmol) was added, a very strong orange color appeared. The mixture was heated at refluxing conditions for 2 hours and the solvents were removed *in vacuo*. The crude product was purified by flash chromatography (1% MeOH/DCM) to obtain product **cp028** as an orange solid (83.0 mg, 78%). The product was isolated as a 1:1 mixture of the isomers E and Z. **¹H NMR (CDCl₃, 400 MHz):** δ 1.13 (t, *J*=7.6 Hz, 3H), 2.44 (q, *J*=7.6 Hz, 2H), 6.95 (dd, *J*=4.0, 0.6 Hz, 1H), 7.08–7.14 (m, 3H), 7.25-7.30 (m, 1H), 7.33-7.39 (m, 2H), 7.79 (dd, *J*=9.0, 5.2 Hz, 2H), 7.90 (s, 1H), 8.43 (s, 1H), 8.74 (d, *J*=3.9 Hz, 1H).**¹³C NMR (CDCl₃, 100 MHz):** δ 14.0, 24.1, 109.4, 111.4, 116.6, 116.7, 125.0, 125.1, 127.2, 128.0, 128.8, 129.4, 129.9, 132.7, 133.1, 140.9, 141.6, 149.7, 150.9, 161.0, 161.9, 163.3, 163.4, 165.0. **¹⁹F NMR (CDCl₃,100 MHz):** δ -108.1 ppm. **HRMS:** calc. for [M+H]⁺ $C_{23}H_{18}N_2O_4F$: 405.12451, found 405.12437

(+/-)-1-(2-ethylphenyl)-5-((5-(4-fluorophenyl)furan-2-yl)methyl)pyrimidine-2,4,6(1H,3H,5H)-trione (161):
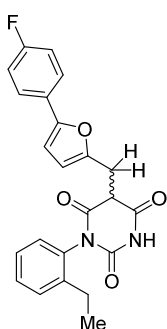
To a solution of **cp028** (0.050 g, 0.124 mmol) in EtOH (1.2 mL, 0.1 M) at 0°, sodium borohydride (0.014 g, 0.371 mmol) was added. The mixture was allowed to reach room temperature and stir for one hour before removing the solvents *in vacuo*. To the crude product HCl 1M was added and a white solid precipitated, the solid was filtered and purified by preparative HPLC to yield compound **161** (32.8 mg, 65%) as a white solid. **¹H NMR (CDCl₃, 400 MHz):**δ 0.75 (t, *J*=7.6 Hz, 1.5H), 1.16 (t,*J*=7.6 Hz, 1.5H), 1.87 (q, *J*=8.0 Hz, 1H), 2.43 (q, *J*=7.6 Hz, 1H), 3.61-3.78 (m, 2H), 3.88-3.91 (m, 1H), 6.21 (d, *J*=3.1 Hz, 0.5), 6.25 (d, *J*=3.3 Hz, 0.5H), 6.48 (d, *J*=3.3 Hz, 0.5H), 6.52 (d, *J*=7.5 Hz, 0.5H) 6.64 (d, *J*=7.5 Hz, 0.5H), 6.98-7.11 (m, 3H), 7.24-7.27 (m, 1H), 7.33-7.39 (m, 1.5H), 7.48-7.57 (m, 2H), 8.85 (s, 0.5H), 9.01 (s, 0.5H). **HRMS:** calc. for [M+H]⁺ $C_{23}H_{20}N_2O_4F$: 407.14016, found 407.14009

(E/Z)-5-((5-(4-acetylphenyl)furan-2-yl)methylene)-1-(2-ethylphenyl)pyrimidine-2,4,6(1H,3H,5H)-trione (1:1 mixture of E/Z isomers) (168):
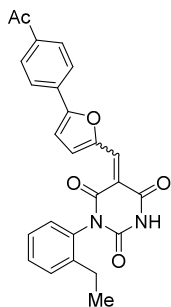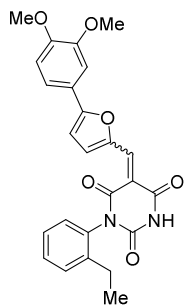
Compound **168** (77%, orange solid) was synthesized as described for **cp028**. **^{1}H NMR (CDCl$_3$,400 MHz):** δ 1.20 (t, *J*=7.6 Hz, 3H), 2.48-2.54 (m, 2H), 2.65 (s, 3H), 7.09 (d, *J*=4.1 Hz, 0.5H), 7.16-7.19 (m, 1.5H), 7.34-7.38 (m, 1H), 7.41-7.48 (m, 2H), 7.94 (d, *J*=13.0, 8.4 Hz, 2H), 8.06 (dd, *J*=8.5, 1.9 Hz, 2H), 8.18 (s, 0.5H), 8.25 (s, 0.5H), 8.53 (s, 0.5H), 8.59 (s, 0.5H), 8.76 (d, *J*=4.1 Hz, 0.5H), 8.81 (d, *J*=4.1 Hz, 0.5H). **^{13}C NMR (CDCl$_3$, 100 MHz):** δ 13.8, 13.9, 23.9, 26.7, 110.4, 110.6, 112.9, 125.7, 127.1,127.3, 128.7, 128.8, 129.2, 129.2, 129.3, 129.8, 129.9, 131.6, 132.1, 132.3, 132.4, 132.5, 132.9, 137.9, 137.9, 140.5, 140.9, 141.5, 141.6, 149.3, 149.3, 149.4, 151.3, 151.4, 160.3, 160.7, 160.8, 161.5, 161.8, 163.0, 197.1, 197.1 **HRMS:** calc. for [M+H]$^+$ C$_{25}$H$_{21}$N$_2$O$_5$: 429.14450, found 429.14433.

(E/Z)-5-((5-(4-(dimethylamino)phenyl)furan-2-yl)methylene)-1-(2-ethylphenyl)pyrimidine-2,4,6(1H,3H,5H)-trione (1.5:1 mixture of E/Z isomers) (167):
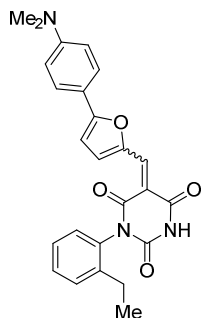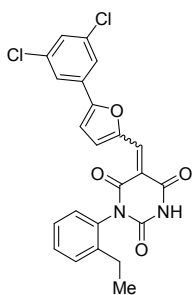
Compound **167** (83%, dark purple solid) was synthesized as described for **cp028**. **^{1}H NMR (CDCl$_3$,400 MHz):** δ 1.20 (t, *J*=7.6 Hz, 3H), 2.52 (m, 2H), 3.09 (s, 6H), 6.79 (dd, *J*=9.0, 3.1 Hz, 2H), 6.84 (d, *J*=4.3 Hz, 0.6H), 6.92 (d, *J*=4.3 Hz, 0.4H), 7.17 (d, *J*=8.0 Hz, 0.4H), 7.19 (d, *J*=7.9 Hz, 0.6H), 7.33-7.46 (m, 3H), 7.75 (t, *J*=8.3 Hz, 2H), 7.88 (s, 0.4H), 7.95 (s, 0.6H), 8.44 (s, 0.4), 8.49 (s, 0.6H), 8.85 (d, *J*=3.7 Hz, 0.6H), 8.90 (bs, 0.4H). **HRMS:** calc. for [M+H]$^+$ C$_{25}$H$_{23}$N$_3$O$_4$: 430.17613, found 430.17545.

(E/Z)-5-((5-(3,4-dimethoxyphenyl)furan-2-yl)methylene)-1-(2-ethylphenyl)pyrimidine-2,4,6(1H,3H,5H)-trione (1:1 mixture of E/Z isomers) (172):

Compound **172** (64%, dark red solid) was synthesized as described for **cp028**. **^{1}H NMR (CDCl$_3$, 400 MHz):** δ 1.20 (t, *J*=7.6 Hz, 3H), 2.48-2.55 (m, 2H), 3.87 (s, 6H), 6.55 (t, *J*=2.2 Hz, 1H), 6.96 (d, *J*=4.1 Hz, 0.5H), 6.99 (dd, *J*=3.7, 2.3 Hz, 2H), 7.04 (d, *J*=4.0 Hz, 0.5H), 7.18 (t, *J*=8.6 Hz, 1H), 7.35 (ddd, *J*=14.7, 2.3 Hz, 1H), 7.40-7.48 (m, 2H), 8.30 (s, 0.5H), 8.39 (s, 0.5H), 8.52 (s, 0.5H), 8.58 (s, 0.5H), 8.76 (d, *J*=3.9 Hz, 0.5H), 8.83 (d, *J*=4.0 Hz, 0.5H). **HRMS:** calc. for [M+H]$^+$ C$_{25}$H$_{23}$N$_2$O$_6$: 447.15506, found 447.15477.

(E/Z)-5-((5-(3,5-dichlorophenyl)furan-2-yl)methylene)-1-(2-ethylphenyl)pyrimidine-2,4,6(1H,3H,5H)-trione (1:1 mixture of E/Z isomers) (170):
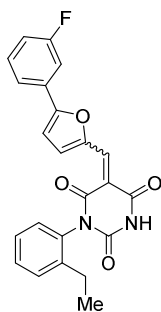
Compound **170** (78%, orange solid) was synthesized as described for **cp028**. **¹H NMR (CDCl₃, 400 MHz):** δ 1.20 (t, *J*=7.6 Hz, 3H), 2.48-2.54 (m, 2H), 7.00 (d, *J*=4.1 Hz, 0.5H), 7.07 (d, *J*=4.0 Hz, 0.5H), 7.17, (t, *J*=7.16 Hz, 1H), 7.35 (dd, *J*=14.3, 6.7 Hz, 1H), 7.40-7.38 (m, 3H), 7.70 (dt, *J*=4.1, 2.1 Hz, 2H), 8.23 (s, 0.5H), 8.30 (s, 0.5H), 8.48 (s, 0.5H), 8.55 (s, 0.5H), 8.72 (d, *J*=4.0 Hz, 0.5H), 8.78 (d, *J*=4.1 Hz, 0.5H). **HRMS:** calc. for [M+H]⁺ $C_{23}H_{17}Cl_2N_2O_4$: 455.05599, found 455.0599. Calc. for [M+H]⁺ $C_{23}H_{17}Cl^{37}ClN_2O_4$: 457.05284, found 457.05304.

(E/Z)-1-(2-ethylphenyl)-5-((5-(3-fluorophenyl)furan-2-yl)methylene)pyrimidine-2,4,6(1H,3H,5H)-trione (1.2:1 mixture of E/Z isomers) (164):

Compound **164** (80%, orange solid) was synthesized as described for **cp028**. **¹H NMR (CDCl₃, 400 MHz):** δ1.20 (t, *J*=7.60 Hz, 3H), 2.48-2.55 (m, 2H), 6.99 (dd, *J*=4.1, 0.7 Hz, 0.55H), 7.07 (dd, *J*=4.0, 0.7 Hz, 0.45H), 7.17 (t, *J*=7.9 Hz, 1H), 7.32-7.48 (m, 5H), 7.48-7.70 (m, 1H), 7.81-7.83 (m, 1H), 8.50 (s, 0.45H), 8.57 (s, 0.55H), 8.61 (bs, 0.45H), 8.63 (bs, 0.55H), 8.75 (d, *J*=4.1 Hz, 0.55H), 8.82 (d, *J*=4.0 Hz, 0.45H). **HRMS:** calc. for [M+H]⁺ $C_{23}H_{18}N_2O_4F$: 405.12451, found 405.12435

(E/Z)-5-((5-(3-chlorophenyl)furan-2-yl)methylene)-1-(2-ethylphenyl)pyrimidine-2,4,6(1H,3H,5H)-trione (1:1 mixture of E/Z isomers) (165):
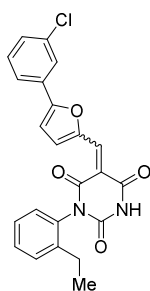
Compound **165** (82%, orange solid) was synthesized as described for **cp028**. **¹H NMR (CDCl₃, 400 MHz):** δ 1.20 (td, *J*=7.6, 0.5 Hz, 3H), 2.48-2.55 (m, 2H), 6.99 (dd, *J*=4.1, 0.8 Hz, 0.5H), 7.07 (dd, *J*=4.1, 0.8 Hz, 0.5H), 7.12-7.20 (m, 2H), 7.36 (ddd, *J*=14.1, 7.6, 2.4 Hz, 1H), 7.40-7.49 (m, 3H), 7.51-7.56 (m, 1H), 7.63 (t, *J*=8.2 Hz, 1H), 8.01 (s, 0.5H), 8.08 (s, 0.5H), 8.50 (s, 0.5H), 8.56 (s, 0.5H), 8.75 (d, *J*=4.1 Hz, 0.5H), 8.81 (d, *J*=4.1 Hz, 0.5H). **HRMS:** calc. for [M+H]⁺ $C_{23}H_{17}ClN_2O_4$: 421.09496, found 421.09481. Calc. for [M+H]⁺ $C_{23}H_{18}^{37}ClN_2O_4$: 423.09201, found 423.09191.

(E/Z)-5-(4-chlorobenzylidene)-1-(2-ethylphenyl)pyrimidine-2,4,6(1H,3H,5H)-trione(1:1 mixture of E/Z isomers)(1:1 mixture of E/Z isomers)(173):
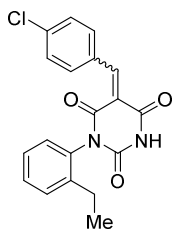
To a solution of barbituric acid **157** (0.050g, 0.213mmol) in EtOH (2.7mL, 0.08M), 4-fluorobenzaldehye (0.030g, 0.213mmol) was added. The mixture was heated at refluxing conditions for 2 hours and the solvents are evaporated. The crude product was purified by flash chromatography (1% MeOH/DCM) to obtain product **173** as awhite solid (66.5mg, 88%). The product is isolated as a 1:1 mixture of the isomers E and Z. **¹H NMR (CDCl₃, 400 MHz):** δ 1.20 (td, *J*=7.6, 4.4 Hz, 3H), 2.50 (qd, *J*=7.6, 2.5 Hz, 2H), 7.15 (d, *J*=7.9 Hz, 1H), 7.35 (t, *J*=7.4 Hz, 1H), 7.39-7.49 (m, 4H), 7.97 (s, 0.5H), 8.09 (s, 0.5H), 8.15 (t, *J*=8.2 Hz, 2H), 8.56 (s, 0.5H), 8.60 (s, 0.5H). **HRMS:** calc. for [M+H]⁺ $C_{19}H_{16}ClN_2O_3$: 355.08440, found 355.06739; Calc. for [M+H]⁺ $C_{19}H_{16}{}^{37}ClN_2O_3$: 357.08145, found 357.07858.

(E/Z)-5-(4-bromobenzylidene)-1-(2-ethylphenyl)pyrimidine-2,4,6(1H,3H,5H)-trione (1.7:1 mixture of isomers E/Z) (174):
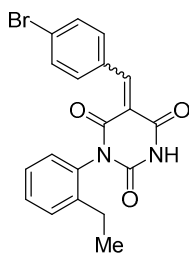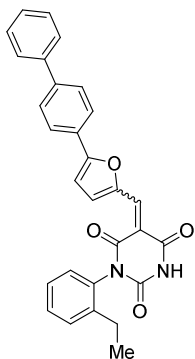
Compound **174** (67%, white solid) was synthesized as described for **173**. **¹H NMR (CDCl₃, 400 MHz):** δ 1.13 (td, *J*=7.6, 4.8 Hz, 3H), 2.43 (qd, *J*=7.6, 3.2 Hz, 2H), 7.08 (d, *J*=8.0 Hz, 1H), 7.25-7.30 (m, 1H), 7.34-7.40 (m, 1H), 7.50 (d, *J*=8.6 Hz, 0.63H) 7.57 (d, *J*=8.6 Hz, 0.37H), 7.90 (bs, 0.63H), 7.98 (t, *J*=8.5 Hz, 2H), 8.02 (bs, 0.37H), 8.47(s, 0.63H), 8.51 (s, 0.37H). **HRMS:** calc. for [M+H]⁺ $C_{19}H_{16}BrN_2O_3$: 399.03388, found 399.03388; for $C_{19}H_{16}{}^{81}BrN_2O_3$: 401.03183, found 401.03182

(E/Z)-5-((5-(3,4-dichlorophenyl)furan-2-yl)methylene)-1-(2-ethylphenyl)pyrimidine-2,4,6(1H,3H,5H)-trione (1.4:1 mixture of isomers E/Z) (171):
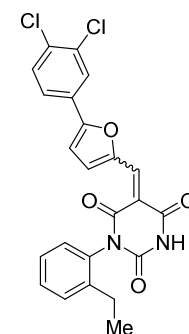
Compound **171** (85%, yellow solid) was synthesized as described for **cp028**. **¹H NMR (CDCl₃, 400 MHz):** δ 1.20 (t, *J*=7.6 Hz, 3H), 2.48-2.50 (m, 2H), 6.97 (d, *J*=4.1 Hz, 0.4H), 7.04 (d, *J*=4.0 Hz, 0.6H), 7.17 (t, *J*=7.4 Hz, 1H), 7.35 (ddd, *J*=14.5, 6.9, 2.2 Hz, 1H), 7.40-7.48 (m, 2H), 7.52 (s, 0.4H), 7.54 (s, 0.6H), 7.64 (ddd,*J*=8.0, 5.8, 2.0 Hz, 1H), 7.89 (d, *J*=4.1 Hz, 1H), 8.47 (s, 0.6H), 8.54 (s, 0.4H), 8.72 (d, *J*=4.1 Hz, 0.4H), 8.79 (d, *J*=4.0Hz, 0.6H), 9.07 (s, 0.6H), 9.13 (s, 0.4H).**HRMS:** calc. for [M+H]⁺ $C_{23}H_{17}Cl_2N_2O_4$: 455.05599, found 455.0599; Calc. for [M+H]⁺ $C_{23}H_{16}Cl^{37}ClN_2O_4$: 457.05284, found 457.05304.

(E/Z)-5-((5-([1,1'-biphenyl]-4-yl)furan-2-yl)methylene)-1-(2-ethylphenyl)pyrimidine-2,4,6(1H,3H,5H)-trione (1:1 mixture of isomers E/Z) (169):
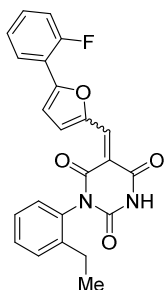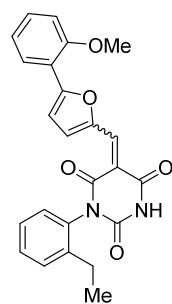
Compound **169** (85%, orange solid) was synthesized as described for **cp028**. **^{1}H NMR (CDCl$_3$, 400 MHz):** δ 1.21 (td, *J*=7.6, 1.2 Hz, 3H), 2.49-2.56 (m, 2H), 7.03 (dd, *J*=4.1, 0.8 Hz, 0.5H), 7.12 (dd, *J*=4.1, 0.8 Hz, 0.5H), 7.16-7.21 (m, 1H), 7.33-7.50 (m, 6H), 7.65 (d, *J*=7.1 Hz, 2H), 7.73 (d, *J*=7.9 Hz, 2H), 7.91-7.95 (m, 2H), 8.03 (bs, 0.5H), 8.09 (bs, 0.5H), 8.53 (s, 0.5H), 8.59 (s, 0.5H), 8.81 (d, *J*=4.1 Hz, 0.5H), 8.86 (d, *J*=3.8 Hz, 0.5H). **HRMS:** calc. for [M+H]$^+$ C$_{29}$H$_{23}$N$_2$O$_4$: 463.16523, found 463.16491

(E/Z)-1-(2-ethylphenyl)-5-((5-(2-fluorophenyl)furan-2-yl)methylene)pyrimidine-2,4,6(1H,3H,5H)-trione (1.5:1 mixture of isomers E/Z) (163):

Compound **163** (76%, yellow solid) was synthesized as described for **cp028**. **^{1}H NMR (CDCl$_3$, 400 MHz):** δ 1.21 (t, *J*=7.6, 0.5 Hz, 3H), 2.48-2.56 (m, 2H), 7.13-7.48 (m, 8H), 8.00 (t, *J*=7.5 Hz, 1H), 8.53-8.60 (m, 2H), 8.77 (d, *J*=4.1 Hz, 0.6H), 8.83 (m, *J*=4.1 Hz, 0.4H). **HRMS:** calc. for [M+H]$^+$ C$_{23}$H$_{18}$N$_2$O$_4$F: 405.12451, found 405.12440

(E/Z)-1-(2-ethylphenyl)-5-((5-(2-methoxyphenyl)furan-2-yl)methylene)pyrimidine-2,4,6(1H,3H,5H)-trione (~1.7:1 mixture of isomers E/Z) (162):

Compound **162** (82%, yellow solid) was synthesized as described for **cp028**. **^{1}H NMR (CDCl$_3$, 400 MHz):** δ 1.20 (td, *J*=7.6, 1.3 Hz, 3H), 2.49-2.56 (m, 2H), 3.98 (s, 1.9H), 4.00 (s, 1.1H), 7.02 (dd, *J*=8.3, 4.2 Hz, 1H), 7.08-7.12 (m, 1H), 7.18 (dd, *J*=12.6, 7.5 Hz, 1H), 7.26-7.28 (m, 1H), 7.32-7.38 (m, 1H), 7.46-7.48 (m, 3H), 8.03 (dt, *J*=7.8, 1.4 Hz, 1H), 8.14 (bs, 0.4H), 8.17 (bs, 0.6H), 8.51 (bs, 0.4H), 8.58 (bs, 0.6H), 8.79 (d, *J*=4.1 Hz, 0.6H), 8.84 (d, *J*=3.4 Hz, 0.4H). **HRMS:** calc. for [M+H]$^+$ C$_{24}$H$_{21}$N$_2$O$_5$: 417.14450, found 417.14431

(E/Z)-1-(2-ethylphenyl)-5-((5-(p-tolyl)furan-2-yl)methylene)pyrimidine-2,4,6(1H,3H,5H)-trione (1:1 mixture of isomers E/Z) (166):

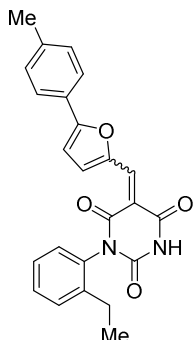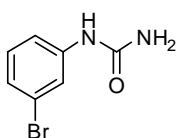Compound **166** (78%, orange solid) was synthesized as described for **cp028**. **¹H NMR (CDCl₃, 400 MHz):** δ 1.20 (t, *J*=7.6 Hz, 3H), 2.40 (s, 3H), 2.52 (qd, *J*=7.5, 3.5 Hz, 2H), 6.93 (d, *J*=4.1 Hz, 0.5H), 7.01 (d, *J*=4.1 Hz, 0.5H), 7.17 (t, *J*=7.8 Hz, 1H), 7.27 (d, *J*=7.7 Hz, 2H), 7.30-7.36 (m, 1H), 7.39-7.46 (m, 2H), 7.73 (dd, *J*=8.2, 2.8 Hz, 2H), 8.49 (s, 0.5H), 8.57 (s, 0.5H), 8.78 (d, *J*=4.1 Hz, 0.5H), 8.87 (d, *J*=4.0 Hz, 0.5H), 9.09 (d, *J*=4.8 Hz, 1H). **HRMS:** calc. for [M+H]⁺ C₂₄H₂₁N₂O₄: 401.14958, found 401.14927

1-(3-bromophenyl)urea:

1-(3-Bromophenyl)urea was synthesised following reported procedure for urea **156**. **¹H NMR (DMSO, 400 MHz):** δ 3.37 (d, J=18.4 Hz, 2H), 4.22 (dd, J=13.9, 6.9 Hz, 1H), 7.30 (d, J=7.6 Hz, 1H), 7.43 (t, J=6.9 Hz, 1H), 7.53 (s, 1H), 7.64 (t, J=7.7 Hz, 1H).

1-(3-bromophenyl)pyrimidine-2,4,6(1H,3H,5H)-trione:
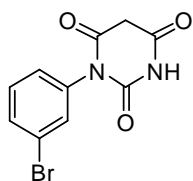
1-(3-bromophenyl)pyrimidine-2,4,6(1H,3H,5H)-trione:(0.266 g, 40 %) was synthesised as described for compound **157**. **¹H NMR (MeOD, 400 MHz):** δ 3.37 (d, *J*=18.4 Hz, 2H), 4.22 (dd, *J*=13.9, 6.9 Hz, 1H), 7.30 (d, *J*=7.6 Hz, 1H), 7.43 (t, *J*=6.9 Hz, 1H), 7.53 (s, 1H), 7.64 (t, *J*=7.7 Hz, 1H).

(E/Z)-1-(3-bromophenyl)-5-((5-(3-chlorophenyl)furan-2-yl)methylene)pyrimidine-2,4,6(1H,3H,5H)-trione (194) (1:1 mixture of E/Z isomers):
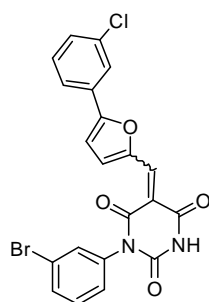
Compound **194** was synthesised as described for compound **cp028**, using 1-(3-bromophenyl)pyrimidine-2,4,6(1H,3H,5H)-trione and aldehyde **A₃** as starting materials. **¹H NMR (CDCl₃, 400 MHz):** δ 7.02 (dd, *J*=4.1, 0.6 Hz, 0.5H), 7.08 (dd, *J*=4.1, 0.6 Hz, 0.5H), 7.38-7.43 (m, 3H), 7.47 (dt, *J*=7.8, 1.8 Hz, 1H), 7.60-7.64 (m, 1H), 7.62 (t, *J*=17.7 Hz, 1H), 7.79-7.77 (m, 1H), 7.84 (s,), 8.07 (s, 0.5H), 8.14 (s, 0.5H), 8.44 (s, 0.5H), 8.56 (s, 0.5H), 8.74 (d, *J*=4.0 Hz, 0.5H), 8.81 (d, *J*=4.1 Hz, 0.5H). **HRMS:** calc. for [M+H]⁺ C₂₁H₁₃N₂O₄BrCl: 470.97417, found 470.97396

(E/Z)-1-(3-bromophenyl)-5-((5-(3-bromophenyl)furan-2-yl)methylene)pyrimidine-2,4,6(1H,3H,5H)-trione (193) (1:1 mixture of E/Z isomers):
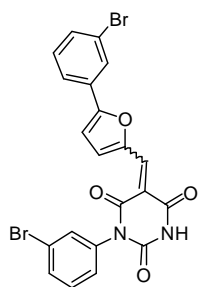
Compound **193** was synthesised as described for compound **cp028** using 1-(3-bromophenyl)pyrimidine-2,4,6(1H,3H,5H)-trione and aldehyde **A$_{12}$** as starting materials. **^{1}H NMR (CDCl$_3$, 400 MHz):** δ 6.92 (d, *J*=3.9 Hz, 0.5H), 6.98 (d, *J*=4.8 Hz, 0.5H), 7.03 (d, *J*=8.6 Hz, 1H), 7.37-7.52 (m, 3H), 7.61 (t, *J*=7.9 Hz, 1H), 7.75 (t, *J*=8.6 Hz, 1H), 7.86-7.88 (m, 1.5H), 7.95 (bs, 0.5H), 8.46 (bs, 0.5H), 8.53 (bs, 0.5H), 8.76 (d, *J*=4.2 Hz, 0.5H), 8.83 (d, *J*=3.6 Hz, 0.5H). **HRMS:** calc. for [M+H]$^+$ C$_{21}$H$_{13}$N$_2$O$_4$Br$_2$: 514.92366, found 514.92348
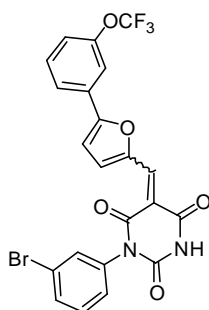
(E/Z)-1-(3-bromophenyl)-5-((5-(3-(trifluoromethoxy)phenyl)furan-2-yl)methylene)pyrimidine-2,4,6(1H,3H,5H)-trione (196) (1:1 mixture of E/Z isomers):

Compound **196** was synthesised as described for compound **cp028** using 1-(3-bromophenyl)pyrimidine-2,4,6(1H,3H,5H)-trione and aldehyde **A$_{13}$** as starting materials. **^{1}H NMR (CDCl$_3$, 400 MHz):** δ 7.05 (d, *J*=4.1 Hz, 0.5H), 7.10 (d, *J*=4.0 Hz, 0.5H), 7.23-7.25 (m, 1H), 7.30 (d, *J*=8.2 Hz, 1H), 7.41 (q, *J*=7.8 Hz, 1H), 7.46 (t, *J*=1.9 Hz, 0.5H), 7.48 (t, *J*=1.9 Hz, 0.5H), 7.53 (td, *J*=8.1, 1.6 Hz, 1H), 7.62 (t, *J*=7.7 Hz, 1H), 7.69 (bs, 1H), 7.78 (t, *J*=8.3Hz, 1H), 7.99 (bs, 0.5H), 8.06 (bs, 0.5H), 8.50 (bs, 0.5H), 8.57 (bs, 0.5H), 8.74 (d, *J*=4.1 Hz, 0.5H), 8.81 (d, *J*=4.1 Hz, 0.5H). **HRMS:** calc. for [M+H]$^+$ C$_{21}$H$_{13}$N$_2$O$_5$BrF$_3$: 520.99545, found 520.99491

(E/Z)-1-(3-bromophenyl)-5-((5-(3-chloro-4-methoxyphenyl)furan-2-yl)methylene)pyrimidine-2,4,6(1H,3H,5H)-trione (195) (1.2:1 mixture of E/Z isomers):
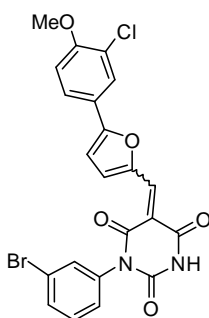
Compound **195** was synthesised as described for compound **cp028** using 1-(3-bromophenyl)pyrimidine-2,4,6(1H,3H,5H)-trione and aldehyde **A$_{14}$** as starting materials. **^{1}H NMR (CDCl$_3$, 400 MHz):** δ 2.17 (s, 3H), 7.02 (dd, *J*=4.1, 0.6 Hz, 0.55H), 7.08 (dd, *J*=4.1, 0.6 Hz, 0.45H), 7.22-7.25 (m, 1H), 7.36 (td, *J*=7.9, 1.4 Hz, 1H), 7.36 (td, *J*=7.9, 1.4 Hz, 1H), 7.40 (dd, *J*=15.3, 7.8 Hz, 1H), 7.46 (t, *J*=1.9 Hz, 0.45H), 7.48 (t, *J*=1.8 Hz, 0.55H), 7.56-7.59 (m, 1H), 7.78 (t, *J*=8.4 Hz, 1H), 7.99 (dd, *J*=3.7, 1.8 Hz, 1H), 8.06 (bs, 0.45H), 8.13 (bs, 0.55H), 8.49 (s, 0.45H), 8.56 (s, 0.55H), 8.74 (d, *J*=4.1 Hz, 0.55H), 8.81 (d, *J*=4.0 Hz, 0.45 H). **HRMS:** calc. for [M+H]$^+$ C$_{22}$H$_{15}$N$_2$O$_5$BrCl: 500.98474, found 500.98451

4-((tert-butyldimethylsilyl)oxy)aniline (198):
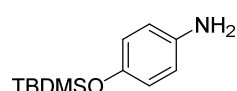
Compound **198** (3.54 g, 87%) was synthesised as described for urea **156.** **^{1}H NMR (DMSO-d$_6$, 400 MHz):** δ 0.15 (s, 6H), 0.94 (s, 9H), 5.70 (s, 2H), 6.70 (d, *J*=8.8 Hz, 2H), 7.23 (d, *J*=8.9 Hz, 2H), 8.30 (s, 1H). **HRMS:** calc. for [M+H]$^+$ C$_{13}$H$_{23}$N$_2$O$_2$Si: 267.15233, found 267.15342. Calc. for [M+Na]$^+$ C$_{13}$H$_{22}$N$_2$O$_2$SiNa: 289.13428 found 289.13524

1-(4-((tert-butyldimethylsilyl)oxy)phenyl)urea:
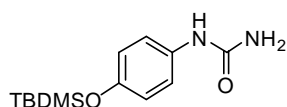
1-(4-((tert-butyldimethylsilyl)oxy)phenyl)urea (0.61 g, 51%) was synthesised as described for urea **156**. **^{1}H NMR (DMSO-d$_6$, 400 MHz):** δ 0.15 (s, 6H), 0.94 (s, 9H), 5.70 (s, 2H), 6.70 (d, *J*=8.8 Hz, 2H), 7.23 (d, *J*=8.9 Hz, 2H), 8.30 (s, 1H). **HRMS:** calc. for [M+H]$^+$ C$_{13}$H$_{23}$N$_2$O$_2$Si: 267.15233, found 267.15342. Calc. for [M+Na]$^+$ C$_{13}$H$_{22}$N$_2$O$_2$SiNa: 289.13428 found 289.13524

1-(4-((tert-butyldimethylsilyl)oxy)phenyl)pyrimidine-2,4,6(1H,3H,5H)-trione:
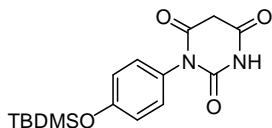
1-(4-((tert-butyldimethylsilyl)oxy)phenyl)pyrimidine-2,4,6(1H,3H,5H)-trione (0.167g, 44%) was synthesised as described for compound **157**. **^{1}H NMR (CDCl$_3$, 400 MHz):** δ 0.22 (s, 6H), 0.99 (s, 9H), 3.74 (s, 2H), 6.89 (d, *J*=8.8 Hz, 2H), 7.01 (d, *J*=8.8 Hz, 2H), 9.01 (s, 1H). **HRMS:** calc. for [M+H]$^+$ C$_{16}$H$_{23}$N$_2$O$_4$Si: 334.13488, found 334.13503.

(E/Z)-1-(4-((tert-butyldimethylsilyl)oxy)phenyl)-5-((5-(4-fluorophenyl)furan-2-yl)methylene)pyrimidine-2,4,6(1H,3H,5H)-trione (199):
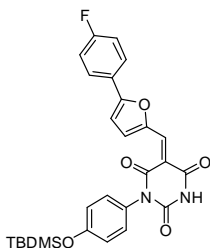
Compound **199** (55 mg, 66%) was synthesised as described for compound **cp028** . This compound was directly taken into the next step. **HRMS:** calc. for [M+H]$^+$ C$_{27}$H$_{28}$N$_2$O$_5$Si: 507.17460, found 507.17464

(E/Z)-1-(2-ethylphenyl)-5-((5-(4-fluorophenyl)furan-2-yl)methylene)-3-methylpyrimidine-2,4,6(1H,3H,5H)-trione (201):
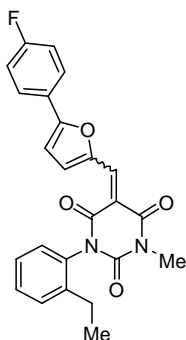
To a solution of compound **cp028** (0.050 g, 0.124 mmol) in DMF (0.5 mL, 0.237 M), sodium hydride (60 % in mineral oil) (5.36 mg, 0.134 mmol) was added and the mixture was allowed to stir for 5 min before adding methyl iodide (8.5 µL, 0.136 mmol). The mixture was allowed to stir further for 2 h. at 85º. The mixture was partitioned between H_2O/brine (1:1) and DCM, and the organic phase was washed with the same mixture (3x). The crude product was purified by chromatography (10% ethyl acetate/DCM) to afford compound **201** (35.6 mg, 69 %) as a bright yellow solid. **^{1}H NMR (CDCl$_3$, 400 MHz):** δ 1.08 (t, *J*=7.6 Hz, 3H), 2.44 (q, *J*=7.6 Hz, 2H), 3.29 (s, 3H), 7.24-7.41 (m, 6.5H), 7.48 (d, *J*=4.0 Hz, 0.5H), 8.00-8.06 (m, 2H), 8.20 (s, 0.5H), 8.30 (s, 0.5H), 8.48 (d, *J*=4.0 Hz, 0.5H), 8.67 (d, *J*=4.0 Hz, 0.5H). **HRMS:** calc. for $[M+H]^+$ $C_{24}H_{20}N_2O_4F$: 419.14016, found 419.14000

Tert-butyl (1-bromo-2-oxo-7,10,13-trioxa-3-azahexadecan-16-yl)carbamate (200):
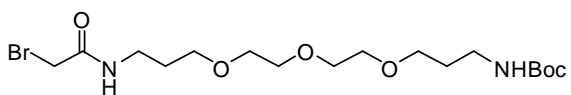
Compound **200** (0.29 g) was synthesised according to the literature procedure for the chloro analogue.[92] **^{1}H NMR (CDCl$_3$, 400 MHz):** δ 1.44 (s, 9H), 1.72-1.79 (m, 2H), 1.82 (dt, *J*=11.7, 5.9 Hz, 2H), 3.22 (dd, *J*=12.3, 6.1, 2H), 3.42 (dd, *J*=12.1, 5.8 Hz, 2H), 3.54 (t, *J*=6.0 Hz, 2H), 3.58-3.69 (m, 10H), 3.85 (s, 2H), 4.93 (bs, 1H), 7.18 (bs, 1H).

tert-butyl (E/Z)-(1-(3-(2-ethylphenyl)-5-((5-(4-fluorophenyl)furan-2-yl)methylene)-2,4,6-trioxotetrahydropyrimidin-1(2 h.)-yl)-2-oxo-7,10,13-trioxa-3-azahexadecan-16-yl)carbamate (1.5:1 mixture of E/Z isomers) (202):
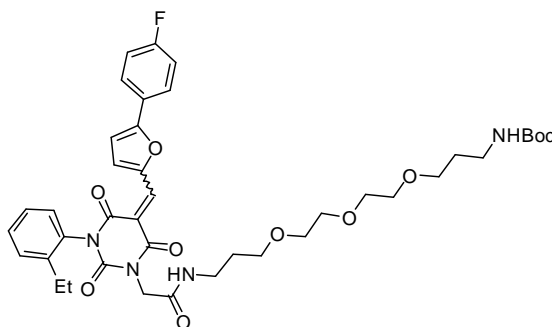
To a solution of **cp028** (0.020 g, 0.049 mmol) in DMF (0.5 mL, 0.1M), sodium hydride (60% in mineral oil) (2.2 mg, 0.054 mmol) was added. After 15 minutes, **200** (0.108 g, 0.245 mmol) was added and the mixture was allowed to stir for 16 hours at 80º before stopping the reaction. The

mixture was subjected to preparative HPLC to afford compound **202** (13.5 mg, 43%). **^{1}H NMR (CDCl$_3$, 400 MHz):**δ 1.18 (t, *J*=7.6 Hz, 3H), 1.42 (s, 9H), 1.71-1.77 (m, 2H), 1.78-1.82 (m, 2H), 2.52 (quin, *J*=7.5 Hz, 2H), 3.20 (bs, 2H), 3.43 (dd, *J*=11.8, 5.8 Hz, 2H), 3.51-3.54 (m, 2H), 3.58-3.62 (m, 6H), 3.63-3.66 (m, 4H), 4.64-4.72 (m, 2H), 4.92-4.99 (m, 1H), 6.71 (bs, 0.6H), 6.91 (d, *J*=4.0 Hz, 0.6H), 6.98 (d, *J*=4.0 Hz, 0.4H), 7.15-7.21 (m, 3.4 H), 7.30-7.35 (m, 1H), 7.38-7.44 (m, 2H), 7.80-7.86 (m, 2H), 8.51 (s, 0.4H), 8.56 (s, 0.6H), 8.75 (d, *J*=4.1 Hz, 0.6H), 8.82 (d, *J*=4.0 Hz, 0.4H). **HRMS:** calc. for [M+H]$^+$ C$_{40}$H$_{50}$N$_4$O$_{10}$F: 765.35055, found 765.35267

(E/Z)-N-(2-(2-(2-azidoethoxy)ethoxy)ethyl)-2-(3-(2-ethylphenyl)-5-((5-(4-fluorophenyl)furan-2-yl)methylene)-2,4,6-trioxotetrahydropyrimidin-1(2 h.)-yl)acetamide (204):
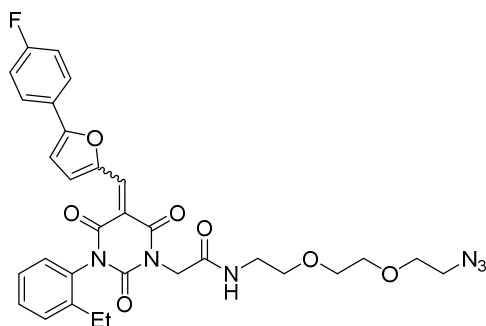
To a solution of **cp028** (0.05 g, 0.124 mmol) in DMF (0.5 mL, 0.1M), sodium hydride (60% in mineral oil) (2.2 mg, 0.054 mmol) was added. After 15 minutes, compound **203** (0.109 g, 0.371 mmol) was added and the mixture was allowed to stir for 16 hours before stopping the reaction. The crude product was purified by chromatography (20% ethyl acetate/DCM) and subsequently by preparative HPLC to afford **204** (15.0 mg, 19%). The compound was directly subjected to the next step.

N-((1-(2-(2-(2-((Z)-3-(2-ethylphenyl)-5-((5-(4-fluorophenyl)furan-2-yl)methylene)-2,4,6-trioxotetrahydropyrimidin-1(2 h.)-yl)acetamido)ethoxy)ethoxy)ethyl)-1H-1,2,3-triazol-4-yl)methyl)-5-((3aS,4S,6aR)-2-oxohexahydro-1H-thieno[3,4-d]imidazol-4-yl)pentanamide (206):
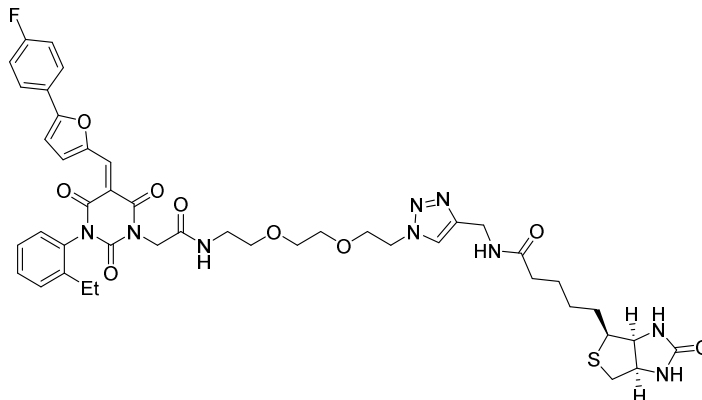
To a solution of compound **204** (15.0 mg, 0.024 mmol) in a mixture of tBuOH/H$_2$O (1:1, 2 ml, 0.007 M), CuSO$_4$.5H$_2$O (0.0024 mmol, 0.6 mg) and **205** (10.2 mg, 0.036 mmol) were added and the mixture was allowed to stir at room temperature for 20 h. The crude product was purified by preparative HPLC to yield **206** (2.1 mg, 10.4%). **HRMS:** calc. for [M+H]$^+$ C$_{44}$H$_{51}$N$_9$O$_9$FS: 900.35090, found 900.35213

(+/-)-N-((1-(2-(2-(2-(3-(2-ethylphenyl)-5-((5-(4-fluorophenyl)furan-2-yl)methyl)-2,4,6-trioxotetrahydropyrimidin-1(2 h.)-yl)acetamido)ethoxy)ethoxy)ethyl)-1H-1,2,3-triazol-4-yl)methyl)-5-((3aS,4S,6aR)-2-oxohexahydro-1H-thieno[3,4-d]imidazol-4-yl)pentanamide (207):
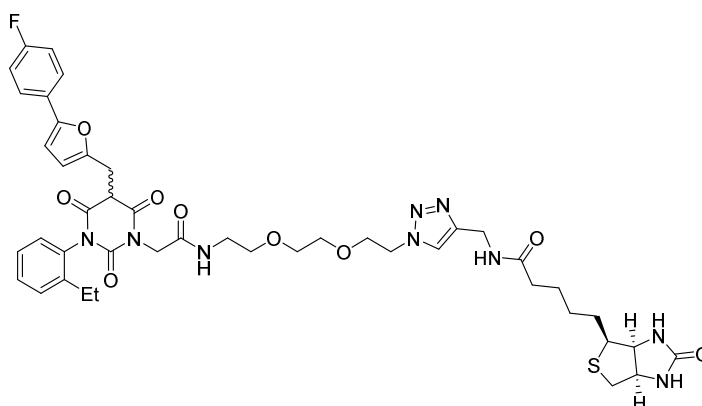
To a solution of crude **206** (0.016 mmol) in MeOH (0.1 mL), sodium borohydride (2.4 mg, 0.064 mmol) was added and the mixture was allowed to stir at room temperature for 3 h.The

crude product was purified by preparative HPLC to yield **207** (1.2 mg, 8.3 %). **HRMS:** calc. for $[M+H]^+$ $C_{44}H_{53}N_9O_9FS$: 902.366550, found 902.36747

11.List of Abbreviations

2-DG	2-Deoxy-D-glucose
2DG6P	2-Deoxy-D-glucose-6-phosphate
2DGA6P	6-Phospho-2-deoxy-D-glucoronic acid
3-BrPA	3-Bromopyruvate
ACN	Acetonitrile
ADP	Adenosine diphosphate
AKT	Protein kinase B
ATP	Adenosine triphosphate
Bn	Benzyl
Boc	tert-Butyloxycarbonyl
BP	Branching point
BRET	Bioluminescence resonance energy transfer
CBz	Carboxybenzyl
CDK11	Cyclin-dependent kinase 11
DCA	dichloroacetate
DCE	1,2-Dichloroethane
DCM	Dichloromethane
DHAP	Dihydroxyacetonephosphate
DHP	Dihydropyran
DIPEA	Diisopropyl ethylamine
DMAP	4-Dimethylaminopyridine
DMF	Dimethyl formamide
DMSO	Dimethyl sulfoxide
DNA	Deoxyribonucleic acid
DYRK3	dual specificity tyrosine phosphorylation regulated kinase 3
EM	Electron microscopy
ER	Endoplasmic reticulum
FADH2	Flavin adenine dinucleotide H2
FRET	Fluorescence resonance energy transfer
GLUT	Facilitative glucose transporters
GPA	Glucopiericidin A
GSK3A	Glycogen synthase kinase-3 alpha
HIF-1	Hypoxia inducible factor 1
HK	Hexokinase

HPLC	High pressure liquid chromatography
HRMS	High resolution mass spectrometry
HRP	Horse radish peroxidase
HTS	High-throughput screening
IC	Intracellular domain
IL-3	Interleukin-3
LDH	Lactate dehydrogenase
MAP2K6	Dual specificity mitogen-activated protein kinase kinase 6
mRNA	messenger ribonucleic acid
MS	Mass spectrometry
mTOR	mammalian target of rapamycin
NAD(P)H	Nicotinamide adenine dinucleotide phosphate H
NAD+	Nicotinamide adenine dinucleotide +
NADH	Nicotinamide adenine dinucleotide H
NEK2	(Never in Mitosis Gene A)-Related Kinase
NMR	Nuclear magnetic resonance
NOE	Nuclear overhauser effect
OXPHOS	Oxidative phosphorylation
PA	Piericidin A
PAGE	Polyacrylamide gel electrophoresis
PDH	pyruvate dehydrogenase
PDHK	pyruvate dehydrogenase kinase
PEG	Polyethylene glycol
PFK	phosphofructokinase
PI3K	Phosphoinositide 3-kinase
PK	Pyruvate kinase
PKC	Protein kinase C
PKM1	Pyruvate kinase spliced variant M1
PKM2	Pyruvate kinase spliced variant M2
PPTS	pyridinium p-toluensulfonate
pre-mRNA	premature messenger ribonucleic acid
PTC	Phase transfer catalyst
Pyr.	Pyridine
r.t.	room temperature
RNA	Ribonucleic acid
ROS	Reactive oxygen species

SAR	Structure activity relationship
SF2/ASF	Serine/arginine-rich splicing factor 1
SF3b	Splicing factor 3b
SGLT	Sodium-glucose transporter
snRNA	Small nuclear ribonucleic acid
snRNP	Small nuclear ribonucleoproteins
SOCl2	Thionyl chloride
SR	Serine rich
SRPK	Serine-arginine protein kinase
SS	Splicing site
TAMRA	5/6-Carboxytetramethylrhodamine
TBAF	Tetrabutylammonium fluoride
TBAI	Tetrabutylammonium iodide
TBDMSCl	Tert-butyldimethylsilyl chloride
TBS	tert-Butylsilyl
TBTU	*O*-(Benzotriazol-1-yl)-N,N,N´,N´-tetramethyluroniumtetrafluoroborate
TCA	Tricarboxylic acid cycle
TFA	Trifluoroacetic acid
THF	Tetrahydrofuran
THP	Tetrahydropyran
TLC	Thin layer chromatography
UDP	Uridine diphosphate
VEGF	Vascular endothelial growth factor

12. References

1.   Wood, I. S.; Trayhurn, P., Glucose transporters (GLUT and SGLT): expanded families of sugar transport proteins. *Br J Nutr* **2003,** *89* (1), 3-9.

2.   Scheepers, A.; Joost, H.-G.; Schürmann, A., The Glucose Transporter Families SGLT and GLUT: Molecular Basis of Normal and Aberrant Function. *Journal of Parenteral and Enteral Nutrition* **2004,** *28* (5), 364-71.

3.   Wu, X.; Freeze, H. H., GLUT14, a Duplicon of GLUT3, Is Specifically Expressed in Testis as Alternative Splice Forms. *Genomics* **2002,** *80* (6), 553-557.

4.   Simpson, I. A.; Carruthers, A.; Vannucci, S. J., Supply and demand in cerebral energy metabolism: the role of nutrient transporters. *J Cereb Blood Flow Metab* **2007,** *27* (11), 1766-91.

5.   Patching, S. G., Glucose Transporters at the Blood-Brain Barrier: Function, Regulation and Gateways for Drug Delivery. *Mol Neurobiol* **2016**.

6.   Burant, C. F.; Bell, G. I., Mammalian Facilitative Glucose Transporters: Evidence for Similar Substrate Recognition Sites in Functionally Monomeric Proteins. *Biochemistry* **1992,** *31* (42), 10414-20.

7.   Schuit, F. C., Is GLUT2 required for glucose sensing? *Diabetologia* **1997,** *40* (1), 104-11.

8.   Rolland, F.; Winderickx, J.; Thevelein, J. M., Glucose-sensing mechanisms in eukaryotic cells. *Trends Biochem Sci* **2001,** *26* (5), 310-15.

9.   Leto, D.; Saltiel, A. R., Regulation of glucose transport by insulin: traffic control of GLUT4. *Nat Rev Mol Cell Biol* **2012,** *13* (6), 383-96.

10.   Colas, C.; Ung, P. M.; Schlessinger, A., SLC Transporters: Structure, Function, and Drug Discovery. *Medchemcomm* **2016,** *7* (6), 1069-1081.

11.   Deng, D.; Xu, C.; Sun, P.; Wu, J.; Yan, C.; Hu, M.; Yan, N., Crystal structure of the human glucose transporter GLUT1. *Nature* **2014,** *510* (7503), 121-5.

12.   Deng, D.; Sun, P.; Yan, C.; Ke, M.; Jiang, X.; Xiong, L.; Ren, W.; Hirata, K.; Yamamoto, M.; Fan, S.; Yan, N., Molecular basis of ligand recognition and transport by glucose transporters. *Nature* **2015,** *526* (7573), 391-6.

13.   Nomura, N.; Verdon, G.; Kang, H. J.; Shimamura, T.; Nomura, Y.; Sonoda, Y.; Hussien, S. A.; Qureshi, A. A.; Coincon, M.; Sato, Y.; Abe, H.; Nakada-Nakura, Y.; Hino, T.; Arakawa, T.; Kusano-Arai, O.; Iwanari, H.; Murata, T.; Kobayashi, T.; Hamakubo, T.; Kasahara, M.; Iwata, S.; Drew, D., Structure and mechanism of the mammalian fructose transporter GLUT5. *Nature* **2015,** *526* (7573), 397-401.

14.   Sun, L.; Zeng, X.; Yan, C.; Sun, X.; Gong, X.; Rao, Y.; Yan, N., Crystal structure of a bacterial homologue of glucose transporters GLUT1-4. *Nature* **2012,** *490* (7420), 361-6.

15.   Kapoor, K.; Finer-Moore, J. S.; Pedersen, B. P.; Caboni, L.; Waight, A.; Hillig, R. C.; Bringmann, P.; Heisler, I.; Muller, T.; Siebeneicher, H.; Stroud, R. M., Mechanism of inhibition of human glucose transporter GLUT1 is conserved between cytochalasin B and phenylalanine amides. *Proc Natl Acad Sci U S A* **2016,** *113* (17), 4711-6.

16.   McCoy, K. D.; Ahmed, N.; Tan, A. S.; Berrige, M. V., The Hemopoietic Growth Factor, Interleukin-3, Promotes Glucose Transport by Increasing the Specific Activity and Maintaining the Affinity for Glucose of Plasma Membrane Glucose Transporters. *The Journal of Biological Chemistry* **1997,** *272* (28), 17276-82.

17.   James, D. E.; Brown, R.; Navarro, J.; Pilch, P. F., Insulin-regulatable tissues express a unique insulin-sensitive glucose transport protein. *Nature* **1988,** *333*, 183-85.

18.   Edinger, A. L.; Thompson, C. B., Akt maintains cell size and survival by increasing mTOR-dependent nutrient uptake. *Mol Biol Cell* **2002,** *13* (7), 2276-88.

19.   DeBerardinis, R. J.; Lum, J. J.; Hatzivassiliou, G.; Thompson, C. B., The biology of cancer: metabolic reprogramming fuels cell growth and proliferation. *Cell Metab* **2008,** *7* (1), 11-20.

20.   Denko, N. C., Hypoxia, HIF1 and glucose metabolism in the solid tumour. *Nat Rev Cancer* **2008,** *8*, 705-13.

21.   Osthus, R. C.; Shim, H.; Kim, S.; Li, Q.; Reddy, R.; Mukherjee, M.; Xu, Y.; Wonsey, D.; Lee, L. A.; Dang, C. V., Deregulation of glucose transporter 1 and glycolytic gene expression by c-Myc. *J Biol Chem* **2000,** *275* (29), 21797-800.

22.   Ojeda, P.; Perez, A.; Ojeda, L.; Vargas-Uribe, M.; Rivas, C. I.; Salas, M.; Vera, J. C.; Reyes, A. M., Noncompetitive blocking of human GLUT1 hexose transporter by methylxanthines reveals an exofacial regulatory binding site. *Am J Physiol Cell Physiol* **2012,** *303* (5), C530-9.

23.   Blodgett, D. M.; De Zutter, J. K.; Levine, K. B.; Karim, P.; Carruthers, A., Structural basis of GLUT1 inhibition by cytoplasmic ATP. *J Gen Physiol* **2007,** *130* (2), 157-68.

24.   Liu, Q.; Vera, J. C.; Peng, H.; Golde, D. W., The Predicted ATP-Binding Domains in the Hexose Transporter GLUT1 Critically Affect Transporter Activity. *Biochemistry* **2001,** *40* (26), 7874-81.

25.   Rungaldier, S.; Oberwagner, W.; Salzer, U.; Csaszar, E.; Prohaska, R., Stomatin interacts with GLUT1/SLC2A1, band 3/SLC4A1, and aquaporin-1 in human erythrocyte membrane domains. *Biochim Biophys Acta* **2013,** *1828* (3), 956-66.

26.   Lee, E. E.; Ma, J.; Sacharidou, A.; Mi, W.; Salato, V. K.; Nguyen, N.; Jiang, Y.; Pascual, J. M.; North, P. E.; Shaul, P. W.; Mettlen, M.; Wang, R. C., A Protein Kinase C Phosphorylation Motif in GLUT1 Affects Glucose Transport and is Mutated in GLUT1 Deficiency Syndrome. *Mol Cell* **2015,** *58* (5), 845-53.

27.   Asano, T.; Katagiri, H.; Takata, K.; Lin, J.; Ishihara, H.; Inukai, K.; Tsukuda, K.; Kikuchi, M.; Hirano, H.; Yazaki, Y.; Oka, Y., The Role of *N*-Glycosylation of GLUT1 for Glucose Transport Activity. *The Journal of Biological Chemistry* **1991,** *266* (36), 24632-36.

28.   Wilson, J. E., Isozymes of mammalian hexokinase: structure, subcellular localization and metabolic function. *Journal of Experimental Biology* **2003,** *206* (12), 2049-2057.

29.   Underwood, A. H.; Newsholme, E. A., Properties of Phosphofructokinase from Rat Liver and their Relation to the Control of Glycolysis and Gluconeogenesis. *Biochem. J.* **1965,** *95*, 868-75.

30.   Passonneau, J. V.; Lowry, O. H., Phosphofructokinase and the Pasteur Effect. *Biochemical and Biophysical Researc Communications* **1962,** *7* (1), 10-15.

31.   Liemburg-Apers, D. C.; Willems, P. H.; Koopman, W. J.; Grefte, S., Interactions between mitochondrial reactive oxygen species and cellular glucose metabolism. *Arch Toxicol* **2015,** *89* (8), 1209-26.

32.   Hanukoglu, I.; Rapoport, R., Routes and regulation of NADPH production in steroidogenic mitochondria. *Endocrine Research* **2009,** *21* (1-2), 231-241.

33.   Andrisse, S.; Koehler, R. M.; Chen, J. E.; Patel, G. D.; Vallurupalli, V. R.; Ratliff, B. A.; Warren, D. E.; Fisher, J. S., Role of GLUT1 in regulation of reactive oxygen species. *Redox Biol* **2014,** *2*, 764-71.

34.   Warburg, O.; Minami, S., Versuche an Überlebendem Carcinomgewebe. *Klin. Wochenschr.* **1923,** *2* (17), 776-77.

35.   Otto, A. M., Warburg effect(s)-a biographical sketch of Otto Warburg and his impacts on tumor metabolism. *Cancer Metab* **2016,** *4*, 5.

36.   Warburg, O.; Posener, K.; Negelein, E., Ueber den Stoffwechsel der Tumoren. *Biochemische Zeitschrift* **1924,** *152*, 319-44.

37.   Weinhouse, S., The Warburg Hypothesis Fifty Years Later. *Z. Krebsforsch.* **1976,** *87*, 115-26.

38.   Krzeslak, A.; Wojcik-Krowiranda, K.; Forma, E.; Jozwiak, P.; Romanowicz, H.; Bienkiewicz, A.; Brys, M., Expression of GLUT1 and GLUT3 glucose transporters in endometrial and breast cancers. *Pathol Oncol Res* **2012,** *18* (3), 721-8.

39.   Carvalho, K. C.; Cunha, I. W.; Rocha, R. M.; Ayala, F. R.; Cajaíba, M. M.; Begnami, M. D.; Vilela, R. S.; Paiva, G. R.; Andrade, R. G.; Soares, F. A., GLUT1 expression in malignant tumors and its use as an immunodiagnostic marker. *Clinics* **2011,** *66* (6), 965-972.

40.   Vander Heiden, M. G.; Cantley, L. C.; Thompson, C. B., Understanding the Warburg Effect: The Metabolic Requirements of Cell Proliferation. *Science* **2009,** *324*, 1029-33.

41.   Liberti, M. V.; Locasale, J. W., The Warburg Effect: How Does it Benefit Cancer Cells? *Trends Biochem Sci* **2016,** *41* (3), 211-8.

42.   Gatenby, R. A.; Gillies, R. J., Why do cancers have high aerobic glycolysis? *Nat Rev Cancer* **2004,** *4* (11), 891-9.

43.   Lunt, S. Y.; Vander Heiden, M. G., Aerobic glycolysis: meeting the metabolic requirements of cell proliferation. *Annu Rev Cell Dev Biol* **2011,** *27*, 441-64.

44.   Hedeskov, C. J., Early Effects of Phytohaemagglutinin on Glucose Metabolism of Normal Human Lymphocytes. *Biochem. J.* **1968,** *110*, 373-80.

45.   Semenza, G. L., Targeting HIF-1 for cancer therapy. *Nat Rev Cancer* **2003,** *3* (10), 721-32.

47.   Hanahan, D.; Weinberg, R. A., Hallmarks of cancer: the next generation. *Cell* **2011,** *144* (5), 646-74.

48.   Vander Heiden, M. G., Targeting cancer metabolism: a therapeutic window opens. *Nat Rev Drug Discov* **2011,** *10* (9), 671-84.

49.   Tennant, D. A.; Duran, R. V.; Gottlieb, E., Targeting metabolic transformation for cancer therapy. *Nat Rev Cancer* **2010,** *10* (4), 267-77.

50.   Elf, S. E.; Chen, J., Targeting glucose metabolism in patients with cancer. *Cancer* **2014,** *120* (6), 774-80.

51.   Hamanaka, R. B.; Chandel, N. S., Targeting glucose metabolism for cancer therapy. *J Exp Med* **2012,** *209* (2), 211-5.

52.   Landau, B. R.; Laszlo, J.; Stengle, J.; Burk, D., Certain Metabolic and Pharmacologic Effects inCancer Patients Given Infusions of 2-Deoxy-D-Glucose. *J. Natl. Cancer Inst.* **1958,** *21* (3), 485-94.

53.   Clem, B. F.; O'Neal, J.; Klarer, A. C.; Telang, S.; Chesney, J., Clinical development of cancer therapeutics that target metabolism. *QJM* **2016,** *109* (6), 367-72.

54.   Raez, L. E.; Papadopoulos, K.; Ricart, A. D.; Chiorean, E. G.; Dipaola, R. S.; Stein, M. N.; Rocha Lima, C. M.; Schlesselman, J. J.; Tolba, K.; Langmuir, V. K.; Kroll, S.; Jung, D. T.; Kurtoglu, M.; Rosenblatt, J.; Lampidis, T. J., A phase I dose-escalation trial of 2-deoxy-D-glucose alone or combined with docetaxel in patients with advanced solid tumors. *Cancer Chemother Pharmacol* **2013,** *71* (2), 523-30.

55.   Pelicano, H.; Martin, D. S.; Xu, R. H.; Huang, P., Glycolysis inhibition for anticancer treatment. *Oncogene* **2006,** *25* (34), 4633-46.

56.   Christofk, H. R.; Vander Heiden, M. G.; Harris, M. H.; Ramanathan, A.; Gerszten, R. E.; Wei, R.; Fleming, M. D.; Schreiber, S. L.; Cantley, L. C., The M2 splice isoform of pyruvate kinase is important for cancer metabolism and tumour growth. *Nature* **2008,** *452* (7184), 230-3.

57.   Vander Heiden, M. G.; Christofk, H. R.; Schuman, E.; Subtelny, A. O.; Sharfi, H.; Harlow, E. E.; Xian, J.; Cantley, L. C., Identification of small molecule inhibitors of pyruvate kinase M2. *Biochem Pharmacol* **2010,** *79* (8), 1118-24.

58.   Wang, D.; Chu, P. C.; Yang, C. N.; Yan, R.; Chuang, Y. C.; Kulp, S. K.; Chen, C. S., Development of a novel class of glucose transporter inhibitors. *J Med Chem* **2012,** *55* (8), 3827-36.

59.   Liu, Y.; Cao, Y.; Zhang, W.; Bergmeier, S.; Qian, Y.; Akbar, H.; Colvin, R.; Ding, J.; Tong, L.; Wu, S.; Hines, J.; Chen, X., A small-molecule inhibitor of glucose transporter 1 downregulates glycolysis, induces cell-cycle arrest, and inhibits cancer cell growth in vitro and in vivo. *Mol Cancer Ther* **2012,** *11* (8), 1672-82.

60.   Kobori, M.; Shinmoto, H.; Tsushida, T.; Shinohara, K., Phloretin-induced apoptosis in B 16 melanoma 4A5 cells by inhibition of glucose transmembrane transport. *Cancer Lett* **1997,** *119*, 207-12.

61.   Granchi, C.; Fortunato, S.; Minutolo, F., Anticancer agents interacting with membrane glucose transporters. *Medchemcomm* **2016,** *7* (9), 1716-1729.

62.   Kletzien, R. F.; Perdue, J. F.; Springer, A., Cytochalasin A and B. *J Biol Chem* **1972,** *247* (9), 2964-66.

63.   Hall, C.; Wu, M.; Crane, F. L., Piericidin A: a New Inhibitor of Mitochondrial Electron Transport. *Biochem Biophys Res Comm* **1966,** *25* (4), 373-77.

64.   Ulanovskaya, O. A.; Cui, J.; Kron, S. J.; Kozmin, S. A., A pairwise chemical genetic screen identifies new inhibitors of glucose transport. *Chem Biol* **2011,** *18* (2), 222-30.

65.   Siebeneicher, H.; Bauser, M.; Buchmann, B.; Heisler, I.; Muller, T.; Neuhaus, R.; Rehwinkel, H.; Telser, J.; Zorn, L., Identification of novel GLUT inhibitors. *Bioorg Med Chem Lett* **2016,** *26* (7), 1732-7.

66.   Liu, Y.; Zhang, W.; Cao, Y.; Liu, Y.; Bergmeier, S.; Chen, X., Small compound inhibitors of basal glucose transport inhibit cell proliferation and induce apoptosis in cancer cells via glucose-deprivation-like mechanisms. *Cancer Lett* **2010,** *298* (2), 176-85.

67.   Frerichs, H.; Ball, E. g., Studies on the Metabolism of Adipose Tissue. XVI. Inhibition by Phlorizin and Phloretin of the Insulin-stimulated Uptake of Glucose. *Biochemistry* **1964,** *3* (7), 981-85.

68.   Cao, X.; Fang, L.; Gibbs, S.; Huang, Y.; Dai, Z.; Wen, P.; Zheng, X.; Sadee, W.; Sun, D., Glucose uptake inhibitor sensitizes cancer cells to daunorubicin and overcomes drug resistance in hypoxia. *Cancer Chemother Pharmacol* **2007,** *59* (4), 495-505.

69.   Murata, H.; Hruz, P. W.; Mueckler, M., Indinavir inhibits the glucose transporter isoform Glut4 at physiologic concentrations. *AIDS* **2002,** *16*, 859-63.

70.   Kitagawa, M.; Ikeda, S.; Tashiro, E.; Soga, T.; Imoto, M., Metabolomic identification of the target of the filopodia protrusion inhibitor glucopiericidin A. *Chem Biol* **2010,** *17* (9), 989-98.

71.   Siebeneicher, H.; Cleve, A.; Rehwinkel, H.; Neuhaus, R.; Heisler, I.; Muller, T.; Bauser, M.; Buchmann, B., Identification and Optimization of the First Highly Selective GLUT1 Inhibitor BAY-876. *ChemMedChem* **2016**.

72.   Ung, P. M.; Song, W.; Cheng, L.; Zhao, X.; Hu, H.; Chen, L.; Schlessinger, A., Inhibitor Discovery for the Human GLUT1 from Homology Modeling and Virtual Screening. *ACS Chem Biol* **2016,** *11* (7), 1908-16.

73.   Cowley, P. M.; Wise, A.; Brown, T. J.; Isherwood, M.; Chakrabartu, A., SLC2A Transporter Inhibitors. *World Intellectual Property Organization* **2014**, WO 2014/187922 A1.

74.   Younes, M.; Brown, R. W.; Stephenson, M.; Gondo, M.; Cagle, P. T., Overexpression of Glut1 and Glut3 in Stage I Nonsmall Cell Lung Carcinoma Is Associated with Poor Survival. *Cancer 80* (6), 1046-1051.

75.   Yamamoto, N.; Sato, T.; Kawasaki, K.; Murosaki, S.; Yamamoto, Y., A nonradioisotope, enzymatic assay for 2-deoxyglucose uptake in L6 skeletal muscle cells cultured in a 96-well microplate. *Anal Biochem* **2006,** *351* (1), 139-45.

76.   Yamamoto, N.; Kawasaki, K.; Kawabata, K.; Ashida, H., An enzymatic fluorimetric assay to quantitate 2-deoxyglucose and 2-deoxyglucose-6-phosphate for in vitro and in vivo use. *Anal Biochem* **2010,** *404* (2), 238-40.

77.   Morrison, G. C.; Waite, R. O.; Caro, A. N.; Shavel, J., 2,5-Dimethylindolo[2,3-f]morphan. *J Org Chem* **1967,** *32*, 3691-93.

78.   Morrison, G. C.; Waite, R. O.; Serafin, F.; Shavel, J., Alternate Precursors in Biogenetic-Type Syntheses. I. The Synthesis of Cyclohex[j]indolo[2,3-f]morphan. *J Org Chem* **1967,** *32*, 2551-55.

79.   Morrison, G. C.; Waite, R. O.; Serafin, F.; Shavel, J., Alternate Precursors in Biogenetic-Type Syntheses. II. The Synthesis of Cyclohex[j]indolo[2,3-f]morphan-15-one. *J Org Chem* **1967,** *32*, 2555-57.

80.   Shavel, J.; Morrison, G. C.; Morrison, M., Indolomorphans and Process for their Production. **1966**.

81.   Bonjoch, J.; Boncompte, F.; Casamitjana, N.; Bosch, J., Benzomorphan Related Compounds. XXII. Reduction of 3-(tetrahydropyridyl)indoles to Indolines. Synthesis of a New Type of Indolomorphan. *Tetrahedron* **1986,** *42* (24), 6693-6702.

82.   Liu, R. R.; Li, B. L.; Lu, J.; Shen, C.; Gao, J. R.; Jia, Y. X., Palladium/l-Proline-Catalyzed Enantioselective alpha-Arylative Desymmetrization of Cyclohexanones. *J Am Chem Soc* **2016,** *138* (16), 5198-201.

83.   Fischer, E.; Hess, O., Synthese von Indol-derivaten. *European Journal of Inorganic Chemistry* **1884,** *17* (1), 559-68.

84.   Diaba, F.; Bonjoch, J., Asymmetric synthesis of 2-azabicyclo[3.3.1]nonanes by a microwave-assisted organocatalysed tandem desymmetrisation and intramolecular aldolisation. *Org Biomol Chem* **2009,** *7* (12), 2517-9.

85.   Boriack-Sjodin, A.; Carcanague, D. R.; Dussault, D. D.; Hatoum-Mokdad, H.; Hull, K. G.; Ioannidis, G.; Manchester, J. I.; McGuire, H. M.; McKinney, D. C.; Stokes, S., Heterocyclic Derivatives and Methods Thereof. *World Intellectual Property* **2010,** (WO 2010/038081 A2).

86.   Schmidt, B.; Nave, S., Palladium-CatalyzedO-Allylation of α-Hydroxy Carbonyl Compounds. *Advanced Synthesis & Catalysis* **2006,** *348* (4-5), 531-537.

87.   Beaumont, K.; Webster, R.; Gardner, I.; Dack, K., Design of Ester Prodrugs to Enhance Oral Absorption of Poorly Permeable Compounds: Challenges to the Discovery Scientist. *Current Drug Metabolism* **2003,** (4), 461-85.

88.   Johnson, M. G.; Liu, J. J.; Li, A. R.; van Lengerich, B.; Wang, S.; Medina, J. C.; Collins, T. L.; Danao, J.; Seitz, L.; Willee, A.; D'Souza, W.; Budelsky, A. L.; Fan, P. W.; Wong, S. G., Solving time-dependent CYP3A4 inhibition for a series of indole-phenylacetic acid dual antagonists of the PGD(2) receptors CRTH2 and DP. *Bioorg Med Chem Lett* **2014,** *24* (13), 2877-80.

89.   Thomae, D.; Jeanty, M.; Coste, J.; Guillaumet, G.; Suzenet, F., Extending the Scope of the Aza-Fischer Synthesis of 4- and 6-Azaindoles. *European Journal of Organic Chemistry* **2013,** *2013* (16), 3328-3336.

90.   Fink, B. E.; Zhao, Y.; Borzilleri, R. M.; Zhang, L.; Kim, K. S.; Kamau, M. G.; Tebben, A. J., TGF BETA R ANTAGONISTS. **2016,** (US 2016/0176871 A1).

91.   Chataigner, I.; Lebreton, J.; Durand, D.; Guingant, A.; Villiéras, J., A New Approach for the Determination of the Absolute Configuration of Secondary Alcohols by 1H NMR with *O*-Substituted Mandelate Derivatives. *Tetrahedron Letters* **1998,** *39*, 1759-62.

92.   Winter, G. E.; Buckley, J.; Paulk, J.; Roberts, J. M.; Souza, A.; Dhe-Paganon, S.; Bradner, J. E., Phthalimide conjugation as a strategy for in vivo protein degradation. *Science* **2015,** *348* (6241), 1376-81.

93.   Ast, G., How did alternative splicing evolve? *Nat Rev Genet* **2004,** *5* (10), 773-82.

94.   Keren, H.; Lev-Maor, G.; Ast, G., Alternative splicing and evolution: diversification, exon definition and function. *Nat Rev Genet* **2010,** *11* (5), 345-55.

95.   Kaida, D.; Schneider-Poetsch, T.; Yoshida, M., Splicing in oncogenesis and tumor suppression. *Cancer Sci* **2012,** *103* (9), 1611-6.

96.   Will, C. L.; Luhrmann, R., Spliceosome structure and function. *Cold Spring Harb Perspect Biol* **2011,** *3* (7).

97.   Matera, A. G.; Wang, Z., A day in the life of the spliceosome. *Nat Rev Mol Cell Biol* **2014,** *15* (2), 108-21.

98.   Madhani, H. D., snRNA catalysts in the spliceosome's ancient core. *Cell* **2013,** *155* (6), 1213-5.

99.   Fica, S. M.; Tuttle, N.; Novak, T.; Li, N. S.; Lu, J.; Koodathingal, P.; Dai, Q.; Staley, J. P.; Piccirilli, J. A., RNA catalyses nuclear pre-mRNA splicing. *Nature* **2013,** *503* (7475), 229-34.

100.   Ritchie, D. B.; Schellenberg, M. J.; MacMillan, A. M., Spliceosome structure: piece by piece. *Biochim Biophys Acta* **2009,** *1789* (9-10), 624-33.

101.   Golas, M. M.; Sander, B.; Bessonov, S.; Grote, M.; Wolf, E.; Kastner, B.; Stark, H.; Luhrmann, R., 3D cryo-EM structure of an active step I spliceosome and localization of its catalytic core. *Mol Cell* **2010,** *40* (6), 927-38.

102.   Boehringer, D.; Makarov, E. M.; Sander, B.; Makarova, O. V.; Kastner, B.; Luhrmann, R.; Stark, H., Three-dimensional structure of a pre-catalytic human spliceosomal complex B. *Nat Struct Mol Biol* **2004,** *11* (5), 463-8.

103.   Yan, C.; Wan, R.; Bai, R.; Huang, G.; Shi, Y., Structure of a yeast step II catalytically activated spliceosome. *Science* **2016,** *10.1126/science. aak9979*.

104.   Effenberger, K. A.; Urabe, V. K.; Jurica, M. S., Modulating splicing with small molecular inhibitors of the spliceosome. *Wiley Interdiscip Rev RNA* **2016**.

105.   Lee, S. C.; Abdel-Wahab, O., Therapeutic targeting of splicing in cancer. *Nat Med* **2016,** *22* (9), 976-86.

106.   Kaida, D.; Motoyoshi, H.; Tashiro, E.; Nojima, T.; Hagiwara, M.; Ishigami, K.; Watanabe, H.; Kitahara, T.; Yoshida, T.; Nakajima, H.; Tani, T.; Horinouchi, S.; Yoshida, M., Spliceostatin A targets SF3b and inhibits both splicing and nuclear retention of pre-mRNA. *Nat Chem Biol* **2007,** *3* (9), 576-83.

107.   Kotake, Y.; Sagane, K.; Owa, T.; Mimori-Kiyosue, Y.; Shimizu, H.; Uesugi, M.; Ishihama, Y.; Iwata, M.; Mizui, Y., Splicing factor SF3b as a target of the antitumor natural product pladienolide. *Nat Chem Biol* **2007,** *3* (9), 570-5.

108.   Kuhn, A. N.; van Santen, M. A.; Schwienhorst, A.; Urlaub, H.; Luhrmann, R., Stalling of spliceosome assembly at distinct stages by small-molecule inhibitors of protein acetylation and deacetylation. *RNA* **2009,** *15* (1), 153-75.

109.   Samatov, T. R.; Wolf, A.; Odenwalder, P.; Bessonov, S.; Deraeve, C.; Bon, R. S.; Waldmann, H.; Luhrmann, R., Psoromic acid derivatives: a new family of small-molecule pre-mRNA splicing inhibitors discovered by a stage-specific high-throughput in vitro splicing assay. *Chembiochem* **2012,** *13* (5), 640-4.

110.   Pilch, B.; Allemand, E.; Facompré, M.; Bailly, C.; Riou, J.; Soret, J.; Tazi, J., Specific Inhibition of Serine- and Arginine-rich Splicing Factors Phosphorylation, Spliceosome Assembly, and Splicing by the Antitumor Drug NB-506. *Cancer Research* **2001,** *61*, 6876-84.

111.   O'Brien, K.; Matlin, A. J.; Lowell, A. M.; Moore, M. J., The biflavonoid isoginkgetin is a general inhibitor of Pre-mRNA splicing. *J Biol Chem* **2008,** *283* (48), 33147-54.

112.   Baell, J.; Walters, M. A., Chemical con artists foil drug discovery. *Nature* **2014,** *513*, 481-83.

113.   Tang, Q.; Zhang, G.; Du, X.; Zhu, W.; Li, R.; Lin, H.; Li, P.; Cheng, M.; Gong, P.; Zhao, Y., Discovery of novel 6,7-disubstituted-4-phenoxyquinoline derivatives bearing 5-(aminomethylene)pyrimidine-2,4,6-trione moiety as c-Met kinase inhibitors. *Bioorganic & medicinal chemistry* **2014,** *22* (4), 1236-49.

114.   Kastl, J.; Braun, J.; Prestel, A.; Moller, H. M.; Huhn, T.; Mayer, T. U., Mad2 Inhibitor-1 (M2I-1): A Small Molecule Protein-Protein Interaction Inhibitor Targeting the Mitotic Spindle Assembly Checkpoint. *ACS Chem Biol* **2015,** *10* (7), 1661-6.

115.   Laudien, R.; Mitzner, R., Phenylureas. Part 1. Mechanism of the basic hydrolysis of phenylureas. *Journal of the Chemical Society, Perkin Transactions 2* **2001,** (11), 2226-2229.

116.   Schneider, M.; Hsiao, H. H.; Will, C. L.; Giet, R.; Urlaub, H.; Luhrmann, R., Human PRP4 kinase is required for stable tri-snRNP association during spliceosomal B complex formation. *Nat Struct Mol Biol* **2010,** *17* (2), 216-21.

117. Liu, Q.; Sabnis, Y.; Zhao, Z.; Zhang, T.; Buhrlage, S. J.; Jones, L. H.; Gray, N. S., Developing irreversible inhibitors of the protein kinase cysteinome. *Chemistry & biology* **2013,** *20* (2), 146-59.

118. Patel, N. A.; Kaneko, S.; Apostolatos, H. S.; Bae, S. S.; Watson, J. E.; Davidowitz, K.; Chappell, D. S.; Birnbaum, M. J.; Cheng, J. Q.; Cooper, D. R., Molecular and genetic studies imply Akt-mediated signaling promotes protein kinase CbetaII alternative splicing via phosphorylation of serine/arginine-rich splicing factor SRp40. *J Biol Chem* **2005,** *280* (14), 14302-9.

119. Caputi, M.; Freund, M.; Kammler, S.; Asang, C.; Schaal, H., A bidirectional SF2/ASF- and SRp40-dependent splicing enhancer regulates human immunodeficiency virus type 1 rev, env, vpu, and nef gene expression. *J Virol* **2004,** *78* (12), 6517-26.

120. Debdab, M.; Carreaux, F.; Renault, S.; Soundararajan, M.; Fedorov, O.; Filippakopoulos, P.; Lozach, O.; Babault, L.; Tahtouh, T.; Baratte, B.; Ogawa, Y.; Hagiwara, M.; Eisenreich, A.; Rauch, U.; Knapp, S.; Meijer, L.; Bazureau, J. P., Leucettines, a class of potent inhibitors of cdc2-like kinases and dual specificity, tyrosine phosphorylation regulated kinases derived from the marine sponge leucettamine B: modulation of alternative pre-RNA splicing. *J Med Chem* **2011,** *54* (12), 4172-86.

121. Raingeaud, J.; Whitmarsh, A. J.; Barrett, T.; Derijard, B.; Davis, R. J., MKK3- and MKK6-Regulated Gene Expression Is Mediated by the p38 Mitogen-Activated Protein Kinase Signal Transduction Pathway. *Mol Cell Biol* **1996,** *16* (3), 1247-55.

122. van der Houven van Oordt, W.; Diaz-Meco, M. T.; Lozano, J.; Krainer, A. R.; Moscat, J.; Caceres, J. F., The MKK 3/6-p38–signaling Cascade Alters the Subcellular Distribution of hnRNP A1 and Modulates Alternative Splicing Regulation. *J Cell Biol* **2000,** *149* (2), 307-16.

123. Naro, C.; Barbagallo, F.; Chieffi, P.; Bourgeois, C. F.; Paronetto, M. P.; Sette, C., The centrosomal kinase NEK2 is a novel splicing factor kinase involved in cell survival. *Nucleic Acids Res* **2014,** *42* (5), 3218-27.

124. Hu, D.; Mayeda, A.; Trembley, J. H.; Lahti, J. M.; Kidd, V. J., CDK11 complexes promote pre-mRNA splicing. *J Biol Chem* **2003,** *278* (10), 8623-9.

125. Sidarovich, A.; Will, C. L.; Anokhina, M. M.; Ceballos, J.; Sievers, S.; Agafonov, D. E.; Samatov, T. R.; Bao, P.; Kastner, B.; Urlaub, H.; Waldmann, H.; Lührmann, R., Identification of a small molecule inhibitor that stalls splicing at an early step of spliceosome activation. *eLIFE* **2017,** (just accepted).

126. Echavarren, A. M., Intramolecular Reactions of Alkynes with Furans and Electron Rich Arenes Catalyzed by PtCl2: The Role of Platinum Carbenes as Intermediates. *Journal of the American Chemical Society* **2003,** *125* (19), 5757-5766.

127. Hussein, M.; Bettio, M.; Schmitz, A.; Hannam, J. S.; Theis, J.; Mayer, G.; Dosa, S.; Gutschow, M.; Famulok, M., Cyplecksins are covalent inhibitors of the pleckstrin homology domain of cytohesin. *Angewandte Chemie* **2013,** *52* (36), 9529-33.

128. Trinh, T. N.; Hizartzidis, L.; Lin, A. J.; Harman, D. G.; McCluskey, A.; Gordon, C. P., An efficient continuous flow approach to furnish furan-based biaryls. *Org Biomol Chem* **2014,** *12* (47), 9562-71.

129. Mitsch, A.; Wissner, P.; Silber, K.; Haebel, P.; Sattler, I.; Klebe, G.; Schlitzer, M., (p-Ac and p-F) Non-thiol farnesyltransferase inhibitors: N-(4-tolylacetylamino-3-benzoylphenyl)-3-arylfurylacrylic acid amides. *Bioorganic & medicinal chemistry* **2004,** *12* (17), 4585-600.

130. Liégault, B. L., D.; Caron, L.; Vlassova, A.; Fagnou, K. , (m-F) Establishment of Broadly Applicable Reaction Conditions for the Palladium-Catalyzed Direct Arylation of Heteroatom-Containing Aromatic Compounds. *J. Org. Chem.* **2009,** *74*, 1826-1834.

131. Cosner, C. C.; Markiewicz, J. T.; Bourbon, P.; Mariani, C. J.; Wiest, O.; Rujoi, M.; Rosenbaum, A. I.; Huang, A. Y.; Maxfield, F. R.; Helquist, P., (m,p-Cl) Investigation of N-aryl-3-alkylidenepyrrolinones as potential Niemann-Pick type C disease therapeutics. *J Med Chem* **2009,** *52* (20), 6494-8.

132.   Murasawa, S.; Iuchi, K.; Sato, S.; Noguchi-Yachide, T.; Sodeoka, M.; Yokomatsu, T.; Dodo, K.; Hashimoto, Y.; Aoyama, H., (2m-Cl and m-Br) Small-molecular inhibitors of Ca(2)(+)-induced mitochondrial permeability transition (MPT) derived from muscle relaxant dantrolene. *Bioorganic & medicinal chemistry* **2012,** *20* (21), 6384-93.

133.   Umezawa, K.; Matsui, A.; Nakamura, Y.; Citterio, D.; Suzuki, K., (o-OMe)Bright, color-tunable fluorescent dyes in the Vis/NIR region: establishment of new "tailor-made" multicolor fluorophores based on borondipyrromethene. *Chemistry* **2009,** *15* (5), 1096-106.

13. Curriculum Vitae

Javier de CeballosCerrajería
16, Olpe
44135, Dortmund, Germany
Mobile: 0049 157 871 474 69
Mail: javierceballos5@gmail.com
27 years old – Single

M.Sc., Ph. D. Student in Chemical Biology

<u>Education & Training</u>

2012-present: Ph.D. student at the Max Planck Institute ofMolecular Physiology, Dortmund
- Research Topic*: "Synthesis of Glucose Uptake Inhibitors"*
- Supervisor*: Prof. Herbert Waldmann*

2011-2012 M. Sc. "Synthesis and Catalysis" at the Institute of Chemical Research of Catalonia (ICIQ),[1] Tarragona (Spain)(9/10)
- Master thesis*:"Metal-free Electrophilic 2-Amination of Indoles"*
- Supervisor: *Prof. Kilian Muñiz*

2006-2011   Licenciatura[2]in Chemistry at the University of Oviedo(Spain)(8.5/10)
- Specialization in Organic Chemistry

<u>Fellowships</u>

2012-2015: MaxPlanck Fellowship for Research during *Ph.D.* studies
- Research Project: "*Synthesis of Glucose Uptake Inhibitors*"

2012-present: Member of the *International Max Planck Research School in Chemical and Molecular Biology (IMPRS-CMB)*[3]

---

[1] Institute of Chemical Research of Catalonia (ICIQ) provides a M. Sc. title in cooperation with University RoviraiVirgili (Tarragona, Spain)

[2]Licenciatura was at the time the basic Spanish University degree in Chemistry. Licenciatura consisted of 5 years of chemical education, in the last year it was possible to orient one-self into an area of chemistry. Average grade is evaluated with 1 being the best possible and 5 the worst.

[3]IMPRS-CMB is a joint initiative of the Max-Planck-Institute of Molecular Physiology in Dortmund and three partner universities, the TU Dortmund, the Ruhr-University-Bochum and the University of Duisburg-Essen. (www.imprs-cmb.mpg.de)

2010-2011: Research collaboration fellowship in the Group of Prof. Vicente Gotor at the University of Oviedo, Oviedo (Spain)

- Research project*: "Enzymatic regioselective acylation and hydrolysis reactions on 3´and 5´positions of cyanobased-nucleosides"*
- Supervisor*: Prof. Miguel Ferrero*

Publications

- *"*Iodine(III)-Mediated Selective Intermolecular C-H Amination for the Chemical Diversification of Tryptamines*"* Bosnidou A.E.; Millan A.; Ceballos J.; Martínez C.; Muniz, K.*; *J. Org. Chem.* **2016**, *81*, 6496-6504.

- *"Identification of a small molecule inhibitor that stalls splicing at an early step of spliceosome activation"* Sidarovich, A.; Will, C. L.; Anokhina, M. M.; Ceballos, J.; Sievers, S., Agafonov, D. E.; Samatov, T.; Kastner, B.; Urlaub, H.; Waldmann, H.; Lührmann, R.*; *eLIFE, just accepted*

Conferences

- Talk: "*Glupins- A Novel Class of Glucose Uptake Inhibitors*"at JCS Ruhr 2016, Dortmund.

- Poster presentation at the IMPRS retreat. "*Study of the Splicing Process by Small Molecule Induced Inhibition"* October, 2015.

- Attendance to CHEM21 workshop and Symposium at the Royal Society of Chemistry, London, June 2016.

- Organizing Committee of the *5th IMPRS-CMB Student Symposium*.

- Poster Presentation at ICIQ Summer School, July 2012, Tarragona.

Teaching

- Supervision of the Bio-organic practical course for Bachelor studies at the TU Dortmund (2013-2016)
- Supervision of a laboratory technician trainee (Dec. 2015 to Aug. 2016)

Languages

- Spanish: Mother tongue
- English: Proficient
- German: Intermediate
- French: Intermediate

14. Acknowledgements

Finally, to my love, Helena Gelabert Chasco, with whom I have shared, and will continue to do so for many years, my life.